



Wissenschaftszentrum Weihenstephan für Ernährung, Landnutzung und Umwelt

Lehrstuhl für Botanik

**Genetic basis of water use efficiency and yield potential in  
*Arabidopsis thaliana***

Zhenyu Yang

Vollständiger Abdruck der von der Fakultät Wissenschaftszentrum Weihenstephan für Ernährung, Landnutzung und Umwelt der Technischen Universität München zur Erlangung des akademischen Grades eines

Doktors der Naturwissenschaften

genehmigten Dissertation.

Vorsitzender: Prof. Dr. Kay H. Schneitz

Prüfer der Dissertation:

1. Prof. Dr. Erwin Grill

2. Prof. Dr. Ramon A. Torres Ruiz

Die Dissertation wurde am 16.11.2016 bei der Technischen Universität München eingereicht und durch die Fakultät Wissenschaftszentrum Weihenstephan für Ernährung, Landnutzung und Umwelt am 08.12.2016 angenommen.



---

# Content

Content.....	2
List of Figures.....	6
Abbreviations .....	10
Summary .....	14
Zusammenfassung.....	16
1.Introduction.....	18
1.1 Crop yield.....	18
1.2 The drought .....	20
1.3 Drought scenarios .....	20
1.4 Strategies to cope with drought.....	21
1.4.1 Escape strategy.....	21
1.4.2 Avoidance strategy .....	22
1.4.3 Tolerance strategy .....	23
1.5 Strategies to save water .....	23
1.5.1 Technical strategies .....	23
1.5.2 Plant-based strategy (high water use efficiency) .....	24
1.6 Drought-induced ABA signaling.....	25
1.6.1 ABA synthesis .....	26
1.6.2 ABA signaling.....	28
1.6.2.1 Receptor complex.....	29
1.6.3.2 SnRK2s .....	31
1.6.3.3 Ion channel.....	32
1.6.3.4 Transcriptional factors .....	32
1.7 Drought-induced MAPKs signaling.....	33
1.8 Nighttime stomatal opening.....	34
1.9 Stomatal oscillation .....	36
1.10 The aim of this work.....	38
2. Materials and methods .....	40
2.1 Material .....	40
2.1.1 Chemicals .....	40
2.1.2 Equipment .....	40
2.1.3 Bacteria strains .....	41
2.1.4 Plant materials.....	42
2.1.5 Vector and primers.....	44
2.2 Methods .....	45
2.2.1 Seed sterilization and seedling growth conditions .....	45
2.2.2 Plant growth conditions .....	45

2.2.3 Progressive drought .....	45
2.2.4 Deficit irrigation.....	49
2.2.5 Yield potential under well-watered conditions.....	50
2.2.6 Leaf area, biomass, water use efficiency and energy measurements .....	52
2.2.7 Thermal imaging.....	52
2.2.8 Carbon and oxygen isotope composition.....	53
2.2.9 Gas exchange.....	54
2.2.9.1 Gas exchange under well-watered conditions and progressive drought .....	54
2.2.9.2 Mesophyll conductance .....	56
2.2.9.3 Nighttime stomatal opening and stomatal oscillation .....	61
2.2.10 Stomatal aperture, density, size and index .....	63
2.2.11 Genomic DNA isolation from plants.....	63
2.2.12 Cloing techniques .....	64
2.2.13 Statistic analysis .....	64
3. Results .....	65
3.1 System establishment .....	65
3.1.1 Progressive drought .....	66
3.1.2 Deficit irrigation testing system .....	68
3.1.3 Thermal imaging and gas exchange analysis during progressive drought .	71
3.2 Enhanced water use efficiency conferred by ectopic expression RCARs .....	72
3.2.1 Water productivity conferred by ectopic expression of RCARs during progressive drought .....	74
3.2.1.1 Leaf surface temperatures and growth in well-watered phase of progressive drought .....	74
3.2.1.2 Water consumption.....	76
3.2.1.3 Biomass accumulation and WUE .....	78
3.2.1.4 Water use efficiency determined by using stable isotopes .....	80
3.2.1.5 Associations among biomass gain, leaf surface temperatures, leaf growth and WUE .....	83
3.2.1.6 Water productivity conferred by overexpression of RCAR1, RCAR6, and RCAR10.....	85
3.2.1.7 Insight into mechanisms by gas exchange analysis.....	86
3.2.1.7.1 Stomatal limitation.....	86
3.2.1.7.1.1 Estimation of $g_s$ , $A_n$ and $C_i$ in well-watered conditions and during progressive drought .....	86
3.2.1.7.1.2 Estimation of $g_s$ , $A_n$ and $C_i$ during progressive drought .....	88
3.2.1.7.2 Mesophyll conductance and photosynthetic biochemical limitations.....	89
3.2.1.7.2.1 Estimation of $g_m$ , $V_{c,max}$ , $J_{max}$ , $V_{TPU}$ using C3 plant photosynthesis model .....	89
3.2.1.7.2.2 Compensation of reduced stomatal conductance by increased $CO_2$ gradient.....	91
3.2.1.7.2.3 Estimation of $g_m$ , $V_{c,max}$ , $J_{max}$ , $V_{TPU}$ using C3 plant photosynthesis model .....	92
3.2.1.7.2.4 Compensation of reduced stomatal conductance by	

---

increased CO <sub>2</sub> gradient.....	94
3.2.1.7.3 Estimation of mesophyll conductance by analysis of <sup>13</sup> C discrimination.....	96
3.2.1.8 Shoot and root contributions to WUE.....	97
3.2.1.9 Biomass and WUE affected by ambient temperatures.....	98
3.2.2 Water productivity of RCAR6 and RCAR10 lines under well-watered conditions.....	99
3.2.2.1 Biomass and WUE of plants grown under moderate light.....	99
3.2.2.2 Biomass and WUE of plants grown under saturation light.....	102
3.2.3 Water productivity of Arabidopsis under deficit irrigation.....	103
3.2.3.1 Leaf surface temperatures.....	104
3.2.3.2 Biomass formation and water use efficiency.....	105
3.2.4 Stomatal density and size in RCAR6 and RCAR10 lines.....	107
3.3 Natural variation of water use efficiency in Arabidopsis ecotypes.....	109
3.3.1 Natural variation of WUE under progressive drought conditions.....	110
3.3.1.1 Arabidopsis accessions under well-watered conditions.....	110
3.3.1.2 Water productivity of Arabidopsis accessions under progressive drought.....	111
3.3.1.3 Associations among biomass, leaf surface temperatures, leaf growth and water use efficiency.....	112
3.3.1.4 Water productivity of Arabidopsis accessions in an independent progressive drought.....	113
3.3.1.5 Gas exchange of Arabidopsis accessions under well-watered and progressive drought conditions.....	116
3.3.1.6 Stomatal aperture and size contribute to leaf temperature differences between Col-0 and Cvi-0.....	119
3.3.2 Quantitative trait locus mapping of cool leaf temperature gene MPK12 and its function in the regulation of WUE.....	120
3.3.2.1 Variation in leaf surface temperature during the progressive drought .....	120
3.3.2.2 Leaf surface temperatures of Col-0, Cvi-0 and reciprocal F1 and F2 generations.....	121
3.3.2.3 Leaf surface temperatures of Col-0, Cvi-0, and recombinant inbred lines.....	122
3.3.2.4 Mapping the QTL locus responsible for the leaf surface temperature .....	123
3.3.2.5 Recombination events in F2 mapping population.....	127
3.3.2.6 Candidate genes.....	129
3.3.2.7 MPK12 is the gene responsible for "cool" leaf surface temperature.....	130
3.3.2.8 Amino acid alignments of MPK12.....	133
3.3.2.9 Water use efficiency conferred by the MPK12 gene.....	133
3.4 Nighttime stomatal opening and stomatal oscillation in Arabidopsis.....	135
3.4.1 Quantitative trait locus analysis of nighttime stomatal opening and stomatal oscillation in Arabidopsis.....	137
3.4.1.1 The phenomena of nighttime stomatal opening and stomatal oscillation.....	137

## Content

---

3.4.1.2 Mapping the locus responsible for nighttime stomatal opening .....	143
3.4.1.3 Mapping the loci responsible for the oscillation period .....	147
3.4.2 The MPK12 gene is responsible for nighttime stomatal opening but not for oscillation periods .....	150
3.4.2.1 Nighttime stomatal opening controlled by the MPK12 gene.....	150
3.4.2.2 Oscillation periods are not controlled by the MPK12 gene .....	154
3.4.3 Stomatal oscillation does not occur at random .....	156
4. Discussion .....	159
4.1 Drought assay system .....	159
4.2 Potential to enhance water use efficiency in Arabidopsis .....	164
5. Appendix .....	185
6. References .....	192
Acknowledgements .....	218
Lebenslauf .....	219

# List of Figures

Figure 1-1 US maize yield trends from 1966-2005, and the technological innovations that contributed to this yield advance	18
Figure 1-2 Trends of yield increase of the three major cereal crops in selected regions since the start of the 1960s	19
Figure 1-3 ABA biosynthesis pathway in plants	26
Figure 1-4 ABA core signaling to modulate stomatal movement and to initiate transcription of downstream genes	28
Figure 1-5 Phylogenetic tree of ABA binding proteins from Arabidopsis	30
Figure 2-1 Soil preparation and evaluation of water status	46
Figure 2-2 The calibration curve of the soil water content and soil water potential	47
Figure 2-3 Experimental setup of the whole-rosette gas exchange measurement	55
Figure 3-1 Growth performance, biomass and WUE in <i>Arabidopsis thaliana</i> wild type Columbia during progressive drought	68
Figure 3-2 Growth performance, biomass and WUE of wild type Columbia grown under water deficit conditions	70
Figure 3-3 Thermal imaging and gas exchange analysis during progressive drought	72
Figure 3-4 Prescreening of Arabidopsis lines with ectopic expression of ABA receptors	75
Figure 3-5 Overexpression of ABA receptors affects growth and leaf temperatures of Arabidopsis Columbia lines	77
Figure 3-6 Water consumption of RCAR lines under progressive drought	78
Figure 3-7 Water productivity conferred by ectopic expression of ABA receptors	79
Figure 3-8 Carbon isotope composition, carbon isotope discrimination and integrated WUE conferred by ectopic expression of RCAR receptors	81
Figure 3-9 Oxygen isotope composition in extracted cellulose fractions conferred by ectopic expression of RCAR receptors	83
Figure 3-10 Associations among biomass gain, leaf surface temperatures, leaf growth and WUE in Arabidopsis lines overexpressing RCARs	84
Figure 3-11 Water productivity conferred by overexpression of ABA receptor RCAR1, RCAR6, and RCAR10 during progressive drought	86
Figure 3-12 Gas exchange analysis revealed enhanced water productivity conferred by ectopic expression of RCAR6 and RCAR10 under well-watered conditions	88
Figure 3-13 Gas exchange parameters and insWUE of Columbia, RCAR6-3 and RCAR10-4 at various soil water contents	89

## List of Figures

---

Figure 3-14 Gas exchange analysis using Col and RCAR6-3 lines under saturating light and variable ambient CO <sub>2</sub> conditions	91
Figure 3-15 Compensation for reduced stomatal conductance by a steeper CO <sub>2</sub> gradient between the atmosphere and chloroplast	92
Figure 3-16 Gas exchange analysis using Columbia, RCAR6-3 and RCAR10-4 lines under saturating light and variable ambient CO <sub>2</sub> conditions	94
Figure 3-17 Compensation of reduced stomatal conductance by a steeper CO <sub>2</sub> gradient between the atmosphere and chloroplast	95
Figure 3-18 Estimation of mesophyll conductance by on-line $\Delta^{13}\text{C}$ measurements	97
Figure 3-19 Organ-mediated changes in WUE analyzed by grafting of RCAR10-4 line and wild type Columbia	98
Figure 3-20 Water productivity conferred by ectopic expression of ABA receptors under different ambient temperatures	99
Figure 3-21 Biomass production under a well-watered growth regime	101
Figure 3-22 Growth performance, biomass accumulation and $\Delta^{13}\text{C}$ -derived integrated WUE of RCAR6-3 plants under high photon flux density conditions	103
Figure 3-23 Leaf surface temperatures of wild type Columbia and RCAR lines in response to soil water content	104
Figure 3-24 Biomass formation and water productivity conferred by ectopic expression of RCAR6 and RCAR10 under deficit irrigation	106
Figure 3-25 Stomatal density, size and index of lines ectopically expressing RCAR6 and RCAR10	108
Figure 3-26 Leaf growth and leaf surface temperatures of eight Arabidopsis ecotypes under well-watered conditions	110
Figure 3-27 Water productivity of Arabidopsis accessions under progressive drought conditions	111
Figure 3-28 Correlations among leaf temperature, leaf area, leaf expansion rate, biomass and WUE in Arabidopsis accessions	113
Figure 3-29 Water productivity of Arabidopsis accessions	114
Figure 3-30 Gas exchange analysis of Arabidopsis accession Col-0, Mr-0, Mt-0, Sorbo and Tu-0	116
Figure 3-31 Enhanced insWUE in Arabidopsis accessions by reduced soil water content	117
Figure 3-32 Lower insWUE in Arabidopsis accession Cvi-0	118
Figure 3-33 Cool leaf temperature and high stomatal conductance in accession Cvi-0 caused by larger stomatal pores and stomatal size	119
Figure 3-34 Leaf surface temperatures of Col-0 and Cvi-0 in relation to the depletion	



of soil water content	120
Figure 3-35 Leaf temperatures of Col-0, Cvi-0 and their reciprocal F1 and F2 generations	122
Figure 3-36 Leaf surface temperatures of Col-0, Cvi-0, and their recombinant inbred lines	123
Figure 3-37 Genome and genotype of Col, Cvi and their F2 and RILs populations	124
Figure 3-38 Fine mapping of the Cvi "cool" leaf temperature gene to a 137kb region on chromosome 2	128
Figure 3-39 Increased leaf surface temperature of Cvi transformants homozygous for Col MPK12 allele	131
Figure 3-40 Reduced leaf surface temperature of knockout MPK12 mutant <i>mpk12</i> in Columbia background	132
Figure 3-41 Alignment of deduced amino acid sequence of MPK12	133
Figure 3-42 Water productivity conferred by MPK12 gene	134
Figure 3-43 Nighttime stomatal opening and stomatal oscillation of Arabidopsis accessions Col-0 and Cvi-0	138
Figure 3-44 Stomatal oscillations of Arabidopsis accessions Col-0 and Cvi-0	141
Figure 3-45 Nighttime stomatal openings and stomatal oscillations of F1 hybrids and recombinant inbred lines derived from Arabidopsis accessions Col-0 and Cvi-0	143
Figure 3-46 Alignment of genotypes and nighttime stomatal conductance phenotypes of Col-0, Cvi-0 and their RILs populations	146
Figure 3-47 Alignment of genotypes and oscillation period phenotypes of Col-0, Cvi-0 and their RILs populations	149
Figure 3-48 Nighttime stomatal opening and stomatal oscillations of Arabidopsis accessions Col-0, Cvi-0 and Cvi plants homozygous for the Col MPK12 allele	151
Figure 3-49 Stomatal oscillation of Arabidopsis accessions Col-0, Cvi-0 and Cvi plants homozygous for the Col MPK12 allele	155
Figure 3-50 Stomatal oscillation does not occur at random and maybe associated with soil water availability	156
Figure 4-1 Protein structure of MPK12 homologous	178
Figure 4-2 Alignment of the promoter sequence in Col and Cvi	180
Figure 6-1 Biomass and water consumption in Arabidopsis thaliana wild type Columbia during progressive droughts	185
Figure 6-2 Water productivity conferred by ectopic expression of ABA receptors	186
Figure 6-3 Biomass production during progressive droughts	187
Table 2-1 Equipments	40

## List of Figures

---

Table 2-2 <i>Escherichia coli</i> strains	41
Table 2-3 <i>Agrobacterium tumefaciens</i> strain	41
Table 2-4 Collections of ecotypes of <i>Arabidopsis thaliana</i>	42
Table 2-5 Candidate genes which were cloned transformed into wild type Cvi-0 plants	43
Table 3-1 Photosynthetic parameters of Columbia and RCAR6-3 deduced from An-Ci curve at saturating light	92
Table 3-2 Photosynthetic parameters of Columbia, RCAR6-3 and RCAR10-4 deduced from An-Ci curve at saturating light	95
Table 3-3 Candidate gene list between marker c2_18883 and marker c2_19020	129
Table 3-4 Nighttime stomatal conductance of <i>Arabidopsis</i> accessions Col-0, Cvi-0 and their F1 hybrids and RILs populations	145
Table 3-5 Oscillation periods of stomatal conductance of <i>Arabidopsis</i> accessions Col-0 and Cvi-0 and their genetic populations	148
Table 3-6 Nighttime stomatal conductance of <i>Arabidopsis</i> accessions Col-0, Cvi-0, and Cvi plants homozygous for the Col MPK12 allele	154
Table 3-7 Oscillation periods of stomatal conductance of <i>Arabidopsis</i> accessions Col-0, Cvi-0 and Cvi plants homozygous harboring the Col MPK12 allele	156
Table 5-1 Primers for identifying genes responsible for a cool leaf temperature	188
Table 5-2 Primers for identifying homozygous T-DNA insertion lines	189
Table 5-3 Uniform primers for identifying homozygous T-DNA insertion lines	189
Table 5-4 Primers for cloning genes listed in Table 2-5	190
Table 5-5 Strains used in this study	191

# Abbreviations

AAO3	Abscisic aldehyde oxidase
ABA	Abscisic Acid
ABA2	ABA Deficient 2
ABI1/ABI2	ABA insensitive 1/2; A type PP2C
ABI4	APETALA 2 (AP2) domain transcriptional factor ABA insensitive 4
ABRE	ABA-responsive element
ABER / ABFs	ABRE-binding proteins/factors
Amp	Ampicillin
$A_n$	Net carbon assimilation rate
APETALA 2	A transcription factor containing the ERF domain
AREBs / ABFs	ABRE-binding proteins/factors
ATAF1	<i>Arabidopsis thaliana</i> activating factor 1
ATP	Adenosine triphosphate
Bypass	An function-unknown gene in <i>Arabidopsis thaliana</i>
bZIP TF	Basic leucine zipper transcription factor
C3	C3 carbon fixation pathway
C4	C4 carbon fixation pathway
$C_a$	Ambient CO <sub>2</sub> concentration
$C_a - C_c$	CO <sub>2</sub> gradient between ambient and chloroplast
$C_a - C_i$	CO <sub>2</sub> gradient between ambient and intercellular space
$C_i$	Intercellular CO <sub>2</sub> concentration
$C_i - C_c$	CO <sub>2</sub> gradient between intercellular space and chloroplast
$C_i^*$	Intercellular photocompensation point
CAT1	Catalase 1
CDS	Coding sequence
CE	Coupling element
Cool1	Gene encode the cool leaf temperature trait
CRF5	A gene encodes one of the six cytokinin response factors
CTAB	Hexadecyl trimethyl-ammonium bromide
Cv <sup>i</sup> MPK12	Cvi transformants homozygous for Col MPK12 allele
DFG motif	The Asp-Phe-Gly motif
$E$	Transpiration rate

## Abbreviations

---

$E_{night}$	Nighttime transpiration rate
<i>er2</i>	An ERECTA mutant in Columbia background in <i>Arabidopsis thaliana</i>
<i>era1-2</i>	An farnesyltransferase knockout mutant in Columbia background
ERECTA	A Leucine rich repeat receptor kinase
ERF	Ethylene- Responsive Element binding factors
FLOWERING LOCUS T (FT)	A florigen gene
FRI (FRIGIDA)	A gene affecting growth rate, WUE and flowering time
$F_m'$	Maximum fluorescence
$F_s$	Steady-state fluorescence
$g_i$	Internal conductance
GIGANTEA (GI)	A flower-promoting gene
GK	A source of Arabidopsis knockout lines from University of Bielefeld
$g_m$	Mesophyll conductance
$g_s$	Stomatal conductance
$g_{s\_day}$	Daytime stomatal conductance
$g_{s\_night}$	Nighttime stomatal conductance
$h$	Humidity
HAB1 and HAB2	Homology to ABI1 1/2; A type PP2C
HB6	Arabidopsis Homeobox Protein 6; HD-ZIP TF
iWUE	Intrinsic water use efficiency
insWUE	Instantaneous water use efficiency
IPP	Isopentylidiphosphate
IRT	IR thermogram
$J_{max}$	Maximum electron transport rate
Kan	Kanamycin
KAT1/2	Potassium channel in Arabidopsis 1/2
$K_c$	Michaelis-Menten constants of Rubisco for CO <sub>2</sub>
$K_o$	Michaelis-Menten constants of Rubisco for O <sub>2</sub>
Lcbk2	A gene encoding a putative sphingosine kinase
LEA	Late embryogenesis abundant
LEA1	LEA hydroxyproline-rich glycoprotein 1
LEA2	LEA hydroxyproline-rich glycoprotein 2
$L_p$	Projected leaf area
MAPK	Mitogen-activated protein kinase

MAPKK	MAPK kinase
MAPKKK	MAPK kinase kinase
MEP	2-C-methyl-D-erythritol-4-phosphate
<i>mpk12</i>	Knockout mutant of MPK12
mRNA	Messenger RNA
MS medium	Murashige and Skoog medium
NASC	Nottingham Arabidopsis Stock Center
NAC TF	NAC transcription factor
NCED	9-cis-epoxycarotenoid dioxygenase
NILs	Near isogenic lines
OST1	OPEN STOMATA 1
PP2C	Type 2C protein phosphatase
PAR	Photosynthetic active radiation
PD98059	A MAP2K inhibitor
PYR	Pyrabactin Resistance Protein
PYL	PYR-Like proteins
PYR1 <sup>MANDI</sup>	Hextuple mutant derived from RCAR11/PYR1
QTL	Quantitative trait locus
QUAC1	Quick-Activating Anion Channel 1
ROS	Reactive oxygen species
RCAR	Regulatory Components of ABA Receptors
$R_d$	The respiration rate in the daytime
Rif	Rifampicin
RILs	Recombinant inbred lines
$R_{sample}$	The <sup>18</sup> O/ <sup>16</sup> O ratio of the sample
$R_{standard}$	The <sup>18</sup> O/ <sup>16</sup> O ratio of the Vienna standard Mean Ocean Water standard
<i>RWC3</i>	A water channel protein
$r_i$	Internal resistance
$r_m$	Stomatal conductance
$r_s$	Stomatal resistance
SALK	A source of Arabidopsis knockout lines from Salk institute
SDR1	Short-chain dehydrogenase/reductase 1
Ser/Thr	Serine/Threonine
SLAC1	Slow Anion Channel-Associated 1

## Abbreviations

---

SnRK2.6/SRK2	Subfamily 2 of sucrose nonfermenting 1 (SNF1)-related kinase
SNPs	Single nucleotide polymorphisms
SSLPs	Simple sequence length polymorphisms
SWC	Soil water content
SWP	Soil water potential
$T_{ring}$	Temperature in the ring chamber
TRIP	A gene encoding a homolog of mammalian TGF-beta receptor interacting protein
$T_{cuvette}$	Temperature in the cuvette
TWIN SISTER OF FT (TSF)	A florigen gene
UV	Ultraviolet
UVA	Long wave ultraviolet A
UVB	Short wave ultraviolet B
$V_{cmax}$	Maximum carbon assimilation rate
VPD	Vapor pressure difference
$V_{TPU}$	The rate of triose phosphate utility
$W_a$	Water vapor concentration
Yield	Actual quantum efficiency of photosystem II
ZEP	Zeaxanthin epoxidase
$^{16}\text{O}$	Oxygen 16 isotope
$^{18}\text{O}$	Oxygen 18 isotope
$^{12}\text{C}$	Carbon 12 isotope
$^{13}\text{C}$	Carbon 13 isotope
$\delta^{13}\text{C}$	Carbon isotope composition ( $^{12}\text{C}$ and $^{13}\text{C}$ )
$\delta^{18}\text{O}$	Oxygen isotope discrimination ( $^{16}\text{O}$ and $^{18}\text{O}$ )
$\Delta^{13}\text{C}$	$^{13}\text{C}$ discrimination
$\Delta^{18}\text{O}$	$^{18}\text{O}$ enrichment
$\Delta^{13}\text{C}_{bulk}$	$^{13}\text{C}$ discrimination of bulk samples
$\Delta^{13}\text{C}_{cellulose}$	$^{13}\text{C}$ discrimination of cellulose samples
$\Delta e$	$^{18}\text{O}$ enrichment at the evaporation site in the stomata
$\epsilon_k$	Kinetic fractionation
$\epsilon^+$	Liquid-vapor equilibrium fractionation
$\Gamma^*$	The chloroplastic $\text{CO}_2$ photocompensation point

## Summary

Most plants inevitably confront drought in nature, and have evolved sophisticated strategies to cope with drought, among which drought avoidance is more compatible with the interests of agriculture. Reducing water loss and improving water uptake enable drought avoidance by plants. The reduction in water loss for carbon fixation, i.e. improved water use efficiency (WUE) of plants, is a most interesting trait for drought resistance. Previous researches have engendered the wide consensus that WUE of plants can be enhanced under water-limited conditions. However, few successes have been achieved to translate this insight into crops in field conditions. The failure is due to the difficulty of "recognizing and targeting the correct trait and phenotype under the relevant stress conditions", lack of knowledge on genes and gene networks regulating WUE and the negative correlation between WUE and plants' growth.

In this study, for analysis of plants' drought resistance, a prolonged progressive drought system was established to simulate the slow soil drying in the field under drought. Using the leaf temperature and leaf growth, along with measurements of soil water potential provide simple parameters to classify the severity of drought stress. These parameters were found to be a powerful tool for identifying natural accessions and transgenic lines that combine enhanced WUE with maintenance of growth. Moreover, measuring gas exchange under the variable severity of drought conditions facilitated to elucidate the adaptive mechanisms of plants.

Transpiration and carbon uptake through stomatal pores are intrinsically associated, and the aperture of stomatal pores is best-known to be regulated by the Phytohormone abscisic acid (ABA). The activation of ABA signaling promotes stomatal closing, reducing water loss in plants, but simultaneously restricts the uptake of CO<sub>2</sub>, thereby affecting plant growth. This delicate balance of transpiration and CO<sub>2</sub> uptake can be modulated by a family of ABA receptors. Investigation of WUE in *Arabidopsis* via expressing ABA receptors revealed that plants overexpressing RCAR6/PYL12 were found to combine maintained leaf growth with up to 40% enhanced WUE compared with wild type, i.e., are water productive. Water productivity was associated with the maintenance of net carbon assimilation rate

caused by the compensation of reduced stomatal conductance by an increased CO<sub>2</sub> gradient between ambient air and chloroplasts, and may also be due to a simultaneous increase in photosynthetic capacity.

Naturally occurring variations in WUE within a single species are valuable resources for understanding plants' WUE. Investigation of variation in leaf temperature between the accessions Columbia and Cape Verde led to an identification of MPK12 gene which was further found to regulate plants' WUE. MPK12 gene encodes a protein kinase of 372 amino acid residues. In accession Cvi-0, glycine is substituted by arginine at residue 53 which is located in the glycine-rich loop of the ATP binding pocket. This single substitution may interfere with the phosphorelay to target substrates, thereby affecting the signal transduction and finally, the physiological responses.

The gas exchange analysis of Col-0 and Cvi-0 reveal nighttime stomatal opening and stomatal oscillation. Both phenomena were analyzed by using F1 hybrids and recombinant inbred lines derived from Col-0 and Cvi-0. The results indicated a QTL at the end of chromosome 2 that may explain the variations of recombinant inbred lines (RILs) in the nighttime stomatal conductance, and quantitative trait locus at the end of chromosome 2 and 3 may be responsible for the periods of stomatal oscillation. Owing to the similar location of MPK12 gene, both traits of Cvi-0 plants harboring Col MPK12 allele were assessed, and the results revealed that the MPK12 gene could regulate the nighttime stomatal conductance, but not the periods of stomatal oscillation. Reducing nighttime water loss is supposed to be a way to increase plants' WUE.



## Zusammenfassung

Pflanzen sind während ihrer Vegetationsperiode oft Phasen der Trockenheit ausgesetzt. Im Laufe der Evolution haben sie verschiedene Strategien entwickelt, um sich an Trockenperioden anzupassen. Für die Landwirtschaft ist besonders die Strategie der Trockenheitsvermeidung von Bedeutung.

Die Reduzierung des Wasserverlustes und die Steigerung der Wasseraufnahme ermöglichen den Pflanzen die Trockenheitsvermeidung. Ein verringerter Wasserverlust bei der Kohlenstofffixierung, d.h. eine verbesserte Wassernutzungseffizienz (WUE) der Pflanzen, ist eine Eigenschaft mit größtem Interesse für den Kulturpflanzenanbau. Bisherige Untersuchungen zeigten, dass es möglich ist, die WUE von Pflanzen unter Wassermangel zu erhöhen. Jedoch ist es bisher kaum gelungen dies auf Kulturpflanzen unter Freilandbedingungen anzuwenden. Dieser mangelnde Erfolg ist auf die Schwierigkeit die richtigen Merkmale und Eigenschaften für die relevante Stressbedingung zu erkennen, mangelnde Kenntnisse über beteiligte Gene und Gennetzwerke, welche die WUE regulieren und die negative Korrelation zwischen WUE mit Pflanzenwachstum zurück zu führen.

In dieser Arbeit wurden zur Untersuchung der Trockenresistenz Pflanzen einer zunehmenden Trockenheit ausgesetzt um ein langsames Austrocknen des Bodens unter Feldbedingungen zu simulieren. Die Blattemperatur und das Blattwachstum zusammen mit dem Wasserpotential des Bodens stellen einfache Parameter zur Ermittlung des Stressausmaßes dar. Diese Parameter waren wirksame Werkzeuge um Akzessionen und transgene Linien zu identifizieren, die eine erhöhte WUE mit unverändertem Wachstum kombinierten. Darüberhinaus ermöglichten Messungen des Gasaustauschs die Anpassungsmechanismen der Pflanzen an unterschiedliche Phasen des Trockenstresses zu untersuchen.

Transpiration und Kohlenstoffaufnahme über die Schließzellen der Pflanzen sind intrinsisch gekoppelt. Der Öffnungsgrad der Schließzellen wird, wie bestens bekannt, über das Phytohormon Abscisinsäure (ABA) reguliert. Die Aktivierung der ABA-Signaltransduktion führt zum Schließen der Stomata und reduziert den Wasserverlust, behindert aber gleichzeitig die Kohlenstoffdioxid-Aufnahme und dadurch das Pflanzenwachstum. Das empfindliche Gleichgewicht zwischen Transpiration und Kohlenstoffdioxid-Aufnahme kann durch die Familie der

ABA-Rezeptoren beeinflusst werden. Untersuchungen der WUE in Arabidopsis nach Expression der RCAR ABA-Rezeptoren zeigten, dass eine Überexpression von RCAR6/PAL12 zu einer um 40 % erhöhten WUE bei gleichzeitig unverändertem Blattwachstum gegenüber dem Wildtyp führte, d.h. diese Linie war wasserproduktiv. Die Wasserproduktivität ging einher mit dem Aufrechterhalten der Nettokohlenstoffassimilationsrate durch Kompensation der reduzierten stomatären Leitfähigkeit über eine Erhöhung des Kohlenstoffdioxid-Gradienten zwischen der umgebenden Luft und den Chloroplasten. Möglicherweise ist auch ein gleichzeitiger Anstieg der Photosynthesekapazität daran beteiligt.

Natürliche Variationen der WUE innerhalb einer Art sind wertvolle Ressourcen um die Mechanismen der WUE von Pflanzen zu entschlüsseln. Untersuchungen der Unterschiede in der Blattoberflächentemperatur zwischen den Akzessionen Columbia (Col-0) und Cape Verde (Cvi-0) führten zur Identifizierung des Gens MPK12 identifiziert werden, das eine Rolle in der Regulation der WUE spielt. MPK12 kodiert für eine Proteinkinase mit einer Länge von 372 Aminosäureresten. In der Akzession Cvi-0 befindet sich in der Glycin-reichen Schleife der ATP-Bindetasche wo ein Aminosäureaustausch von Glycin zu Arginin am Rest 53 stattfand. Dieser einzelne Aminosäureaustausch führt vermutlich zur Beeinträchtigung der Phosphoübertragung zu Zielsubstraten, wodurch die Signaltransduktion und schließlich die physiologische Antwort beeinträchtigt wird.

Untersuchungen des Gasaustauschs in Col-0 und Cvi-0 zeigten ein Öffnen der Stomata in der Nacht sowie stomatäre Oszillationen. Beide Phänomene wurden in F1 Hybriden und rekombinanten Inzuchtlinien (RILs) von Col-0 und Cvi-0 untersucht. Diese Ergebnisse wiesen auf ein quantitatives Merkmal (QTL) am Ende des Chromosoms 2 hin, welches für die Variationen in den RILs bei der stomatären Leitfähigkeit in der Nacht verantwortlich ist. Weiterhin könnten quantitative Merkmale am Ende der Chromosomen 2 und 3 verantwortlich für die Periode der stomatären Oszillation sein. Aufgrund der ähnlichen Lokalisation des MPK12 Gens auf Chromosome 2, wurden beide Phänomene in Cvi-0 Pflanzen mit dem eingeführten Col MPK12 Allel untersucht. Die Ergebnisse zeigten, dass MPK12 die nächtliche stomatäre Leitfähigkeit reguliert, jedoch nicht die Periode der stomatären Oszillation. Die Reduzierung der nächtlichen Transpiration wird als ein Weg zur Verbesserung der WUE gesehen.

# 1. Introduction

## 1.1 Crop yield

Plants absorb and convert solar energy to chemical energy through photosynthesis by taking advantage of simple substances present in their surroundings, like water and CO<sub>2</sub> (Barber, 2009; Zhu *et al.*, 2008). The stored chemical energy is released later into the food chain (Sharma, 2009). Agriculture is an artificial food chain in which crops, as autotrophs, are the initiators and produce carbohydrates to feed heterotrophs humans, for example. The amount of carbohydrates generated by crops and used by humans is referred to as “biomass” or “yield”. Crops reach their maximum yield (yield potential) under non-stress conditions (Blum, 2005). However, crop plants grown in the field can hardly avoid unpleasant environments, such as drought or salt stress, which cause yield reductions. In the 1960s, a green revolution was initiated to improve the yield of crops. The yield gain of maize production in the USA was increased by a rate of 112 kg ha<sup>-1</sup> per year, or 1.2% per year, between 1965 and 2005 (Fig. 1-1) (Cassman and Liska, 2007).

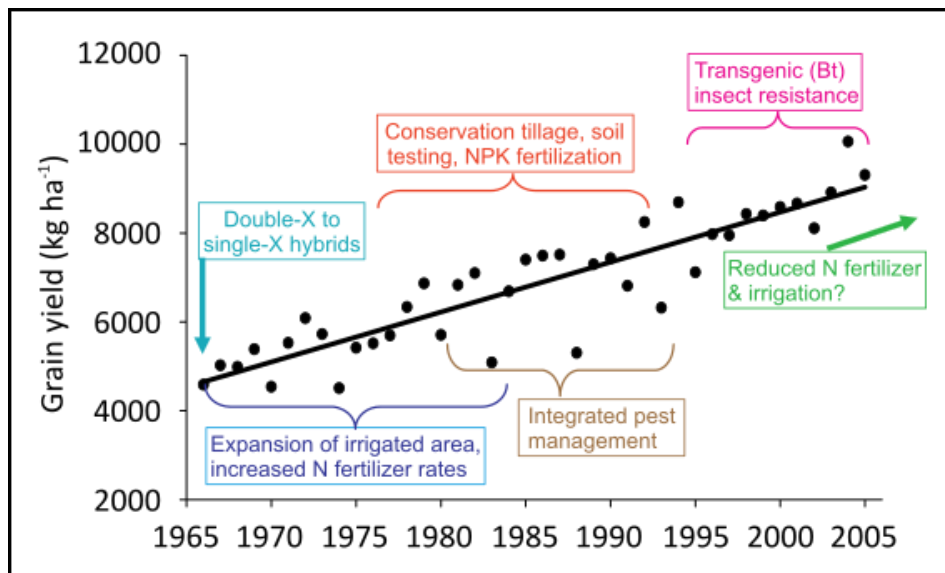


Figure 1-1 US maize yield trends from 1966–2005, and the technological innovations that contributed to this yield advance. (Cassman and Liska, 2007)

New breeding methods, expansion of irrigated areas, soil testing and balanced fertilization of soil, conservation tillage, and integrated pest control were the driving forces for the first 30 years of improvement (Cassman and Liska, 2007). The

continuous increase for the rest of this time was mostly due to the introduction of Bt maize, a crop variety generated by genetic engineering.

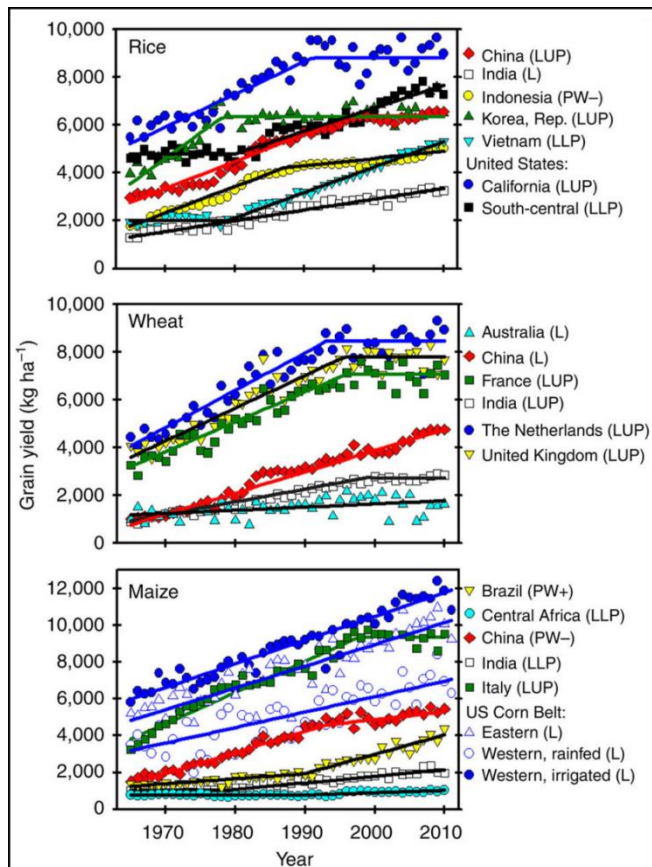


Figure 1-2 Trends of yield increase of the three major cereal crops in selected regions since the start of the 1960s. (Grassini *et al.*, 2013)

However, a similar trend of increase has not appeared for another two important staple crops: rice and wheat. The yields of these have not increased for long periods of time in some developed countries, following an earlier period of steady linear increase (Fig.1-2) (Grassini *et al.*, 2013). Developing countries seem to have the potential to increase their yields to the levels that

developed countries already have, but the average yield increase rate globally could be much lower than Fraley's prediction of 2.3% (Cassman and Liska, 2007). If this is the case, humans may not be able to feed themselves by 2050, when the population on earth will reach 9 billion (Grassini *et al.*, 2013; Ray *et al.*, 2012).

In addition, attempts to further increase crop yields face challenges such as climate change and exhausted groundwater resources. Climate change attracts a lot of attention owing to its tremendous destructive force on crop growth and yield, as was seen in the unprecedented drought confronted by California in 2015. Moreover, the overuse of underground water for agriculture and industry results in its gradual depletion (Bourzac, 2013), and less water is able to be invested in agriculture in future, which in turn, will certainly threaten crop yields. To be well prepared, strategies should be considered. One solution is to enhance the ability of plants to resist drought and increase water use efficiency (WUE).

## 1.2 The drought

Drought is a phenomenon that occurs frequently during the growth season of plants. The definition of drought can be either conceptual or operational (Wilhite and Glantz, 1985). Conceptually, drought is defined as "a long period with no rain, especially during a planting season", while operationally one describes the onset, severity, and termination of drought, and links it to precipitation, evaporation, and evapotranspiration (Wilhite and Glantz, 1985). Changnon (2009) has investigated the impacts of drought thresholds on agriculture in Illinois in the United States, and found that 75% of normal precipitation levels would not affect agricultural activities and production, but 60% levels appeared to have an influence on agricultural production. It has been argued by some scientists that "normal" is not meaningful in this context (Glantz and Katz, 1977). Wilhite and Glantz (1985) suggested that the operational definition of agricultural drought should include descriptions of the responses of crops at different growth stages to the soil water content.

## 1.3 Drought scenarios

Studies on plants' responses to drought stress typically include three methods: the progressive drought, deficit irrigation (controlled drought), and extreme drought-rewatering. The progressive drought simulates the rain-drought scenario. This method allows plants to grow in soil saturated with water to begin with, but no water is administered afterward (Medrano, 2002; Xin *et al.*, 2008). During the progressive drought period, the soil water content is monitored and the performance, yield and other traits of plants are measured to identify germplasms with drought resistance, high yield and enhanced WUE. The other common drought in agriculture is the repeated rain-drought scenario. In practice, water is administered in the most critical growth stages of plants' life cycles. This irrigation regime is called deficit irrigation (controlled drought) (Geerts and Raes, 2009). To simulate this drought scenario in experimental conditions, repeated water is supplied to maintain soil water content at designated levels during certain growth stages (Geerts and Raes, 2009). During deficit irrigation, data concerning soil water levels and the responses of plants are analyzed either to identify varieties with enhanced drought resistance, yield, and WUE or to find the optimum water regimes for the growth of plants. The final drought scenario is extreme drought, which rarely

occurs in agriculture. Studies on extreme drought focus on whether plants experiencing extreme drought are still able to survive after rewatering (Zhao *et al.*, 2016). Choosing different drought scenarios to investigate the responses of plants leads to different results (Tardieu, 2011). A gene that confers a high survival rate to plants in severe drought scenarios may not improve the growth and yield in mild stress scenarios (Tardieu, 2011). This is because different drought scenarios trigger different strategies of plants (Levitt, 1972).

### **1.4 Strategies to cope with drought**

Plants inevitably confront drought in nature, and have evolved sophisticated strategies to cope with drought. These strategies include drought escape, drought avoidance, and drought tolerance (Levitt, 1972).

#### **1.4.1 Escape strategy**

Plants evolve the strategy of escaping from drought by cutting their life cycles down, which ensures the production of seeds before a terminal drought occurs (Farooq *et al.*, 2009). Plants with this strategy exhibit an early flowering phenotype, which allows them to take full advantage of the surrounding resources and grow more quickly finishing their life cycles before intolerable drought starts (Kumar, 2001; Maroco *et al.*, 2000). Considerable variations in flowering time in response to soil water availability have been reported in rice (Xu *et al.*, 2005), *Avena barbata* (Sherrard and Maherali, 2006), *Brassica rapa* (Franks *et al.*, 2007), and *Mimulus* (Ivey and Carr, 2012). A mechanism study that screened *Arabidopsis* flowering time mutants under drought escape triggering conditions revealed that central regulatory components of the flower-promoting gene GIGANTEA (GI) and the florigen genes FLOWERING LOCUS T (FT) and TWIN SISTER OF FT (TSF) were involved in the drought escape response (Riboni *et al.*, 2013). A high degree of developmental plasticity is another trait of plants that escape from drought (Chaves *et al.*, 2003). The growth duration of the plant is interactively modulated by its genotype and environmental factors (Dingkuhn *et al.*, 1999). The adjustment of growth duration to soil water availability allows plants to maximize their yields (Siddique *et al.*, 2003). Moreover, the efficient transport of assimilates from storage organs to fruit in drought-suffering plants is also reported to be associated with drought escape (Rodrigues *et al.*, 1995; Yang *et al.*, 2001). However, the yield is generally considered to be associated with a

life cycle, and therefore shortening the growth period would result in a trade-off of the yield production (Turner *et al.*, 2001).

### **1.4.2 Avoidance strategy**

The drought avoidance strategy confers on plants the ability to maintain relatively high tissue-water potential under water-limited conditions (Mitra, 2001). Studies on the drought avoidance strategy attract a lot of attention because it is more compatible with the interests of agriculture (Morison *et al.*, 2008; Tardieu, 2011). Preventing water loss, improving water uptake, and retaining water in plant cells enable drought avoidance by plants (Chaves *et al.*, 2003). When drought occurs, plants respond rapidly by closing stomata and therefore minimizing water loss. The genes involved in controlling stomatal closure lead to reduced water loss, for example, genes involved in ABA synthesis and ABA signaling (Fujii and Zhu, 2009; Guzel Deger *et al.*, 2015; Iuchi *et al.*, 2001a; Raghavendra *et al.*, 2010). Reduced water loss can also result from having thick leaf cuticles (Park *et al.*, 2010; Riederer and Schreiber, 2001; Xiao *et al.*, 2004). Several studies have revealed genes involved in regulating the development of cuticles (Park *et al.*, 2010; Wang *et al.*, 2011; Xiao *et al.*, 2004). Reduced water loss can also be achieved by cutting down nighttime water loss. Nighttime stomatal opening has been reported in C3 and C4 species (Caird *et al.*, 2007). This source of water loss is not accompanied by carbon gain. Genetic variations in nighttime stomatal opening have been investigated among and within species (Christman *et al.*, 2008). In addition, some plants reduce their own water use through early leaf senescence (Khanna-Chopra *et al.*, 1999; Levy *et al.*, 1999), and shoot architecture (Poorter and Nagel, 2000).

Improvement of water uptake during drought is mainly achieved through roots (Chaves *et al.*, 2003). Some plants are capable of developing a long, dense, and deep root system that captures soil water efficiently (Kavar *et al.*, 2008; Ludlow and Muchow, 1990; Tardieu, 1996; Tardieu and Simonneau, 1998; Turner *et al.*, 2001). The genetic variations in rice roots resulted in a remarkable diversity in terms of growth patterns, architecture, and environmental adaptations, when subjected to drought conditions (Gowda *et al.*, 2011). Moreover, enhanced root water conductivity may also contribute to improvement in water uptake. A study on rice responding to water stress showed variable expression levels in the water channel

protein *RWC3* between upland rice and lowland rice. Overexpression of *RWC3* gene in lowland rice improved root osmotic hydraulic conductivity (Lian, 2004).

### **1.4.3 Tolerance strategy**

The tolerance strategy allows plants to endure water deficit through low tissue water potential (Mitra, 2001). Plants that survive under low tissue water potential evolve the ability to balance cell turgor and water loss (Mitra, 2001). These processes involve variable mechanisms, such as osmotic adjustment (Morgan, 1984), cell detoxification (Castiglioni *et al.*, 2008; Garg *et al.*, 2002) and cell protection (Sunkar *et al.*, 2003). Many of the evergreen shrubs and trees in arid or semi-arid regions have high solute concentrations in living cells, allowing them to survive in such extreme conditions with reduced photosynthesis and stomatal conductance (Faria *et al.*, 1998). The other example is the partial dormancy of the evergreen *Retama raetam*, which allows its survival in the dry season (Mittler *et al.*, 2001). The endogenous levels of photosynthesis genes of *Retama raetam* can be repressed during the dry season and re-synthesized within 6 to 24 hours. The same phenomenon was also found in the angiosperm "resurrection plants" and in some ferns, as well as non-vascular plants, algae and lichens (Chaves *et al.*, 2003). The mutual changes from the phase of growth to the phase of dormancy may be caused by rapid changes of messenger RNA (mRNA) (Ingram and Bartels, 1996).

## **1.5 Strategies to save water**

### **1.5.1 Technical strategies**

Agriculture consumes more than two-thirds of the earth's fresh water for the production of food (Gleick and Serageldin, 2014). It is estimated that producing 1 kg wheat requires 900 kg water, and generating 1 kg rice requires 1200 kg water (Pimentel *et al.*, 2004). According to the source of the water invested in agriculture, crop areas are divided into rainfed areas and irrigated areas, which in 2003 accounted for approximately 80% and 20% cropped lands, respectively (FAOSTAT2006). However, almost half the food produced comes from irrigated areas (FAOSTAT2006). In traditional agriculture, furrow irrigation is the most common way of feeding plants with water in the field, but it has been reported to be inefficient, as only 60% of the water provided is utilized by plants for growth, and the other 40% is



lost through soil evaporation or percolation deep into the soil (Bourzac, 2013). In modern years, new irrigation techniques have emerged, such as sprinkling irrigation, drip irrigation, and micro-irrigation, to minimize the water loss through soil evaporation and runoff. Among these techniques, micro-irrigation has the highest irrigation efficiency: 90% (Bourzac, 2013). Replacement of furrow irrigation by micro-irrigation would lead to a 30% reduction in water use. However, this might be overoptimistic. Providing necessary equipment to the 80% of agricultural land that is currently rainfed might be a huge task. Moreover, the operation of the system and its long-term maintenance may also be costly. Taken together, new irrigation techniques do enhance the irrigation efficiency and avoid water loss, and have therefore been applied to some high-value crops, but in the short term, it might be difficult to equip on large scales.

### **1.5.2 Plant-based strategy (high water use efficiency)**

Saving water in agriculture, given the prerequisite of maintaining yield levels, maybe achieved not only through increased irrigation efficiency, but also through enhanced WUE of crops. WUE is an attractive trait for agriculture. Studies of the WUE in plant species emerged in the mid-twentieth century when the Green Revolution occurred. The slogan "more crop per drop" was coined in recent years (Kijne *et al.*, 2003). Reducing water loss and increasing water uptake of drought avoidance strategy are associated with WUE. WUE can be defined as the ratio of a plant's net carbon assimilation rate to its stomatal conductance, or as the biomass over a certain period against the consumed water, or as the ratio of yield to input water (Morison *et al.*, 2008). WUE can be measured in a variety of ways at various spatiotemporal scales, including the gravimetric method, gas exchange measurements, and stable carbon isotope composition (Easlon *et al.*, 2014). Research on this topic has given rise to the wide consensus that the WUE of plants is capable of being enhanced under water-limited conditions, and that an increase of WUE by a factor of 1.5 to 2.5 is achievable (Medrano, 2002; Ranney *et al.*, 1991; Rizza *et al.*, 2012; Wall *et al.*, 2001).

The study of the genetic basis of WUE in several plant species has shown that there is considerable variation in WUE among their natural populations and that WUE is controlled by multiple genetic variants (Hausmann *et al.*, 2005; Juenger *et al.*, 2005; Manzaneda *et al.*, 2015; McKay *et al.*, 2008; Rebetzke *et al.*, 2008; Xu *et al.*, 2008; Xu

*et al.*, 2009). Studies on WUE in two recombination inbred populations (RILs) (Cvi X Ler and Ler X Col) have revealed six quantitative trait loci (QTL) associated with carbon isotope composition. One was identified as a MAP kinase which caused the development of larger stomata and affected the ABA inhibition of stomatal opening (Des Marais *et al.*, 2014; Hausmann *et al.*, 2005). Another study using a RILs population derived from the Arabidopsis accessions Tsu-1 and Kas-1, a pleiotropic mutation, *FRI (FRIGIDA)*, was identified as being responsible for WUE (Lovell *et al.*, 2013). Moreover, the *ERECTA* gene, affecting multiple whole-plant traits, was also found to be able to explain the variation in WUE between Arabidopsis accessions Col-0 and Ler-0 (Masle *et al.*, 2005). Some of the loci which were identified as explaining the carbon isotope composition in Arabidopsis were found to be negatively associated with seed lengths and seed production (Hausmann *et al.*, 2005). The negative association between carbon isotope composition or WUE and yield was also found in barley (López-Castañeda and Richards, 1994; Munoz *et al.*, 1998), durum wheat (Blum, 2005), tomato (Martin *et al.*, 1999). These results indicate that selection for high WUE may result in a genetic shift towards traits like reduced yield, early flowering, and small leaves (Blum, 2009). A successful case in this field was achieved in wheat by introgression into elite material of genomic regions, which conferred a high WUE with maintained carbon assimilation rates (Rebetzke *et al.*, 2002). If this example is not an exception, breeding plants combining improved WUE and maintained growth would be more practicable than expanding the water-saving techniques in the rainfed agriculture.

### **1.6 Drought-induced ABA signaling**

Ideally, plants maintain water homeostasis (Christmann *et al.*, 2013). This delicate balance can be interrupted by reduced soil water potential caused by drought. Reduced soil water potential leads to a transduction of hydraulic signal which is originated from a water tension-, turgor- or osmotic-potential-induced drop of root water potential and is perceived by hydraulic sensors (Christmann *et al.*, 2013). The relay of the initial hydraulic signal in rigid pipes is driven by the cohesion and tension properties of water. The speed of relay of hydraulic signal can be as fast as sound (Christmann *et al.*, 2013; Malone, 1993). After being recognized by unknown hydraulic sensors, the hydraulic signal is converted into the chemical signal ABA (Christmann *et al.*, 2013).

### 1.6.1 ABA synthesis

Hydraulic signals induce the endogenous levels of ABA by three mechanisms, enhanced biosynthesis (Endo *et al.*, 2008; Qin and Zeevaart, 1999), the inhibition of ABA degradation (Okamoto *et al.*, 2009), and the liberation of ABA from its conjugate, ABA glucosy ester (Xu *et al.*, 2012). Among these sources, ABA biosynthesis accounts for most of the ABA generation (Christmann *et al.*, 2013). The primary site of ABA biosynthesis has been reported to occur at the parenchyma cells of the vasculature (Endo *et al.*, 2008).

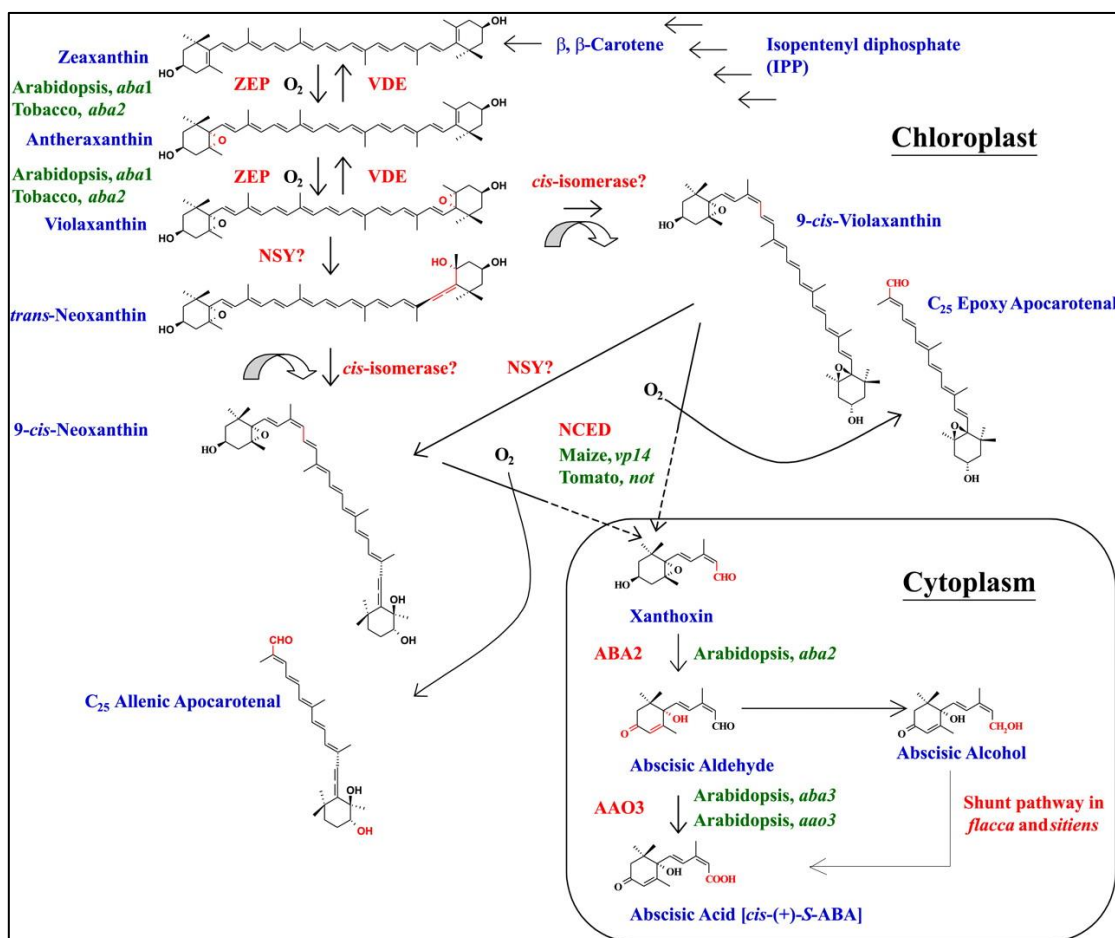


Figure 1-3 ABA biosynthesis pathway in plants. (Wasilewska *et al.*, 2008)

The ABA biosynthesis pathway has been demonstrated in different plant species (Christmann *et al.*, 2006; Finkelstein, 2013; Nambara and Marion-Poll, 2005; Schwartz *et al.*, 2003; Wasilewska *et al.*, 2008; Xiong, 2003), and is initiated by a five-carbon (C5) precursor, isopentenyl diphosphate (IPP). In *Arabidopsis thaliana*, ABA is derived by 2-C-methyl-D-erythritol-4-phosphate (MEP) pathway (Eisenreich *et al.*,

2004; Kuzuyama, 2014; Lichtenthaler, 1999). The initial steps of ABA biosynthesis are confined to the chloroplasts, where glyceraldehydes 3-phosphate and pyruvate are combined and rearranged to produce IPP. This leads to the production of phytoene and lycopene as intermediates, the latter of which is cyclized and hydroxylated to form zeaxanthin, the first oxygenated carotenoid (C40). Four distinct enzymes are possible candidates for catalyzing the conversion of zeaxanthin to the C15 intermediate xanthoxin in plastids - zeaxanthin epoxidase (ZEP) (Agrawal, 2001; Marin *et al.*, 1996), neoxanthin synthase (NSY) (North *et al.*, 2007), an unidentified epoxy carotenoid isomerase, and 9-cis-epoxycarotenoid dioxygenase (NCED) (Luchi *et al.*, 2001b; Schwartz *et al.*, 2001).

"A series of enzyme-catalyzed epoxidations and isomerizations via violaxanthin, and the final cleavage of the C40 carotenoid by a dioxygenation reaction yields the proximal ABA precursor, xanthoxin, which is then further oxidized to abscisic aldehyde and finally to ABA" (Nambara *et al.*, 2005). A variety of studies have indicated that NCED is the rate-limiting enzyme in ABA biosynthesis (Qin & Zeevaart, 1999; Thompson *et al.*, 2000; Luchi *et al.*, 2001).

Concerning the water deficit-induced ABA synthesis, three important ABA biosynthetic enzymes - NCED3, ABA2 and AAO3 - are co-localized in the vascular parenchyma cells (Endo *et al.*, 2008; Koiwai *et al.*, 2004). The expression of NCED3 is up-regulated by drought stress (Tan *et al.*, 2003) via a stress-inducible NAC TF ATAF1 that directly binds to the NCED3 promoter (Jensen *et al.*, 2008; Jensen *et al.*, 2013). Therefore, stress-induced ABA is predominately synthesized in the vascular tissue and subsequently transported into surrounding responsive cells. In Arabidopsis, tobacco, and tomato plants, the expression of ZEP/ABA1 is drought-induced in roots but not in leaves (Audran *et al.*, 1998; Thompson *et al.*, 2000), whereas the cowpea ZEP transcripts are not drought responsive at all (Luchi *et al.*, 2000). Only the SDR1/ABA2 expression appears not to be regulated by stress, but up-regulated by sugar (Cheng *et al.*, 2002). Taken together, these results strongly support that drought positively regulates the expression of components in the ABA biosynthesis pathway.

## 1.6.2 ABA signaling

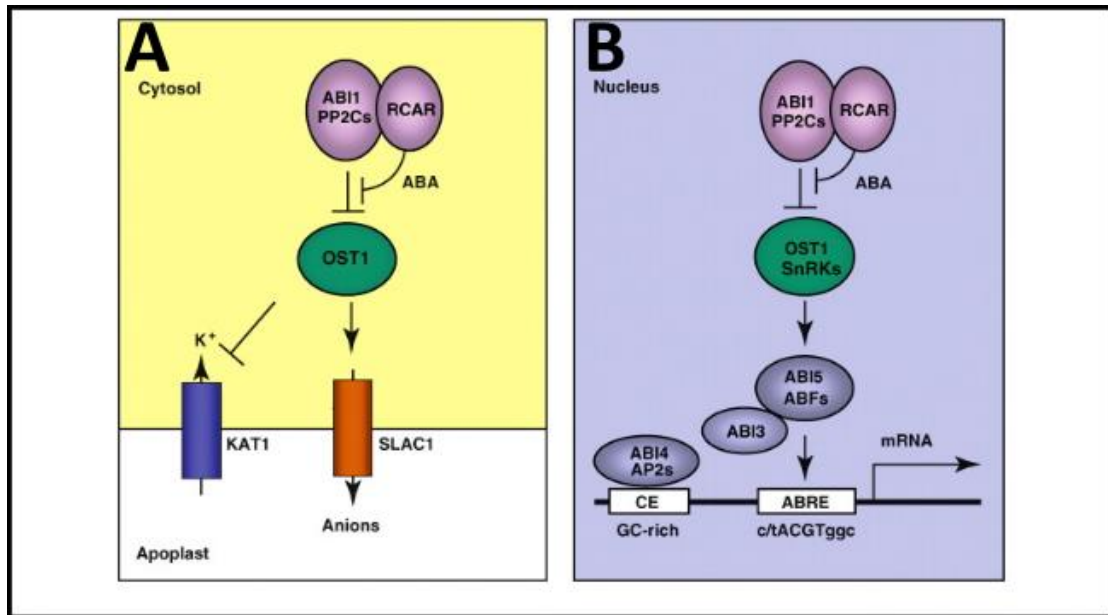


Figure 1-4 ABA core signaling to modulate stomatal movement and to initiate transcription of downstream genes. Simplified ABA signaling models shown here are according to (Raghavendra *et al.*, 2010).

To trigger ABA signaling, drought-induced ABA is transported from the site of synthesis to the bundle sheath cell apoplastic area, is diffused passively with the flow of water to sites of transpiration, and is finally transported to the guard cells (Umezawa *et al.*, 2010). Subsequently, the ABA core signaling pathway is triggered. ABA is recruited by an ABA-binding regulatory component RCAR/PYR1/PYL and an associated protein phosphatase of type 2C (PP2C) (Ma *et al.*, 2009). OPEN STOMATA 1 (OST1/SRK2E/SnRK2.6) protein kinase is subsequently activated, which results in the phosphorelay of Ost1 protein to SLAC1 ion channel and KAT1 cation channel in guard cells to trigger stomatal closure. Moreover, Ost1 and other related SnRK2 protein kinases phosphorylates transcription factors (AREBs/ABFs/ABI5/ABI4) to bind to the promoter elements (ABRE/CE) of downstream genes thereby activate their expression (Fujii *et al.*, 2007; Fujii *et al.*, 2009; Fujita *et al.*, 2009; Geiger *et al.*, 2009; Lee, S. C. *et al.*, 2009; Ma *et al.*, 2009; Park *et al.*, 2009; Raghavendra *et al.*, 2010; Sato *et al.*, 2009; Yoshida *et al.*, 2010). As a consequence, the adaption responses of plants to drought are mediated in both short term and long term ways (Raghavendra *et al.*, 2010).

### 1.6.2.1 Receptor complex

High affinity ABA binding proteins in *Arabidopsis thaliana* were identified independently by two groups (Ma *et al.*, 2009; Park *et al.*, 2009). Sean Cutler's group screened mutants using an ABA agonist, the synthetic chemical pyrabactin (Park *et al.*, 2009). The mutants insensitive to this growth regulator were cloned and the Pyrabactin Resistance 1 (PYR1) locus was identified (Park *et al.*, 2009). Further analysis revealed PYR1 and several PYR-related homologues of *Arabidopsis* capable of inhibiting Mg<sup>2+</sup>- and Mn<sup>2+</sup>-dependent serine/threonine phosphatases type 2C (PP2C) (Park *et al.*, 2009). Prototypes of PP2Cs - abscisic Acid Insensitive 1 (ABI1) and its close homologue ABI2 - were reported to be involved in the network of ABA signal transduction and be able to repress ABA responses (Park *et al.*, 2009).

In Erwin Grill's group, the Regulatory Component of ABA Receptor 1 (RCAR1), identical to PYL9, was found to interact with ABI1 and ABI2 through a yeast two hybrid screen (Ma *et al.*, 2009). Binding studies of the RCAR1 exhibited a dissociation constant of 0.7  $\mu$ M for the physiologically active ABA, (S)-ABA, using isothermal calorimetry, which indicates a strong RCAR1–ABA interaction (Ma *et al.*, 2009). By contrast, the selective and rapid inhibition of protein phosphatase activity by (S)-ABA was revealed in *in vitro* analysis of purified RCAR1 and ABI2, which displayed a dissociation constant of 0.06  $\mu$ M ABA, approximately ten-fold lower than the value for RCAR alone. This result suggests that interaction of the two proteins provides the high affinity binding site required for ABA responses (Ma *et al.*, 2009). The stereoisomers (R)-ABA and trans-ABA were more than 1000-fold less active in mediating ABI1 and ABI2 inhibition (Ma *et al.*, 2009). Taken together, RCAR1, PYR1, and several PYL proteins of *Arabidopsis* display high binding affinity to ABA and, as shown for RCAR1 and RCAR3, with stereoselectivity (Ma *et al.*, 2009).

In *Arabidopsis*, there are 14 members in the RCAR protein family which are classified into three subfamilies (Ma *et al.*, 2009; Park *et al.*, 2009; Raghavendra *et al.*, 2010). Moreover, approximately 80 PP2Cs exist in *Arabidopsis*, within which six of the nine PP2Cs in clade A, such as ABI1, ABI2, HAB1 and HAB2 have been identified to negatively regulate ABA responses (Kuhn *et al.*, 2006; Merlot *et al.*, 2001; Nishimura *et al.*, 2007; Robert *et al.*, 2006; Rubio *et al.*, 2009; Saez *et al.*, 2006; Schweighofer *et al.*, 2004; Yoshida *et al.*, 2006). There would be 80 different combinations of the

receptor complex, each of which would trigger a variety of downstream components and vary in their affinity to the hormone, thereby allowing the adjustment of ABA signaling to strongly variable ABA levels (Raghavendra *et al.*, 2010).

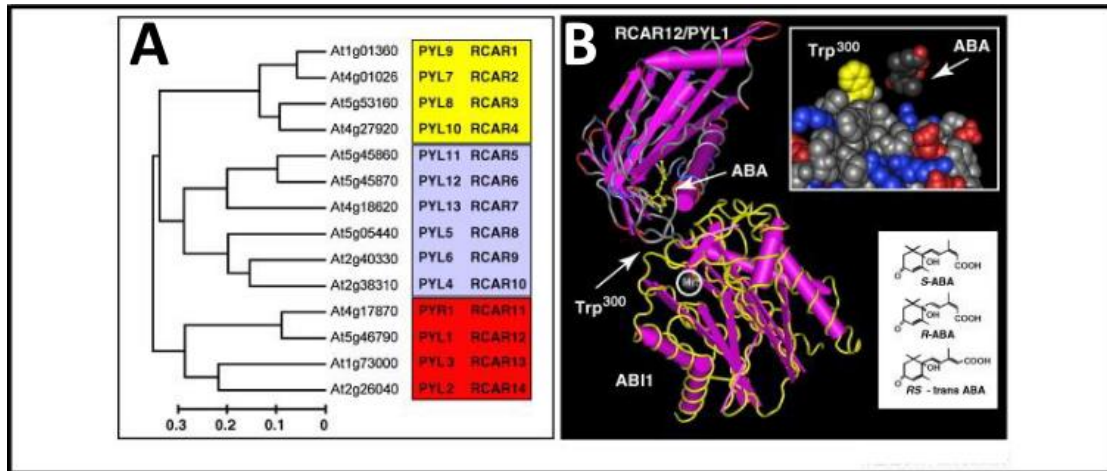


Figure 1-5 Phylogenetic tree of ABA binding proteins from Arabidopsis and ABA binding by the heteromeric RCAR12/ABI1 complex according to the crystal structure provided in (Miyazono *et al.*, 2009). Both figure shown here are from (Raghavendra *et al.*, 2010).

The mechanism whereby ABA binds to RCARs and the mechanism of the inhibition of the protein phosphatase activity of PP2Cs by RCARs have both been elucidated through X-ray diffraction studies, firstly of PYR1 (RCAR11) in a complex with ABA (Nishimura *et al.*, 2009; Santiago, Dupeux *et al.*, 2009), and secondly of trimeric complexes of ABA/ABI1/RCAR12 (PYL1) (Melcher *et al.*, 2009; Miyazono *et al.*, 2009; Yin *et al.*, 2009). The RCAR provides a cavity in the center, engaged by seven  $\beta$ -sheets and two  $\alpha$ -helical domains, which functions as a ligand binding site. Thus RCAR proteins have an open ligand binding pocket that is closed upon ABA binding by a conformational change of two  $\beta$ -sheets engulfing the ABA molecule, reminiscent of a gate/latch mechanism (Melcher *et al.*, 2009; Raghavendra *et al.*, 2010). The docking of RCAR to the catalytic site of the PP2C is induced by their conformational change caused by ABA binding, and blocks the approach of the substrate to the phosphatase. A conserved tryptophan residue of the PP2C is involved in ABA binding by contacting ABA via a bound water molecule. The spatial occupation by RCAR at the active site of the PP2C in the trimeric receptor complex reasonably explains ABA-mediated non-competitive inhibition of ABI1 and ABI2 (Ma *et al.*, 2009; Szostkiewicz *et al.*, 2010).

### 1.6.3.2 SnRK2s

SnRK2 kinases belong to a plant-specific serine/threonine kinase family, sucrose nonfermenting 1 (SNF1)-related kinases (SnRKs). That SnRK2s are involved in osmotic stress and plant development has been reported for a variety of species (Boudsocq *et al.*, 2004; Huai *et al.*, 2008; Li *et al.*, 2000; Mao *et al.*, 2010; Mikołajczyk *et al.*, 2000). There are 10 SnRK2s (SnRK2.1-10), which are classified into three subgroups (Kulik *et al.*, 2011). All SnRK2s share an N-terminal Ser/Thr kinase domain and a C-terminal regulatory domain (Domain I), which are involved in ABA-independent osmotic stress response (Belin *et al.*, 2006; Kobayashi *et al.*, 2004). Specifically, the ABA-activated kinases of SnRK2 group 3, including SnRK2.2, SnRK2.3, and SnRK2.6, contain a C-terminal ABA-specific box (Domain II) (Yoshida *et al.*, 2006).

SnRK2.6 has been identified as being responsible for stomatal movement, and is highly expressed in guard cells. Leaf temperature analysis through thermal imaging displays a cool leaf temperature in the mutant *ost1* compared with wild type and a wilted phenotype (Mustilli, 2002). Both phenotypes in the *ost1* mutant were caused by impaired stomatal closure (Mustilli, 2002; Yoshida, 2002). Two homologs, SnRK2.2 and SnRK2.3, were reported to affect the ABA response in seed germination, dormancy and seedling growth (Fujii *et al.*, 2007), which may be associated with their non-tissue specific expression. Studies on the triple mutant *snrk2.2/3/6* demonstrated its poor growth and its extreme insensitivity to ABA (Fujii *et al.*, 2009; Fujita *et al.*, 2009; Nakashima *et al.*, 2009), which implies the redundancy of SnRK2.6, SnRK2.2 and SnRK2.3 in ABA signaling during plant development and stress tolerance. Taken together, these findings indicate that SnRK2s are activated by ABA and positively regulate ABA response in various tissues.

The physical interaction of group A PP2Cs with SnRK2s in various combinations has been reported, and found to efficiently inactivate ABA-activated SnRK2s through the dephosphorylation of multiple Ser/Thr residues in the activation loop (Umezawa *et al.*, 2009). The inactivation of SnRK2s by group A PP2Cs is suppressed by the RCAR/PYR ABA receptors in response to ABA (Umezawa *et al.*, 2009). These results demonstrate that group A PP2Cs act as 'gatekeepers' of subclass III SnRK2s, unraveling an important regulatory mechanism of ABA signaling (Umezawa *et al.*, 2009).



### 1.6.3.3 Ion channel

Stomatal closure is a response modulated by ABA-activated guard cell voltage-independent slow (S)-type anion channel (SLAC1) and the voltage-dependent rapid (R)-type anion channel (QUAC1) (Vahisalu, Kollist, Wang, Nishimura, Chan, Valerio, Lamminmaki *et al.*, 2008) (Imes *et al.*, 2013; Meyer *et al.*, 2010). The activated channels induce a transient membrane depolarization followed by the efflux of Cl<sup>-</sup> and malate<sup>2-</sup> from guard cells, which decrease the cytosolic osmotic potential, in turn resulting in stomatal closure (Roelfsema *et al.*, 2004). The SLAC1 channel has been reported to be activated by OST1/SnRK2.6 (Negi *et al.*, 2008; Vahisalu, Kollist, Wang, Nishimura, Chan, Valerio, Lamminmäki *et al.*, 2008). In vitro analysis has revealed that OST1/SnRK2.6 phosphorylates the N-terminus of SLAC1 to activate the anion channel currents. In contrast, the co-expression of PP2Cs such as ABI1 and PP2CA with OST1/SnRK2.6 successfully inhibits the activation of the anion channel (Geiger *et al.*, 2009; Lee, S. C. *et al.*, 2009). ABA-dependent activation of OST1/SnRK2.6 was also shown to activate the QUAC1 channel (Imes *et al.*, 2013).

The K<sup>+</sup> influx through heteromultimeric channels, which is formed by the inward-rectifying potassium channel KAT1 and its homolog KAT2, results in stomatal opening (Kwak *et al.*, 2001; Lebaudy *et al.*, 2010; Pilot *et al.*, 2001). In vitro, OST1/SnRK2.6 phosphorylates two positions of the cytosolic C-terminus of KAT1 (Thr306 and Thr308). A further point mutation assay implied that the phosphorylation at Thr306 is responsible for the functional inhibition of KAT1 (Sato *et al.*, 2009). Therefore, the ion channel activity of KAT1 is inhibited by OST1/SnRK2.6, maintaining ABA-dependent stomatal closure.

### 1.6.3.4 Transcriptional factors

ABA-responsive element binding factors and proteins (ABFs/AREBs) and basic region/leucine zipper (bZIP)-type transcriptional regulators are key transcriptional regulators of ABA-dependent gene expression (Choi *et al.*, 2005; Finkelstein *et al.*, 2005). Both of these two types of transcriptional factors have been identified as substrates of SnRK2s in the nucleus (Fujita *et al.*, 2012). A vitro assay shows that ABF2/AREB1 is phosphorylated by SnRK2s (Fujii *et al.*, 2007; Fujii *et al.*, 2009; Fujita *et al.*, 2009; Yoshida *et al.*, 2010). Moreover, the SnRK2 kinases have been reported

to phosphorylate directly multiple Ser/Thr residues of the R-X-X-S/T sites in N-terminal conserved regions of bZIP TFs to fully activate the TFs (Furihata *et al.*, 2006; Kobayashi *et al.*, 2005). Subsequently, the multi-phosphorylated homo- or hetero-dimeric AREBs/ABFs/ABI5 (Lindemose *et al.*, 2013; Yoshida *et al.*, 2010) bind to the ABA-responsive cis-element (ABRE: ACGTGT/GC) in the promoter region of ABA-induced genes to activate the transcription (Raghavendra *et al.*, 2010).

B3 domain TF ABA INSENSITIVE 3 (ABI3) also plays a role in ABA-induced transcription, mainly through interacting with ABI5 to enhance its action (Giraudat *et al.*, 1992, McCarty *et al.*, 1991). In addition, transcription factors, such as the APETALA 2 (AP2) domain TF ABA INSENSITIVE 4 (ABI4) and MYC/MYB-type regulators, act as positive ABA-response regulators (Finkelstein *et al.*, 1998). In contrast, the homeodomain leucine zipper AtHB6 serves as a transcription factor that suppresses ABA responses through interaction with ABI1 (Himmelbach *et al.*, 2002; Valdés *et al.*, 2012).

### **1.7 Drought-induced MAPKs signaling**

When drought occurs, ABA is synthesized and plays a major role in plants' adaptations to water-limited conditions. It has been demonstrated that the ABA-dependent activation of OST1/SnRK2E/SnRK2.6 is able to activate SLAC1 and QUAC anion channels and inactivate KAT1 cation channel, thereby inducing stomatal closure. Other signaling pathways have also been implicated in ABA signal transduction. Not just ABA signaling pathway, other signaling pathways have been reported to be involved in drought stress, such as MAPK signaling pathway (Danquah *et al.*, 2015). MAPK signaling cascades minimally include an MAP3K (MAP2K kinase), an MAP2K (MAPK kinase) and an MAPK (Colcombet and Hirt, 2008). Environmental cues are firstly recognized by plasma membrane receptors, which then activate the MAP3Ks. The phosphorelay from activated MAP3Ks facilitates the activation of the MAP2Ks and subsequently the MAPKs. MAPKs then target various downstream proteins in the cytoplasm or nucleus, which include other kinases, enzymes, or transcriptional factors (Khokhlatchev *et al.*, 1998). MAP3Ks are serine or threonine kinases that phosphorylate MAP2Ks at a conserved S/T-X3-5-S/T motif, and MAP2Ks phosphorylate threonine and tyrosine residues of MAPKs at a conserved T-X-Y motif (Chang and Karin, 2001). MAPK cascades are conserved signaling modules in all

eukaryotic cells (Colcombet and Hirt, 2008). In Arabidopsis, 80 MAPKK kinases (MAPKKKs), 10 MAPK kinase (MAPKKs/MKKs) and 20 MAP kinases (MAPKs/MPKs) have been characterized (Ichimura *et al.*, 2002). The MAPK cascades have been reported to be involved in biotic responses such as pathogen responses (Cardinale *et al.*, 2002; del Pozo *et al.*, 2004; Frye *et al.*, 2001), and abiotic responses such as drought stress (Danquah *et al.*, 2015), salt stress (Xing *et al.*, 2007), cold stress (Teige *et al.*, 2004), and ozone stress (Ahlfors *et al.*, 2004). Moreover, MAPK cascades also play roles in plant development (Wang *et al.*, 2007).

The first indication of the involvement of MAPK cascades in ABA-induced responses was the fact that an MAP2K inhibitor, PD98059, was able to decrease ABA-induced stomatal closure (Burnett *et al.*, 2000). A more direct evidence is that in Arabidopsis MPK3 antisense plants, the ABA-promoted inhibition of stomatal opening partially failed, which indicates that MPK3 is involved in ABA-dependent stomatal closure (Gudesblat *et al.*, 2007). A recent study showed MPK9 and MPK12 were highly expressed in guard cells and were able to mediate ABA-induced guard cell closure (Jammes *et al.*, 2009). Some MAPKs, such as MPK1 and MPK2, showed increased activity after ABA treatment (Hwa and Yang, 2008; Ortiz-Masia *et al.*, 2007; Umezawa *et al.*, 2013). (Xing *et al.*, 2008) have demonstrated that the ABA-dependent MKK1-mediated activation of MPK6 regulates CATALASE1 (CAT1) expression in ROS homeostasis. A more systematic study on ABA-induced MAPKs was performed by (Danquah *et al.*, 2015). Their results indicate that ABA induces the activation of two functionally redundant MAP3Ks, MAP3K17 and MAP3K18, and both MAP3Ks further activate an MAP2K - MKK3 which subsequently stimulates the activity of the four C group MAPKs: MPK1, MPK2, MPK7, and MPK14.

## 1.8 Nighttime stomatal opening

Plants lose water mainly through their stomata, which is driven by leaf-to-air vapor pressure difference (VPD) (Caird *et al.*, 2007). VPD is defined as the difference between the vapor pressure in the air at a given temperature and the saturation vapor pressure in the air at the same temperature (Abtew and Melesse, 2013). The vapor pressure levels in the substomatal cavity of the leaf is assumed to be close to saturation (Farquhar and Raschke, 1978), which causes an inevitable water efflux from the substomatal cavity into the atmosphere in cases of stomatal opening,

according to Fick's diffusion law. In the daytime, light-induced stomatal opening (Roelfsema and Hedrich, 2005) leads to substantial water loss in plants, as well as carbon assimilation (Christman *et al.*, 2008). In darkness, the stomata are closed, but incomplete stomatal closure at night has been reported in both C3 and C4 plants (Caird *et al.*, 2007; Dawson *et al.*, 2007; Marks and Lechowicz, 2007; Musselman and Minnick, 2000), and shows considerable variation among species (Caird *et al.*, 2007; Dawson *et al.*, 2007). Genetic variations in nighttime stomatal opening have been investigated in different accessions of *Arabidopsis*, and the tested accessions displayed up to a 3-fold difference (Christman *et al.*, 2008). Three near isogenic lines (NILs) derived from either Ler-0 and Cvi-0 or from Tsu-1 and Kas-1, which show divergent compositions of stable carbon isotopes ( $\delta^{13}\text{C}$ ) or daytime stomatal conductance, exhibited significant differences in nighttime stomatal conductance when compared with their parental lines (Christman *et al.*, 2008). The results of studies of the NILs revealed one QTL responsible for nighttime stomatal opening (Christman *et al.*, 2008).

Stomatal conductance is not constant at night. Spontaneous, gradual increases in nighttime stomatal conductance during predawn have been observed in many species under both field conditions and controlled growth conditions (Schwabe, 1952). In the *Arabidopsis* accession Columbia, a 38% increase of nighttime stomatal conductance, from  $0.117 \text{ mmol m}^{-2} \text{ s}^{-1}$  to  $0.161 \text{ mmol m}^{-2} \text{ s}^{-1}$ , has been reported (Lasceve *et al.*, 1997). Further research found that the predawn increase of nighttime stomatal conductance did not occur in *Arabidopsis* mutants with disordered circadian rhythms and starch deficiencies (Dodd *et al.*, 2004; Dodd *et al.*, 2005). These results imply that the nighttime stomatal opening might be associated with circadian rhythms and starch metabolism.

Nighttime stomatal conductance can also be modulated by variable cues in the environment (Caird *et al.*, 2007), such as salt stress, drought, high leaf-to-air VPD, and the availability of nutrition (Cavender-Bares *et al.*, 2007; Daley and Phillips, 2006; Dawson *et al.*, 2007; Donovan *et al.*, 1999; Hubbart *et al.*, 2007; Rawson and Clarke, 1988). Unirrigated desert shrubs had lower nighttime stomatal conductance than irrigated ones in field conditions (Donovan *et al.*, 2003). The same conclusion was also obtained using wheat in a greenhouse experiment (Rawson and Clarke, 1988).

Seasonal changes in nighttime stomatal conductance were also reported and were regarded to be associated with seasonal changes in the soil water availability (Donovan *et al.*, 2003; Grulke *et al.*, 2004, James *et al.*, 2006). For example, nighttime stomatal conductance of *Chrysothamnus nauseosus* was reduced under water deficit conditions at the end of growing season (Grulke *et al.*, 2004).

The implications of these studies of nighttime stomatal opening have been drawn by (Caird *et al.*, 2007). Nighttime stomatal opening may lead to a disequilibrium between predawn leaf water potential and soil water potential (Donovan *et al.*, 1999; Donovan *et al.*, 2003), which makes problematic the use of predawn leaf water potential as a way of inferring soil water potential (Caird *et al.*, 2007; Hubbart *et al.*, 2007). Nighttime transpiration may affect hydraulic redistribution (Richards and Caldwell, 1987), which occurs in soil with heterogeneous water distribution. Some roots tend to absorb water from the wet part of the soil while some roots lose their water to the dry part of the soil. Nighttime transpiration may prevent or reduce water loss from roots to the dry areas of soil, due to the water potential gradient formed by the soil-plant-atmosphere continuum (Caird *et al.*, 2007). Nighttime stomatal opening may also be beneficial to plants that grow under drought conditions (Caird *et al.*, 2007). Having more open stomata at night allows plants to have a higher potential for early morning carbon assimilation, when temperatures and VPD are low (Caird *et al.*, 2007). Nighttime stomatal conductance may also influence the isotope signature of respiratory CO<sub>2</sub> (Barbour *et al.*, 2005) and O<sup>18</sup> composition in leaves (Caird *et al.*, 2007). Nighttime stomatal opening may facilitate the uptake of nutrients at night and the remobilization of nutrients (Meinzer *et al.*, 1988). These integrated effects of nighttime water use, nighttime nutrition uptake, and remobilization imply the indirect effect of nighttime stomatal opening on plant growth (Caird *et al.*, 2007). Finally, nighttime stomatal conductance may also be associated with air pollution uptake (Grulke *et al.*, 2004; Takahashi *et al.*, 2005).

## **1.9 Stomatal oscillation**

The phenomenon of autonomic, cyclic opening, and closing movements of stomata has been described in the past as either cyclic variation in stomatal aperture or stomatal oscillation (Barrs, 1971; Cowan, 1972). This phenomenon is widespread and has been documented in different species (Brun, 1961; Apel, 1966; Apel, 1967; Barrs

and Klepper, 1968; Bertsch and Domes, 1969; Brown and Rosenberg, 1970; Cox, 1968; Ehrler *et al.*, 1965; Hunt *et al.*, 1968; Kanemasu and Tanner, 1969; Kriedemann, 1968; Nunes *et al.*, 1968; Parkhurst and Gates, 1966). The induction of stomatal oscillation requires a pulse or stepwise changes in a plant's environment (Barrs and Klepper, 1968). Such changes could be in any factor that affects stomatal aperture (Apel, 1967; Barrs, 1971; Hopmans, 1969). The manipulation of light conditions in a plant's environment was able to trigger stomatal oscillation, which can be interrupted by a dark period (Apel, 1967; Bertsch and Domes, 1969; Ehrler *et al.*, 1965). Moreover, changes in light quality were also able to induce stomatal oscillation (Apel, 1967). Other factors, such as atmospheric CO<sub>2</sub>, temperature, humidity, soil water content, and soil temperature have also been reported to be able to elicit stomatal oscillation.

The oscillation of stomata can be observed directly using a microscope (Kuiper, 1961; Went, 1944) or leaf surface impressions (Apel, 1966; Hopmans, 1969), and indirectly by measuring related plant properties, including stomatal conductance, net carbon assimilation rate, transpiration rate, leaf water status, and stem parameter (Barrs, 1971).

Stomatal oscillation can be either damped or sustained after its initial occurrence (Barrs and Klepper, 1968). The period of oscillations in most of the species varies from 10 to 50 minutes (Barrs, 1971; Barrs and Klepper, 1968; Caird *et al.*, 2007; Cardon *et al.*, 1994; Farquhar and Cowan, 1974; Teoh and Palmer, 1971). The amplitude of oscillations is difficult to assess, especially for damped oscillations (Barrs and Klepper, 1968). Moreover, the amplitude can be less variable in some species and more variable in others. For example, the amplitude of oscillation in sunflowers (Hunt *et al.*, 1968) and sugar beets (Brown and Rosenberg, 1970) exhibited little variation, from 1.0 to 1.5 sec/cm (leaf diffusivity), whereas more than ten-fold variations, from 3.5 to 49 sec/cm (leaf diffusivity), have been reported in beans (Ehrler *et al.*, 1965). The variability of stomatal oscillation may be the consequence of the interaction between species and environmental conditions (Barrs, 1971).

Physiological and model studies explain that stomatal oscillation is the result of

positive feedback responses of stomatal apertures to changes in ambient conditions, such as light and temperature, and negative feedback responses to the variations of plant water potential (Cowan, 1972; Raschke, 1970). Moreover, Raschke (1970) has suggested a third feedback loop in stomatal oscillation, which involves the response of stomatal aperture to the concentration of CO<sub>2</sub> in intercellular spaces, possibly due to the role of CO<sub>2</sub> in controlling the generation and degradation of osmotica in guard cells. For example, after a plant experiences darkness for a certain period of time, illumination is given. The sudden increase in light intensity leads to a fast response of stomatal opening, which in turn increases the plant's transpiration. Water loss, due to either strong transpiration or less water uptake, results in a decrease in leaf water content or water potential, and therefore induces stomatal closure. At this moment, oscillation begins. To maintain the oscillation, two prerequisites are needed, as proposed by Barrs and Klepper (1968). The first is a time lag between the development of maximum water stress (the lowest leaf water potential) and maximum transpiration rate. Concurrent measurements of transpiration rate and leaf water potential showed that maximum water stress was reached about 10 minutes after maximum transpiration rate (Barrs and Klepper, 1968). The second prerequisite is the unknown mechanisms that induce water stress under well-watered conditions. Skidmore and Stone have pointed out that the occurrence of water stress may be caused by appreciable resistances to water flow within the plant, resulting in the rate of water loss exceeding the rate of water uptake (Skidmore and Stone, 1964). Stomatal oscillation is a response of plants adjusting their water relations in a changing environment. However, detailed studies on the implications of this phenomenon are rare.

### **1.10 The aim of this work**

Plants are sessile organisms that cannot escape from unfavorable environmental conditions. Instead, they evolve sophisticated strategies to adapt to their living habitats, such as drought escape, drought avoidance, and drought tolerance. Among these, drought avoidance is most compatible with natural drought scenarios. The reduction in water loss and increase in water uptake of the drought avoidance strategy are associated with WUE, which is the most interesting trait to agriculture. Generating plants with enhanced WUE and understanding the mechanisms hidden behind it would help to solve food production problems.

The aims of this work include: (1) establishing a progressive drought system to simulate a rain-drought scenario for Arabidopsis plants in the field by slow, progressive soil drying. (2) Establishing a deficit irrigation system to simulate a repeated rain-drought scenario for Arabidopsis plants in nature, by repeated watering to maintain a certain soil water content. (3) Evaluating transgenic plants overexpressing ABA receptors to identify the RCARs that confer high WUE, by analyzing leaf surface temperatures, leaf growth, above-ground dry biomass, and WUE derived from gravimetric methods and carbon isotope discrimination. (4) Analyzing the mechanisms of enhanced WUE in plants. (5) Searching for natural variation genes modulating drought-adapted responses and WUE in Arabidopsis. (6) Natural variation studies on occasionally observed phenomena of stomata - nighttime stomatal opening and stomatal oscillation.



## 2. Materials and methods

### 2.1 Material

#### 2.1.1 Chemicals

General chemicals used in this work were obtained from Sigma-Aldrich ([www.sigmaaldrich.com](http://www.sigmaaldrich.com), Munich, Germany), J. T. Baker ([www.avantomaterials.com](http://www.avantomaterials.com), Deventer, Holland), and Roth (<https://www.carlroth.com/de>, Karlsruhe, Germany). (S)-ABA was purchased from CHEMOS ([www.chemos.de](http://www.chemos.de), Regenstauf, Germany). Soda Chargers from iSi GmbH (<http://www.isi.com>, Austria). Humidifying granules was purchased from Pall Schumacher GmbH ([www.pall.com](http://www.pall.com), Crailsheim, Germany). Primers used in this study were synthesized by Eurofins MWG Operon (<https://www.eurofinsgenomics.com>, Ebersberg, Germany). The DNA ladders such as 1 kb, 100 bp, and  $\lambda$ HindIII DNA ladders were applied by Thermo scientific (<http://www.thermofisher.com/de/de/home.html>, Thermo scientific GmbH, Munich). The molecular biology enzymes, including restriction enzymes, T4-ligase, alkaline phosphatase, GoTaq-polymerase, Phusion-HiFi polymerase, and so on) were obtained from Thermo scientific or New England Biolabs ([www.neb-online.de/en/](http://www.neb-online.de/en/), NEB GmbH, Frankfurt a. M).

#### 2.1.2 Equipment

Table 2-1 Types of equipment used in this study.

Equipment	Model	Company
Centrifuge	Avanti J-25	Beckman Coulter
Electrophoresis Power Supply	EPS 200/EPS 3500 XL	Pharmacia Biotech
Lab Balance	Handy	Satorius Analytic
Laboratory Incubator	ED53	WTC Binder
Magnetic Stirrer	Stuart	Bibby
Micro-centrifuge	5415D	Eppendorf
PCR Cycler	T-Gradient	Biometra
Pipetman	classic	Gilson
Thermomixer	Comfort	Eppendorf
Vortex	MS1	IKA
Sterile Bench	Laminar Flow Workstation	Microflow
plant growth cabinet	E15	Conviron
Thermo Camera	IR-TCM 384	InfraTec
pF Meter		UGT
Tissuelyser II	Tissuelyser II	QIAGEN
Gas exchange system	GFS-3000	Heinz Walz
Gas exchange system	LI-6400	Li-cor

## Materials and Methods

PAM-Fluorometer Growth cabinet	3055-FL E15	Heinz Walz Convicon
-----------------------------------	----------------	------------------------

### 2.1.3 Bacteria strains

Table 2-2 Escherichia coli strains.

Strain	Genotype	Resistance	Company
DH5 $\alpha$	F $^-$ $\Phi$ 80 <i>lacZ</i> $\Delta$ M15 $\Delta$ ( <i>lacZYA-argF</i> ) U169 <i>recA1 endA1 hsdR17</i> ( <i>rK</i> $^-$ , <i>mK</i> $^+$ ) <i>phoA supE44</i> $\lambda^-$ <i>thi-1 gyrA96 relA1</i>	no	Invitrogen
XL1-blue	<i>recA1 endA1 gyrA96 thi-1</i> <i>hsdR17 supE44 relA1 lac</i> [F' <i>proAB lacIq Z</i> $\Delta$ M15 Tn10 (Tetr )]	Tetracycline	Invitrogen

Prepared competent cells according to the method described by (Sambrook and Russell, 2001). *E.coli* strains were cultured either on solid LB medium (invert the plates during incubation) or in liquid LB medium (with shaking at 200 rpm) with proper antibiotics at 37 °C for 12-16 hours.

Table 2-3 Agrobacterium tumefaciens strain.

Strain	Genotype	Resistance	Company
C58pGV3101	Ti-Plasmid: Ppmp90 (Koncz and Schell, 1986)	Rifampicin and Gentamycin	Csaba Koncz (MPI Cologne)

The *Agrobacterium tumefaciens* strain C58pGV3101 was used for plant transformation through inflorescence dip (Harrison *et al.*, 2006). *Agrobacterium* strain was grown either on solid LB medium (invert the plates during incubation) or in liquid LB medium (with shaking at 200rpm) with proper antibiotics at 30°C for 2 days.

<b>LB (Luria-Bertani) medium:</b>	NaCl	10 g/L
	Peptone	10 g/L
	Yeast extract	5 g/L
	Agar (for plates)	18 g/L
	Autoclaved, pH 7.0	

After the medium was cooled down to 60 °C, antibiotics were applied.

Ampicillin: 100 mg/L (stock solution 100 mg/mL in *milli-Q* H<sub>2</sub>O).

Kanamycin: 50 mg/L (stock solution 50 mg/mL in *milli-Q* H<sub>2</sub>O).

Rifampicillin: 50 mg/L (stock solution 50 mg/mL in *milli-Q* H<sub>2</sub>O).

## 2.1.4 Plant materials

### Arabidopsis accessions

Table 2-4 Collections of ecotypes of *Arabidopsis thaliana*. Ten ecotypes of *Arabidopsis thaliana* grown in different habitats distributed in different countries are shown. "-" means no information available for the habitats. The information of habitats and locations of these accessions are obtained from the database of either Salk 1001 genome or the Web service VNAT. Ten ecotypes of *Arabidopsis thaliana* are listed in the Table 2-4. Arabidopsis accession Cvi-0 was obtained as a gift from Prof. Sonnewald's lab and the rests of accessions were ordered from NASC (Nottingham *Arabidopsis* Stock Center).

Accession	habitat	Country
Col-0	-	Gorzpw, Wielkopolski, Poland
Cvi-0	Rocky wall with moss	Cape Verdi Islands
Ler-0	-	Gorzpw, Wielkopolski, Poland
Mr-0	-	Monte/Tosso, Italy
Mt-0	-	Martuba/Cyrenaika, Libya
Rld-1		Rschew, Russia
Sorbo	mountains	Sorbo, Tadjikistan
Tu-0	-	Turin, Italy
Van-0	Field border	Vancouver, Canada
Ws-0	-	Wassilewskija, Russia

### Col-0 and Cvi-0 hybrids

F1 hybrids were generated by intercrossing accessions Col-0 (female parent) and Cvi-0 (male parent). Anthers of mature flower from Cvi-0 plants were tapped on well-developed, non-pollinated stigmata from Col-0 plants. The Col-0 plants with pollinated stigmata were allowed to grow for approximately three weeks to generate the F1 hybrid seeds.

### F2 generations

The F1 hybrids plants derived from Col-0 and Cvi-0 were self-crossed and let them

grow for two to three months for obtaining F2 seeds.

### **Recombinant inbred lines**

Twenty RILs used to search for the QTL responsible for "cool" leaf temperature phenotype were ordered from Versailles Arabidopsis Stock Center. Generation of RILs is described in (Simon *et al.*, 2008).

### **Transgenic *Arabidopsis thaliana***

Transgenic lines with ectopic expression of ABA binding regulatory component of ABA receptors (RCAR1-14) were established by transferring an expression cassette for RCARs under control of the *cauliflower mosaic virus* 35S promoter into Arabidopsis wild type Columbia (Col-0), and selecting for homozygous lines as carried out for RCAR1 (Ma *et al.*, 2009). All the RCAR overexpressors (RCAR1-14) were provided by Stefanie V. Tischer (2016).

Table 2-5 Candidate genes which were cloned transformed into wild type Cvi-0 plants. Gene IDs, names are shown in the table.

<b>Gene</b>	<b>Other name</b>
AT2G45910	U-box ubiquitin
AT2G46070	MPK12
AT2G46080	BYPASS
AT2G46090	Lcbk2
AT2G46140	LEA1
AT2G46150	LEA2
AT2G46250	Myosin
AT2G46280	TRIP-1
AT2G46310	CRF5

Transgenic lines used to identify the "cool" leaf temperature genes in wild type Cvi-0 plants background were generated by first cloning ten Col-0 genes with their endogenous promoters (Table 2-5) into pBI121 vector and transforming these constructs into wild type Cvi-0 plants through floral dip, and selecting for homozygous lines as carried out for RCAR1 (Ma *et al.*, 2009).

### **Mutants of *Arabidopsis thaliana***

*Erecta* mutant *er2*, farnesyltransferase knockout mutant *era1-2* with Columbia background used as additional controls in gas exchange analysis. Knockout mutants of MPK12 (SALK074849, SALK075365, and GK103D08) served in identifying its

function in controlling the leaf temperature, WUE, nighttime stomatal conductance, and stomatal oscillation.

### **Grafts of *Arabidopsis thaliana***

The grafts of *Arabidopsis* wild type (Col) and RCAR- overexpressing line (RCAR10-4) were generated using 5-day-old seedlings according to a micrografting technique (Turnbull *et al.*, 2002). Specifically, seeds were positioned close to the channel generated by removing two strips of agar from a Murashige and Skoog (MS) plate. After incubation at 4 °C for 2 days, the seeds were incubated at 22 °C for 3 days under continuous illumination and at 50  $\mu\text{mol m}^{-2} \text{s}^{-1}$ . Afterward, they were allowed to grow another 2 days with dim light (10  $\mu\text{mol m}^{-2} \text{s}^{-1}$ ) at 22 °C. At this point, the seedlings were cut at the position of hypocotyls with a sterile razor on a sterile black nitrocellulose membrane under a dissecting microscope, and shoots and roots of the donors lines were aligned together. The grafts displaying perfect alignment were then first incubated one week at weak light (10  $\mu\text{mol m}^{-2} \text{s}^{-1}$ ) and at 22 °C and afterward, one week under short day conditions (8 hours light/16 hours dark) at a photon flux density of 150  $\mu\text{mol m}^{-2} \text{s}^{-1}$  and at 22 °C in the daytime and 17 °C at night. Subsequently, the successful grafts were transferred in a new plate and incubated one week. The grafts were then ready to use for other experiments. The combinations of grafts in this study were Col-Col, Col-RCAR10, RCAR10-Col, and RCAR10-RCAR10 (shoot-root).

## **2.1.5 Vector and primers**

### **Vectors for cloning**

pBI121Ascl vector was used for generating constructs with desired genes. The host organism for this vector is C58pGV3101. The selection marker for this vector is kanamycin. Ascl in the vector is the cloning site.

### **Primers for identifying genes responsible for a "cool" leaf temperature trait**

Primers for identifying genes responsible for a "cool" leaf temperature trait between *Arabidopsis* accessions Col-0 and Cvi-0, primers for identifying homozygous knockout lines and primers for generating transgenic plants were displayed in the Appendix (Table 5-1, Table 5-2, Table 5-3 and Table 5-4).

## 2.2 Methods

### 2.2.1 Seed sterilization and seedling growth conditions

*Arabidopsis thaliana* seeds were added with 1 mL of 80% ethanol containing 0.1% (v/v) Triton X-100 and incubated and shaken constantly for 20 minutes at 1000 rpm. After the supernatant was removed, the seeds were washed with 1 mL of 3% sodium hypochlorite for three minutes. Subsequently, the seeds were washed five times with sterile *milli-Q* H<sub>2</sub>O to remove residual chemical agents. Finally, the seeds were cultivated in Petri dishes containing MS medium, supplemented with 10 g/L sucrose (or 5 g/L sucrose) and 0.9% agar as described in (Christmann *et al.*, 2005). The plates were kept in a 4 °C cold room for 2 days to improve germination; afterward the plates were kept in the culture room at 22 °C under continuous illumination (60  $\mu\text{mol m}^{-2} \text{s}^{-1}$ ) until the seedlings were ready for use in the experiments.

### 2.2.2 Plant growth conditions

The seedlings were grown in 1/2 MS medium for 7 days and transferred to the soil (Classic Profi Substrate Einheitserde Werkverband). All plants other than those grown under specific conditions were grown under the conditions described in this section.

The plants in pots with volumes of either 200 mL or 600 mL were arranged randomly in trays. Domes were placed on the trays for seven days to maintain proper humidity for the transplanted plantlets. After one week of growth, the domes were removed, and the plantlets were grown under a short-day condition with an 8-hour light and 16-hour dark photoperiod, at photon flux density of 150  $\mu\text{mol m}^{-2} \text{s}^{-1}$ . The temperature and relative humidity of the plants' growth cabinet (Convicon E15, Convicon, Winnipeg, Canada) stabilized at 22°C and 50% in the daytime, and 17°C and 60% at night. Water was administrated twice a week.

### 2.2.3 Progressive drought

#### Soil preparation and water status evaluation

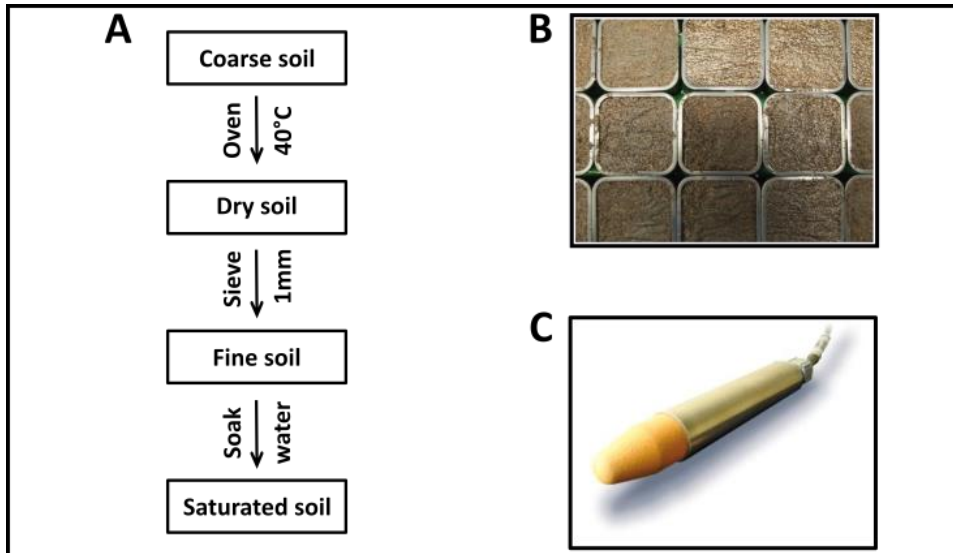


Figure 2-1 Soil preparation and evaluation of water status. A) The soil preparation scheme used in the progressive drought experiment. The original coarse soil was used as a source of cultivation substrate and saturated soil B) was obtained and followed by a drying and sieving processes. C) A pF-meter was used to measure water potential in soil.

The coarse soil was dried in the oven and sieved to obtain the fine soil that was used to prepare the soil saturated with water (Fig. 2-1A and B). The density of the soil used in this study was  $0.17 \text{ g cm}^{-3}$ . Therefore, 33.4 g of dried, fine soil were loaded in 200 mL pots or 100.2 g of soil were loaded for 600 mL pots (Figure 2-1B). All the pots with the same amount of soil were then saturated in a large water tank for 2 to 3 days. After saturation, the soil water content (SWC) of each pot was determined to reach the field capacity. To evaluate the soil water availability of the plants, a gravimetric method and a pF-meter (Fig.2-1C) were used to obtain readouts on SWC and soil water potential (SWP).

It is impractical to use a pF-meter to measure SWP when an experiment is ongoing because of the interruption of plant growth, but SWC is easy to be determined by weighing pots and this method does not disturb plants. A calibration curve of SWC against SWP was determined and was utilized to convert SWC to SWP. The calibration curve follows a power function relationship (Figure 2-2A). 66% SWC has about -0.03 bar SWP. Decreasing SWC led to a reduced SWP.

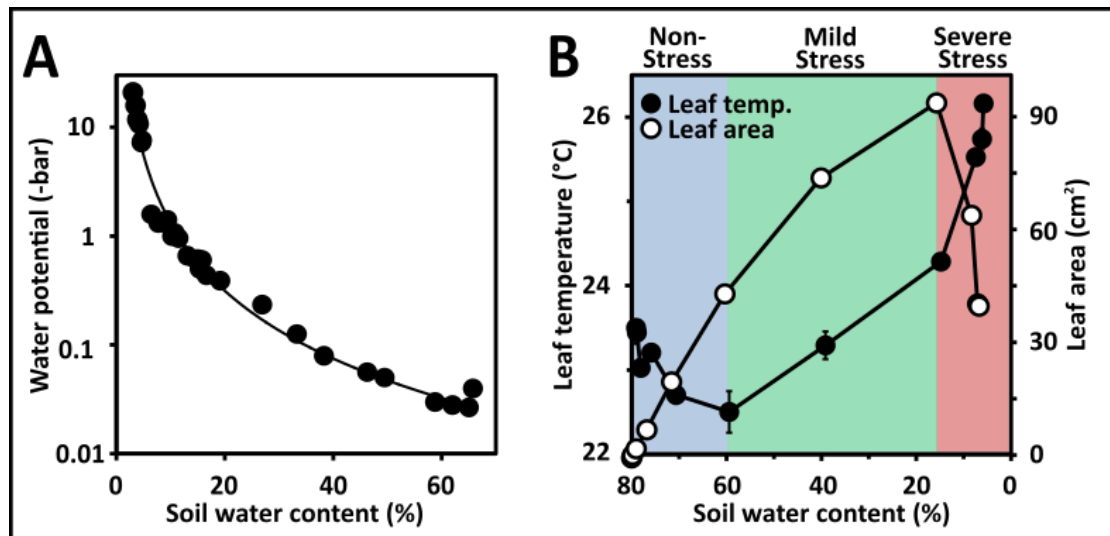


Figure 2-2 The calibration curve of the soil water content and soil water potential. A) Calibration curve of soil water content (SWC) against soil water potential (SWP). SWP was measured by pF-meter and SWC was determined by the gravimetric method. B) Classification of the severity of drought throughout progressive drought was based on the leaf temperature (filled circles) and leaf area (open circles) results of *Arabidopsis* wild type Columbia plants. Progressive drought was classified into non-stress (well-watered; SWC > 60% or SWP > -0.03 bar; blue box), mild stress (mild drought; 15% < SWC < 60% or -0.5 bar < SWP < -0.03 bar; green box) and severe stress (severe drought; SWC < 15% or SWP < -0.5 bar; red box) phases. A) Single measurement. B) n=4 biological replicates, mean  $\pm$  SEM.

### Progressive drought

Two phases are included in a progressive drought experiment: a preparation phase and a progressive drought phase. The preparation phase included germination of seeds, seedling growth and covering the pots with Parafilms. The progressive drought phase included repeated measurements of pot weight, leaf area, and leaf temperature. Seeds were sown first on 1/2 MS medium and incubated at 4 °C for 2 days to let the seeds germinate well. Afterward, the seeds were incubated at 22 °C with continuous illumination ( $60 \mu\text{mol m}^{-2} \text{s}^{-1}$ ) for 7 days. At this moment, two cotyledons emerged, and the seedlings were transferred into the fine soil with saturated water in 200 mL pots (SWC  $\approx$  77%; SWP  $\approx$  -0.02 bar). The plantlets were then allowed to grow under short day conditions with an 8-hour light and 16-hour dark photoperiod and at a photon flux density of  $150 \mu\text{mol m}^{-2} \text{s}^{-1}$ . The temperature and relative humidity in the plants' growth cabinet stabilized at 22°C and 50% in the daytime, and 17°C and 60% at night. To avoid stressing the seedlings, each pot was covered with a transparent plastic wrap to maintain high humidity. The wraps were removed after 7 days of growth of the plantlets. At this time, the plantlets had four to five fully expanded leaves (two cotyledons and two to three true leaves). Subsequently, the surface of the soil was covered with two pieces of Parafilm (5 cm x



10 cm for each piece) to prevent soil water evaporation and the holes at the bottom of the pots were also sealed with adhesive tape. In order to ensure that each pot had a similar soil water status at the onset of the progressive drought, a certain amount of water was injected into the soil using a syringe. At this point, the progressive drought was started, and no water was administered to the soil. In this experimental setup, the progressive drought lasted two months, during which the weight of the pots was recorded and, optical photos and thermal pictures were taken in 5-day intervals. After day 58 of progressive drought, the plant shoots were harvested to determine the dry biomass.

In addition, the progressive drought was classified into well-watered phase (SWC > 60% or SWP > -0.03 bar), mild drought phase (15% < SWC < 60% or -0.5 bar < SWP < -0.03 bar) and severe drought phase (SWC < 15% or SWP < -0.5 bar) (Fig. 2-2A and B). 60% SWC or -0.03 bar was used as a boundary to classify the well-water phase and the mild drought phase because the leaf temperature of plants of *Arabidopsis* wild type Columbia began to increase (Fig. 2-2A and B). The determination of 15% SWC or -0.5 bar as the boundary between the mild drought phase and the severe drought phase was due to that the leaf area of plants began to wilt (Fig. 2-2A and B).

### **Progressive drought under variable ambient temperatures**

The progressive drought experiments were also performed at different ambient temperatures in growth chambers. The preparation phase was the same as in the progressive drought at 22 °C. In the progressive drought phase, the ambient temperatures were set to 17 °C, 27 °C and 32 °C in the daytime; the temperatures at night were 5°C less than the corresponding daytime temperatures. All plants were grown under short day conditions (8 hours light / 16 hours dark photoperiod) at a photon flux density of 150  $\mu\text{mol m}^{-2} \text{s}^{-1}$  and 50% relative humidity in the daytime and 60% relative humidity at night. 18-day-old plantlets were subjected to progressive drought for 70 days at 17 °C, 50 days at 27 °C, and 40 days at 32 °C. Using these experimental setups, the weight of the pots was recorded and optical photos and thermal pictures were taken in 5-day intervals. At the end of each progressive drought experiments, the shoot parts of the plants were harvested to determine the dry biomass.

The progressive drought experiment using Col-0, RCAR10-4 and their grafts were performed under short day conditions with an 8 hours light and 16 hours dark photoperiod and at a photon flux density of  $150 \mu\text{mol m}^{-2} \text{s}^{-1}$ . The temperature and relative humidity in the plants' growth cabinet stabilized at  $22^\circ\text{C}$  and 50% in the daytime, and  $17^\circ\text{C}$  and 60% at night. 28-day-old plants were transferred into the soil saturated with water and covered with Parafilms. In this experimental setup, the progressive drought lasted ten weeks. Thermograms were taken two weeks after the onset of the progressive drought. After the 70th day of progressive drought, plant shoots were harvested to determine the dry biomass.

The progressive drought experiment performed to assess the response of Arabidopsis accessions RLD-0, Ler-0, Col-0, and Cvi-0 to progressive drought differed from the progressive drought experiments shown above. In this experiment, pots with a volume of  $600 \text{ cm}^3$  volume were used, and 100.2 g of dry soil were loaded into each pot. No water was administered after the soil was saturated with water. Seven-day-old seedlings were transferred into pots and grew under domes for seven days. Subsequently, the domes were removed and all plantlets were allowed to grow for another four days. At this point, the pots were covered, and the progressive drought was started. Around 220 g of water were present in the soil in each pot (37% SWC) at the onset of this progressive drought experiment. All plants were grown under short day conditions (8 hours light / 16 hours dark photoperiod) at a photon flux density of  $150 \mu\text{mol m}^{-2} \text{s}^{-1}$  and at  $22^\circ\text{C}$  and 50% relative humidity in the daytime and  $17^\circ\text{C}$  and 60% relative humidity at night. Using this experimental setup, the weight of pots was recorded and optical photos and thermal pictures were taken in 7-day intervals. After the 49th day of progressive drought, plant shoots were harvested to determine the dry biomass.

### **2.2.4 Deficit irrigation**

Performing a deficit irrigation experiment required 25 days of preparation from sowing seeds to covering pots with parafilms. This experiment also required a 35-day deficit irrigation phase during which the SWC was controlled at 80%, 60%, 40% and 20% through repeated watering in three-day intervals. Specifically, seeds were sowed first on 1/2 MS medium and incubated at  $4^\circ\text{C}$  for 2 days; afterward, they were incubated for 7 days at  $22^\circ\text{C}$  and under continuous illumination ( $60 \mu\text{mol m}^{-2}$

s<sup>-1</sup>). At this point, seedlings were transferred into the fine soil saturated with water in 200 mL pots (SWC  $\approx$  77%; SWP  $\approx$  -0.02 bar) and allowed to grow under short day conditions with an 8 hours light and 16 hours dark photoperiod and at a photon flux density of 150  $\mu\text{mol m}^{-2} \text{s}^{-1}$ . The temperature and relative humidity in the plant growth chamber stabilized at 22°C and 50% in daytime, and 17°C and 60% at night. Each pot was covered with a transparent plastic wrap to maintain high humidity. This wrap was removed after 7 days of growth of the plantlets. Subsequently, watering was stopped for another 7 days to allow the soil water content of all pots to reduce to 30%. The pots of plantlets that were designed to grow under 80%, 60%, and 40% SWC were covered with Parafilms, and water was administrated to their corresponding levels, while that with 20% SWC was covered 4 days later when its SWC reached to 20%. The holes at the bottom of the pots were also sealed with adhesive tape. At this point, the deficit irrigation experiment was started and lasted 35 days, during which the weight of pots was recorded, optical photos and thermal pictures were taken in five-day or six-days intervals. At the end of the deficit irrigation, the plant shoots were harvested to determine the dry biomass.

## 2.2.5 Yield potential under well-watered conditions

### Yield potential under low photon flux density

With regard to the yield potential experiment under moderate light conditions, the seven-day-old seedlings were transferred into pots (200 mL) and grown under domes for seven days. Subsequently, the domes were removed, and a thin layer of sand was spread on the soil surface to inhibit the growth of green algae. All plants were grown under long day conditions with a 16 hours light and 8 hours dark photoperiod and at a photon flux density of 150  $\mu\text{mol m}^{-2} \text{s}^{-1}$ . The temperature and relative humidity of the plant growth chamber stabilized at 22°C and 50% in daytime, and 17°C and 60% at night. In addition, when the plants started bolting, an aracon was mounted over the rosette of each plant, and a transparent, air-permeable plastic bag was placed over each plant afterward to prevent pollen contamination from other individual plants. Water was administrated twice a week to keep plants in well-watered conditions. After four months of growth, the seeds and the straws of the plants were harvested separately. The total biomass that the plants generated is defined as the sum of the weight of the seeds and the weight of the dry straw part.

### **Yield potential under high photon flux density**

This experiment was carried out in the sun simulator at the Helmholtz Center in Munich, Germany. The simulated photobiological conditions provided exposure very similar to global solar radiation from UV rays to near infrared radiation using a combination of four different types of lamps (metal halide lamps: Osram Powerstar HQI-TS 400W/D, quartz halogen lamps: Osram Haloline IRC 400W, blue fluorescent tubes: Philips TL-D 36W/BLUE, and UV-B fluorescent tubes: Philips TL 40W/12). The arrangement of many of these lamps in several groups also allowed the simulation of the diurnal variation of solar radiation by switching appropriate groups on and off. Glass filters (Pyran 6 mm, Schott, Germany) were used to prevent the biological material from damage from UV-C radiation (100 - 280 nm) emitted by the UV-B fluorescence tubes, and to adjust the short-wave cut-off in the UV-B spectrum (280 - 315 nm). (Thiel *et al.*, 1996) and (Döhning *et al.*, 1996) have provided a detailed description of the sun simulator's general functionality.

In the sun simulator growth chamber, seven-day-old seedlings were transferred into the pots (600 mL) and grown under domes for 7 days. Subsequently, the domes were removed. All plants were grown under short day conditions with a photoperiod of 8 hours light and 16 hours dark and at 22°C and 50% relative humidity in the daytime and 17°C and 60% relative humidity at night. Water was administrated once or twice a week to keep the plants in well-watered conditions. A maximum photosynthetic active radiation (PAR, 400 - 700 nm) of  $900 \mu\text{mol m}^{-2} \text{s}^{-1}$  was reached two hours after the onset of light and kept constant for four hours, followed by a stepwise decrease for two hours to get dark. UV-A radiation (315 - 400 nm) followed the course of PAR with a maximum of  $19 \text{ W m}^{-2}$ , whereas UV-B radiation was switched on two hour after the visible light to simulate the natural behavior of UV-B radiation compared to natural conditions, reaching a maximum value of  $0.1 \text{ W m}^{-2}$ , corresponding to a biologically effective UV-B radiation of  $25 \text{ mW m}^{-2}$  (calculated by the generalized plant action spectrum of Caldwell, 1971, normalized at 300 nm). The spectroradiometric assessment of UV and PAR were performed using a double monochromator system TDM300 of Bentham (Reading, UK). Dry biomass was obtained by drying the aerial parts of the plantlets after 42 days of growth.

## 2.2.6 Leaf area, biomass, water use efficiency and energy measurements

The projected leaf area of the Arabidopsis rosettes was determined according to the photographs taken in the progressive drought and deficit irrigation experiments. A 4 cm<sup>2</sup> red square paper was used as a reference when taking photos. Photoshop Elements software (Adobe) was used to obtain the pixel values of the selected regions. Projected leaf area ( $L_p$ ) was then calculated according to the following equation:

$$L_p = \text{pixel}_{\text{leaf}} \times 4 / \text{pixel}_{\text{ref}} \quad (1)$$

where  $\text{pixel}_{\text{leaf}}$  and  $\text{pixel}_{\text{ref}}$  are the pixel values of the selected leaf region and the reference region. Under well-watered conditions (SWC > 60% or SWP > -0.03 bar), the logarithmic growth phase was used to derive the maximal linear leaf expansion rate as the square root function of the daily growth rate of the projected leaf area.

The above-ground parts of plants were harvested at the end of the progressive drought. The dry biomass was determined after drying the material for 3 days at 60 °C to achieve a constant weight. Water use efficiency was then calculated as the ratio of dry biomass to consumed water.

The energy content of each Arabidopsis line was determined by combusting aliquots of dried plant material under a high oxygen atmosphere using a Calorimeter C2000 (IKA) calibrated with benzoic acid provided by the supplier.

## 2.2.7 Thermal imaging

Thermograms were obtained using a thermographic system (InfraTec, Germany). Real-time visualization of thermograms and the operation of a thermal camera were achieved using an external laptop. The thermal camera was vertically positioned above trays containing 24 pots, and the upper and lower boundaries of the visual fields of the thermograms were aligned with the upper and lower edges of the trays. Thermograms of plants grown under well-watered conditions, progressive drought, or deficit irrigation conditions were taken four to five hours after the light photoperiod started. Parafilm covering the soil surface provided a thermal background that can be easily distinguished from leaves in a thermogram. The

thermograms were saved as .irb format on the memory card of the thermal camera and downloaded onto the external laptop. Leaf temperature values were obtained by analyzing thermal images using IRBIS3 software (InfraTec, Germany).

## 2.2.8 Carbon and oxygen isotope composition

The carbon isotope composition of whole-shoot biomass and extracted cellulose was analyzed using an elemental analyzer (NA1110; Carlo Erba Instruments) interfaced (ConFlo II, Finnigan MAT) with a continuous-flow isotope ratio mass spectrometer (Delta Plus; Finnigan MAT), EA-CF-IRMS. Each sample was measured against standard CO<sub>2</sub> calibrated with an isotope standard (International Atomic Energy Agency CH6, accuracy of calibration ± 0.06 ‰ SD). The precision of sample repeats was 0.08 ‰ (SD) for bulk biomass and 0.13 ‰ for cellulose and included deviations by subsampling, cellulose extraction, and EA-CF-IRMS measurement.

<sup>13</sup>C discrimination ( $\Delta^{13}\text{C}$ , in ‰) was calculated using the following equation (Farquhar *et al.*, 1989):

$$\Delta^{13}\text{C} = (\delta^{13}\text{C}_{\text{air}} - \delta^{13}\text{C}_{\text{plant}}) / (1 + \delta^{13}\text{C}_{\text{plant}} / 1000) \quad (2)$$

where  $\delta^{13}\text{C}_{\text{air}}$  and  $\delta^{13}\text{C}_{\text{plant}}$  are the carbon isotope composition in the air and the plant, respectively. Intrinsic WUE has been defined as follows (Farquhar *et al.*, 1989):

$$iWUE = 0.625 \cdot C_a \cdot (1 - C_i/C_a) \quad (3)$$

where the factor 0.625 gives the ratio of the diffusivities of CO<sub>2</sub> and H<sub>2</sub>O in air, and  $C_a$  and  $C_i$  designate the CO<sub>2</sub> concentration in ambient air and intercellular space. In the growth cabinet,  $C_a$  was  $422 \pm 12 \mu\text{mol mol}^{-1}$  with an approximated  $\delta^{13}\text{C}_{\text{air}}$  value of -9.7‰.

The simplified Farquhar model (Farquhar *et al.*, 1980) based on non-limiting mesophyll conductance was applied to estimate  $C_i/C_a$  (Farquhar *et al.*, 1989):

$$\Delta^{13}\text{C} = a + (b - a) \cdot C_i/C_a \quad (4)$$

where the term  $a$  (4.4 ‰) denotes the fractionation of <sup>13</sup>CO<sub>2</sub> relative to <sup>12</sup>CO<sub>2</sub> during

diffusion through the stomatal pores, and  $b$  (27.6‰) represents the net fractionation during carboxylation reactions.

Oxygen isotope composition (in ‰) was expressed as follows:

$$\delta^{18}\text{O} = \left( \frac{R_{\text{sample}}}{R_{\text{standard}}} - 1 \right) \cdot 1000 \quad (5)$$

where  $R_{\text{sample}}$  and  $R_{\text{standard}}$  are the  $^{18}\text{O}/^{16}\text{O}$  ratios of the sample and the Vienna standard Mean Ocean Water standard (V-SMOW), respectively. Cellulose samples were dried at 40 °C for 24 hours, 700 µg aliquots packed in silver cups (size: 3.3 × 5 mm, LüdiSwiss, Flawil, Switzerland) and stored above orange Silica Gel (2 mm - 5 mm, ThoMar OHG, Lüttau, Germany) in exsiccator vessels. To analyze  $^{18}\text{O}$ , samples were pyrolysed at 1400 °C in a pyrolysis oven (HTO, HEKAtech, Wegberg, Germany), equipped with a helium-flushed zero blank auto-sampler (Costech Analytical Technologies, Valencia, CA, USA) and interfaced (ConFlo III, Finnigan MAT, Bremen, Germany) to a continuous-flow isotope ratio mass spectrometer (Delta Plus, Finnigan MAT). Solid internal laboratory standards (SILS, cotton powder) were run as a control after every fifth sample. All samples and SILS were measured against a laboratory working standard carbon monoxide gas, that was previously calibrated against a secondary isotope standard (IAEA-601). The long-term precision of the internal laboratory standards was better than 0.3 ‰ (SD for repeated measurements).

## 2.2.9 Gas exchange

### 2.2.9.1 Gas exchange under well-watered conditions and progressive drought

Gas exchange measurements were carried out for analysis of net carbon assimilation rate ( $A_n$ ), stomatal conductance ( $g_s$ ), transpiration rate ( $E$ ) and intercellular  $\text{CO}_2$  levels ( $C_i$ ) in the whole plant configuration and at the single-leaf level using the GFS-3000 gas exchange system equipped with custom-built cuvettes (ring chamber or clamp-on leaf cuvette) and the provided software (Heinz Walz, Germany). The whole-rosette gas exchange measurements for well-watered Col-0, RCAR6-3,

RCAR10-4, *era1-2*, and *er2* and Arabidopsis accessions were made on 31 day  $\pm$  1-day old Arabidopsis plants at a photon flux density of 150  $\mu\text{mol m}^{-2} \text{s}^{-1}$ , 420  $\mu\text{mol mol}^{-1}$  external  $\text{CO}_2$ , and a vapor pressure deficit of 13 Pa  $\text{kPa}^{-1} \pm 2 \text{ Pa kPa}^{-1}$ . Instantaneous leaf water use efficiency (insWUE) was calculated as the ratio  $A_n/g_s$ . The experimental setup of the whole-rosette gas exchange measurement was displayed in Fig. 2-3A-C. The sealing of the plants was achieved by inserting four pieces of Parafilm with "v" gap from four directions below the Arabidopsis plants and adjusted them to be as close as possible to the stem (Fig. 2-3C). The overlapped regions of Parafims were then closed using

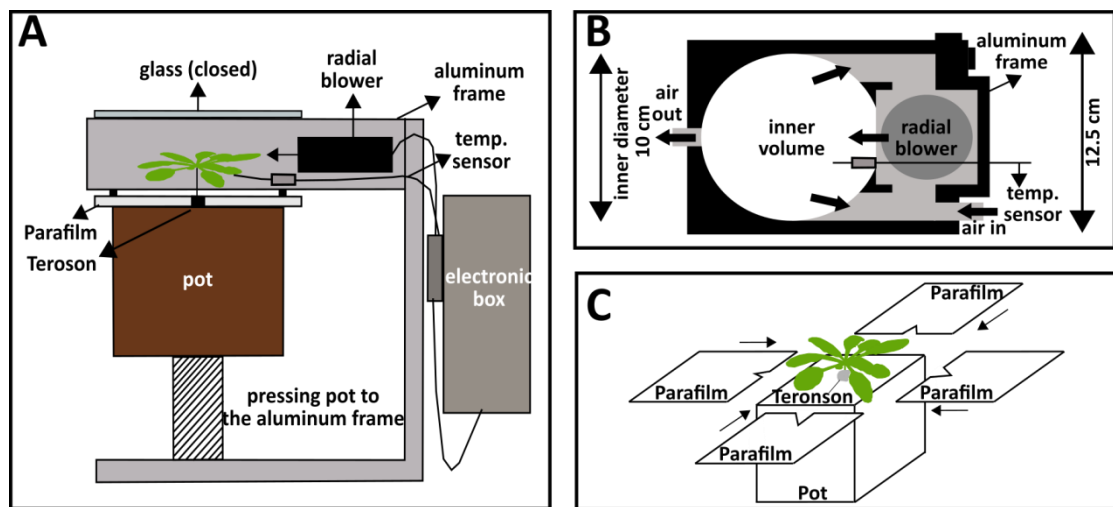


Figure 2-3 Experimental setup of the whole-rosette gas exchange measurement. A) Side view and B) vertical view of the experimental setup of the whole-rosette gas exchange measurement. C) Shoot part of the Arabidopsis plants was sealed using Parafilms and Teroson (a vehicle glue; gray). Sealing of the pots needs insertion of four pieces of Parafilms with a "v" gap from four directions below the Arabidopsis plants and adjusted them to be as close as possible to the stem. The overlapped regions of Parafim were then closed using adhesive tapes, and the intersection site of four Parafilms was sealed using Teroson. Sealed rosette was then enclosed in the ring chamber where the upper part was closed with glass. Approaching of the pot to the ring chamber was achieved by an adjustable spring lifter. The volume of the ring chamber is 240 mL. The gas exchange measurement started after the airtightness was checked. A) and B) were modified according to manufacturer's description.

adhesive tape, and the intersection site of four Parafilms was sealed using Teroson (Fig. 2-3C). The sealed rosette was then enclosed in the ring chamber where the upper part was closed with glass (Fig. 2-3A). Approaching of the pot to the ring chamber was achieved by an adjustable spring lifter (Fig. 2-3A). The gas exchange measurement was started after examination of the air tightness.



The whole-rosette gas exchange measurements for Col-0, RCAR6-3 and RCAR10-4 plants or Arabidopsis accessions throughout the progressive drought were performed at a photon flux density of  $150 \mu\text{mol m}^{-2} \text{s}^{-1}$ ,  $420 \mu\text{mol mol}^{-1}$  external  $\text{CO}_2$  and a vapor pressure deficit of  $13 \text{ Pa kPa}^{-1} \pm 2 \text{ Pa kPa}^{-1}$ .

Gas exchange measurements for single leaves of 30-day old Arabidopsis accessions Col-0 and Cvi-0 grown under well-watered conditions were performed at a photon flux density of  $200 \mu\text{mol m}^{-2} \text{s}^{-1}$ , an external  $\text{CO}_2$  level of  $380 \mu\text{mol mol}^{-1}$ , and a vapor pressure deficit of  $15 \text{ Pa kPa}^{-1} \pm 1 \text{ Pa kPa}^{-1}$ .

Gas exchange measurements for the whole rosette of 26-day-old Arabidopsis accessions Col-0 and Cvi-0 grown under well-watered conditions were performed at a photon flux density of  $200 \mu\text{mol m}^{-2} \text{s}^{-1}$ , an external  $\text{CO}_2$  level of  $380 \mu\text{mol mol}^{-1}$ , and a vapor pressure deficit of  $15 \text{ Pa kPa}^{-1} \pm 1 \text{ Pa kPa}^{-1}$ . The anatomical properties of the leaves were measured after the gas exchange measurements.

### 2.2.9.2 Mesophyll conductance

#### Theory

According to Fick's diffusion law,  $A_n$  can be written as follows:

$$A_n = (C_a - C_i) \cdot g_s \quad (6)$$

or

$$A_n = (C_i - C_c) \cdot g_m \quad (7)$$

Equation (6) describes the stomatal limitation of photosynthesis, and equation (7) describes the limitation of  $\text{CO}_2$  diffusion from intercellular space to the site of carboxylation in the chloroplast. (Farquhar *et al.*, 1980) further extended this model by taking the biochemical reactions of photosynthesis into account. Farquhar's model demonstrated the photochemical limitations of the photosynthesis of C3 plants: the activity of Rubisco, the regeneration of Ribulose-1,5-disphosphate (RuBP), or the release of phosphate during the metabolism of triose phosphate to either starch or sucrose. When the activity of Rubisco limits photosynthesis,  $A_n$  can be described as follows:

$$A_n = \frac{V_{cmax} \cdot C_c}{C_c + K_c \cdot (1 + O/K_o)} \cdot \left(1 - \frac{\Gamma^*}{C_c}\right) - R_d \quad (8)$$

where  $V_{cmax}$  is the  $V_{max}$  of Rubisco for carboxylation,  $K_c$  and  $K_o$  are the Michaelis-Menten constants of Rubisco for  $CO_2$  and  $O_2$ , respectively.  $C_c$  and  $O$  are the chloroplastic  $CO_2$  and  $O_2$  concentrations.  $\Gamma^*$  is the chloroplastic  $CO_2$  photocompensation point, and  $R_d$  is the respiration rate in the daytime. With the substitution of  $C_c$  with  $C_i - A_n/g_m$  according to equation (7), equation (8) is the following:

$$A_n = \frac{V_{cmax} \cdot (C_i - A_n/g_m)}{(C_i - A_n/g_m) + K_c \cdot (1 + O/K_o)} \cdot \left(1 - \frac{\Gamma^*}{(C_i - A_n/g_m)}\right) - R_d \quad (9)$$

When RuBP regeneration limits photosynthesis,  $A_n$  can be described as follows:

$$A_n = J \cdot \frac{(C_i - A_n/g_m) - \Gamma^*}{4 \cdot [(C_i - A_n/g_m) + 2\Gamma^*]} - R_d \quad (10)$$

where  $J$  is the electron transport rate; 4 arises by assuming 4 electrons per carboxylation or oxygenation.

When the rate of the use of triose phosphate ( $TPU$ ) limits photosynthesis,  $A_n$  can be described as follows:

$$A_n = 3TPU - R_d \quad (11)$$

One commonly reported response to photosynthesis is the response of  $A_n$  to  $C_i$ . As  $C_i$  increases from its minimum concentration to a certain concentration,  $dA_n / dC_i$  increases and is determined by the activity of Rubisco. Further increase in  $C_i$  results in an inflection to a lower  $dA_n / dC_i$  that approaches zero due to the limitation of RuBP-regeneration. In some cases, a further increase in  $C_i$  may result in a negative  $dA_n / dC_i$  if triose-phosphate utilization ( $TPU$ ) becomes limited.

### Constant J method

The constant J method assumes that J is constant with the variable  $C_i$  when photosynthesis is limited by RuBP regeneration. Rearranging the equation (10), J can be expressed as shown in equation (12). Harley *et al.*, (1992) has suggested to estimate J according to equation (12) using dummy values for  $g_m$  together with a series of  $A_n$  and  $C_i$  in which the fluorescence data indicates that J is constant. The value of  $g_m$  that gives the minimum  $V_J$  (variance of J) estimated according to equation (13) is the best estimate of  $g_m$ . The actual quantum efficiency of photosystem II (Yield) was determined by measuring steady-state fluorescence ( $F_s$ ) and maximum fluorescence ( $F_m'$ ) during a light-saturating pulse of c.  $5400 \mu\text{mol m}^{-2} \text{s}^{-1}$  according to the procedures of (Genty *et al.*, 1989), and determination of J was achieved according to equation (14) and equation (15). In equation (13),  $J_a$  is the average value of the electron transport rate and  $J_i$  is the value of J for each  $C_i$ . In equation (15), PAR is the photosynthetic active radiation and  $\alpha$  is the total light absorption of the leaf. PAR is divided by 2 because it is assumed that the absorbed light is equally distributed into photosystem I and II.

$$J = (A + R_d) \cdot \frac{4 \cdot [(C_i - A_n / g_m) + 2\Gamma^*]}{(C_i - A_n / g_m) - \Gamma^*} \quad (12)$$

$$V_J = \sum_{i=1}^n \frac{(J_a - J_i)^2}{(n-1)} \quad (13)$$

$$\text{Yield} = (F_m' - F_s) / F_m' \quad (14)$$

$$J = \text{Yield} \cdot \text{PAR} / 2 \cdot \alpha \quad (15)$$

Specifically,  $A_n$  and  $C_i$  values in equation (12) can be obtained from an  $A_n - C_i$  curve. Before performing the measurement, leaves were adapted for half an hour at a photon flux density of  $1500 \mu\text{mol m}^{-2} \text{s}^{-1}$ , a  $\text{CO}_2$  concentration in the cuvette ( $C_a$ ) of  $400 \mu\text{mol mol}^{-1}$ , a leaf temperature of  $23 \text{ }^\circ\text{C}$ , and a leaf-to-air vapor pressure deficit between  $14 \text{ Pa kPa}^{-1}$  and  $18 \text{ Pa kPa}^{-1}$ . The gas exchange and chlorophyll fluorescence of light-adapted leaves were measured first at  $400 \mu\text{mol mol}^{-1}$ , and then  $C_a$  was decreased to  $50 \mu\text{mol mol}^{-1}$  in six steps at a  $50 \mu\text{mol mol}^{-1}$  intervals. When the

measurement of the lowest  $C_a$  was completed,  $C_a$  was returned to  $400 \mu\text{mol mol}^{-1}$  to restore the original  $A_n$ . Afterward,  $C_a$  was increased stepwise to either  $2000 \mu\text{mol mol}^{-1}$  for the experiment using  $23 \pm 2$  leaves from two-month-old Arabidopsis plants or  $1400 \mu\text{mol mol}^{-1}$  for the experiment using  $16 \pm 3$  leaves two weeks after emergence. The cut-off point of  $C_i$  for distinguishing Rubisco-activity-limited phase of photosynthesis and RuBP-regeneration-limited phase of photosynthesis in this study was determined at  $260 \mu\text{mol mol}^{-1}$  according to fluorescence measurements. The estimation of  $C_i^*$  (intercellular photocompensation point) and  $R_d$  consisted of measuring  $A_n - C_i$  curves at three different photon flux densities ( $450 \mu\text{mol m}^{-2} \text{s}^{-1}$ ,  $150 \mu\text{mol m}^{-2} \text{s}^{-1}$ , and  $50 \mu\text{mol m}^{-2} \text{s}^{-1}$ ) with seven different  $C_a$  ranging from  $100 \mu\text{mol mol}^{-1}$  to  $40 \mu\text{mol mol}^{-1}$  ( $10 \mu\text{mol mol}^{-1}$  intervals) at each light intensity. The intersection point of the three  $A_n - C_i$  curves was used to determine  $C_i^*$  (x-axis) and  $R_d$  (y-axis). The chloroplastic  $\text{CO}_2$  photo compensation point  $\Gamma^*$  was calculated using a simultaneous equation with  $g_m$  ( $C_i^* + R_d / g_m = \Gamma^*$ ) according to (Warren and Dreyer, 2006). Subsequently, a dummy value was given to  $g_m$  in the equation (12), and the value of  $g_m$  that gives the minimum  $V_J$  (variance of J) estimated according to equation (13) is the best estimate of  $g_m$ . This procedure was achieved by using sequential iterations until convergence was found. The sequential iterations were performed using the software package Solver of Microsoft Excel.

### Curve fitting method

The curve fitting method fits  $A_n - C_i$  curves with a nonrectangular hyperbola version of the Farquhar photosynthesis model of C3 plants (Farquhar *et al.*, 1980). The assumption is that  $g_m$  reduces the curvature of the Rubisco-limited portion of an  $A_n - C_i$  curve with an infinite  $g_m$  (Ethier and Livingston, 2004). Minimizing the sum of squared model deviations from the data by non-linear curve fitting,  $g_m$  can be achieved from observed data. (Sharkey *et al.*, 2007) have published an estimator utility based on the principles described above to facilitate the estimation of  $g_m$ ,  $V_{max}$ ,  $J_{max}$ ,  $V_{TPU}$ , and  $R_d$ . The estimation of  $g_m$ ,  $V_{max}$ ,  $J_{max}$ ,  $V_{TPU}$  and  $R_d$  in this study using the curve fitting method was achieved using this estimator utility (Sharkey *et al.*, 2007). The  $A_n - C_i$  curves used in the curve fitting method are the same as those used in the constant J method. The values of  $K_c$ ,  $K_o$ , and  $\Gamma^*$  and their temperature responses used for these estimations were according to the  $C_c$ -based *in vivo* values of (Bernacchi *et al.*, 2002) and integrated into the estimator utility. The  $C_i$  cut-off point

was as described in the constant J method.

### On-line measurement

Gas exchange and the concurrent carbon isotope discrimination in light ( $\Delta_{NL}$ ) were measured with the comparable fully expanded leaves using the clamp-on leaf cuvette of the same LI-6400. Leaves were placed in a 10 cm<sup>2</sup> cuvette supplied with 400  $\mu\text{mol mol}^{-1}$  CO<sub>2</sub>, at a photon flux density of 500  $\mu\text{mol m}^{-2} \text{s}^{-1}$ , and a leaf temperature of 22 °C. For each measurement, the  $\delta^{13}\text{C}$  measurement was triggered and gas exchange data was stored after a stable gas exchange rate was observed. The study employed a mesocosm <sup>13</sup>CO<sub>2</sub>/<sup>12</sup>CO<sub>2</sub> gas exchange facility (Schnyder *et al.*, 2003) and a portable gas exchange system with a clamp-on leaf cuvette (LI-6400). The air supplied to the mesocosm and leaf cuvette was a mix of CO<sub>2</sub>-free, dry air and CO<sub>2</sub> of known carbon isotope compositions (Schnyder *et al.*, 2003). CO<sub>2</sub> concentration inside the mesocosm (CM) was monitored with an infrared gas analyzer (LI-6262, Li-Cor Inc.). The mesocosm and cuvette systems were coupled to a continuous-flow isotope ratio mass spectrometer (IRMS) (Deltaplus Advantage equipped with GasBench II, ThermoFinnigan, Bremen, Germany) via a stainless steel capillary. Sample air was drawn through the capillary with a peristaltic pump and passed through a 0.25 mL sample loop attached to the 8-port Valco valve of the GasBench II. Sample air in the loop was introduced into the IRMS via an open split after passage of a dryer (Nafion) and a GC column (25 m × 0.32 mm Poraplot Q; Chrompack, Middleburg, the Netherlands). After every second sample, a VPDB-gauged CO<sub>2</sub> reference gas was injected into the IRMS via the open split. The whole-system precision (SD) of repeated measurements was 0.10‰ (n = 50).

The estimation of the mesophyll conductance of C3 plants was derived from equation (7). Estimates of  $C_c$  were obtained by comparing observed  $\Delta_P$  and estimates of  $\Delta_{Pi}$  for infinite  $g_m$ . A modified model of C3 discrimination including photorespiration was used:

$$\Delta_{Pi} = a \cdot \frac{C_a - C_i}{C_a} + b \cdot \frac{C_i}{C_a} - f \cdot \frac{\Gamma^*}{C_a} \quad (16)$$

$$\Delta_P = a \cdot \frac{C_a - C_i}{C_a} + a_m \cdot \frac{C_i - C_c}{C_a} + b \cdot \frac{C_c}{C_a} - f \cdot \frac{\Gamma^*}{C_a} \quad (17)$$

$$\Delta_{p_i} - \Delta_p = (b - a_m) \cdot \frac{C_i - C_c}{C_a} \quad (18)$$

In this model,  $a = 4.4\text{‰}$ ,  $b = 28.9\text{‰}$ ,  $a_m = 1.8\text{‰}$  (Evans, JR *et al.*, 1986; Pons *et al.*, 2009) and  $f = 1\text{‰}$  (Ghashghaie *et al.*, 2003). The calculation of  $\Gamma^*$  was according to (Brooks and Farquhar, 1985).

Plants used in the on-line measurements were grown under short day conditions with an 8 hours light / 16 hours dark photoperiod, at a maximum photon flux density of  $500 \mu\text{mol m}^{-2} \text{s}^{-1}$  and supplied with  $400 \mu\text{mol mol}^{-1}$  with a carbon isotope composition of  $-10 \text{‰}$ . Water was provided twice a week to keep all plants growing in well-watered conditions.

### **2.2.9.3 Nighttime stomatal opening and stomatal oscillation**

In order to analyze the nighttime stomatal conductance and stomatal oscillation, gas exchange measurements were performed from nighttime to daytime and lasted more than 20 hours. For each gas exchange measurement,  $380 \mu\text{mol mol}^{-1}$  of  $\text{CO}_2$  and  $12 \text{mmol mol}^{-1}$  of  $\text{H}_2\text{O}$  were continuously supplied. No external light source was mounted over either the ring chamber or the cuvette, and temperature control was switched off. Therefore, the photon flux density and temperature in the ring chamber and the cuvette were dependent on the light source and temperature in the growth chamber. According to the illumination regime, three phases of the gas exchange measurements were defined: the dark phase, the phase of transition between dark and daytime, and the daytime phase.

With regard to the whole-rosette gas exchange measurements, well-watered, 20 days  $\pm$  8 days old *Arabidopsis* plants were sealed in the ring chamber. During the dark phase (from 18:00 to 9:00), no illumination occurred. The temperature in the growth chamber was set to  $17 \text{ °C}$ , and temperatures in the ring chamber ( $T_{ring}$ ) were around  $22 \text{ °C}$ .  $\text{CO}_2$  concentration in the ring chamber ( $C_a$ ) was maintained at  $380 \mu\text{mol mol}^{-1}$  and the concentration of water vapor ( $W_a$ ) was stabilized at  $14 \text{mmol mol}^{-1}$ . The  $W_a$  and the nighttime  $T_{ring}$  resulted in leaf-to-air VPDs reaching approximately  $15 \text{ Pa kPa}^{-1}$  at night. During the transition from dark to light (9:00 to

9:30), the light intensity increased stepwise from  $0 \mu\text{mol m}^{-2} \text{s}^{-1}$  to  $150 \mu\text{mol m}^{-2} \text{s}^{-1}$ . The temperature in the growth chamber increased from  $17 \text{ }^\circ\text{C}$  to  $22 \text{ }^\circ\text{C}$ , and  $T_{ring}$  increased from  $22 \text{ }^\circ\text{C}$  to  $27 \text{ }^\circ\text{C}$ . The ambient  $\text{CO}_2$  in the ring chamber decreased from  $380 \mu\text{mol mol}^{-1}$  to  $370 \mu\text{mol mol}^{-1}$ , while  $W_a$  increased steadily from  $12.5 \text{ mmol mol}^{-1}$  to up to  $17 \text{ mmol mol}^{-1}$ . The increase in  $T_{ring}$  and  $W_a$  caused an increase in the leaf-to-air VPDs from  $15 \text{ Pa kPa}^{-1}$  to up to  $27 \text{ Pa kPa}^{-1}$ . During the daytime phase (9:30 to 17:30), light intensity stabilized at  $150 \mu\text{mol m}^{-2} \text{s}^{-1}$  and  $T_{ring}$  remained at  $27 \text{ }^\circ\text{C}$ . Other conditions such as  $C_a$ ,  $W_a$ , and VPD were around  $370 \mu\text{mol mol}^{-1}$ ,  $17 \text{ mmol mol}^{-1}$  and  $27 \text{ Pa kPa}^{-1}$ , respectively.

In terms of the single-leaf gas exchange measurements, the comparable single leaves of  $37 \pm 4$ -day-old *Arabidopsis* plants grown under well-watered conditions were clamped into the cuvette. During the dark phase (18:00 to 9:00), no illumination occurred, the temperature in the growth chamber was set to  $17 \text{ }^\circ\text{C}$ , and the temperatures in the cuvette ( $T_{cuvette}$ ) for all measurements was around  $19 \text{ }^\circ\text{C}$ . The  $\text{CO}_2$  concentration in the cuvette ( $C_a$ ) was around  $380 \mu\text{mol mol}^{-1}$ . Water vapor concentration ( $W_a$ ) stabilized at  $12 \text{ mmol mol}^{-1}$  and together with the  $T_{ring}$  resulted in approximately  $12.5 \text{ Pa kPa}^{-1}$  VPDs for all measurements. During the phase of transition from dark to light (9:00 to 9:30), the light intensity increased stepwise from 0 to  $180 \mu\text{mol m}^{-2} \text{s}^{-1}$ . The temperature in the growth chamber increased from  $17 \text{ }^\circ\text{C}$  to  $22 \text{ }^\circ\text{C}$ , and  $T_{cuvette}$  increased from  $19 \text{ }^\circ\text{C}$  to  $24 \text{ }^\circ\text{C}$ .  $C_a$  was maintained at  $380 \mu\text{mol mol}^{-1}$ .  $W_a$  increased from  $12 \text{ mmol mol}^{-1}$  to  $12.5 \text{ mmol mol}^{-1}$  for the measurements of Col-0;  $W_a$  increased from  $12 \text{ mmol mol}^{-1}$  to  $13.5 \text{ mmol mol}^{-1}$  for the measurements of Cvi-0. Leaf-to-air VPD in this phase increased from  $12.5 \text{ Pa kPa}^{-1}$  to  $21.5 \text{ Pa kPa}^{-1}$  for Col-0 and from  $12.5 \text{ Pa kPa}^{-1}$  to  $23.5 \text{ Pa kPa}^{-1}$  for Cvi-0. During the daytime phase (17:00 to 9:00), light intensity stabilized at  $180 \mu\text{mol m}^{-2} \text{s}^{-1}$ , and the leaf temperatures of all tested lines were around  $25 \text{ }^\circ\text{C}$ .  $C_a$  still stabilized at  $380 \mu\text{mol mol}^{-1}$ .  $W_a$  stabilized at  $11.5 \text{ mmol mol}^{-1}$  for the measurements of Col-0, while  $W_a$  was  $13 \text{ mmol mol}^{-1}$  for the measurements of Cvi-0. VPDs of Col-0 and Cvi-0 were around  $20 \text{ Pa kPa}^{-1}$  and  $22.5 \text{ Pa kPa}^{-1}$ , respectively.

Nighttime stomatal conductance is calculated as the average value of the stomatal conductance throughout the night. The oscillation period of stomatal conductance at the first cycle (from the first crest to the second crest) was used as a measurement





	100 mM EDTA
	Not autoclaved
<b>1×TE buffer:</b>	10 mM Tris HCl (pH 8.0)
	1 mM EDTA

### **2.2.12 Cloning techniques**

Standard cloning techniques, such as the polymerase chain reaction (PCR), agarose gel electrophoresis, restriction enzyme digestion, plasmid DNA mini-preparation, dephosphorylation via alkaline phosphatase, DNA ligation, transformation etc. were performed according to either manufacturers' protocols or the standard protocols from (Sambrook and Russell, 2001). The constructs generated in this study are displayed in Appendix (Table 5-5).

### **2.2.13 Statistic analysis**

For the sample size of most of our experiment, we chose  $n=4$  of plant individual per genotype and treatment. Analysis of large sample size experiments revealed that normal distribution occurred with an SD,  $\sigma$ , of 10%. The sample size was computed with the G\*Power 3.1.9.2 software program under the assumption that a difference of 30% ( $3*\sigma$ ) between RCAR-overexpressing lines and the wild type would occur, with presumed values for  $\alpha$  and  $\beta$  of 0.05 and 0.1, respectively. The cohort size of four individuals is recommended based on these parameters for an unpaired, two-sided  $t$ -test. The data was analyzed by using methods of one-way ANOVA and linear regression analysis with the SPASS version 16.0 software for Windows.

## 3. Results

### 3.1 System establishment

Plants play a dominant role in mobilizing water from the terrestrial surface to the atmosphere, mainly through the process of transpiration (Jasechko *et al.*, 2013). This universal process, driven by the water potential gradient between the root zone and the atmosphere, is sustained by efficient water capture by plants' root systems (Cowan, 1972; Steudle, 2000). Stomata play pivotal role in regulating transpiration (Cowan, 1972; van den Honert, 1948) and, simultaneously, allow CO<sub>2</sub> to diffuse from the atmosphere to sites of assimilation located within chloroplasts (Chaves *et al.*, 2008). The uptake of CO<sub>2</sub> through stomatal pores leads to a concomitant mass efflux of water vapor, and this process is the major reason why more than two-thirds of the fresh water resources used by the world's population are channeled into agriculture for crop production (Gleick and Serageldin, 2014). However, this water use is not sustainable. The replenishing of fresh water resources does not meet the demands of both agricultural and domestic water use, which will make water a precious resource in the future (Gleick and Serageldin, 2014; Oki and Kanae, 2006).

Understanding how plants respond to limited water may provide tools for reducing the water consumption of plants, and could improve crop performance and yield given water limitations. Many studies have investigated the strategies and mechanisms involved in the adaptation of plants to drought conditions, such as stress avoidance and true tolerance. Some species or cultivars tend to finish their life cycles earlier to escape the drought period. This strategy is accomplished by rapid, plastic development and the remobilization of pre-anthesis assimilates to regenerative organs (Berger and Ludwig, 2014; Franks *et al.*, 2007; Kooyers, 2015). Some plant species try to avoid drought by closing the stomata, developing deep root systems and enhancing water use efficiency (Farooq *et al.*, 2009; Kavar *et al.*, 2008; Rebetzke *et al.*, 2002; Tardieu, 1996; Tardieu, 2011; Tardieu and Simonneau, 1998). Other species evolve the ability to tolerate drought by osmotic adjustment, cell detoxification and protection mechanisms (Castiglioni *et al.*, 2008; Garg *et al.*, 2002; Nelson *et al.*, 2007; Smith-Espinoza *et al.*, 2003; Sunkar *et al.*, 2003). However, few of these studies have succeeded in translating these insights into improving the yield of crops in the field. Tardieu (2011) pointed out that a specific gene might bring

spectacular results in one given drought scenario but not in others. In addition, Skirycz *et al.* (2011) has highlighted that many studies investigated severe drought scenarios and scored plants' drought resistance solely based on their improved survival rate, without investigating plant performance, biomass and yield gain under mild drought stress.

In this first chapter, a method was established to simulate for *Arabidopsis* plants a rain-drought scenario in the field, by slow, progressive soil drying. In addition, the water deficit was combined with repeated watering to mimic deficit irrigation. Both methods facilitated subsequent evaluations on growth performance, biomass gain and WUE.

### 3.1.1 Progressive drought

Progressive drought is an extreme delay in timing or failure of rainfall in nature (Wilhite and Glantz, 1985). To simulate such a progressive drought in studies, water was supplied to the field capacity of soils, but watering was subsequently discontinued until all of the available water had been utilized by plants (Flexas *et al.*, 1999; Gosti *et al.*, 1995; Xin *et al.*, 2008). During the soil-drying procedure, the gravimetric method was used to give readouts for soil water content, which could then be converted to soil water potential according to the calibration curve of soil water content and water potential (see section 2.2.3). Using this traditional progressive drought method showed that soil drying occurred quickly. In the absence of plants, the soil in the pots (200 mL) lost 60% of their water through evaporation within two weeks (Fig. 3-1A). Evaporation can be reduced by placing a cover of parafilm over the soil surface (Fig. 3-1A). Using this setup, seven-day-old wild type Columbia seedlings were transferred to the pots (200 mL) and grown for 11 days under well-watered conditions (SWC  $\geq$  77%; SWP  $\geq$  -0.02 bar) (Fig. 3-1E). The pots of plantlets at an age of 18 days were then covered and the plants were subjected to a progressive drought by no longer administering water (Fig. 3-1E). The plants were cultivated under short day conditions (8h light / 16h dark photoperiod at photon flux density of  $150 \mu\text{mol m}^{-2} \text{s}^{-1}$ ) to keep the *Arabidopsis* at a vegetative growth phase for two months (Fig. 3-1E).

In a separate experiment, Columbia plants were exposed to the progressive drought

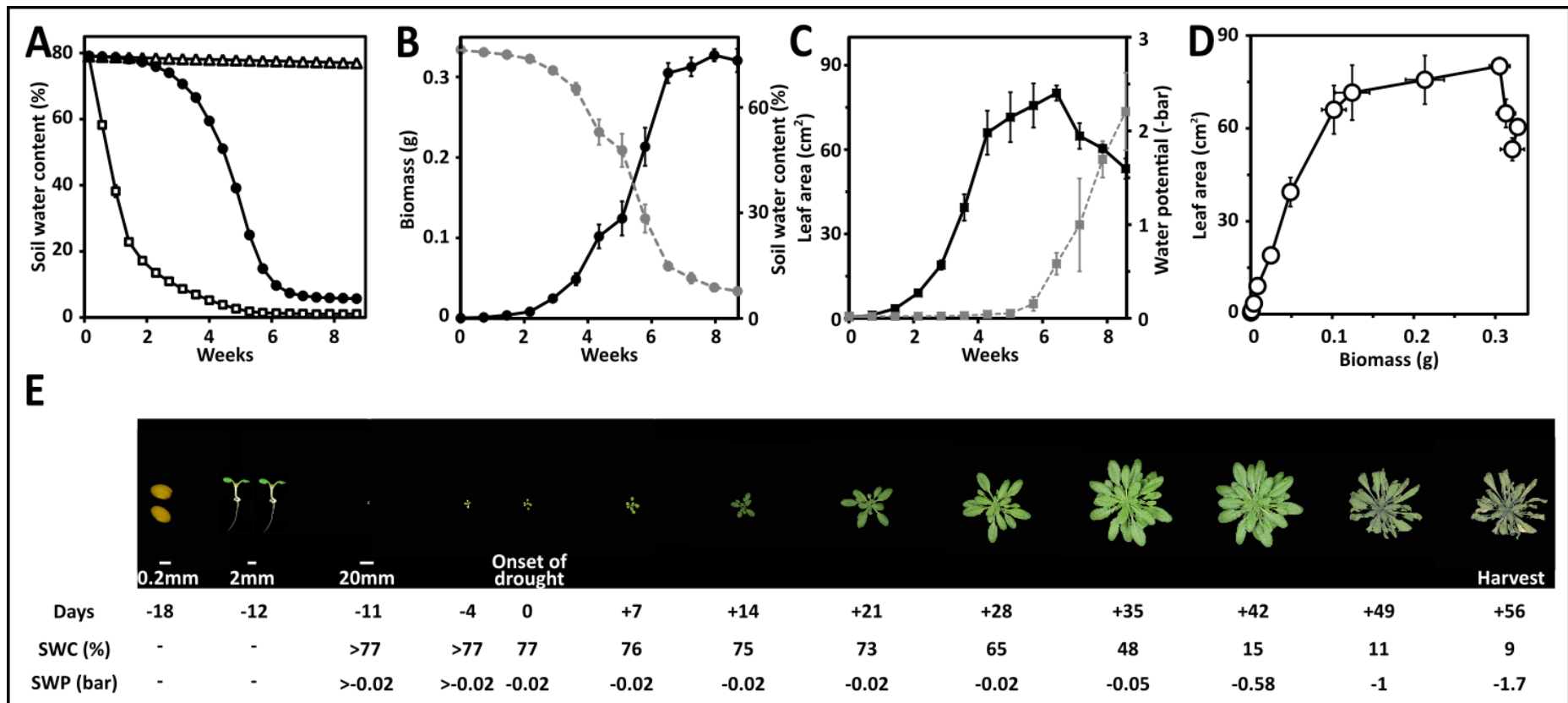


Figure 3-1 Growth performance, biomass and WUE in *Arabidopsis thaliana* wild type Columbia during progressive drought. A) The soil water content of covered pots with Columbia plants (filled circles) or without plants (open triangles) and uncovered pots without plants (open squares) was recorded during drought (60 days without watering). The water loss per day in the covered control was quite constant, at 0.07 mL day<sup>-1</sup>. B) Changes in biomass in gram dry weight (black filled circles) together with the soil water content (gray filled circles) and C) leaf area (black filled squares) together with water potential (gray filled squares) were determined at five-day intervals. D) The association between leaf area and biomass during the progressive drought. E) Developmental stages of *Arabidopsis* plants and time outlined in days. Day "0" refers to the onset of the progressive drought and the days prior to the drought are indicated by negative numbers.

The approximate soil water content (SWC) and soil water potential (SWP) are given below the image. Plants were grown in an 8h light / 16h dark photoperiod at a photon flux density of  $150 \mu\text{mol m}^{-2} \text{s}^{-1}$  and  $22^\circ\text{C}$  and 50% relative humidity in the daytime and  $17^\circ\text{C}$  and 60% relative humidity at night. A)  $n=4$  biological replicates for each data point and B-D)  $n=6$  biological replicates for each data point, mean  $\pm$  SEM.

to analyze biomass acquisition over time. During the course of the experiment, the above-ground part of individual plants was harvested, five plants every five days to determine the dry biomass (Fig. 3-1B). In addition, water consumption was gravimetrically determined by weighing the pots, and the leaf expansion was measured by taking photographs of the leaf rosettes (Fig. 3-1B and C). The analysis provided data on projected leaf area, above-ground dry biomass, and soil water status during the drought experiment. For instance, little water was consumed in the first three weeks because of the lower leaf area (Fig. 3-1C). In the following three weeks, the plants accumulated  $80 \text{ cm}^2 \pm 3 \text{ cm}^2$  leaf area and  $0.32 \text{ g} \pm 0.01 \text{ g}$  dry biomass, and there was an accompanying significant drop in soil water content, from 65% to 15% (reduced SWP by 0.63 bar) (Fig. 3-1B and C). A further 10% of the water was transpired (reduced SWP by 1.85 bar) without contributing very much to biomass formation (Fig. 3-1B and C), which implied the onset of the severe drought. This method of progressive drought was further proved to be reproducible by performing another two independent experiments (Appendix Fig. 5-1).

Plotting the projected leaf area against the above-ground dry biomass displayed a triphasic relationship during the progressive drought (Fig. 3-1D). A positive linear correlation between the projected leaf area and biomass was found in the well-watered phase (Fig. 3-1D). Moreover, although a positive linear relationship was observed under mild drought, the ratio of biomass to leaf area was higher than that under well-watered conditions, which can be explained by the overlapping leaves and thicker leaves under drought (Fig. 3-1D). The projected leaf area was negatively correlated with biomass under severe water stress owing to the wilting of leaves (Fig. 3-1D).

### 3.1.2 Deficit irrigation testing system

Deficit irrigation is an optimized water regime that allows plants an adequate water supply in drought-sensitive growth stages, and limits their supply in less critical stages (Geerts and Raes, 2009). Controlled irrigation of plants requires the data of

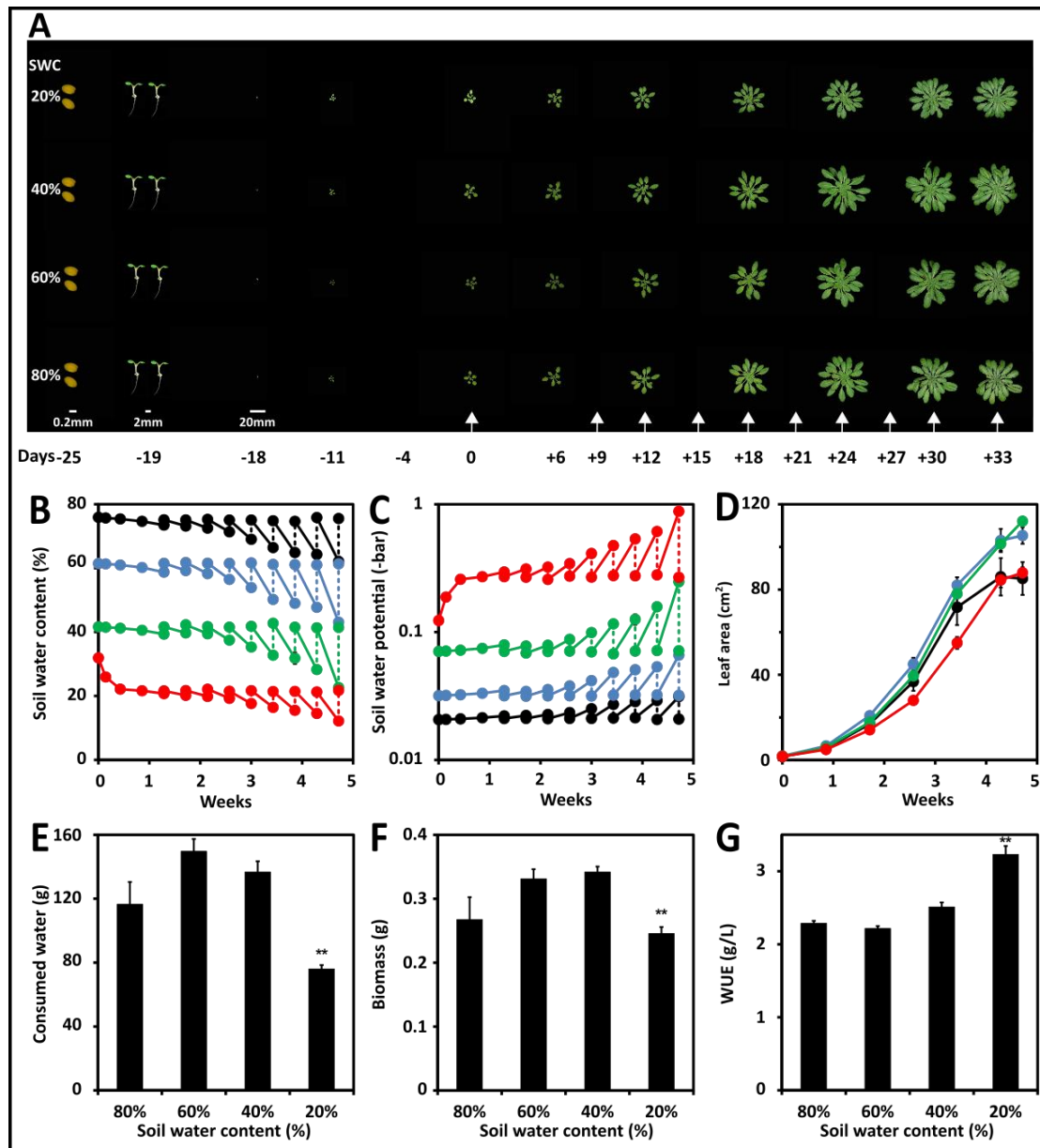


Figure 3-2 Growth performance, biomass and WUE of wild type Columbia grown under water deficit conditions. A) Scheme of the water deficit experiment. After germination and growth in 1/2 MS medium, seven-day-old plantlets were transferred into soil. To maintain the comparable growth of Col-0 plants in each water regime, watering was stopped for seven days until the soil water content of all deficit irrigation regimes reached 30% SWC. Subsequently, plants were covered and then were watered to designed soil water content, 80%, 60% and 40%, while the pots of plantlets grown under the 20% SWC regime were covered four days later when their soil water content had dropped to 20%. White arrows indicate the time of water supply. The scale bars in the pictures of seeds, seedlings and plants represent 0.2 mm, 2 mm and 20 mm respectively. Texts on the left side of the picture indicate designated soil water content in deficit irrigation. Texts under each picture show days in each developmental stage, and the negative numbers represent days before the onset of deficit irrigation. B) Soil water content was controlled at 80% (black line), 60% (blue line), 40% (green line) and 20% (red line), and corresponding soil water potential C) was calculated based on the calibration curve of soil water content and potential. B-C) Solid lines represent water content before applying water, while dotted lines indicate values after adjustments. Leaf area D) is shown as projected leaf area of rosettes. The color codes are the

same as for A) and B). Total water consumption E), dry biomass F) and WUE G) were determined after five weeks of deficit irrigation. Plants were grown with a photoperiod of 8h light / 16h dark photoperiod at photon flux density of  $150 \mu\text{mol m}^{-2} \text{s}^{-1}$  and  $22^\circ\text{C}$  and 50% relative humidity in the daytime and  $17^\circ\text{C}$  and 60% relative humidity at night. B-G)  $n=4$  biological replicates for each data point, mean  $\pm$  SEM. E-G)  $**P<0.001$  compared with values of plantlets grown under 40% soil water condition.

water demand and the physiological responses of plants. Deficit irrigation becomes an acknowledged method for investigating the growth performance and the biomass or yield gain of plants in response to designated severities of drought. To establish a deficit irrigation system for Arabidopsis, wild type Columbia was exposed to different soil water contents. Figure 3-2A shows the developmental stages of Arabidopsis during the experiment which includes 25-day preparation from sowing seeds to covering pots with parafilms and five-week irrigation to keep the soil at 80%, 60%, 40% and 20% water content. 7-day old wild type Columbia plantlets were transferred into the pots (200 mL) and were grown under well-watered conditions ( $\text{SWC} \geq 77\%$ ;  $\text{SWP} \geq -0.02$  bar) for 7 d. Subsequently, watering was stopped for another 7 d to allow soil water content of all pots to reduce to 30%. The pots of plantlets which were designed to grow under 80%, 60% and 40% soil water content were covered and water was applied to their corresponding levels while that with 20% soil water were covered four days later when its soil water content reached to 20%. Here, it was assumed that water consumption would be negligible for plants grown under 20% SWC regime during those four days. Subsequently, water was applied according to the designed regimes in three-day intervals. Soil water content (Fig. 3-2B) and the corresponding water potential (Fig. 3-2C) were recorded during the experimental period. Results of soil water content and water potential are shown in Fig. 3-2B and C. Fluctuations of soil water content were caused by the plants' water use (solid lines) and repeated watering (dotted lines) (Fig. 3-2B and C).

The leaf area experiment indicated that 40% and 60% SWC regimes had comparable results and 80% SWC regime also did not show a clear difference in rosette size compared with those. The 20% soil water content regime displayed consistently small rosettes (Fig. 3-2D). At the end of deficit irrigation, plants grown at different SWC regimes showed considerable variations in final water consumption, above-ground dry biomass and WUE (Fig. 3-2E-G). Plants grown at 40% and 60% SWC regimes generated  $0.34 \text{ g} \pm 0.01 \text{ g}$  and  $0.33 \text{ g} \pm 0.02 \text{ g}$  dry biomass by consuming  $137 \text{ g} \pm 7 \text{ g}$  and  $150 \text{ g} \pm 8 \text{ g}$  soil water while plants grown at 20% and 80% SWC regimes

accumulated  $0.25 \text{ g} \pm 0.01 \text{ g}$  and  $0.27 \text{ g} \pm 0.03 \text{ g}$  dry biomass by using  $76 \text{ g} \pm 2 \text{ g}$  and  $117 \text{ g} \pm 14 \text{ g}$  soil water. As a consequence, plants grown at 40% SWC and 60% SWC regimes achieved a WUE of  $2.5 \text{ g/L} \pm 0.1 \text{ g/L}$  and  $2.2 \text{ g/L} \pm 0.03 \text{ g/L}$  and compared with those, WUE of plants grown at 20% SWC showed a higher value while that of plants grown at 80% SWC regime reduced slightly.

### 3.1.3 Thermal imaging and gas exchange analysis during progressive drought

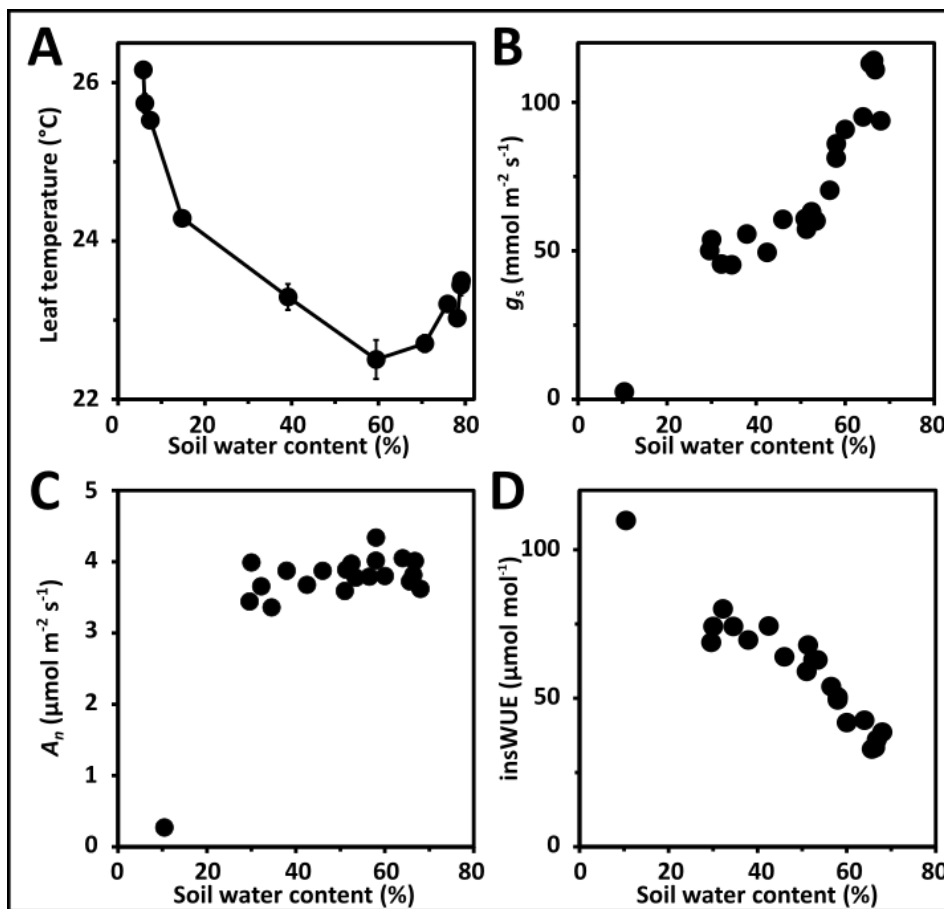


Figure 3-3 Thermal imaging and gas exchange analysis during progressive drought. A) Leaf temperatures of wild type Columbia plants were recorded at six-day intervals. Single plants were grown for 18 days prior to the discontinuation of watering at SWP =  $-0.02 \text{ bar}$ .  $n=4$  biological replicates per data point, mean  $\pm$  SEM. B-D) Whole rosette gas exchange measurements using Col. Stomatal conductance ( $g_s$ ) B), net carbon assimilation rate ( $A_n$ ) C) and insWUE D) defined as the ratio of  $A_n$  to  $g_s$  were analyzed in response to soil water content during progressive drought. Gas exchange measurements were conducted at photon flux density of  $150 \mu\text{mol m}^{-2} \text{s}^{-1}$ ,  $420 \mu\text{mol mol}^{-1}$  external  $\text{CO}_2$  and vapor pressure deficit of  $13 \text{ Pa kPa}^{-1} \pm 2 \text{ Pa kPa}^{-1}$ . A-D) Growth condition of plants as described in Fig. 3-1. B-D) Single plant measurements with 10 technical replicates per data point.

Most of the water loss in plants occurs through stomata. This process can be detected by IR thermogram (IRT), which allows non-contact and high throughput



visualization of leaf surface temperatures, and therefore reflects the transpiration of plants (Hamlyn G. Jones, 2004). When water is transpired in C3 species, CO<sub>2</sub> simultaneously diffuses along its concentration gradient in the atmosphere and the site of carboxylation (Chaves *et al.*, 2008). The gas exchange can be traced by a gas exchange system which is designed to trace the water vapor as well as CO<sub>2</sub> at the inlet and outlet of the cuvette where plant samples are clamped. Analysis of the thermal imaging and the gas exchange during progressive drought using single leaves or whole rosettes, facilitates identification of plants with high WUE and elucidates possible mechanisms.

During progressive drought, the leaf surface temperatures of Col plants varied by more than three degrees (Fig. 3-3A). The initial drop of soil water content from 80% to 60% did not result in elevated leaf surface temperatures, but rather a one-degree decrease. Further soil water depletion led to a consistent elevation in leaf surface temperatures, indicating that water shortage had emerged and stomata had started to react to it (Fig. 3-3A). Consistent with the leaf temperature results, the stomatal conductance ( $g_s$ ) of the whole Col rosette showed a continuous reduction when soil water content was below 60% (Fig. 3-3B). In contrast to stomatal conductance ( $g_s$ ), net carbon assimilation rate ( $A_n$ ) responded little to the drop in soil water content from 68% to 30% (Fig. 3-3C). As a result, insWUE (the ratio of net carbon assimilation rate to stomatal conductance) was enhanced by a factor of up to 2.4 under the progressive drought compared with well-watered conditions (Fig. 3-3D).

### **3.2 Enhanced water use efficiency conferred by ectopic expression RCARs**

When adapting to their habitats, plants need to regulate the relationship between growth and water availability. This relationship can be expressed as WUE. High WUE is an attractive agronomic trait in agriculture. The enhancement of WUE by a factor of 1.5 to 2.5 under drought conditions has been reported in wheat and other crops (Gu *et al.*, 2013; Medrano, 2002; Rizza *et al.*, 2012; Torrecillas *et al.*, 1999). Likewise, a two-fold increase in WUE under drought conditions was also found in *Arabidopsis thaliana* accessions Columbia (Col) and Landsberg (Ler) (Des Marais *et al.*, 2014; Easlon *et al.*, 2014; Juenger *et al.*, 2005; Masle *et al.*, 2005). These facts indicate that high WUE is achievable and can be modulated by drought stress. However, the

underlying molecular mechanisms still have not been fully elucidated. Genes involved in regulating stomatal density or size were found to control WUE (Des Marais *et al.*, 2014; Masle *et al.*, 2005; Yoo *et al.*, 2010), whereas genes controlling open and close movements of stomatal pores are rarely reported. In addition, whether increased WUE is associated with reduced growth and trade-offs in yield is still debated (Blum, 2005). Some studies found that plants with enhanced WUE are always linked to reduced growth and yield (Blum, 2005; Hausmann *et al.*, 2005; Martin *et al.*, 1999; Munoz *et al.*, 1998), while few studies showed both enhanced WUE and yield potential (Rebetzke *et al.*, 2008).

Drought induces ABA synthesis (Iuchi *et al.*, 2001a). Increments in levels of endogenous ABA trigger ABA-dependent signal transduction after being recruited by an ABA-binding regulatory component, RCAR/PYR1/PYL, and an associated protein phosphatase of type 2C (PP2C) (Kang *et al.*, 2010; Kuromori *et al.*, 2010; Ma *et al.*, 2009; Park *et al.*, 2009). OPEN STOMATA1 (OST1/SRK2E/SnRK2.6) protein kinase is subsequently activated, which results in phosphorelay of OST1 protein to SLAC1 ion channel, KAT1 cation channel in guard cells to trigger stomatal closure. Moreover, OST1 and other related SnRK2 protein kinases phosphorylates transcription factors (AREBs/ABFs/ABI5/ABI4) to activate downstream gene expression in the nucleus (Fujii *et al.*, 2007; Fujii *et al.*, 2009; Fujita *et al.*, 2009; Geiger *et al.*, 2009; Lee, S. C. *et al.*, 2009; Ma *et al.*, 2009; Park *et al.*, 2009; Raghavendra *et al.*, 2010; Sato *et al.*, 2009; Yoshida *et al.*, 2010). As a consequence, adaption responses of plants to drought was mediated in both short term and long term manners. Analogously, the adaption responses of plants can also be modulated by constitutively enhanced ABA signaling through ectopic expression of RCAR genes. There are fourteen RCAR proteins in *Arabidopsis thaliana*, and they are classified into three subclades (Ma *et al.*, 2009; Park *et al.*, 2009; Raghavendra *et al.*, 2010). Transgenic plants in Columbia background with ectopic expression single RCARs induced using the *cauliflower mosaic virus* 35S promoter were generated, and the expression level of these lines was analyzed by my colleague Stefanie V. Tischer (2016). Water productivity of all ectopic expression RCAR lines is investigated in this chapter. Growth performance, biomass, and WUE were evaluated during progressive drought on three levels: immediate net carbon assimilation and transpiration, short-term growth and leaf surface temperature, and long-term growth and water use. Certain RACRs were

found to combine maintained growth with enhanced WUE compared with wild type Col-0. The underlying mechanism was also studied to elucidate when, where and why plants benefit from overexpressing certain ABA receptors. In addition, yield potential was analyzed in both low light and high light intensity conditions, and trade-offs under variable ambient temperatures and deficit irrigation were investigated.

### 3.2.1 Water productivity conferred by ectopic expression of RCARs during progressive drought

#### 3.2.1.1 Leaf surface temperatures and growth in well-watered phase of progressive drought

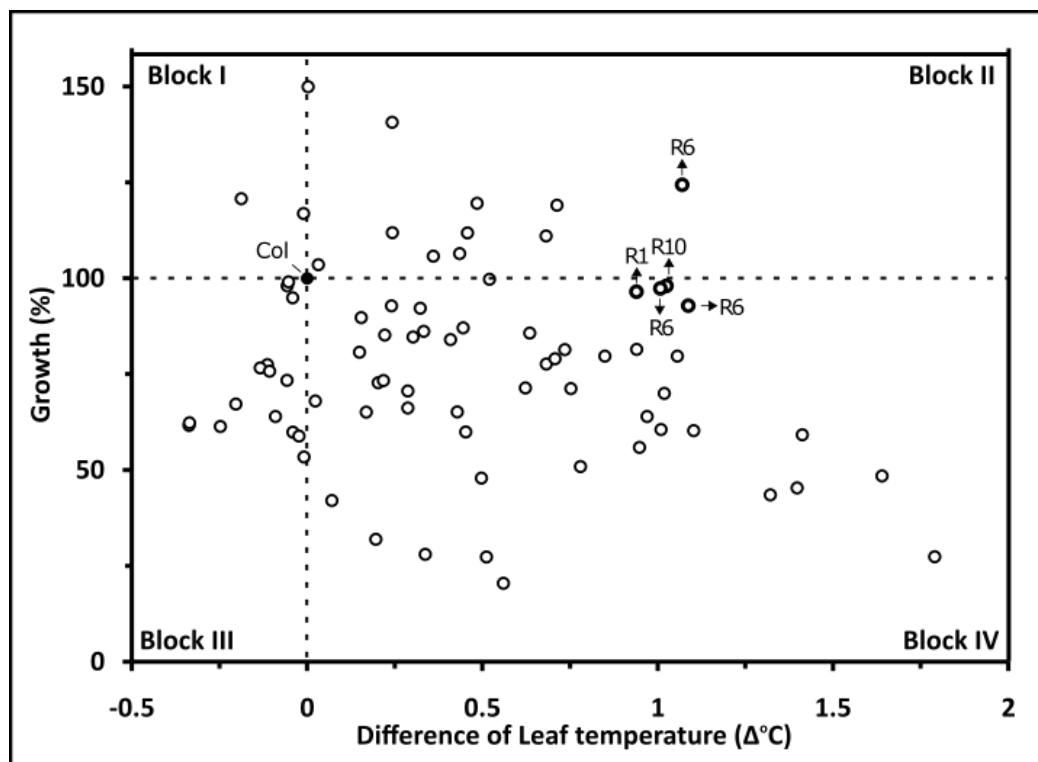


Figure 3-4 Prescreening of *Arabidopsis* lines with ectopic expression of ABA receptors. The relative growths and leaf temperature differences were analyzed for homozygous plants expressing the 14 ABA receptors (open circles) under the constitutive viral promoter 35S, in comparison with *Arabidopsis* wild type Columbia (filled circle). Columbia had leaf area of  $22.7 \text{ cm}^2 \pm 0.1 \text{ cm}^2$  and leaf surface temperature of  $20.2 \text{ }^\circ\text{C} \pm 0.9 \text{ }^\circ\text{C}$ . Both the leaf surface temperatures and the leaf area were determined using 40-day-old plants grown under short day conditions (8 hours light / 16 hours dark photoperiod) at photon flux density of  $150 \mu\text{mol m}^{-2} \text{ s}^{-1}$  and  $22^\circ\text{C}$  and 50% relative humidity in daytime, and  $17^\circ\text{C}$  and 60% relative humidity at night, and at well-watered conditions ( $\text{SWP} \geq -0.02 \text{ bar}$ ). Four plants per line were grown in separate pots at randomized positions. The figure is divided into four blocks (Block I to IV) by dotted lines. Control Columbia (Col) and interesting lines of RCAR1 (R1), RCAR6 (R6) and

## Results

---

RCAR10 (R10) are highlighted by bold circles. Each data point marks a value averaged from four biological replicates.

A prescreening experiment was performed firstly. Three to five independent lines with enhanced expression for each RCAR gene were subjected to progressive drought. At the day 22 of progressive drought, soil water content of all lines was above 60% which was regarded as well-watered phase (see section 2.2.3 Fig. 2-2A and B). Under this condition, all lines were assessed according to their ability to grow comparably to the parental line Columbia, and meanwhile show elevated leaf surface temperatures as a first indication for reduced transpiration. In case, ectopic expression of individual RCARs generated a single plant line that fulfilled the criteria, three independent lines were selected, if not, only one prototype line was chosen. Figure 3-4 shows the growth in percentage (relative rosette size to Col-0) against the difference in leaf surface temperatures. Dotted lines divide the figure into four blocks (Block I to IV). The cross point represents wild type Columbia (filled circle) and others are lines with ectopic expression of RCARs (open circles). Some lines with enhanced expression RCARs displayed lower leaf temperatures than Col-0 with either increased or reduced growth such as data points in the Block I and Block III (Fig. 3-4). Most of the data points falls into the Block IV, indicating higher leaf surface temperatures of these overexpression RCAR lines than Col-0, but most of them tended to have more reduced growth except lines highlighted and named R6 (RCAR6) and R10 (RCAR10) at the interface between the Block IV and Block II (Fig. 3-4). Lines with ectopic expression RCARs shown in the Block II combined elevated leaf temperatures with comparable or some increase in growth, especially the data point highlighted and named with R1 (RCAR1) (Fig. 3-4). Therefore, three independent lines of RCAR1, RCAR6, and RCAR10 were chosen to fulfill following detailed analysis while one prototype was selected for other RCARs.

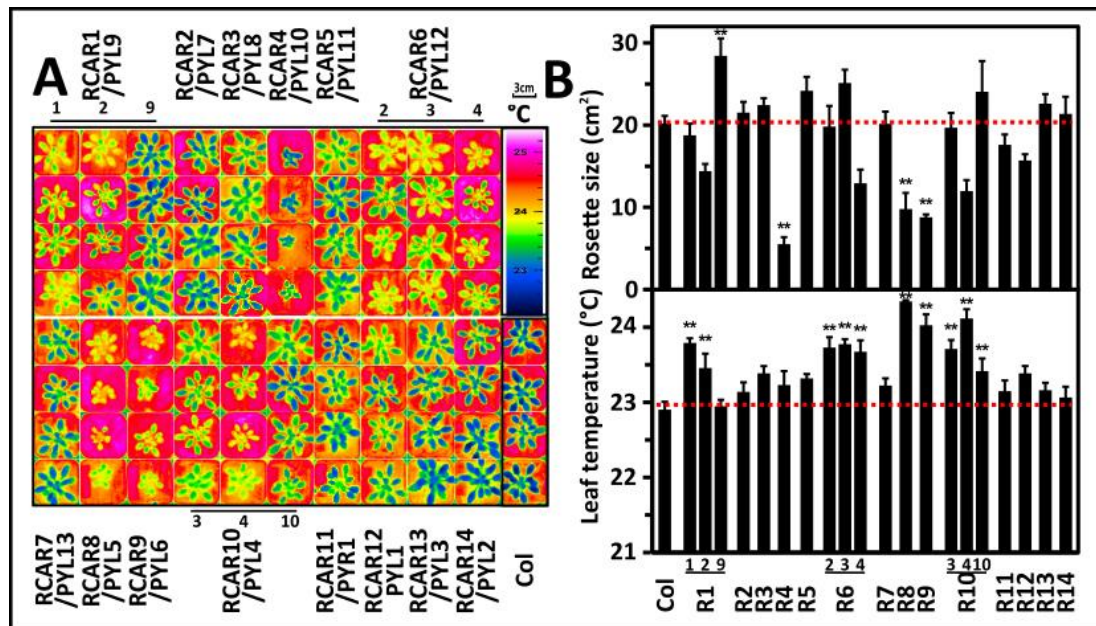


Figure 3-5 Overexpression of ABA receptors affects growth and leaf temperatures of Arabidopsis Columbia lines. Plants homozygous for expressing the 14 ABA receptors (R1-R14; subscript numbers denote independent lines) under the constitutive viral promoter 35S, were analyzed for growth performance and leaf surface temperature. A) Thermogram of the plants grown for 40 days under short day conditions (8 hours light / 16 hours dark photoperiod) at photon flux density of  $150 \mu\text{mol m}^{-2} \text{s}^{-1}$  and  $22^\circ\text{C}$  and 50% relative humidity in daytime and  $17^\circ\text{C}$  and 60% relative humidity at night and in well-watered conditions (SWP  $\geq -0.02$  bar). Four plants were grown per line in separate pots at randomized positions and the thermal pictures were arranged in groups after imaging. B) Rosette size as projected leaf area and leaf temperatures from data shown in A). The threshold value of wild type Columbia (Col) is indicated by a dotted line.  $n=4$  biological replicates per line, mean  $\pm$  SEM.  $**P<0.001$  compared with wild type Col-0.

The selected lines were reanalyzed to confirm the first findings by using again thermal imaging and determining rosette size under the same conditions. The phenotypic assessment confirmed the considerable variations in both leaf surface temperatures and rosette sizes for ectopic expression RCAR lines (Fig. 3-5 A-C). It also confirmed that the Arabidopsis lines RCAR1-1, RCAR6-3 and RCAR10-3 combined higher leaf temperatures with no or minor growth trade-offs, while the RCAR8 and RCAR9 lines showed higher leaf surface temperatures associated with a severely reduced development of the leaf rosette (Fig. 3-5 A-C). Others, such as the RCAR11 to RCAR14 lines, showed no significant or marginal elevation of leaf temperatures and comparable rosette sizes to Col-0 (Fig. 3-5 A-C).

### 3.2.1.2 Water consumption

The variable leaf surface temperatures and rosette sizes of the ectopic expression of

## Results

RCARs under well-watered conditions are indications of different water consumption patterns in the long run. During the progressive drought, the weight of the pots was measured in five-day intervals. Col-0 consumed  $17 \text{ g} \pm 1 \text{ g}$  soil water during the first three weeks, and water consumption increased rapidly to  $129 \text{ g} \pm 1 \text{ g}$  in the subsequent three weeks. Thereafter,  $18 \text{ g} \pm 1 \text{ g}$  water was used until the end of the progressive drought because plants were subjected severe drought stress (see section 2.2.3 Fig. 2-2A and B) and leaves started wilting (see section 3.2.1.3 Fig. 3-7A). 50% of total water consumption of Col-0 occurred at the fifth week, while overexpressing RCAR lines showing elevated leaf surface temperatures and reduced rosette sizes (see Fig. 3-5A-B) displayed at least one week delay for 50% water use, especially RCAR1-1, RCAR1-2 and RCAR4-1 (subclade I), and RCAR6, RCAR8-5, RCAR9-4, RCAR10-3, and RCAR10-4 (subclade II) (Fig. 3-6 A-C). At the end of the

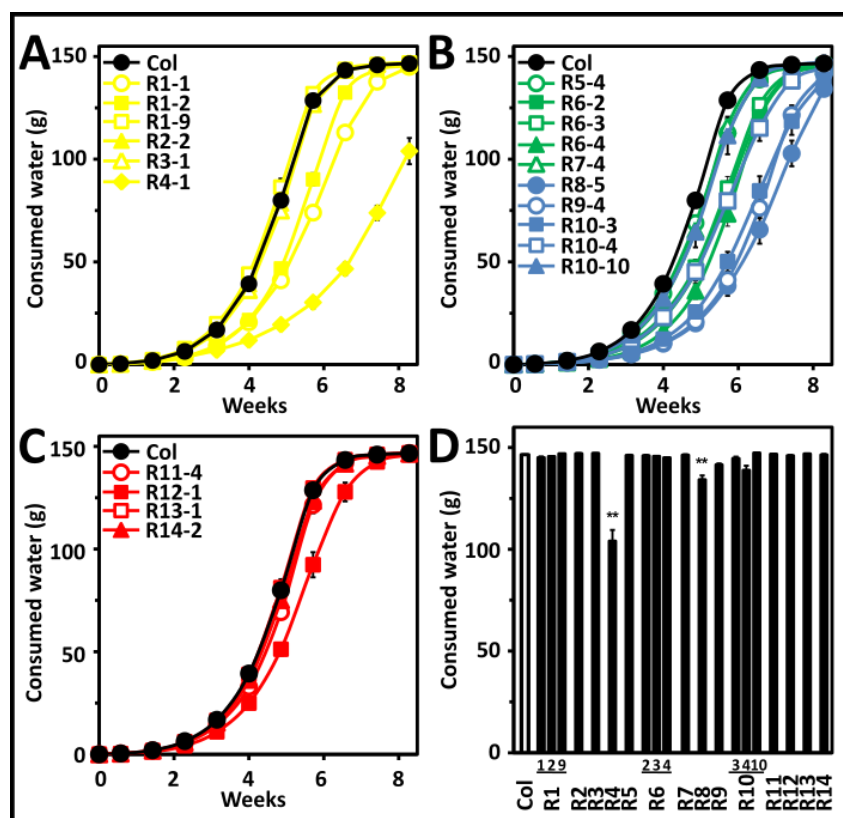


Figure 3-6 Water consumption of RCAR lines under progressive drought. Water consumption in wild type Columbia (black symbols), RCAR1-4 lines (R1-R4, yellow symbols) A), RCAR5-7 (R5-R7, green symbols) and RCAR8-10 (R8-R10, blue symbols) B) and RCAR11-14 (R11-R14, red symbols) C). The line numbers are indicated after the corresponding name of each RCAR. Total water consumption of wild type Columbia (white column) and overexpressing RCAR lines (R1-R14, sub-numbers denote independent lines) are shown in D). Single plantlets were grown for 18 days prior to the discontinuation of watering at soil water potential SWP = -0.02 bar. Plants were grown randomly in 24-pot trays in a single experiment. Growth condition as described in Figure 3-5. A-D) n=4 biological replicates, mean  $\pm$  SEM. \*\*P<0.001 compared

with wild type Col.

progressive drought, Col-0 totally consumed  $146 \text{ g} \pm 0.1 \text{ g}$  water and all other plants had consumed comparable plant-accessible water in the pots (Fig. 3-6D) because the amount of water designed cannot meet their whole-life-cycle water demands except RCAR4-1 and RCAR8-5 (Fig. 3-6D).

### 3.2.1.3 Biomass accumulation and WUE

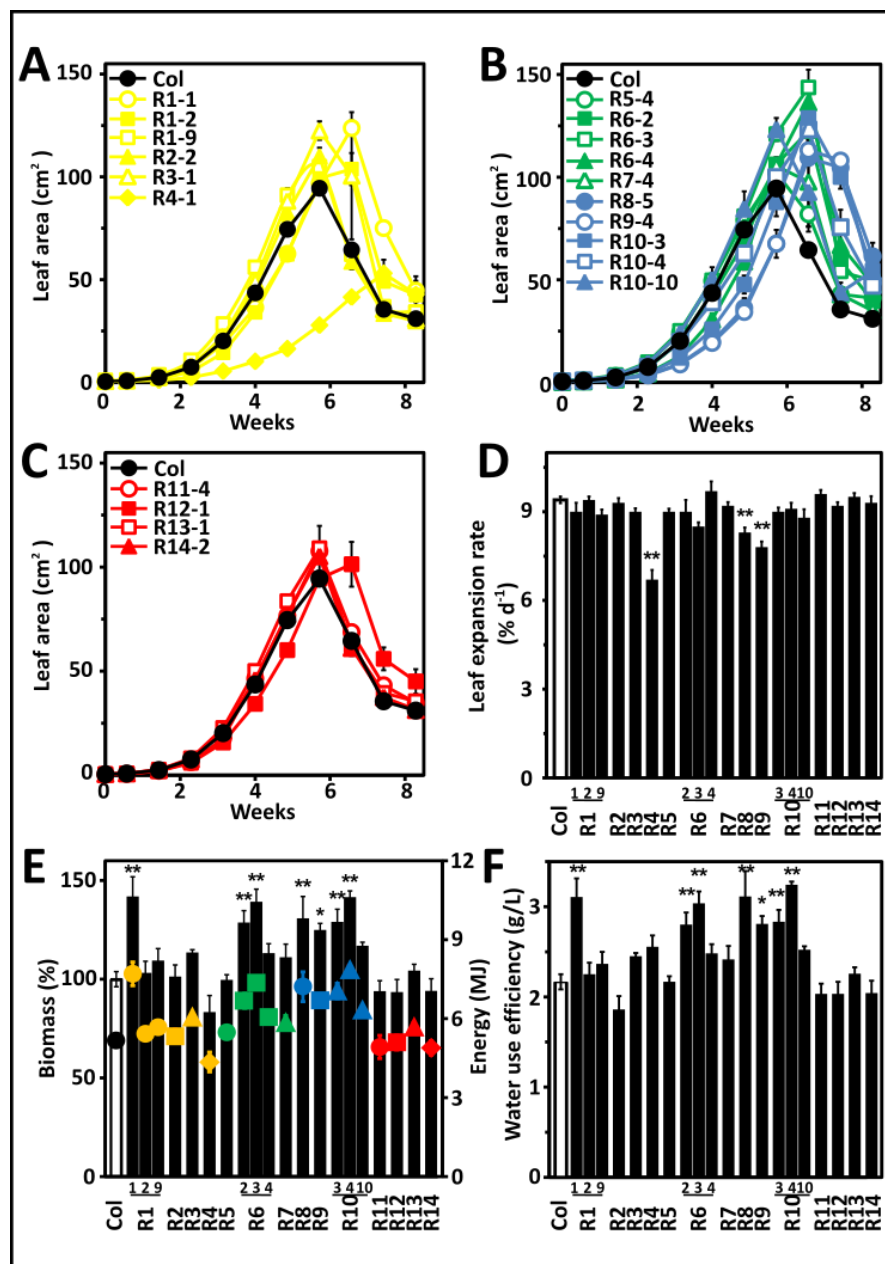


Figure 3-7 Water productivity conferred by ectopic expression of ABA receptors. Dynamic change in projected leaf area of wild type Columbia (black symbols), RCAR1-4 lines (R1-R4, yellow symbols) A), RCAR5-7 (R5-R7, green symbols) and RCAR8-10 (R8-R10, blue symbols)

## Results

---

B) and RCAR11-14 (R11-R14, red symbols) C). The numbers of independent lines are indicated after the corresponding name of each RCAR. D) Maximum leaf expansion rate of wild type Columbia (white column) and overexpression RCAR lines (black columns). E) Above-ground biomass (in percentage of the total dry weight of wild type; columns; Columbia (Col-0) accounted for 0.31 g  $\pm$  0.01 g dry weight per plantlet) and calorimetric yield (energy; symbols) and F) WUE (dry biomass in grams per liter of water consumed) of Arabidopsis plantlets expressing RCAR1 to RCAR14 (R1 to R14, sub-numbers denote independent lines) at the end of drought. Experimental design and plant growth condition as described in Fig. 3-5. A-E) n=4 biological replicates per data point, mean  $\pm$  SEM. \*\*P<0.001 compared with wild type.

Biomass is the sum of a plant's organic matters and is formed mainly through photosynthesis. Owing to the inherent association between carbon assimilation and transpiration, different water consumption patterns can differently impinge on growth patterns under progressive drought. During the progressive drought, the projected leaf area ( $L_p$ ) was measured at five-day intervals. Col-0 showed an increase of leaf area from 0.5 cm<sup>2</sup>  $\pm$  0.1 cm<sup>2</sup> to 94 cm<sup>2</sup>  $\pm$  2 cm<sup>2</sup> in six weeks, with a maximum leaf expansion rate of 9.4 % d<sup>-1</sup>  $\pm$  0.2 % d<sup>-1</sup> during day 0 to day 22. At the end of the experiment, there was a decline of leaf area (Fig.3-7A-D). Reduced leaf area is the consequence of shrinkage of leaves because of loss of turgor in cells during severe drought (Bray, 1997). Overexpressing RCAR lines exhibited different patterns in leaf expansion compared with Col-0 (Fig.3-7A-D). Lines such as RCAR4-1, RCAR8-5, and RCAR9-4 had up to 30% lower maximum leaf expansion rate and showed considerable variations in the maximum leaf area. Some RCARs had both maximum leaf expansion rates and maximum leaf area comparable to Col-0, for example, RCAR2-2, RCAR3-1 (subclade I) and RCAR11-4 to RCAR14-2 (subclade III). Others combined equivalent or only marginally lower growth rate with a higher maximum leaf area, especially RCAR1-1, RCAR6 and RCAR10, which were up to 52% larger. The above-ground dry biomass measurement was consistent with maximum leaf area. RCAR1-1 (subclade I), RCAR6, RCAR8-5, RCAR9-4 and RCAR10 (subclade II) generated up to 40% enhanced biomass in comparison with Col-0, while others showed little or no increase (Fig. 3-7E). In agriculture, farmers pursue a high yield from crops, while in industry, energy is a major concern. Dry biomass samples of all lines were combusted to determine the energy (calorie of the biomass). Col-0 generated 5.2 MJ  $\pm$  0.2 MJ energy by using 146 g water. Overexpressing RCAR lines that showed higher biomass gains generated as much as 40% more energy than Col-0 under comparable growth conditions (Fig. 3-7E). WUE evaluates plants' ability to generate biomass per unit of water given them. Because all lines consumed almost the same amount of water in



the progressive drought, overexpression RCAR lines producing more biomass reflected higher WUE. Indeed, lines like RCAR1-1, RCAR6, RCAR8, RCAR9 and RCAR10 had a WUE that was up to 40% higher than Col-0 (Fig. 3-7F).

### 3.2.1.4 Water use efficiency determined by using stable isotopes

Stable isotopes are powerful tools for tracing biogeochemical processes across spatiotemporal scales, due to isotope effects (Yakir and Sternberg, L. da S. L., 2000). Binary gas diffusions through stomatal pores and carbon assimilation during photosynthesis can be traced by analysis of the abundance of carbon isotopes ( $^{12}\text{C}$  and  $^{13}\text{C}$ ) and oxygen isotopes ( $^{16}\text{O}$  and  $^{18}\text{O}$ ) in plant organic matter (Farquhar *et al.*, 1989; Werner *et al.*, 2012). The compositions of stable carbon isotopes ( $\delta^{13}\text{C}$ ) and oxygen isotopes ( $\delta^{18}\text{O}$ ) in plant organic matter differ from their compositions in the atmosphere and soil water, which implies a discrimination of  $^{13}\text{C}$  and an enrichment of  $^{18}\text{O}$  isotopes ( $\Delta^{13}\text{C}$  and  $\Delta^{18}\text{O}$ ) during processes of carbon and oxygen incorporation

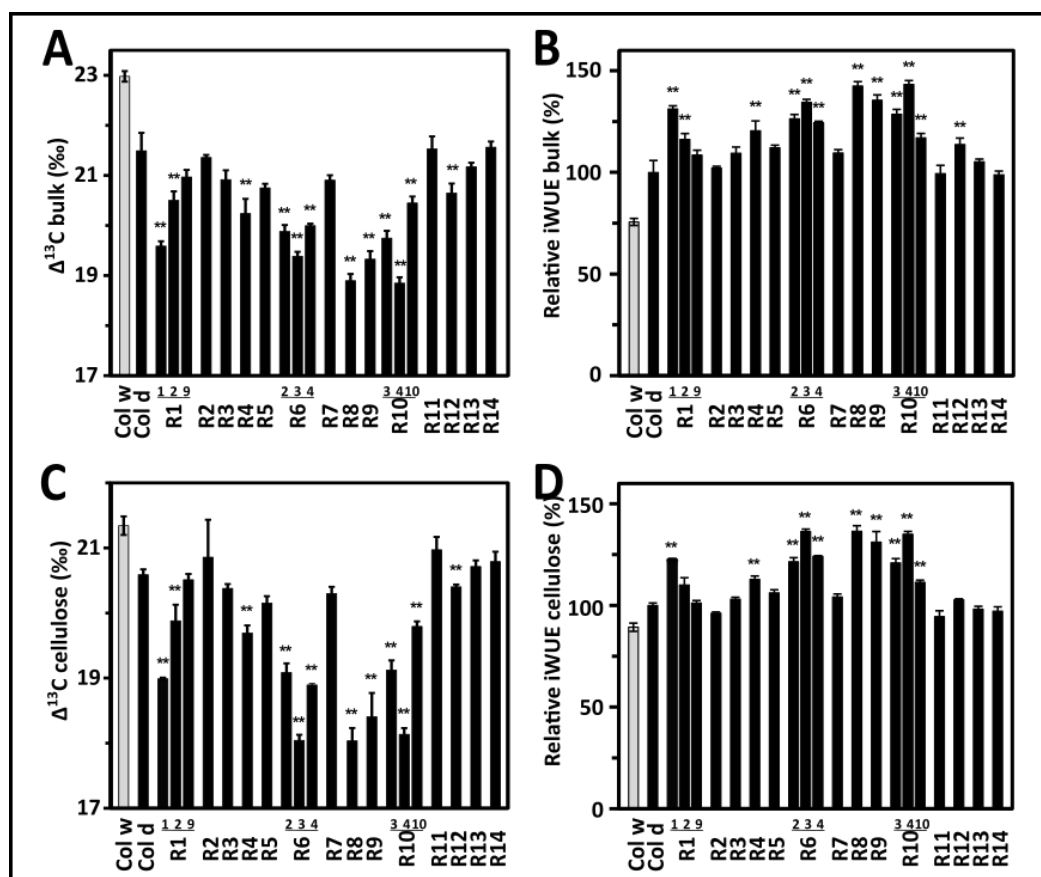


Figure 3-8 Carbon isotope composition ( $\delta^{13}\text{C}$ ), carbon isotope discrimination ( $\Delta^{13}\text{C}$ ) and integrated WUE conferred by ectopic expression of RCAR receptors. A) Bulk  $\Delta^{13}\text{C}$  ( $\Delta^{13}\text{C}_{\text{bulk}}$ ), B) bulk-derived integrated WUE and C)  $\Delta^{13}\text{C}_{\text{cellulose}}$  and D) integrated WUE of extracted cellulose

## Results

---

fractions using plants' dry materials shown in Fig. 3-7E. Wild type Columbia grown under well-watered conditions was introduced as an additional control (gray column, Col w). Integrated WUE values shown in B) and D) were relative to Columbia grown in progressive drought conditions (Col d),  $70 \mu\text{mol mol}^{-1} \pm 8 \mu\text{mol mol}^{-1}$  in bulk and  $80 \mu\text{mol mol}^{-1} \pm 1 \mu\text{mol mol}^{-1}$  in extracted cellulose fractions respectively. A-D) RCAR1 to RCAR14 (R1 to R14, sub-numbers denote independent lines). n=4 biological replicates per data point, mean  $\pm$  SEM. \*\*P<0.001 compared with Col d.

into plant biomass. Drought induces stomatal closure, resulting in less discriminations of  $^{13}\text{C}$  and more enrichment of  $^{18}\text{O}$  during the gas diffusive processes and biochemical processes (Farquhar *et al.*, 1989; Farquhar *et al.*, 2007; Silva *et al.*, 2015). As a consequence, the organic matter of plants with more closed stomata have distinct signatures of carbon and oxygen isotopes compared with those well-watered plants with open stomata. The plant material harvested after the drought experiment were analyzed for the abundance of carbon and oxygen isotopes. Harvested Col-0 plants that had experienced progressive drought discriminated  $21.5 \text{‰} \pm 0.4 \text{‰} \text{ }^{13}\text{C}$ , which was  $1.5 \text{‰} \pm 0.4 \text{‰}$  less than the well-watered Col-0 (Fig. 3-8A). The  $\Delta^{13}\text{C}_{\text{bulk}}$  in ectopic RCAR expression lines displayed less discrimination, especially in RCAR1, RCAR6, RCAR8, RCAR9 and RCAR10, which differed from Col-0 (drought) by at least  $1.5 \text{‰} \pm 0.04 \text{‰}$ . Furthermore, carbon isotope discrimination provides information on the ratio of  $\text{CO}_2$  in the intercellular space to that in the atmosphere (see equation 4 in section 2.2.8). This ratio, in turn, facilitates the calculation of integrated WUE over a certain growth period (see equation 3 in section 2.2.8), which is negatively correlated with  $\Delta^{13}\text{C}_{\text{bulk}}$  (Billings *et al.*, 1989; Farquhar and Richards, 1984b). Indeed, overexpressing RCARs showing less  $\Delta^{13}\text{C}_{\text{bulk}}$  than Col-0 (drought) had a bulk-derived integrated WUE that was enhanced by up to 43% (Fig. 3-8B). Different plant fractions have different carbon isotope compositions ( $\delta^{13}\text{C}$ ) (Park and Epstein, 1961). Among these,  $\delta^{13}\text{C}$  in cellulose is relatively stable and reflects the isotopic compositions of the primary products of photosynthesis (Hietz *et al.*, 2005). Results of cellulose-derived carbon isotope discrimination ( $\Delta^{13}\text{C}_{\text{cellulose}}$ ) indicated that all lines discriminated less  $^{13}\text{C}$  and had higher integrated WUE than did the bulk materials (Fig. 3-8C-D). RCAR overexpression lines with less  $\Delta^{13}\text{C}_{\text{bulk}}$  also showed less  $\Delta^{13}\text{C}_{\text{cellulose}}$  compared with Col-0 (drought), and therefore achieved a higher cellulose-derived integrated WUE, especially the lines RCAR1-1, RCAR6, RCAR8, RCAR9, and RCAR10 (Fig. 3-8C-D).

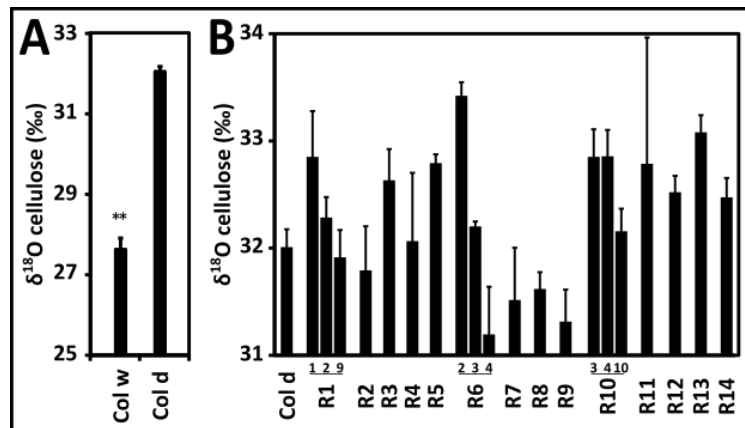


Figure 3-9 Oxygen isotope composition ( $\delta^{18}\text{O}$ ) in extracted cellulose fractions conferred by ectopic expression of RCAR receptors. Oxygen isotope composition ( $\delta^{18}\text{O}_{\text{cellulose}}$ ) was determined using extracted cellulose fractions of A) wild type Columbia grown in well-watered conditions (Col w) and in progressive drought (Col d), and of B) ectopic RCAR lines expression grown in progressive drought. A-B)  $n=4$  biological replicates per data point, mean  $\pm$  SEM. \*\* $P<0.001$  compared with Col d.

It has been suggested that oxygen isotope composition ( $\delta^{18}\text{O}$ ) in plant organic matters may reflect leaf evaporative conditions (Barbour and Farquhar, 2000; Dongmann *et al.*, 1974). Higher transpiration leads to less enrichment of  $^{18}\text{O}$  and therefore less  $\delta^{18}\text{O}$  in plant cellulose under controlled VPD conditions (Barbour and Farquhar, 2000). Drought induces stomatal closure, reducing plant transpiration. As a result, more  $^{18}\text{O}$  is enriched, resulting in more  $\delta^{18}\text{O}$  is incorporated into plant cellulose. Consistent with this theory, the oxygen isotope composition of Col-0 in drought was  $32 \text{‰} \pm 0.2 \text{‰}$ , which is  $4.4 \text{‰} \pm 0.2 \text{‰}$  higher than Col-0 grown in well-watered conditions (Fig. 3-9A). RCAR overexpression lines that showed higher leaf surface temperatures (meaning lower transpiration) in well-watered conditions were expected to have an enrichment of  $^{18}\text{O}$  and higher values of  $\delta^{18}\text{O}$  in plant cellulose, and vice versa. However,  $\delta^{18}\text{O}$  in overexpression RCAR lines varied considerably. Lines possessing higher leaf temperatures such as RCAR1-1, RCAR6-3 and RCAR10-4 displayed higher values of  $\delta^{18}\text{O}$  than Col-0 (Fig. 3-9B; Fig. 3-5A-B). In contrast, RCAR8 and RCAR9 which also had higher leaf temperatures displayed reduced  $\delta^{18}\text{O}$  compared with Col-0 (Fig. 3-9B; Fig. 3-5A-B). The contrasting results were also observed for RCARs in subclade III which had comparable leaf temperatures but exhibited higher value of  $\delta^{18}\text{O}$  (Fig. 3-9B; Fig. 3-5A-B).

### 3.2.1.5 Associations among biomass gain, leaf surface temperatures, leaf growth and WUE

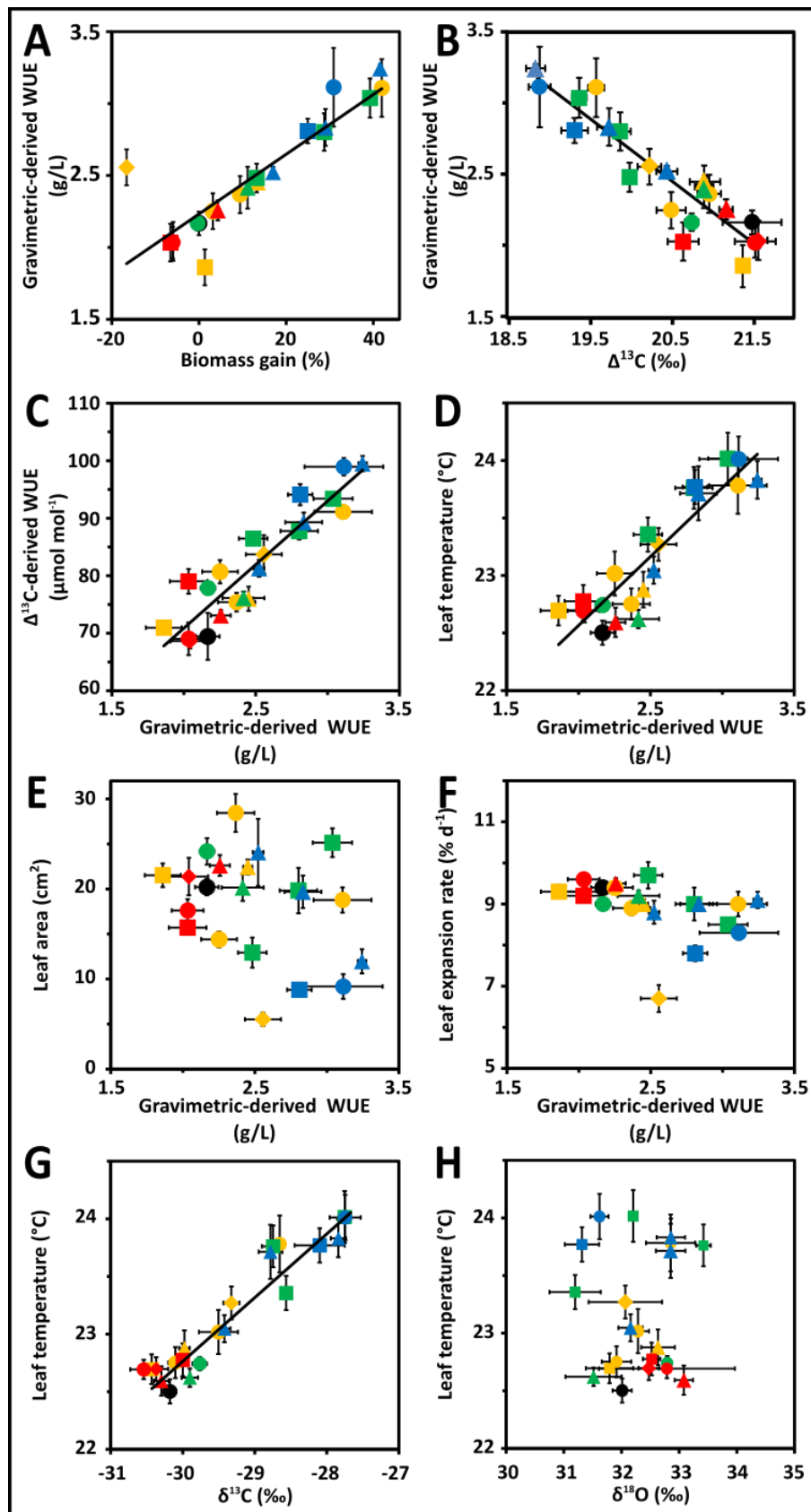


Figure 3-10 Associations among biomass gain, leaf surface temperatures, leaf growth and WUE in Arabidopsis lines overexpressing RCARs. A) Association of gravimetric-derived integrated WUE with biomass gain (percentage increase compared with Col, Col accumulated  $0.31 \text{ g} \pm 0.01 \text{ g}$  dry biomass and biomass gain was set to 0%). B) Association of gravimetric-derived integrated WUE with bulk-derived  $^{13}\text{C}$  discrimination ( $\Delta^{13}\text{C}_{\text{bulk}}$ ). C) Association of gravimetric-derived integrated WUE with  $\Delta^{13}\text{C}_{\text{bulk}}$ -derived integrated WUE. Association of gravimetric-derived integrated WUE with D) leaf temperatures and with E) leaf area of plantlets grown under well-watered conditions at day 22 (SWP > -0.03bar) and with F) maximum leaf expansion rate during progressive drought. Association of leaf temperature with G)  $\delta^{13}\text{C}$  and H)  $\delta^{18}\text{O}$  during progressive drought. A-H) Symbols as described in Fig. 3-7E. Growth conditions as described in Fig. 3-5. n=4 biological replicates per data point, mean  $\pm$  SEM.

Further analysis of the growth performance, biomass accumulation, and integrated WUE in RCAR overexpression lines exposed to progressive drought revealed that gravimetric-derived integrated WUE correlated positively with biomass gain (Fig. 3-10A,  $R = 0.88$ ,  $P < 0.001$ ). The gravimetric-derived integrated WUE showed a strong negatively correlation to  $\Delta^{13}\text{C}_{\text{bulk}}$  and a positive correlation with  $\Delta^{13}\text{C}_{\text{bulk}}$ -derived integrated WUE (Fig. 3-10B,  $R = 0.92$ ,  $P < 0.001$  and C,  $R = 0.92$ ,  $P < 0.001$ ). These associations reveal that most of the RCAR lines have higher integrated WUE than Col-0, especially the lines of overexpression RCAR1, RCAR6, RCAR8, RCAR9, and RCAR10. It was also found that gravimetric-derived integrated WUE was associated positively with leaf temperatures in well-watered conditions (Fig. 3-10D,  $R = 0.91$ ,  $P < 0.001$ ), but not with leaf area or maximum leaf expansion rate in the same conditions (Fig. 3-10E,  $R = 0.31$ ,  $P = 0.169$  and F,  $R = 0.4$ ,  $P = 0.073$ ). RCAR1-1, RCAR6-2, RCAR6-3, and RCAR10-3 all combined elevated leaf surface temperatures with no or minor trade-offs in growth, while RCAR8, RCAR9, and RCAR10-4 all had increased leaf surface temperatures at the expense of some reduction in growth. Taken together, lines such as RCAR1-1, RCAR6-2, RCAR6-3, and RCAR10-3 were capable of increasing their leaf surface temperatures and WUE with little or no reduction in growth. The associations among leaf temperature, biomass gain and leaf growth were further corroborated by an independent experiment (see Appendix Fig. 5-2A-B).

In addition,  $\delta^{18}\text{O}$  in the plant's organic matter can be used to access the time-integrated leaf water loss through stomata during its growth period. However, although The leaf temperature displayed a strong correlation with  $\delta^{13}\text{C}$  (Fig. 3-10G,  $R = 0.96$ ,  $P < 0.001$ ), it did not correlate with  $\delta^{18}\text{O}$  (Fig. 3-10H,  $R = 0.01$ ,  $P = 0.096$ ). This observation is not consistent with a negative correlation between  $\delta^{18}\text{O}$  of the organic

matter and transpiration rate reported in wheat (a positive correlation between  $\delta^{18}\text{O}$  of the organic matter and leaf temperature) (Barbour *et al.*, 2000; Barbour and Farquhar, 2000; Cabrera-Bosquet *et al.*, 2009).

### 3.2.1.6 Water productivity conferred by overexpression of RCAR1, RCAR6, and RCAR10

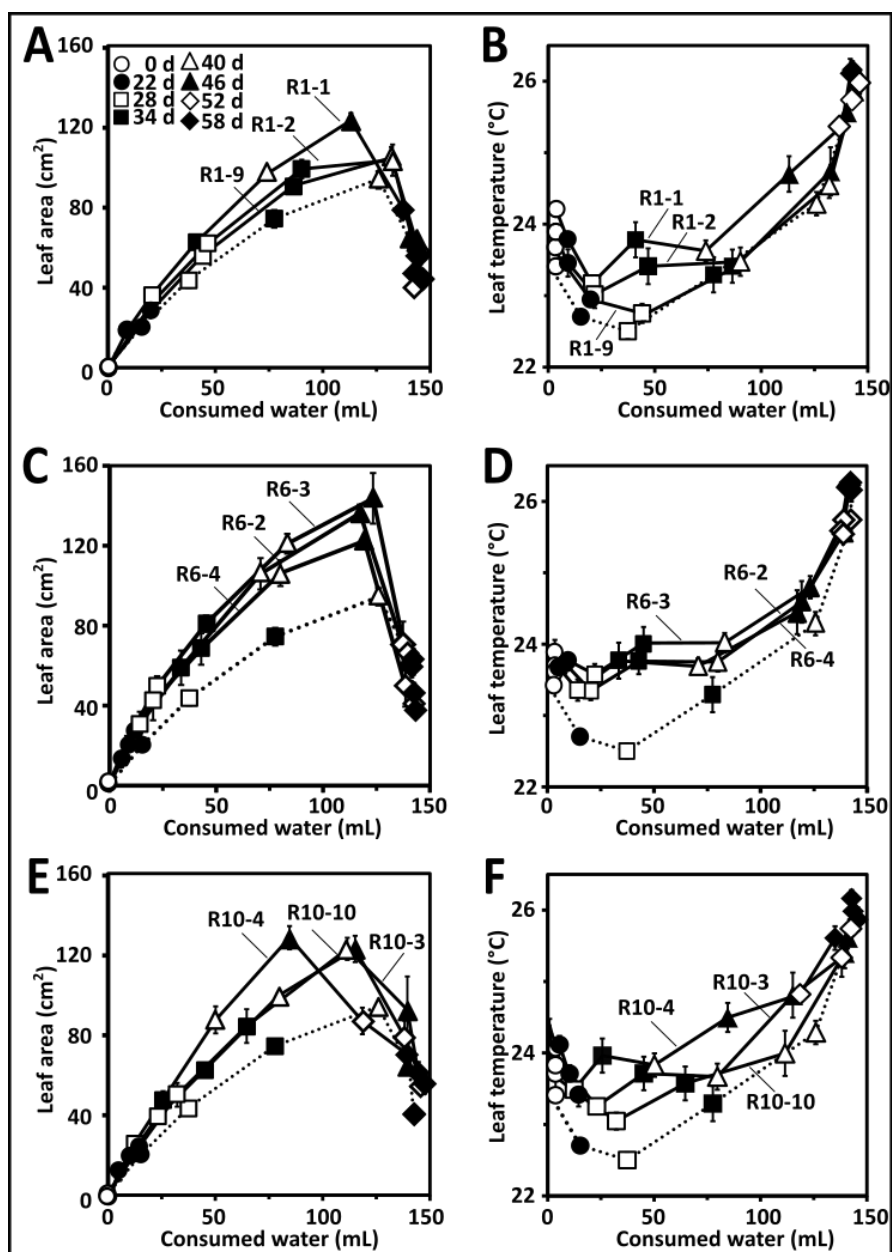


Figure 3-11 Water productivity conferred by overexpression of ABA receptor RCAR1, RCAR6, and RCAR10 during progressive drought. Leaf area and leaf surface temperatures plotted against plant water use for three independent lines from RCAR1 (solid lines) A-B), RCAR6 (solid lines) C-D), RCAR10 (solid lines) E-F) and wild type Columbia (dotted lines). Leaf area was expressed as projected rosette size. Wilting leaves caused the reduction in rosette size. A-E) Symbols shown at the left top corner of Fig. 3-11A represents days after discontinuation

of watering. Growth conditions as described in Fig. 3-5. n=4 biological replicates per data point, mean  $\pm$  SEM.

Gravimetric-derived WUE and  $\Delta^{13}\text{C}$ -derived WUE provide an integrated measure of WUE throughout the whole period of progressive drought, while changes in leaf area in response to consumed water indicate integrated WUE in different development stages throughout the progressive drought except during leaf wilting (at the prerequisite of the positive correlation between leaf area and biomass; see section 3.1.1 Fig. 3-1D). Overexpression lines of RCAR1, RCAR6 and RCAR10 showed an increased leaf area compared to Col-0 when consuming the same amount of water, which indicated enhanced WUE during the course of progressive drought (Fig. 3-11A, C, E). That is to say, to generate the same leaf area, RCAR1, RCAR6 and RCAR10 consumed less water. The reduced water consumptions were consistent with elevated leaf surface temperatures for those lines (Fig. 3-11B, D, F).

### **3.2.1.7 Insight into mechanisms by gas exchange analysis**

Certain ectopic expression of RCARs, like RCAR1, RCAR6, and RCAR10 have been proven to confer Arabidopsis plants an enhanced WUE. Some lines, like RCAR6-2, RCAR6-3, and RCAR10-3, combined this higher WUE with little or no growth penalty, while some lines, such as RCAR6-4 and RCAR10-4 showed reduced growth under well-watered conditions. To further explore the mechanisms of enhanced WUE conferred by overexpressing RCARs, RCAR6-3 and RCAR10-4 were chosen as candidates to analyze the physiological basis of water productivity. Both selected Arabidopsis lines consistently performed better in reiterated and independently conducted experiments (see Appendix Fig. 5-3).

#### **3.2.1.7.1 Stomatal limitation**

##### **3.2.1.7.1.1 Estimation of $g_s$ , $A_n$ and $C_i$ in well-watered conditions and during progressive drought**

Gas exchange system provides instantaneous measurements of transpiration rate ( $E$ ), stomatal conductance ( $g_s$ ), net carbon assimilation rate ( $A_n$ ), and intercellular  $\text{CO}_2$  concentration ( $C_i$ ). Performing gas exchange measurements under plants' growth conditions and comparing these parameters facilitate to reveal the physiological basis of plants' WUE. In this study, gas exchange analysis was conducted using

well-watered, 31 days  $\pm$  1 day old Arabidopsis plants at a photon flux density of 150

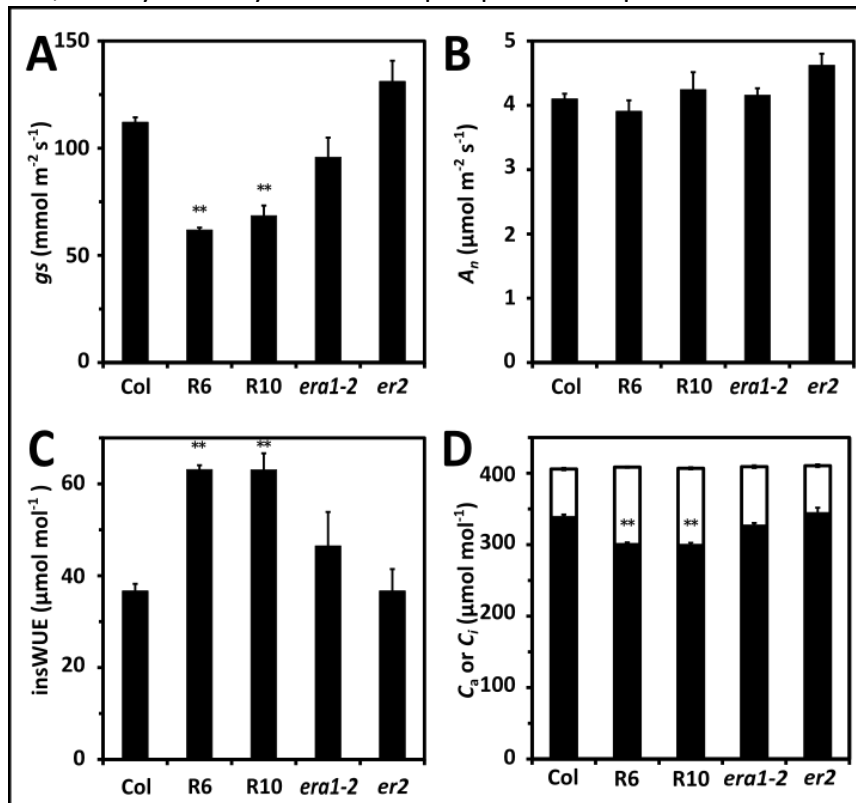


Figure 3-12 Gas exchange analysis revealed enhanced water productivity conferred by ectopic expression of RCAR6 and RCAR10 under well-watered conditions. Stomatal conductance ( $g_s$ ) A) and net carbon assimilation rate ( $A_n$ ) B) with whole rosette measurements of wild type Columbia (Col), RCAR6-3 (R6) and RCAR10-4 (R10) were determined at photon flux density of 150  $\mu\text{mol m}^{-2} \text{s}^{-1}$ , 420  $\mu\text{mol mol}^{-1}$  external  $\text{CO}_2$  and vapor pressure deficit of 13 Pa  $\text{kPa}^{-1} \pm 2$  Pa  $\text{kPa}^{-1}$ . Farnesyltransferase-deficient mutant *era1-2*, which is regarded as drought resistant, and Erecta mutant *er2*, which has been proven to transpire more water, were also analyzed as additional controls. Instantaneous water use efficiency (InsWUE) C) defined as the ratio of  $A_n$  to  $g_s$  and D)  $\text{CO}_2$  concentration at ambient ( $C_a$ , white columns) and intercellular  $\text{CO}_2$  concentration ( $C_i$ , black columns) were determined. Plants of age 31 days  $\pm$  1 day old grown under well-watered conditions (SWP  $\geq -0.02$  bar) were used to perform the gas exchange analysis. All plants were grown under short day conditions (8 hours light / 16 hours dark photoperiod) at photon flux density of 150  $\mu\text{mol m}^{-2} \text{s}^{-1}$  and 22°C and 50% relative humidity in the daytime, and 17°C and 60% relative humidity at night. A-D)  $n=4$  biological replicates with three technical replicates, mean  $\pm$  SEM, \*\* $P < 0.001$  compared with wild type Col.

$\mu\text{mol m}^{-2} \text{s}^{-1}$ , 420  $\mu\text{mol mol}^{-1}$  external  $\text{CO}_2$  and vapor pressure deficit of 13 Pa  $\text{kPa}^{-1} \pm 2$  Pa  $\text{kPa}^{-1}$ . Two additional controls were included in this assay. The Arabidopsis Erecta mutant *er2*, which has been reported to have an increased transpiration rate (Masle *et al.*, 2005), showed comparable instantaneous water use efficiency (insWUE) owing to a concurrent increase of  $g_s$  and  $A_n$  compared with Col-0, whereas the farnesyltransferase-deficient mutant *era1-2*, considered to be drought resistant (Pei,



1998), displayed an insWUE enhanced by a factor of 1.3 (Fig. 3-12A-C). Gas exchange analysis of RCAR6-3 and RCAR10-4 lines showed up to 45% reduced  $g_s$  but  $A_n$ , which resulted in almost double insWUE (Fig. 3-12A-C). Stomatal pores allow gas diffusion from ambient to intercellular air space. This process follows Fick's law of diffusion. The amount of  $\text{CO}_2$  diffused into the stomatal cavity depends on both stomatal resistance ( $r_s$ ) which is the reciprocal of  $g_s$ , and the  $\text{CO}_2$  gradient between ambient ( $C_a$ ) and intercellular space ( $C_i$ ). The equation (6) can be written as  $A_n = (C_a - C_i) / r_s$  or  $A_n = (C_a - C_i) / (1 / g_s)$ . To maintain comparable  $A_n$  in RCAR6-3 and RCAR10-4 with Col-0, an increase in  $\text{CO}_2$  gradient ( $C_a - C_i$ ) is needed to compensate for the reduced  $g_s$ . Indeed, both RCAR6-3 and RCAR10-4 lines had up to  $40 \mu\text{mol mol}^{-1}$  lower  $C_i$ , resulting in as much as a 60% increase in  $C_a - C_i$  (Fig. 3-12D).

### 3.2.1.7.1.2 Estimation of $g_s$ , $A_n$ and $C_i$ during progressive drought

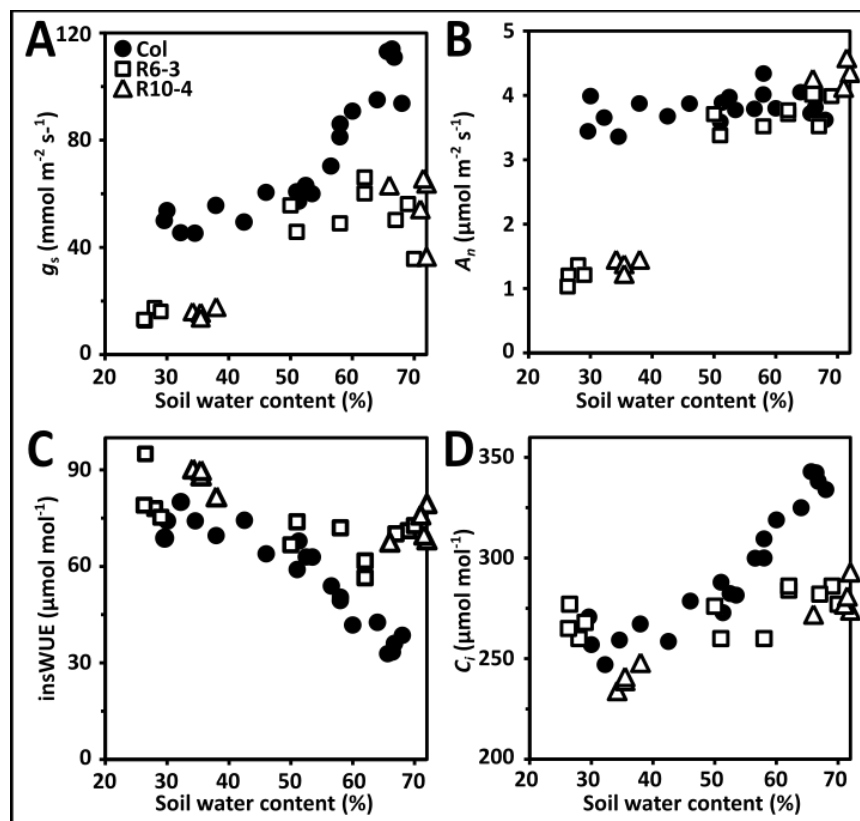


Figure 3-13 Gas exchange parameters and insWUE of Columbia (filled circles), R6 (open squares) and R10 (open triangles) at various soil water contents. The stomatal conductance ( $g_s$ ) A) and net carbon assimilation rate ( $A_n$ ) B), InsWUE C) and  $\text{CO}_2$  concentration in intercellular space ( $C_i$ ) D) of whole rosettes were determined at photon flux density of  $150 \mu\text{mol m}^{-2} \text{s}^{-1}$ ,  $420 \mu\text{mol mol}^{-1}$  external  $\text{CO}_2$  and vapor pressure deficit of  $13 \pm 2 \text{ Pa kPa}^{-1}$ . Four plants for each line were used to conduct the gas exchange measurements. All plants were grown under short day conditions (8h light / 16h dark photoperiod) at photon flux density of  $150 \mu\text{mol m}^{-2} \text{s}^{-1}$  and  $22^\circ\text{C}$  and 50% relative humidity in the daytime and  $17^\circ\text{C}$  and 60%

relative humidity at night. A-D) n=4 biological replicates. Single measurements for each data point with three technical replicates.

The depletion of water from 70% to 30% soil water content under drought resulted in little reduction of  $A_n$  in Col-0, while  $g_s$  and  $C_i$  dropped consistently (Fig. 3-13A-C). The lack of response of the  $A_n$  to soil water content (Fig. 3-13B) was achieved by counterbalancing the reduced  $g_s$  (Fig. 3-13A) with an enhanced CO<sub>2</sub> gradient ( $C_a - C_i$ ). As a consequence, insWUE of Col-0 showed a linear increase from 33  $\mu\text{mol mol}^{-1}$  when soil water content was 70% to 80  $\mu\text{mol mol}^{-1}$  when it was 30% (Fig. 3-13C). In comparison with Col-0, the initially lower  $g_s$  (Fig. 3-13A) in both overexpression RCAR6-3 and RCAR10-4 lines and the higher CO<sub>2</sub> gradient ( $C_a - C_i$ ) caused by a lower  $C_i$  (Fig. 3-13D) resulted in comparable  $A_n$  (Fig. 3-13B), and hence a two-fold higher insWUE at the onset of progressive drought (Fig. 3-13C). However, below 50% soil water content,  $g_s$  of RCAR6-3 and RCAR10-4 dropped and showed lower values than Col-0 (Fig. 3-13A), while  $C_i$  was similar to Col-0 (Fig. 3-13D), which resulted in a reduced  $A_n$  (Fig. 3-13B), therefore the initial advantage of the higher insWUE was attenuated, and both RCAR6-3 and RCAR10-4 exhibited comparable insWUE (Fig. 3-13C).

### **3.2.1.7.2 Mesophyll conductance and photosynthetic biochemical limitations**

#### **3.2.1.7.2.1 Estimation of $g_m$ , $V_{c,\text{max}}$ , $J_{\text{max}}$ , $V_{\text{TPU}}$ using C3 plant photosynthesis model**

Stomata is not the only limiting factor affecting plants' photosynthesis. Before being assimilated by the Rubisco enzyme, CO<sub>2</sub> diffuses from intercellular space to the site of carboxylation (Flexas *et al.*, 2008). A lower  $C_c$  than  $C_i$  implies the existence of resistances along the internal CO<sub>2</sub> diffusion paths (Warren and Dreyer, 2006). This internal resistances ( $R_i$ ) is the reciprocal of internal conductance ( $g_i$ ), hereafter referred to as mesophyll conductance ( $g_m$ ), which was determined by both constant J and curve fitting methods in this study (Ethier and Livingston, 2004; Flexas *et al.*, 2007; Harley *et al.*, 1992; Sharkey *et al.*, 2007). In addition, the activity of Rubisco, the electron transport rate are also the limiting factors of photosynthesis. Gas exchange measurements that performed under plants' growth conditions provide instantaneous readouts of CO<sub>2</sub> uptake and H<sub>2</sub>O loss, but are not able to estimate the mesophyll conductance and the biochemical limitations. The model of C3 plant photosynthesis (Farquhar *et al.*, 1980) provides a way to examine these limitations by solving equations from the response of CO<sub>2</sub> uptake to intercellular CO<sub>2</sub>

concentrations ( $A-C_i$  curve) (see section 2.2.9.2).

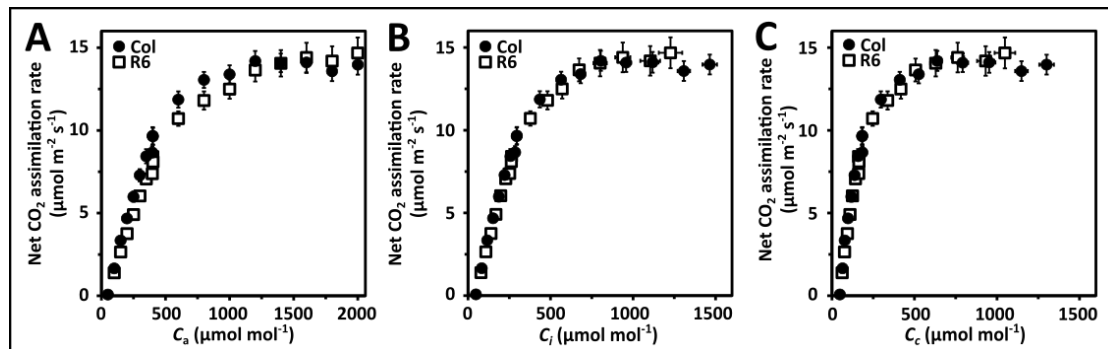


Figure 3-14 Gas exchange analysis using Columbia and RCAR6-3 lines under saturating light and variable ambient  $\text{CO}_2$  conditions. The relationship between A)  $A_n$  and  $C_a$ , B)  $A_n$  and  $C_i$ , C)  $A_n$  and  $C_c$  (curve fitting method derived  $C_c$ ) in wild type Columbia (Col) and overexpression RCAR6-3 (R6) plants. All curves were obtained with variable ambient  $\text{CO}_2$  concentration from  $50 \mu\text{mol mol}^{-1}$  to  $2000 \mu\text{mol mol}^{-1}$  and at photon flux density of  $1500 \mu\text{mol m}^{-2} \text{s}^{-1}$ .  $C_a$  was calculated based on the inlet and outlet  $\text{CO}_2$  concentration of leaf-clamped cuvette.  $C_i$  was determined according to the photosynthesis model developed by Farquhar *et al.*, (1980).  $C_c$  was estimated by using curve fitting method.  $23 \pm 2$  leaves from two-month-old plants grown under well-watered conditions ( $\text{SWP} \geq -0.02$  bar) were used to perform gas exchange analysis. Eight independent leaves from five plants of Col-0 and six independent leaves from five plants of R6 were chosen for gas exchange measurements. All plants were grown under short day conditions (8h light / 16h dark photoperiod) at a photon flux density of  $150 \mu\text{mol m}^{-2} \text{s}^{-1}$  and  $22^\circ\text{C}$  and 50% relative humidity in the daytime and  $17^\circ\text{C}$  and 60% relative humidity at night. A-C)  $n \geq 6$  biological replicates with six technical replicates, mean  $\pm$  SEM.

To understand whether overexpression RCAR6-3 differs from Col-0 in these limitations, the gas exchange measurements were performed using number  $23 \pm 2$  leaves from two-month-old Arabidopsis wild type Columbia and overexpressing RCAR6-3 plants under the light saturation ( $1500 \mu\text{mol m}^{-2} \text{s}^{-1}$ ) and variable ambient  $\text{CO}_2$  conditions. The  $A_n - C_a$  curve is hard to interpret itself owing to the responses are affected by stomatal, mesophyll and photochemical limitations, but this curve can be used to a straightforward comparison of  $A_n$  at any given ambient  $\text{CO}_2$  conditions. In this experiment, Col-0 exhibited slightly higher  $A_n$  than the RCAR6-3 line at the same ambient  $\text{CO}_2$  (Fig. 3-14A). The  $A_n - C_i$  curve eliminates the stomatal limitation, depending on mesophyll process and intrinsic capacity of photosynthesis. Parameterization of the model of C3 plant photosynthesis (Farquhar *et al.*, 1980) yielded a  $g_m$  of  $85 \text{ mmol m}^{-2} \text{s}^{-1} \pm 4 \text{ mmol m}^{-2} \text{s}^{-1}$  (Constant J method),  $87 \text{ mmol m}^{-2} \text{s}^{-1} \pm 6 \text{ mmol m}^{-2} \text{s}^{-1}$  (Curve fitting method), a  $V_{c,max\_C_i}$  of  $51 \mu\text{mol m}^{-2} \text{s}^{-1} \pm 2 \mu\text{mol m}^{-2} \text{s}^{-1}$ , a  $J_{max\_C_i}$  of  $70 \mu\text{mol m}^{-2} \text{s}^{-1} \pm 2.8 \mu\text{mol m}^{-2} \text{s}^{-1}$  and a  $V_{TPU\_C_i}$  of  $6 \mu\text{mol m}^{-2} \text{s}^{-1} \pm 0.8 \mu\text{mol m}^{-2} \text{s}^{-1}$  in Col-0 plants (Fig. 3-14B and Table 3-1). The overexpression RCAR6-3

## Results

line did not differ from Col-0 in  $g_m$ ,  $V_{c,max\_Ci}$ ,  $J_{max\_Ci}$  and  $V_{TPU\_Ci}$ . In addition, the maximum  $C_i$  and  $C_c$  of overexpression RCAR6-3, achieved at ambient  $CO_2$  of 2000  $\mu\text{mol mol}^{-1}$  were lowered by  $237 \mu\text{mol mol}^{-1} \pm 71 \mu\text{mol mol}^{-1}$  and  $253 \mu\text{mol mol}^{-1} \pm 62 \mu\text{mol mol}^{-1}$  lower respectively than those of Col-0 ( $1464 \mu\text{mol mol}^{-1} \pm 44 \mu\text{mol mol}^{-1}$  and  $1301 \mu\text{mol mol}^{-1} \pm 44 \mu\text{mol mol}^{-1}$ ) (Fig. 3-14B and C).

Table 3-1 Photosynthetic parameters of Columbia and RCAR6-3 deduced from  $A_n$ - $C_i$  curve at a saturating light. Mesophyll conductance,  $g_m$ ; the maximum velocity of carboxylation,  $V_{c,max\_Ci}$ ; the maximum capacity for electron transport,  $J_{max\_Ci}$ ; the velocity of triose phosphate utilization,  $V_{TPU\_Ci}$ , were calculated from the gas exchange on the basis of  $C_i$ . Different letters indicate statistically significant differences ( $P < 0.05$ ).

	$g_m$ ( $\text{mmol m}^{-2} \text{s}^{-1}$ )		$V_{c,max\_Ci}$	$J_{max\_Ci}$	$V_{TPU\_Ci}$
	Constant J	Curve fitting	( $\mu\text{mol m}^{-2} \text{s}^{-1}$ )	( $\mu\text{mol m}^{-2} \text{s}^{-1}$ )	( $\mu\text{mol m}^{-2} \text{s}^{-1}$ )
Col-0	$85 \pm 4$ a	$87 \pm 6$ a	$51 \pm 2.0$ a	$70 \pm 2.8$ a	$6 \pm 0.8$ a
R6-3	$76 \pm 5$ a	$84 \pm 7$ a	$49 \pm 3.4$ a	$70 \pm 3.4$ a	$4 \pm 0.1$ a

### 3.2.1.7.2.2 Compensation of reduced stomatal conductance by increased $CO_2$ gradient

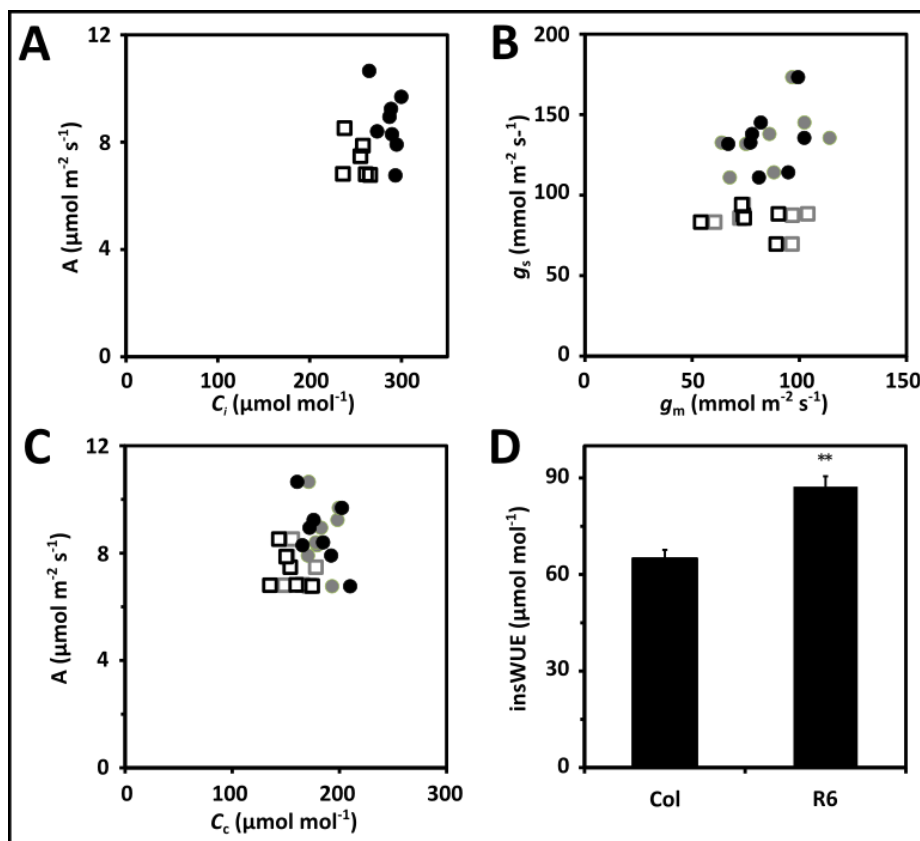


Figure 3-15 Compensation for reduced stomatal conductance ( $g_s$ ) by a steeper  $CO_2$  gradient between the atmosphere and chloroplast ( $C_a - C_i$ ). The RCAR6-3 line had a comparable net carbon assimilation rate ( $A_n$ ) to Col-0 and therefore achieved an enhanced insWUE under 91

well-watered conditions at light saturating during gas exchange measurements. The relationship between A)  $A_n$  and  $C_i$ , B)  $g_s$  and mesophyll conductance ( $g_m$ ), C)  $A_n$  and  $C_c$  of Col (filled circles), overexpression R6 (open squares). B-C) Black symbols were determined by constant J method and gray symbols by curve fitting method. Instantaneous water use efficiency (insWUE) D) was calculated after determination of  $A_n$  and  $g_s$ . Growth conditions as described in Fig. 3-14. Number  $23 \pm 2$  leaves from two-month-old plants grown under well-watered conditions (SWP  $\geq -0.02$  bar) were used to perform gas exchange analysis. Eight independent leaves from six plants of Col and six independent leaves from six plants of R6 were chosen to do gas exchange measurement. A-C) Single measurements with six technical replicates for each data point. D)  $n \geq 6$  biological replicates with six technical replicates, mean  $\pm$  SEM. \*\* $P < 0.001$  compared with wild type Col-0.

At an ambient  $\text{CO}_2$  of  $400 \mu\text{mol mol}^{-1}$  and light saturation conditions,  $A_n$ ,  $g_s$  and  $C_i$  of Col-0 averaged  $8.7 \mu\text{mol m}^{-2} \text{s}^{-1} \pm 0.4 \mu\text{mol m}^{-2} \text{s}^{-1}$ ,  $135 \text{mmol m}^{-2} \text{s}^{-1} \pm 7 \text{mmol m}^{-2} \text{s}^{-1}$  and  $286 \mu\text{mol mol}^{-1} \pm 4 \mu\text{mol mol}^{-1}$ , respectively (Fig. 3-15A-B). Using  $A_n$ ,  $C_i$  and estimated  $g_m$  (see Table 3-1),  $C_c$  can be solved according to the deformed equation (7) -  $A_n = (C_i - C_c) / r_m$  or  $A_n = (C_i - C_c) / (1 / g_m) -$ , based on which the  $C_c$  of Col-0 averaged  $183 \mu\text{mol mol}^{-1} \pm 6 \mu\text{mol mol}^{-1}$  (Constant J method) or  $184 \mu\text{mol mol}^{-1} \pm 4 \mu\text{mol mol}^{-1}$  (Curve fitting method) (Fig. 3-15C). Similarly,  $C_c$  of RCAR6-3 line was  $153 \mu\text{mol mol}^{-1} \pm 6 \mu\text{mol mol}^{-1}$  (Constant J method) or  $162 \mu\text{mol mol}^{-1} \pm 4 \mu\text{mol mol}^{-1}$  (Curve fitting method) (Fig. 3-15C). Compared with Col-0,  $A_n$ ,  $g_s$ ,  $C_i$ , and  $C_c$  of RCAR6-3 line displayed lower value, while  $g_m$  was comparable (Fig. 3-15A-C). Taken together, the total diffusive conductance of  $\text{CO}_2$  from atmosphere to the site of carboxylation ( $1 / (r_s + r_m)$  or  $1 / (1 / g_s + 1 / g_m)$ ) reduced by 23% (Constant J method) and 20% (Curve fitting method), and  $A_n$  showed 15% reduction (Fig. 3-15A-B). Combining the equation (6) and (7), the Fick's diffusion law can be deformed as  $A_n = (C_a - C_c) / (r_s + r_m)$  or  $A_n = (C_a - C_c) \times (1 / (1 / g_s + 1 / g_m))$ . The less reduction in  $A_n$  than total  $\text{CO}_2$  conductance can be explained by the compensation of 14% (Constant J method) or 11% (Curve fitting method) increased total  $\text{CO}_2$  gradient (Fig. 3-15A-C). As a consequence, RCAR6-3 line achieved  $35\% \pm 5\%$  enhanced insWUE in comparison to Col-0 (Fig. 3-15D).

### 3.2.1.7.2.3 Estimation of $g_m$ , $V_{c,\text{max}}$ , $J_{\text{max}}$ , $V_{\text{TPU}}$ using C3 plant photosynthesis model

Young leaves are more active than old ones during photosynthesis. An independent experiment was performed using  $16 \pm 3$  leaves two weeks after emergence under light saturation ( $1500 \mu\text{mol m}^{-2} \text{s}^{-1}$ ) and variable ambient  $\text{CO}_2$  conditions. The  $A_n - C_a$

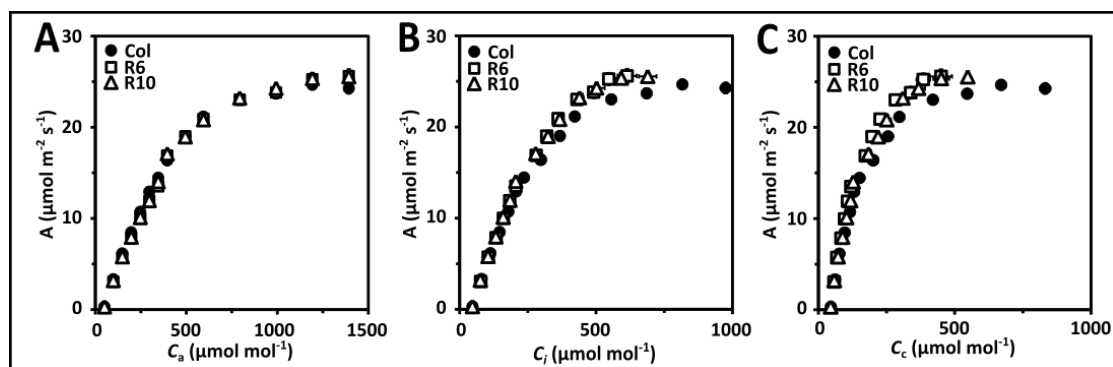


Figure 3-16 Gas exchange analysis using Columbia, RCAR6-3, and RCAR10-4 lines under saturating light and variable ambient CO<sub>2</sub> conditions. The relationship between A)  $A_n$  and  $C_a$ , B)  $A_n$  and  $C_i$ , C)  $A_n$  and  $C_c$  ( $C_c$  derived with curve fitting method) in wild type Columbia (Col) and the overexpression lines RCAR6-3 (R6) and RCAR10-4 (R10). All curves were obtained with variable ambient CO<sub>2</sub> concentration, from 50  $\mu\text{mol mol}^{-1}$  to 1500  $\mu\text{mol mol}^{-1}$ .  $C_a$  was calculated based on the inlet and outlet CO<sub>2</sub> concentration of leaf-clamped corvettes.  $C_i$  was determined according to the photosynthesis model developed by (Farquhar *et al.*, 1980).  $C_c$  was estimated using the curve fitting method. All plants were grown under short day conditions (8h light / 16h dark photoperiod) at photon flux density of 150  $\mu\text{mol m}^{-2} \text{s}^{-1}$  and 22°C and 50% relative humidity in the daytime and 17°C and 60% relative humidity at night. Number  $16 \pm 3$  leaves after two-week emergence in well-watered conditions (SWP  $\geq -0.02$  bar) were used to perform gas exchange analysis. Five independent leaves from five plants of Col-0 and R6, and six independent leaves from five plants of R10 were chosen for gas exchange measurements. A-C)  $n \geq 5$  biological replicates with six technical replicates, mean  $\pm$  SEM.

curve indicated that overexpression lines RCAR6-3 and RCAR10-4 had comparable values for  $A_n$  in response to the same  $C_a$ , compared with Col-0 (Fig. 3-16A). Both the  $A_n - C_i$  and  $A_n - C_c$  curves showed initially steeper slopes and slightly higher  $A_n$  in high  $C_i$  and  $C_c$  (Fig. 3-16B and C). Parameterization of the model of C3 plant photosynthesis (Farquhar *et al.*, 1980) yielded a  $g_m$  of  $172 \text{ mmol m}^{-2} \text{ s}^{-1} \pm 16 \text{ mmol m}^{-2} \text{ s}^{-1}$  (Constant J method) or  $169 \text{ mmol m}^{-2} \text{ s}^{-1} \pm 14 \text{ mmol m}^{-2} \text{ s}^{-1}$  (Curve fitting method), a  $V_{c,\text{max}_{C_i}}$  of  $91 \mu\text{mol m}^{-2} \text{ s}^{-1} \pm 4 \mu\text{mol m}^{-2} \text{ s}^{-1}$ , a  $J_{\text{max}_{C_i}}$  of  $122 \mu\text{mol m}^{-2} \text{ s}^{-1} \pm 2 \mu\text{mol m}^{-2} \text{ s}^{-1}$  and a  $V_{\text{TPU}_{C_i}}$  of  $8 \mu\text{mol m}^{-2} \text{ s}^{-1} \pm 0.2 \text{ m}^{-2} \text{ s}^{-1}$  in Col-0 plants (Table 3-2). Both RCAR6-3 and RCAR10-4 lines had no or little increase in  $g_m$ , but higher  $V_{c,\text{max}_{C_i}}$ ,  $J_{\text{max}_{C_i}}$  and  $V_{\text{TPU}_{C_i}}$  than Col-0. These results are not consistent with the results shown in table 3-1, which might be due to the difference in enzymatic activity of photosynthesis between young and old leaves (Kitajima *et al.*, 1997b; Koike, 1988). The data on  $V_{c,\text{max}_{C_i}}$ ,  $J_{\text{max}_{C_i}}$  and  $V_{\text{TPU}_{C_i}}$  suggest that RCAR gene may play a role in controlling leaf photosynthetic capacity and balancing biochemical and stomatal limitations on photosynthesis. In addition, the maximum  $C_i$  and  $C_c$  achieved were lower in overexpression RCAR6-3 ( $614 \mu\text{mol mol}^{-1} \pm 35 \mu\text{mol mol}^{-1}$  and  $450 \mu\text{mol}$

$\text{mol}^{-1} \pm 40 \mu\text{mol mol}^{-1}$ ) and RCAR10-4 ( $689 \mu\text{mol mol}^{-1} \pm 32 \mu\text{mol mol}^{-1}$  and  $547 \mu\text{mol mol}^{-1} \pm 29 \mu\text{mol mol}^{-1}$ ) than in Col-0 ( $975 \mu\text{mol mol}^{-1} \pm 19 \mu\text{mol mol}^{-1}$  and  $832 \mu\text{mol mol}^{-1} \pm 19 \mu\text{mol mol}^{-1}$ ) (Fig. 3-16B).

Table 3-2 Photosynthetic parameters of Columbia, RCAR6-3 and RCAR10-4 deduced from  $A_n$ - $C_i$  curve at a saturating light. Mesophyll conductance,  $g_m$ ; the maximum velocity of carboxylation,  $V_{c,\max\_C_i}$ ; the maximum capacity for electron transport,  $J_{\max\_C_i}$ ; the velocity of triose phosphate utilization,  $V_{\text{TPU}\_C_i}$ , were calculated from the gas exchange on the basis of  $C_i$ . Different letters indicate statistically significant differences ( $P < 0.05$ ).

	$g_m$ ( $\text{mmol m}^{-2} \text{s}^{-1}$ )		$V_{c,\max\_C_i}$	$J_{\max\_C_i}$	$V_{\text{TPU}\_C_i}$
	Constant J	Curve fitting	( $\mu\text{mol m}^{-2} \text{s}^{-1}$ )	( $\mu\text{mol m}^{-2} \text{s}^{-1}$ )	( $\mu\text{mol m}^{-2} \text{s}^{-1}$ )
Col-0	$172 \pm 16$ a	$169 \pm 14$ a	$91 \pm 3$ a	$122 \pm 2$ a	$8.5 \pm 0.2$ a
R6-3	$172 \pm 10$ a	$160 \pm 5$ a	$118 \pm 15$ b	$141 \pm 7$ b	$9.3 \pm 0.3$ a
R10-4	$187 \pm 12$ a	$190 \pm 21$ a	$103 \pm 4$ ab	$130 \pm 4$ ab	$9.0 \pm 0.2$ a

### 3.2.1.7.2.4 Compensation of reduced stomatal conductance by increased $\text{CO}_2$ gradient

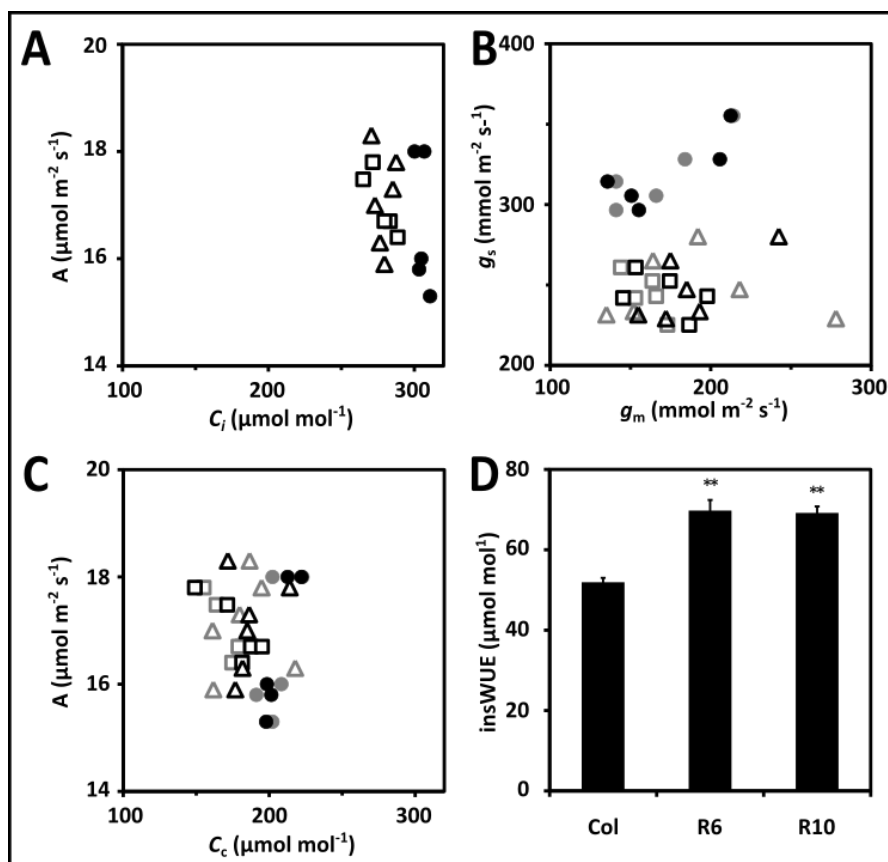


Figure 3-17 Compensation of reduced stomatal conductance ( $g_s$ ) by a steeper  $\text{CO}_2$  gradient between the atmosphere and chloroplast ( $C_a - C_i$ ). The RCAR6-3 (open squares) and RCAR10-4 (open triangles) lines resulted in comparable net carbon assimilation rate ( $A_n$ ) to

## Results

---

Col (filled circles), and therefore achieved an enhanced insWUE under well-watered conditions, by applying saturation light during gas exchange measurements. The relationship between A)  $A_n$  and  $C_i$ , B)  $g_s$  and mesophyll conductance ( $g_m$ ), C)  $A_n$  and  $C_c$  of Col-0, overexpression RCAR6-3, and RCAR10-4. B-C) Black symbols were determined by constant J method and gray symbols by curve fitting method. insWUE D) was calculated after determination of  $A_n$  and  $g_s$ . Growing conditions as described in Fig. 3-16. Two weeks after emergence,  $16 \pm 3$  leaves from plants grown in well-watered conditions ( $SWP \geq -0.02$  bar) were used to perform gas exchange analysis. Five independent leaves from five plants of Col and overexpression R6, and six independent leaves from five plants of R10 were chosen to do gas exchange measurements. A-C) Single measurements with six technical replicates for each data point. D)  $n \geq 5$  biological replicates with six technical replicates, mean  $\pm$  SEM. \*\* $P < 0.001$  compared with wild type Col.

At an ambient  $CO_2$  of  $400 \mu\text{mol mol}^{-1}$  and light saturation conditions,  $A_n$ ,  $g_s$  and  $C_i$  of Col-0 averaged  $16.6 \mu\text{mol m}^{-2} \text{s}^{-1} \pm 0.6 \mu\text{mol m}^{-2} \text{s}^{-1}$ ,  $320 \text{mmol m}^{-2} \text{s}^{-1} \pm 10 \text{mmol m}^{-2} \text{s}^{-1}$  and  $305 \mu\text{mol mol}^{-1} \pm 2 \mu\text{mol mol}^{-1}$ , respectively (Fig. 3-17A-B). Using  $A_n$ ,  $C_i$  and estimated  $g_m$  (see Table 3-2),  $C_c$  can be solved according to  $A_n = (C_i - C_c) / r_m$  or  $A_n = (C_a - C_i) / (1 / g_m)$ , and the  $C_c$  of Col-0 averaged  $206 \mu\text{mol mol}^{-1} \pm 5 \mu\text{mol mol}^{-1}$  (Constant J method) or  $205 \mu\text{mol mol}^{-1} \pm 5 \mu\text{mol mol}^{-1}$  (Curve fitting method) (Fig. 3-17C). Similarly,  $C_c$  of RCAR6-3 line was  $177 \mu\text{mol mol}^{-1} \pm 8 \mu\text{mol mol}^{-1}$  (Constant J method) or  $170 \mu\text{mol mol}^{-1} \pm 5 \mu\text{mol mol}^{-1}$  (Curve fitting method), and  $C_c$  of RCAR10-4 line was  $186 \mu\text{mol mol}^{-1} \pm 6 \mu\text{mol mol}^{-1}$  (Constant J method) or  $184 \mu\text{mol mol}^{-1} \pm 9 \mu\text{mol mol}^{-1}$  (Curve fitting method) (Fig. 3-17C). Compared with Col-0,  $g_s$ ,  $C_i$ , and  $C_c$  of RCAR6-3 and RCAR10-4 lines displayed lower value, while  $A_n$  did not differ from Col-0, and  $g_m$  had a minor increase (Fig. 3-17A-C). Taken together, the total conductance of  $CO_2$  diffusion ( $1 / (r_s + r_m)$  or  $1 / (1 / g_s + 1 / g_m)$ ) from atmosphere to the site of carboxylation reduced by 10% (Constant J method) and 13% (Curve fitting method) for RCAR6-3, and by 5% (Constant J method) and 3% (Curve fitting method) for RCAR10-4 (Fig. 3-17A-C). According to  $A_n = (C_a - C_c) / (r_s + r_m)$  or  $A_n = (C_a - C_c) \times (1 / (1 / g_s + 1 / g_m))$ , the unchanged  $A_n$  but reduced total conductance is due to the fully compensation of 16% (Constant J method) or 18% (Curve fitting method) increased  $CO_2$  gradient for RCAR6-3, and the compensation of 11% (Constant J method) or 11% (Curve fitting method) increased  $CO_2$  gradient for RCAR10-4 (Fig. 3-17A-C). As a consequence, both overexpression RCAR lines achieved an enhancement in insWUE by a factor of 1.3 (Fig. 3-17D).



### 3.2.1.7.3 Estimation of mesophyll conductance by analysis of $^{13}\text{C}$ discrimination

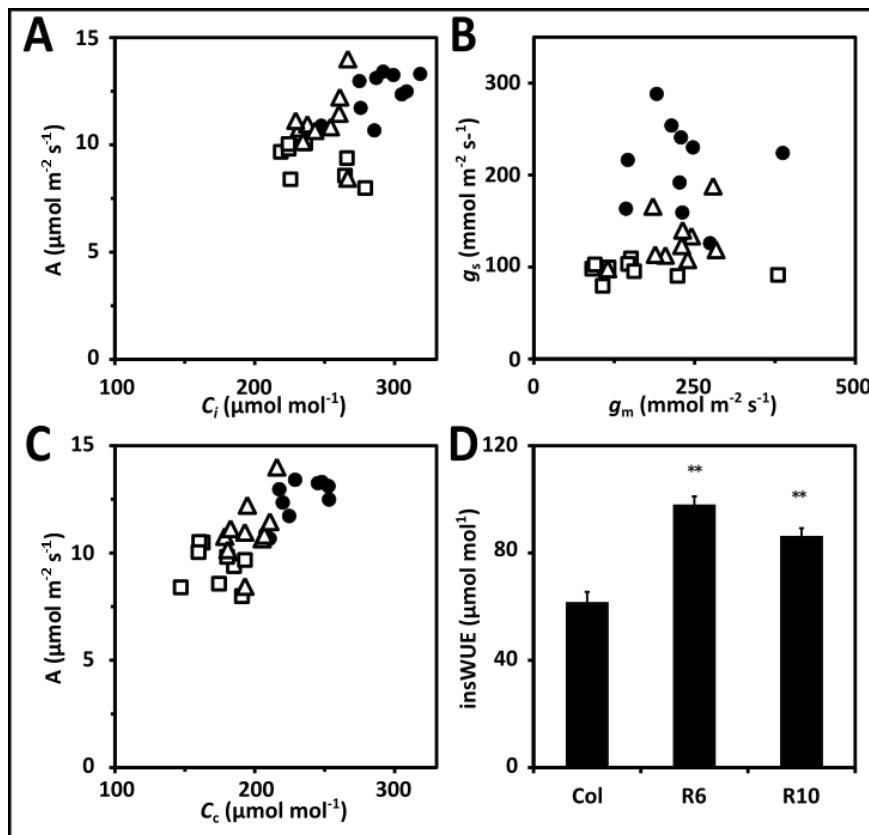


Figure 3-18 Estimation of mesophyll conductance by on-line  $\Delta^{13}\text{C}$  measurements. The relationship between A)  $A_n$  and  $C_i$ , B)  $g_s$  and  $g_m$ , C)  $A_n$  and  $C_c$  of in wild type Col-0 (filled circles), overexpression RCAR6-3(R6) (open squares) and R10-4 (R10) (open triangles). insWUE D) was calculated after determination of  $A_n$  and  $g_s$ . All plants were grown under short day conditions (8h light /16h dark photoperiod) at photon flux density of  $500 \mu\text{mol m}^{-2} \text{s}^{-1}$  and  $22^\circ\text{C}$  and 50% relative humidity in the daytime, and  $17^\circ\text{C}$  and 60% relative humidity at night. Comparable fully expanded young leaves from  $35 \pm 3$  days old Arabidopsis plants grown under well-watered conditions ( $\text{SWP} \geq -0.02$  bar) were used to perform on-line measurements. Ten independent leaves from ten plants of Col-0 and overexpression R6 and R10 were chosen for on-line measurements. A-C) Single measurements with ten technical replicates for each data point. D)  $n \geq 10$  biological replicates with ten technical replicates, mean  $\pm$  SEM. \*\* $P < 0.001$  compared with wild type Col.

Mesophyll conductance was further determined by on-line measurements of  $\Delta^{13}\text{C}$ , in conjunction with gas exchange measurements at a photon flux density of  $500 \mu\text{mol m}^{-2} \text{s}^{-1}$  and ambient  $\text{CO}_2$  of  $400 \mu\text{mol mol}^{-1}$ . Mesophyll conductance of Col-0 averaged  $229 \text{ mmol m}^{-2} \text{s}^{-1} \pm 22 \text{ mmol m}^{-2} \text{s}^{-1}$  (Fig. 3-18B). The gas exchange measurements gave rise to an  $A_n$  of  $12.4 \mu\text{mol m}^{-2} \text{s}^{-1} \pm 0.3 \mu\text{mol m}^{-2} \text{s}^{-1}$ , a  $g_m$  of  $209 \text{ mmol m}^{-2} \text{s}^{-1} \pm 14 \text{ mmol m}^{-2} \text{s}^{-1}$  and a  $C_i$  of  $289 \mu\text{mol mol}^{-1} \pm 6 \mu\text{mol mol}^{-1}$  (Fig. 3-18A and B). Using  $A_n$ ,  $C_i$  and estimated  $g_m$ ,  $C_c$  can be solved according to  $A_n = (C_i - C_c) \times g_m$ , and the  $C_c$  of

## Results

Col-0 averaged  $230.8 \mu\text{mol mol}^{-1} \pm 6 \mu\text{mol mol}^{-1}$  (Fig. 3-18C). Similarly,  $C_c$  of RCAR6-3 line was  $173 \mu\text{mol mol}^{-1} \pm 5 \mu\text{mol mol}^{-1}$ , and  $C_c$  of RCAR10-4 line averaged  $196 \mu\text{mol mol}^{-1} \pm 4 \mu\text{mol mol}^{-1}$  (Fig. 3-18C). Compared with Col-0,  $A_n$ ,  $g_s$ ,  $g_m$ ,  $C_i$ , and  $C_c$  of both RCAR6-3 and RCAR10-4 lines displayed lower values, while the ambient  $C_a$  for RCAR6-3 was  $8 \mu\text{mol mol}^{-1}$  higher than Col-0 (Fig. 3-18A-C). Taken together, the 44% reduction of total  $\text{CO}_2$  conductance in the RCAR6-3 line, compared with Col-0, were fully compensated by a 39% enhanced  $\text{CO}_2$  gradient between ambient and chloroplast ( $C_a - C_c$ ). However, the  $A_n$  of RCAR6-3 reduced by 28% (Fig. 3-18A-C). This might be due to the increased photochemical limitation in RCAR6-3 line. Unlike the RCAR6-3, RCAR10-4 had a 10% decrease in  $A_n$ , which is caused by the compensation of 20% reduced total conductance of  $\text{CO}_2$  diffusion by 19% higher  $C_a - C_c$  (Fig. 3-18A-C). As a consequence, both overexpression RCAR6-3 and RCAR10-4 lines achieved an enhancement in insWUE by a factor of 1.6 and 1.4 respectively (Fig. 3-18A-D).

### 3.2.1.8 Shoot and root contributions to WUE

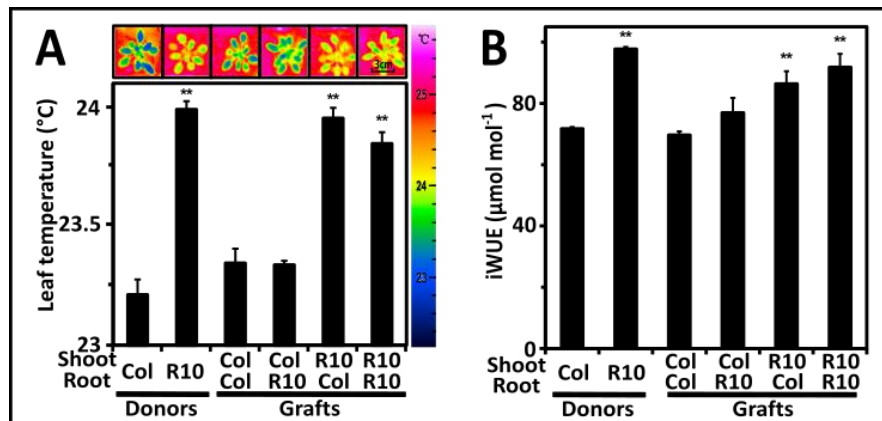


Figure 3-19 Organ-mediated changes in WUE analyzed by grafting of RCAR10-4 line (R10) and wild type Col. A) The leaf surface temperatures of donor lines, self-grafted donor lines and reciprocal grafts of roots and shoots were determined by thermal imaging using six-week-old plants. Scale bar donates 3 cm. B)  $\Delta^{13}\text{C}$ -derived integrated WUE determined by using above-ground dry biomass collected from ten-week-old plants grown under progressive drought. All plants were grown under short day conditions (8h light / 16h dark photoperiod) at photon flux density of  $150 \mu\text{mol m}^{-2} \text{s}^{-1}$  and  $22^\circ\text{C}$  and 50% relative humidity in the daytime and  $17^\circ\text{C}$  and 60% relative humidity at night. A and B)  $n=4$  biological replicates with 2 technical replicates, mean  $\pm$  SEM, \*\* $P<0.001$  compared with wild type Col-0.

The *cauliflower mosaic virus* 35S promoter used to constitutively induce the overexpression of RCARs in plants does not provide a tissue specificity, and thus does not allow to identify the contributions of shoot and root parts to WUE in RCAR

overexpression lines. Therefore, grafts with different combinations (shoot-root: Col-Col, Col-R10, R10-Col and R10-R10) were generated using shoots and roots of Col-0 and RCAR10-4 seedlings as donors. The 28-day-old grafts were transferred into the soil to undergo progressive drought. The leaf surface temperatures of 42-day-old grafts and donor lines (still in the well-watered phase), and  $\Delta^{13}\text{C}$  by using dried biomass from 70-day-old plants (at the end of progressive drought) were analyzed. Similar to the RCAR10-4 donor, reciprocal grafts with RCAR10-4 shoots combined elevated leaf temperatures (Fig. 3-19A) and enhanced integrated WUE compared with Col-0 (Fig. 3-19B), indicating the dominant role of the shoot in improving plants' water productivity. Moreover, grafts with Col-0 shoots and RCAR10-4 roots displayed a slight increase in integrated WUE compared with grafts with Col-0 shoots and Col-0 roots ( $P = 0.204$ ) or Col-0 donor lines ( $P = 0.386$ ). Grafts with RCAR10-4 shoots and Col-0 roots displayed a slight decrease in integrated WUE compared with grafts with the RCAR10-4 shoot and RCAR10-4 root ( $P = 0.340$ ) or RCAR10-4 donor lines ( $P = 0.05$ ). These results tentatively imply a possible contribution from the root (Fig. 3-19B).

### 3.2.1.9 Biomass and WUE affected by ambient temperatures

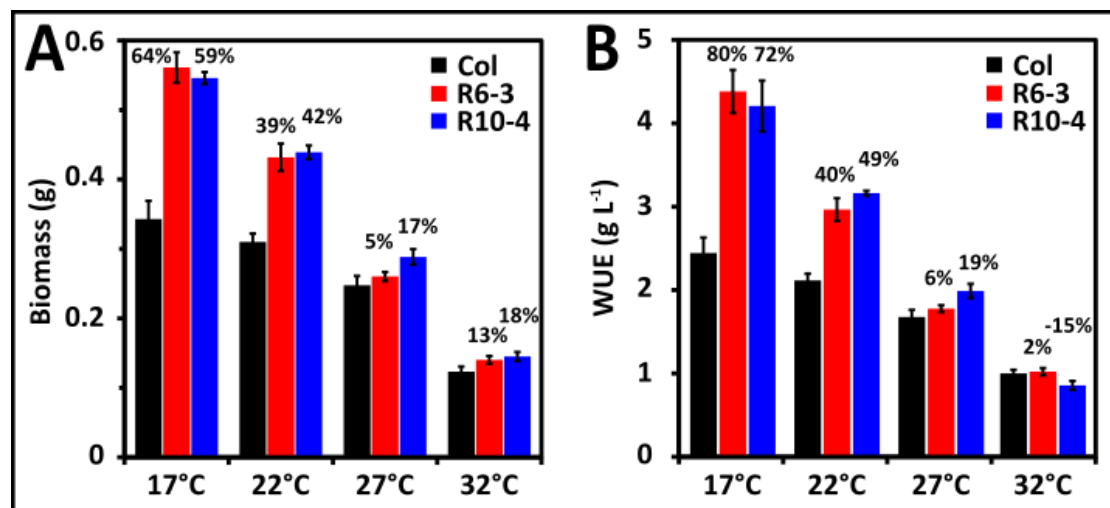


Figure 3-20 Water productivity conferred by ectopic expression of ABA receptors under different ambient temperatures. A) Above-ground biomass of Columbia (Col) (black columns), RCAR6-3 (R6) (red columns), and RCAR10-4 (R10) (blue columns) and B) WUE (dry biomass in grams per liter of water consumed) at the end of the progressive drought under different ambient temperatures of 17 °C, 22 °C, 27 °C, and 32 °C. 18 days old plantlets were subjected to progressive drought for 70 days, 60 days, 50 days, and 40 days respectively. All plants were grown at photon flux density of 150  $\mu\text{mol m}^{-2} \text{s}^{-1}$  and 50% relative humidity in the daytime and 60% relative humidity at night. Temperatures at night were 5°C less than corresponding designated daytime temperatures. A-B)  $n=5$  biological replicates per data

point, mean  $\pm$  SEM,  $**P < 0.001$  compared with wild type Col-0 in corresponding ambient temperatures.

Drought frequently occurs in nature simultaneously with high environmental temperatures. The combined effects of drought and high ambient temperatures may offset the increased biomass and enhanced WUE conferred by overexpressing certain RCARs. To investigate this, progressive drought experiments were performed at 17 °C, 22°C, 27 °C and 32 °C and above-ground dry biomass and WUE were compared between wild type Columbia and RCAR6-3 and RCAR10-4 lines. Indeed, increasing ambient temperature from 17°C to 32°C led to a consistent decline of above-ground dry biomass and gravimetric-derived integrated WUE for all lines (Fig. 3-20A and B). Moreover, at 17 °C, ectopic expression RCAR6-3 and RCAR10-4 lines showed 64% and 59% increase in biomass and a WUE enhanced by 80% and 72% compared with Col-0. With the increase of ambient temperatures, both RCAR lines were still more water efficient, but the advantages became smaller (Fig. 3-20A and B).

### **3.2.2 Water productivity of RCAR6 and RCAR10 lines under well-watered conditions**

Former analyses based on gravimetric methods, carbon isotope discrimination and gas exchange measurements demonstrated the enhanced WUE of RCAR6-3 and RCAR10-4 lines grown under progressive drought, compared with wild type Columbia. However, enhanced WUE is considered to be associated with a trade-off in yield potential (Blum, 2005). Yield potential here refers to the yield of a crop cultivar when grown in environments to which it is adapted, when nutrients and water are not limiting, and pests and diseases are effectively controlled (Evans and Fischer, 1999). To investigate whether enhanced WUE is linked to trade-off in yield potential in Arabidopsis, RCAR6-3 and RCAR10-4 lines were grown under well-watered conditions in both low light (maximum photon flux density of 150  $\mu\text{mol m}^{-2} \text{s}^{-1}$ ) and high light (maximum photon flux density of 900  $\mu\text{mol m}^{-2} \text{s}^{-1}$ ) to evaluate their growth performance, above-ground biomass, and WUE.

#### **3.2.2.1 Biomass and WUE of plants grown under moderate light**

Two experiments were performed under moderate light (a photon flux density of 150  $\mu\text{mol m}^{-2} \text{s}^{-1}$ ) and well-watered conditions. In the first experiment, seven-day-old

seedlings from all lines were transferred to soil and grown with a photoperiod of 16 hours light and 8 hours darkness. Watering was administrated twice a week. The growth performance of eight-week-old RCAR6-3 and RCAR10-4 plants showed little or no visible reduction in comparison to wild type Columbia (Fig. 3-21A higher panel). After four months of growth, the aerial parts of the plants were harvested. The total biomass was defined as the sum of oven-dried straw weight plus the weight of seeds. RCAR6-3 did not differ significantly from Col-0 in total biomass while RCAR10-4 lines showed a reduction of biomass by 11% (Fig. 3-21B). In addition, analysis of  $\Delta^{13}\text{C}$  of seeds materials displayed a 1.2 ‰ less  $^{13}\text{C}$  discrimination of RCAR6-3 than Col-0, and therefore RCAR6-3 achieved a 28% higher iWUE than Col-0 according to equation (3) and (4) (Fig. 3-21D and E).

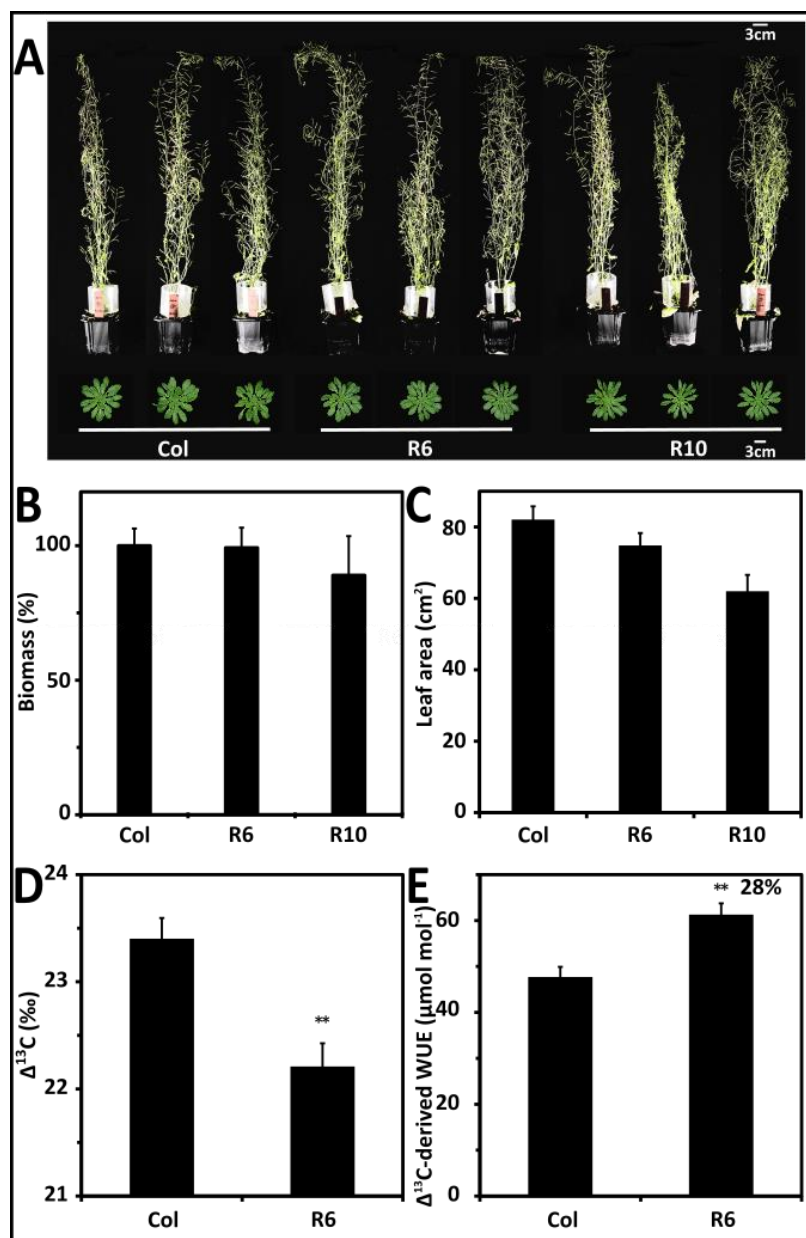


Figure 3-21 Biomass production under a well-watered growth regime. A) Representative pictures of wild type Col, RCAR6-3 (R6) and RCAR10-4 (R10) lines at the age of eight weeks (upper row) grown under long-day conditions (16h light / 8h dark photoperiod) and rosettes aged seven weeks (lower panel) grown in short-day conditions (8h light / 16h dark photoperiod). Both scale bars at the top right and bottom right corners represent 3 cm. B) Relative biomass of above-ground biomass (in percentage relative to Col; biomass equals dry straw weight plus weight of seeds; above-ground biomass of Columbia was  $1.41 \text{ g} \pm 0.11 \text{ g}$  and set to 100%) of Col (n=28), RCAR6-3 (n=28) and RCAR10-4 (n=4) were determined after four-months growth under a well-watered and long-day regime (16h light / 8h dark photoperiod). C) Rosette size of seven-week-old Col-0, RCAR6-3 and RCAR10-4 plants.  $\Delta^{13}\text{C}$  D) and  $\Delta^{13}\text{C}$ -derived iWUE E) of seeds materials of Col-0 and RCAR6-3 shown in the upper panel of A) and B). A-E) All plants were grown at photon flux density of  $150 \mu\text{mol m}^{-2} \text{ s}^{-1}$  and  $22^\circ\text{C}$  and 50% relative humidity in the daytime and  $17^\circ\text{C}$  and 60% relative humidity at night. B, D and E) n=28 biological replicates for Col and RCAR6-3; n=4 for RCAR10-4. C) n=3 biological replicates for all. B-E) mean  $\pm$  SEM, \*\*P<0.001 compared with wild type Col-0.

In the second experiment, seven-day-old seedlings of all lines were transferred into the soil and grown with a photoperiod of 8 hours light and 16 hours dark photoperiod. Their pots were covered and water was supplied once a week. Pictures of rosettes after seven weeks indicated a minor reduction in rosette sizes of the RCAR6-3 line (8%) compared to Col-0 while RCAR10-4 line showed a decrease in rosette size (24%) (Fig. 3-21A lower panel and C).

### 3.2.2.2 Biomass and WUE of plants grown under saturation light

Crops grown in the field always experience full sunlight. High photon flux density promotes the photosynthetic capacity of plants and enhances demand for CO<sub>2</sub>, therefore imposing a strain on the CO<sub>2</sub> gradients between the atmosphere and the site of carboxylation in the plants' chloroplast. The enhanced CO<sub>2</sub> gradient of the RCAR6-3 line found under low light conditions compared with wild type Columbia might be attenuated at saturating light conditions. As a consequence, the increase in the WUE of the overexpression RCAR6-3 line grown under high light might be affected.

To investigate this issue, growth performance, biomass and WUE under high light and well-watered conditions were compared between Col-0 and the RCAR6-3 line. The plants were grown in a sun simulation growth chamber which supplied as much as 900  $\mu\text{mol m}^{-2} \text{s}^{-1}$  light in this experiment (Döhning *et al.*, 1996; Thiel *et al.*, 1996). After six weeks' growth, Col-0 had obtained 251 cm<sup>2</sup>  $\pm$  17 cm<sup>2</sup> leaf area and 1.6 g  $\pm$  0.1 g dry biomass. The RCAR6-3 line showed only a 1% reduced leaf area at the end of the experiment but had 18%  $\pm$  4% reduced above-ground dry biomass compared with Col-0 (Fig. 3-22B-C). Further analysis of  $\Delta^{13}\text{C}$  using the dried above-ground biomass revealed 1 ‰  $\pm$  0.1 ‰ less  $\Delta^{13}\text{C}_{\text{bulk}}$  and 9%  $\pm$  1% higher <sup>13</sup>C-derived integrated WUE than Col-0 (Fig. 3-22D-E).

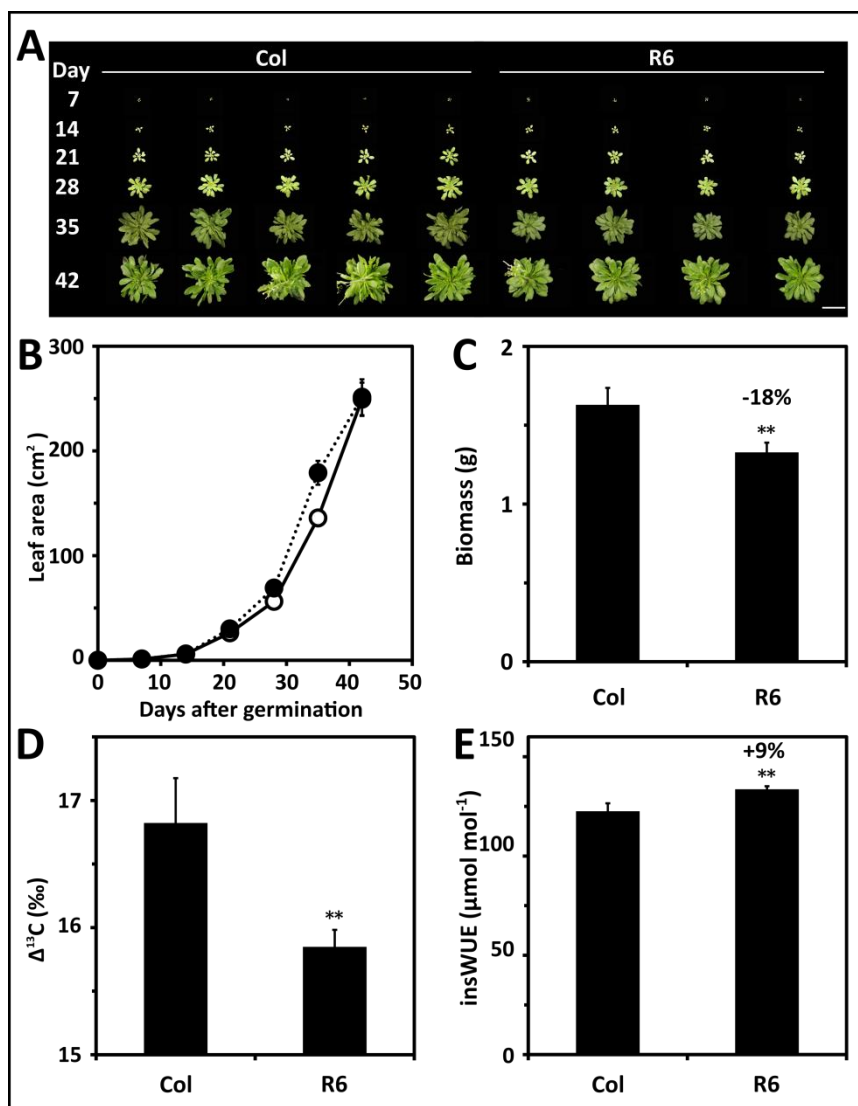


Figure 3-22 Growth performance, biomass accumulation and  $\Delta^{13}\text{C}$ -derived integrated WUE of RCAR6-3 (R6) plants under high photon flux density conditions. A) Pictures of Col and R6 grown under well-watered conditions, an 8h light / 16h dark photoperiod and 22°C, 50% relative humidity in the daytime and 17°C, 60% relative humidity at night. Illumination began in the morning at 9:00 am with a photon flux density of  $140 \mu\text{mol m}^{-2} \text{s}^{-1}$ . It was increased to  $330 \mu\text{mol m}^{-2} \text{s}^{-1}$  at 10:00 am and finally reached  $900 \mu\text{mol m}^{-2} \text{s}^{-1}$  at 11:00 am. Plants grew under the strongest light for four hours till 15:00 pm. Subsequently, light intensity decreased stepwise from  $900$  to  $0 \mu\text{mol m}^{-2} \text{s}^{-1}$  from 15:00 to 17:00. One hour acclimation was allowed when the light intensity was adjusted to a new level. Text on the left side indicates the age of the plants. The scale bar denotes 10 cm. B) Leaf area values of Col (dotted line) and R6-3 (solid line) as shown in A). C) Biomass obtained by drying the aerial part of plantlets after 42 days of growth. Bulk derived  $^{13}\text{C}$  discrimination D) and  $\Delta^{13}\text{C}$ -derived integrated WUE E) were determined by using dry biomass samples from C). B-E)  $n=5$  for Col and 4 for R6-3 biological replicates for each data point, mean  $\pm$  SEM, \*\* $P < 0.001$  compared with wild type.

### 3.2.3 Water productivity of Arabidopsis under deficit irrigation

Ectopic RCAR6 and RCAR10 lines have been proven to have enhanced WUE with little or no reduction in the growth and biomass accumulation under progressive drought



conditions. However, an increase in WUE is considered to have benefits under terminal severe drought stress, like progressive drought, but not in a mild drought scenarios (Tardieu, 2011). To investigate whether RCAR6 and RCAR10 lines could still be water-efficient in different drought scenarios, deficit irrigation (60%, 40%, and 20% soil water content, but not 80% due to unexplained growth see Fig. 3-2) was performed. Seven-day-old seedlings of wild type Columbia, RCAR6-3 and RCAR10-4 were transferred into pots (200 mL) and grown under well-watered conditions (SWC  $\geq$  77%, SWP  $\geq$  -0.02 bar) for seven days. Subsequently, watering was stopped for another seven days period to allow soil water content to drop to 30%. For pots of plantlets designated to grow with 60% and 40% soil water content were adjusted and pots were covered, and water was applied until their respective levels were reached, while those of 20% soil water content were covered four days later when their soil water content had reached 20%. The time point of covering the 40% and 60% water regime pots were defined as day 0 for the deficit irrigation regime assuming that negligible water was consumed by plantlets grown at the 20% SWC in four extra days. Subsequently, water was applied according to maintain the designated regimes in three-day intervals. Leaf surface temperatures, leaf growth, above-ground dry biomass and the WUE of those lines were analyzed.

### 3.2.3.1 Leaf surface temperatures

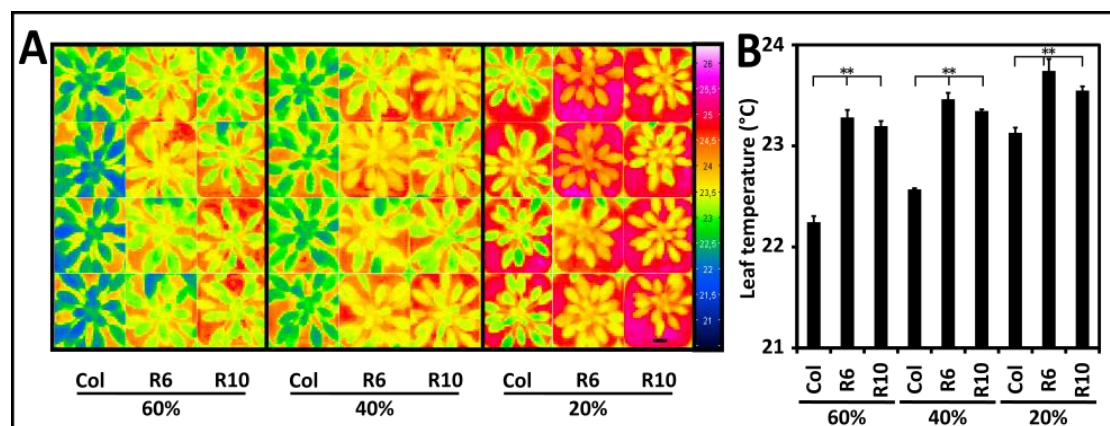


Figure 3-23 Leaf surface temperatures of wild type Columbia and RCAR lines in response to soil water content. Thermogram A) and leaf temperature values B) of 43-day-old Col, RCAR6-3 (R6) and RCAR10-4 (R10) grown at 60%, 40% and 20% soil water content (See Fig. 3-2). Four plants were grown per line in separate pots at randomized positions and thermal pictures were arranged in groups after imaging. Scale bar indicates 2 cm. All plants were grown under short day conditions (8h light /16h dark photoperiod) at photon flux density of  $150 \mu\text{mol m}^{-2} \text{s}^{-1}$  and  $22^\circ\text{C}$  and 50% relative humidity in the daytime and  $17^\circ\text{C}$  and 60% relative humidity at night.  $n=4$  biological replicates for each data point, mean  $\pm$  SEM. \*\* $P < 0.001$  compared with wild type Col-0 in each water regime.

Plants grown for 17 days under water deficit conditions were chosen as examples to show the leaf surface temperatures resulting from different water regimes. In every water regime, both RCAR6-3 and RCAR10-4 lines showed higher leaf temperatures than wild type Columbia. Under the 60% water regime, the leaf temperature of Col averaged  $22.2\text{ }^{\circ}\text{C} \pm 0.1\text{ }^{\circ}\text{C}$ , which was  $1\text{ }^{\circ}\text{C}$  lower than RCAR6-3 ( $23.3\text{ }^{\circ}\text{C} \pm 0.1\text{ }^{\circ}\text{C}$ ) and RCAR10-4 ( $23.2\text{ }^{\circ}\text{C} \pm 0.04\text{ }^{\circ}\text{C}$ ) (Fig. 3-23A and B). Reducing soil water content to 40% resulted in an elevation in leaf temperatures for all lines, but the difference was maintained at  $1\text{ }^{\circ}\text{C}$  between Col-0 and both other lines (Fig. 3-23A and B). A further decrease of soil water content to 20% diminished the difference, but the leaf temperatures of RCAR6-3 and RCAR10-4 were still higher than Col-0 by at least  $0.4\text{ }^{\circ}\text{C}$  (Fig. 3-23A and B).

### **3.2.3.2 Biomass formation and water use efficiency**

In the deficit irrigation experiment, leaf areas of all lines showed a slight increase when soil water content was reduced from 60% to 40% followed by a significant decrease when soil water content was further reduced to 20%. Under the 60% water regime, Col-0 plants consistently increased the leaf area from  $1.8\text{ cm}^2 \pm 0.2\text{ cm}^2$  at the onset of deficit irrigation, to  $105\text{ cm}^2 \pm 4\text{ cm}^2$  at the end, and achieved a maximum leaf expansion rate of  $9.4\text{ \% d}^{-1} \pm 0.2\text{ \% d}^{-1}$  (Fig. 3-24A and D). Compared with Col-0, the RCAR6-3 and RCAR10-4 lines showed a somewhat reduction in leaf area and maximum leaf expansion rate (Fig. 3-24A and D). Reducing soil water content to 40% did not result in a reduced leaf area and maximum leaf expansion rate in Col-0 and RCAR6-3 lines, but the difference between Col-0 and RCAR10-4 lines was attenuated (Fig. 3-24B and D). Further reducing soil water content to 20% led to a significant decrease in both leaf area and maximum leaf expansion rate in all lines, but RCAR6-3 still did not differ from Col-0, while RCAR10-4 showed some reduction (Fig. 3-24C and D).

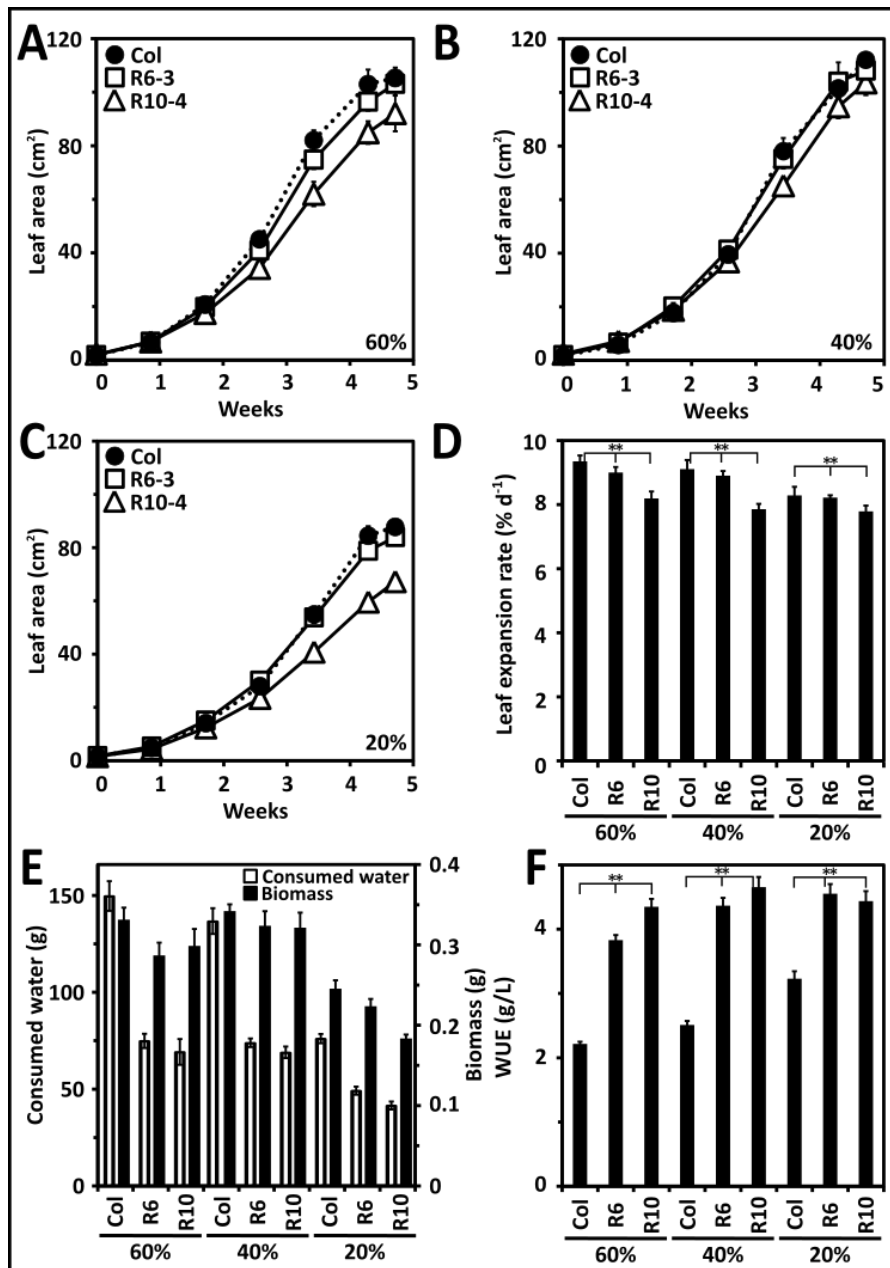


Figure 3-24 Biomass formation and water productivity conferred by ectopic expression of RCAR6 and RCAR10 under deficit irrigation. Leaf area over time of 33 days at A) 60%, B) 40% and C) 20% soil water content and the maximum leaf expansion rate D) in wild type Columbia (Col, filled circles), RCAR6-3 lines (R6, open squares) and RCAR10-4 (R10, open triangles). E) Above-ground biomass and F) WUE (dry biomass in grams per liter of water consumed) at the end of deficit irrigation. Plants were grown in conditions as described in Fig. 3-23. A-F) n=4 biological replicates, mean  $\pm$  SEM, \*\*P<0.001 compared with wild type Col in each water regime.

At the end of deficit irrigation, the biomass accumulation of all lines showed the same tendency as leaf area measurements. A slightly higher under the 40% water regime as compared with the 60%, and a significantly lower under the 20% SWC (Fig. 3-24E and F). The WUE of all lines increased consistently with less water, from 60% to

20% SWC while consumed water showed the opposite trend. Under the 60% water regime, Col-0 generated  $0.33 \text{ g} \pm 0.01 \text{ g}$  dry biomass and consumed  $150 \text{ g} \pm 8 \text{ g}$  water, resulting in a WUE of  $2.2 \text{ g/L} \pm 0.03 \text{ g/L}$ . The overexpression lines RCAR6-3 and RCAR10-4 combined  $13\% \pm 5\%$  and  $9\% \pm 6\%$  reduced biomasses respectively, with  $50\% \pm 2\%$  and  $54\% \pm 4\%$  less water consumption, hence achieving 1.7-fold and 2-fold enhanced WUE (Fig. 3-24E and F). When soil water content was reduced to 40%, both RCAR lines were still water productive. RCAR6-3 and RCAR10-4 combined 1.7-fold and 2-fold enhanced WUEs with  $5\% \pm 5\%$  and  $6\% \pm 5\%$  reduced biomasses respectively, compared with Col-0 (a WUE of  $2.5 \text{ g/L} \pm 0.1 \text{ g/L}$  and a dry biomass of  $0.34 \text{ g} \pm 0.01 \text{ g}$ ) (Fig. 3-24E and F). Further reducing soil water content to 20%, RCAR6-3 combined a 1.4-fold increase in WUE with 7% less dry biomass compared with Col-0, while RCAR10-4 showed the same increase in WUE with a 25% decline in dry biomass (Fig. 3-24E and F). Taken together, RCAR6-3 line achieved enhanced WUE at no or a minor expense to biomass accumulation under different drought scenarios.

### 3.2.4 Stomatal density and size in RCAR6 and RCAR10 lines

Several studies have reported that components of ABA signaling such as ABI1 and RCAR10/PYL4 regulate stomatal development (Arend *et al.*, 2009; Pizzio *et al.*, 2013b). To investigate whether reduced stomatal conductance and elevated leaf surface temperatures were associated, at least partially, with differences in the development of stomata, three independent experiments were performed using leaves of 32, 36 and 40 days old plants, respectively. Results showed considerable variations in stomatal density (Fig. 3-25A, C, F). Two of three experiments displayed up to 35% higher stomatal density in RCAR6-3 and RCAR10-4 lines than wild type Columbia, while one displayed as low as 23% stomatal density (Fig. 3-25A, C, F). In terms of stomatal size, two experiments displayed up to 11% smaller stomata in RCAR6-3 and RCAR10-4 lines than in Col-0, and one experiment gave comparable values (Fig. 3-25B, D, G). RCAR10-4 had similar stomatal index values in two experiments while that of RCAR6-3 were lower than Col-0 in one test but comparable in another test (Fig. 3-25E and H). Taken together, analysis of parameters of stomatal development in three independent experiments indicated that leaves with a higher stomatal density tended to possess a smaller stomatal size, and leaves with lower stomatal density tended to have a larger stomatal size, which implied that overexpressing RCARs may affect the stomatal development, and also may regulate the relationship between

stomatal density and stomatal size.

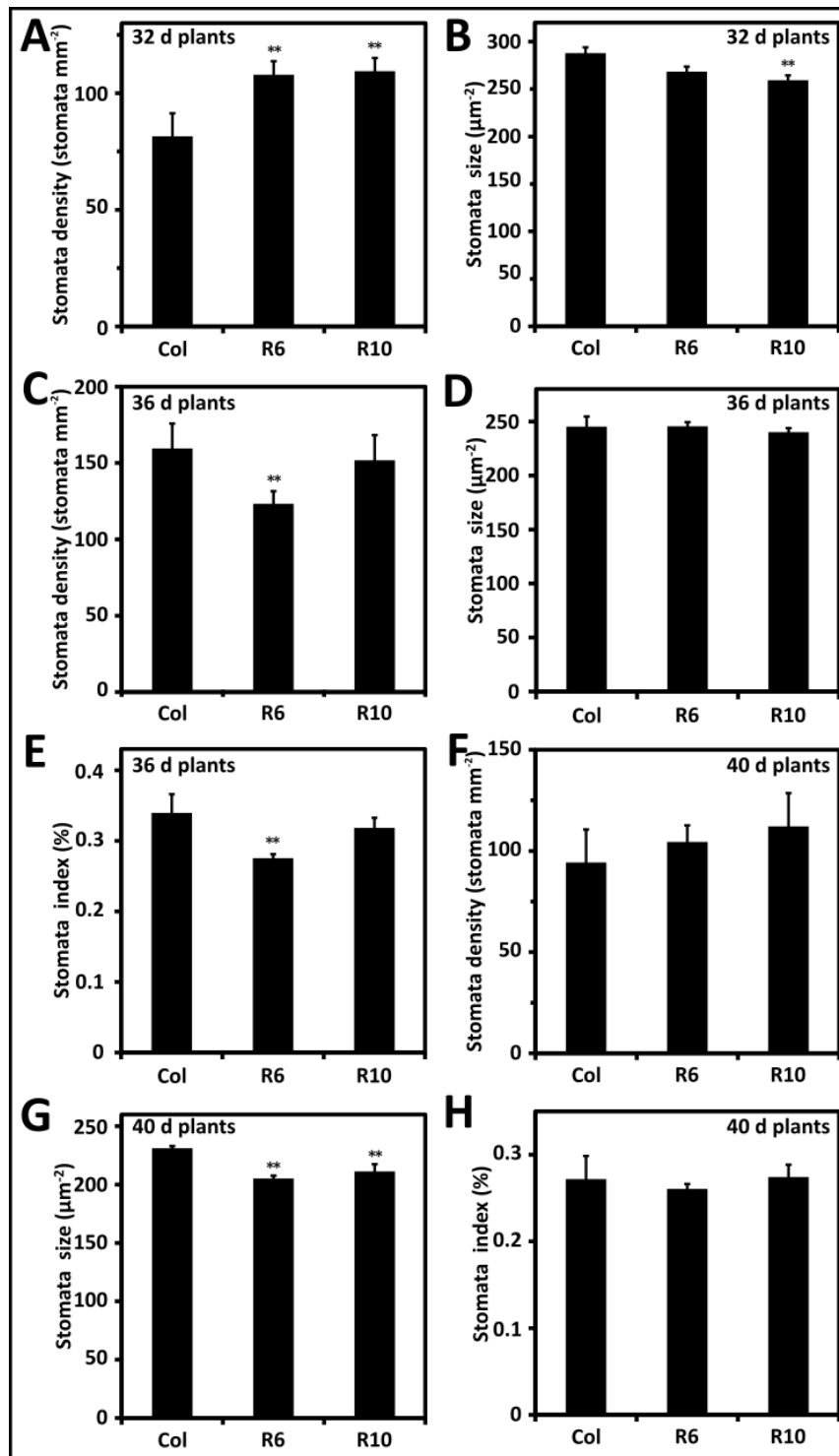


Figure 3-25 Stomatal density, size and index of lines ectopically expressing RCAR6 and RCAR10. Three independent experiments (A-B experiment one; C-E experiment two, F-H experiment three) were performed by using comparable leaves of wild type Columbia, RCAR6-3, and RCAR10-4 plants. Stomatal density A) and stomatal size B) of comparable leaves of 32-day-old plants. Stomatal density C), stomatal size D) and stomatal index (ratio of numbers of guard cells to pavement cells) E) of comparable leaves of 36-day-old plants. Stomatal density E), stomatal size D) and stomatal index E) of comparable leaves of

40-day-old plants. All plants in the three independent experiments were grown under well-watered conditions. The pots of the plants in experiments two and three were covered. Plants growth in conditions as described in Fig. 3-23. A-H) n=3 biological replicates, mean  $\pm$  SEM, \*\*P<0.001 compared with wild type Col.

### **3.3 Natural variation of water use efficiency in Arabidopsis ecotypes**

Natural variation, also named genetic variation, describes naturally occurring differences in a population of the same species after natural selection, which allows them to adapt to their living habitats (Weigel, 2012). The widespread distribution of *Arabidopsis thaliana* around the world suggests natural variation in water use. Moreover, the genomic sequence data of different accessions of Arabidopsis have been generated (<http://signal.salk.edu/atg1001/index.php>). Both advantages of Arabidopsis facilitate the natural variation studies in WUE. Several studies have already investigated the natural variation in WUE of Arabidopsis (Easlon *et al.*, 2014; Juenger *et al.*, 2005) and discovered genes of natural variation controlling the WUE (Des Marais *et al.*, 2014; Easlon *et al.*, 2014; Juenger *et al.*, 2005; Masle *et al.*, 2005). However, the knowledge on natural variation affecting the WUE of plants is still poor.

In this chapter, the WUE of different Arabidopsis ecotypes was evaluated under both well-watered and progressive drought conditions, by measuring growth performance and gas exchange. The obtained results further proved the enhancement of WUE by a factor of two in Arabidopsis under drought (Des Marais *et al.*, 2014; Easlon *et al.*, 2014; Juenger *et al.*, 2005; Masle *et al.*, 2005), and revealed that accessions Cvi-0 and Van-0 had lower leaf temperatures and were less water productive than Col-0. In contrast, the accession RLD-0 showed hotter leaf temperature and achieved a higher WUE. Furthermore, the gene responsible for the variation of leaf surface temperature between accessions Col-0 and Cvi-0 was discovered and proved to be positively associated with WUE.

### 3.3.1 Natural variation of WUE under progressive drought conditions

#### 3.3.1.1 Arabidopsis accessions under well-watered conditions

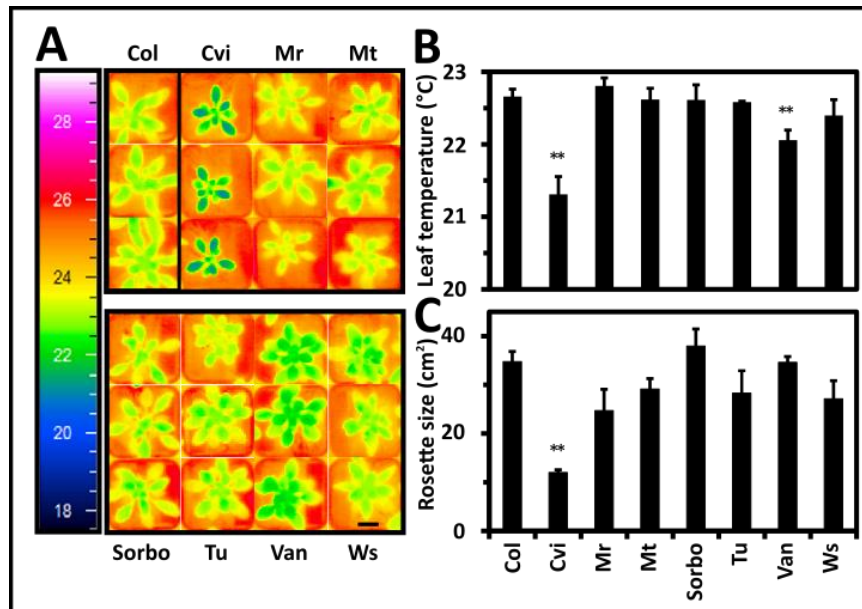


Figure 3-26 Leaf growth and leaf surface temperatures of eight Arabidopsis ecotypes under well-watered conditions. A) Thermogram of Col-0 (Col), Cvi-0 (Cvi), Mr-0 (Mr), Mt-0 (Mt), Sorbo, Tu-0 (Tu), Van-0 (Van) and Ws-0 (Ws), having grown for 40 days under short day conditions (8 h light /16 h dark photoperiod) at photon flux density of  $150 \mu\text{mol m}^{-2} \text{s}^{-1}$ ,  $22^\circ\text{C}$  and 50% relative humidity in daytime, and  $17^\circ\text{C}$  and 60% relative humidity at night, and well-watered conditions ( $\text{SWP} \geq -0.02 \text{ bar}$ ). Three plants were grown per line in separate pots at randomized positions and thermal pictures were arranged in groups after imaging. The scale bar represents 2 cm. B) Leaf temperatures from data shown in A) and leaf area C) as projected rosette size. A-C)  $n=3$  biological replicates per line, mean  $\pm$  SEM,  $**P < 0.001$  compared with Col accession.

Eight ecotypes were scored by evaluating their leaf temperatures and rosette sizes at the day 22 of the progressive drought. The soil water content of all lines at this time was above 60%, which is regarded as the well-watered phase (see section 2.2.3). Under this condition, the leaf surface temperature of Col reached  $22.6^\circ\text{C} \pm 0.1^\circ\text{C}$  and its rosette size averaged  $34.8 \text{ cm}^2 \pm 2 \text{ cm}^2$ . In comparison with Col-0, Cvi-0 had both  $1.3^\circ\text{C} \pm 0.2^\circ\text{C}$  lower leaf temperature and  $66\% \pm 2\%$  smaller leaf area (Fig. 3-26A-C). Van-0 also had a lower leaf temperature, reduced by  $0.6^\circ\text{C} \pm 0.2^\circ\text{C}$ , but its rosette size was comparable to that of Col-0 (Fig. 3-26A-C). The leaf surface temperatures of the other accessions were similar to Col-0, but there were considerable variations in the rosette sizes (Fig. 3-26A-C).

### 3.3.1.2 Water productivity of Arabidopsis accessions under progressive drought

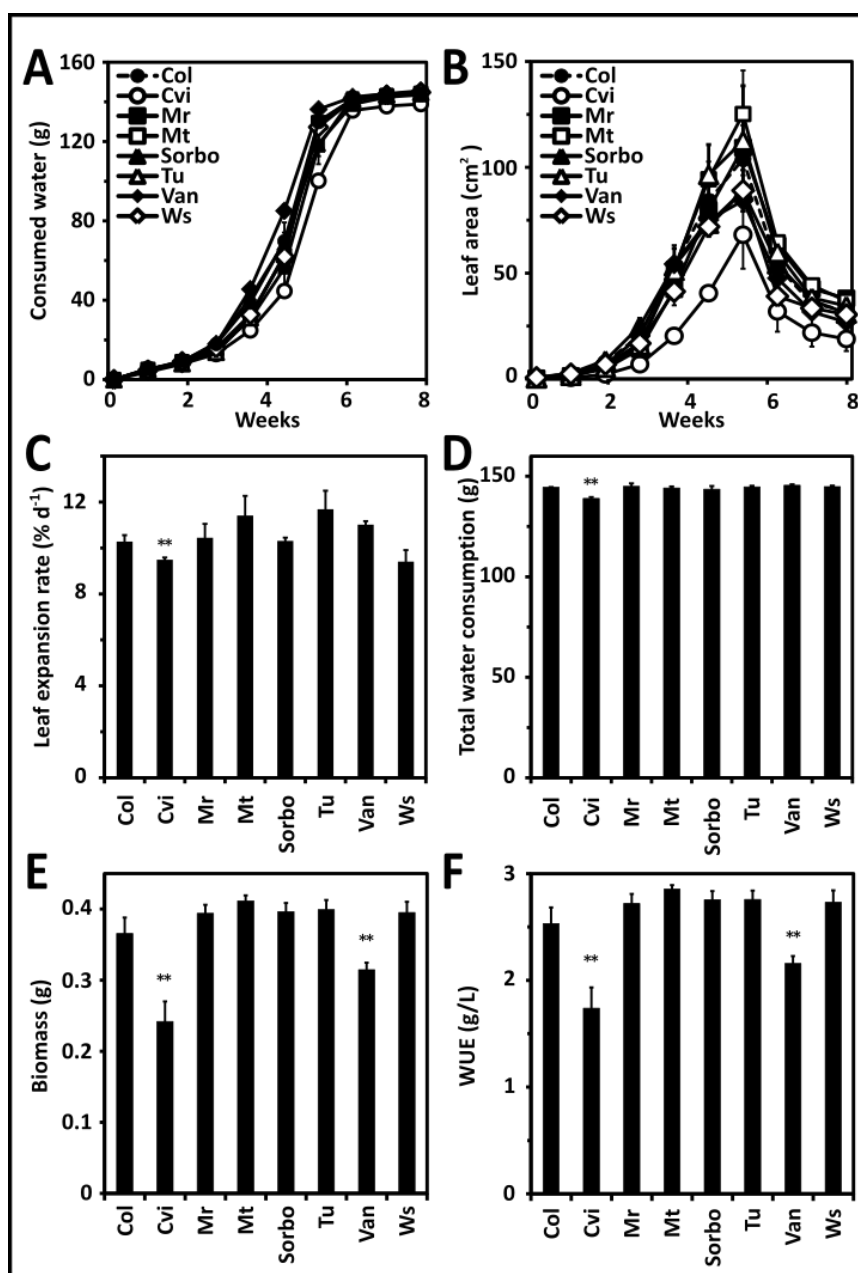


Figure 3-27 Water productivity of Arabidopsis accessions under progressive drought conditions. Changes in water consumption A), leaf area B) and maximum leaf expansion rate C) during the progressive drought of Col-0 (Col, filled circles), Cvi-0 (Cvi, open circles), Mr-0 (Mr, filled squares), Mt-0 (Mt, open squares), Sorbo (filled triangles), Tu-0 (Tu, open triangles), Van-0 (Van, filled diamonds) and Ws-0 (Ws, open diamonds) are depicted. The values are given in percentage increase per day. Total water consumption D), above-ground dry biomass E) and WUE F) of these accessions at the end of the progressive drought. Plants were grown randomly in 24-pot trays in a single experiment. Growth conditions as described in Fig. 3-26. A-D) n=3 biological replicates, mean  $\pm$  SEM, \*\*P<0.001 compared with accession Col-0.



Thermography provided the first sign of differences in leaf transpiration, implying possible different water consumption patterns for *Arabidopsis* accessions in the long run. During the progressive drought, pots of plants were weighed in 5-day intervals and the water consumed by all accessions was determined. Col-0 consumed  $18 \text{ g} \pm 2 \text{ g}$  soil water in the first three weeks, and this increased rapidly to  $130 \text{ g} \pm 1 \text{ g}$  in the subsequent two weeks, after which it consumed a further  $15 \text{ g} \pm 1 \text{ g}$  water by the end of the progressive drought (Fig. 3-27A). 50% of total water consumption of Col-0 occurred at the day 30. Compared with Col-0, Cvi-0 needed more time to consume the half of its total water use, while Van-0 needed 3 days less to use up 50% of its total water consumption (Fig. 3-27B). Leaf areas reflected the biomass accumulation during the progressive drought, and were measured at 5-day intervals. The leaf area of Col-0 increased from  $0.6 \text{ cm}^2 \pm 0.1 \text{ cm}^2$  to  $104 \text{ cm}^2 \pm 4 \text{ cm}^2$  in five and half weeks, with a maximum leaf expansion rate of  $10.3 \% \text{ d}^{-1} \pm 0.3 \% \text{ d}^{-1}$ , followed by a decline in leaf area in the subsequent two weeks (Fig. 3-27C and D). Cvi-0 grew more slowly than Col in the same period, with an 8% lower growth rate and a 40% smaller maximum leaf area (Fig. 3-27C and D). Other ecotypes did not differ clearly from Col-0 in terms of leaf expansion rate or maximum leaf area.

At the end of the progressive drought, Col-0 had accumulated  $0.37 \text{ g} \pm 0.02 \text{ g}$  dry biomass. Accessions like Mr-0, Mt-0, Sorbo, Tu-0 and Ws-0 had a slightly high biomass than Col-0, while Cvi-0 and Van-0 had  $34\% \pm 8\%$  and  $14\% \pm 3\%$  less biomass respectively (Fig. 3-27E). All ecotypes used up a similar amount of water at the end of the drought, implying that accessions which had more biomass would have a higher WUE. Indeed, Mr-0, Mt-0, Sorbo, Tu-0 and Ws-0 had a slightly higher WUE, while that of Cvi-0 and Van-0 were  $31\% \pm 8\%$  and  $14\% \pm 8\%$  lower, respectively (Fig. 3-27F).

### **3.3.1.3 Associations among biomass, leaf surface temperatures, leaf growth and water use efficiency**

Further analysis of the growth performance, biomass accumulation, and integrated WUE in RCAR overexpression lines exposed to progressive drought revealed that gravimetric-derived integrated WUE correlated positively with leaf temperature (Fig. 3-27A,  $R = 0.93$ ,  $P = 0.001$ ) and biomass (Fig. 3-27B,  $R = 0.99$ ,  $P < 0.001$ ). In addition, leaf area ( $R = 0.43$ ,  $P = 0.32$ ) or maximum leaf expansion rate ( $R = 0.40$ ,  $P = 0.32$ ) under well-watered conditions displayed a weak positive association with WUE at the

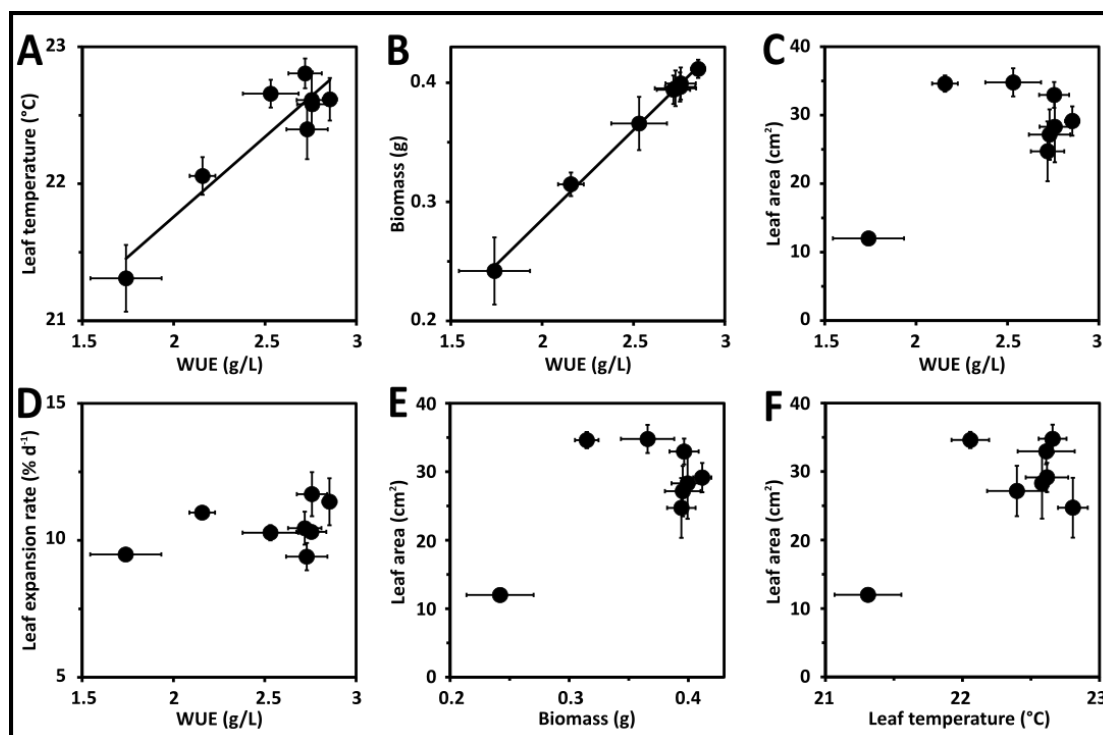


Figure 3-28 Correlations among leaf temperature, leaf area, leaf expansion rate, biomass and WUE in *Arabidopsis* accessions. A) Correlation between leaf temperature and WUE. B) Genetic correlation between biomass and WUE. C) Correlation between leaf area and WUE. D) Genetic correlation between leaf expansion rate and WUE. E) Correlation between leaf area and biomass. F) Correlation between leaf area and leaf temperature. All the data is from the experiment shown in section 3.3.1.1 and 3.3.1.2. Each bivariate data point corresponds to the accession mean values for both traits. A-F)  $n=3$  biological replicates, mean  $\pm$  SEM.

end of a progressive drought (Fig. 3-28C and D). Compared with Cvi-0, other *Arabidopsis* accessions which displayed higher WUE had larger leaf area and faster leaf expansion rate under well-watered conditions (Fig. 3-28C and D). It was also found that leaf area was weakly associated with biomass (Fig. 3-27E,  $R = 0.40$ ,  $P = 0.32$ ) and leaf temperatures under well-watered conditions (Fig. 3-27F,  $R = 0.58$ ,  $P = 0.14$ ). These results suggest that high WUE is not tightly linked reduced growth.

### 3.3.1.4 Water productivity of *Arabidopsis* accessions in an independent progressive drought

An independent progressive drought experiment was performed using *Arabidopsis* accessions RLD-0, Ler-0, Col-0, and Cvi-0. In this experiment, pots of 600 cm<sup>3</sup> volume were used, and 100 g dry soil was loaded into each. After saturating the soil, no further water was administered. Seven-day-old seedlings were transferred into the pots and grew under domes for seven days. Subsequently, the domes were removed

and all plantlets grew for another four days. The pots were then covered and the

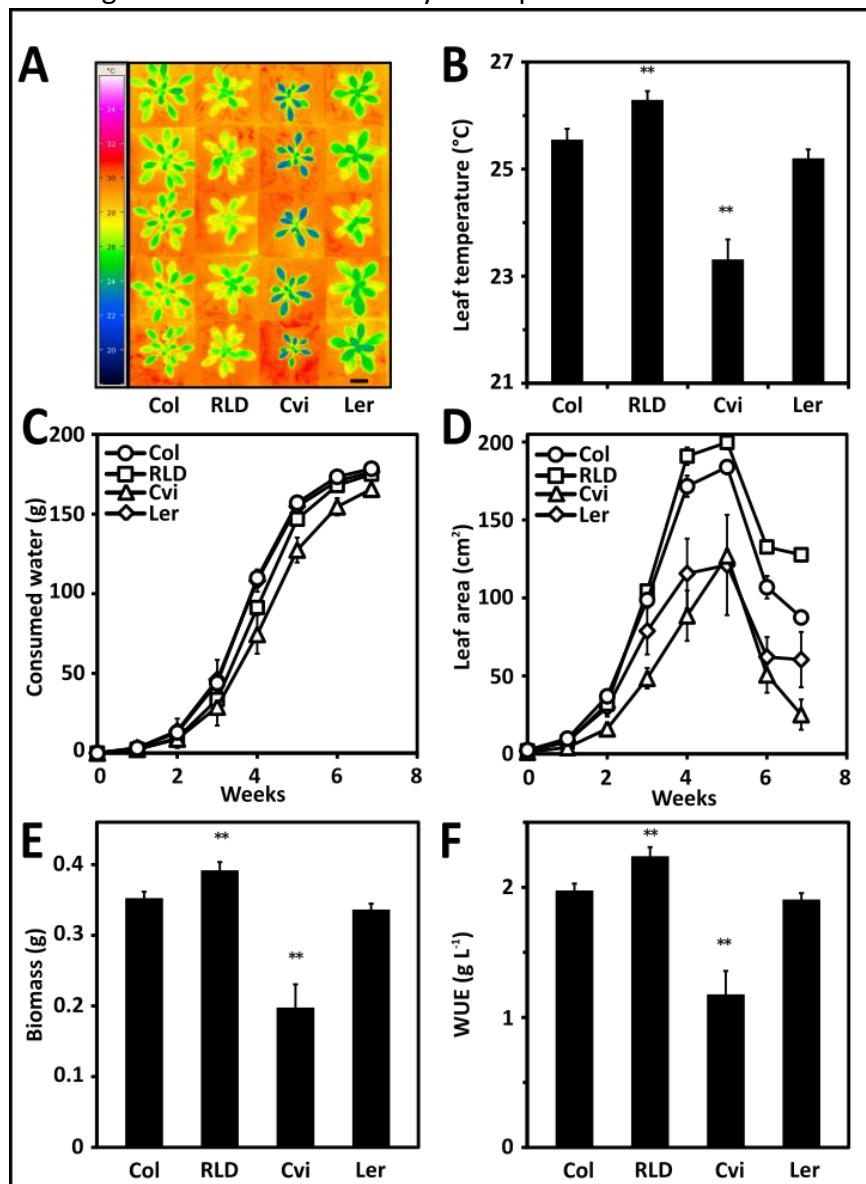


Figure 3-29 Water productivity of Arabidopsis accessions. A) Thermogram and B) leaf temperatures of 37-day-old plants of Arabidopsis accessions Col-0 (Col), RLD-0 (RLD), Cvi-0 (Cvi), Ler-0 (Ler). Changes in water consumption C) and leaf area D) of Col (open circles), RLD (open squares), Cvi-0 (open triangles), Ler-0 (open diamonds) during the progressive drought. Final above-ground dry biomass E) and WUE F) of these accessions at the end of the progressive drought. There was 220 g water in the soil (37% soil water content) at the onset of the progressive drought. In this experiment, pots of 600 cm<sup>3</sup> volume were filled with 100 g dry soil. After saturating the soil with water, seven-day-old seedlings were transferred into the pots and allowed to grow under a dome without watering for seven days. Subsequently, the domes were removed and all plantlets grew for another four days without watering. The pots were covered and the progressive drought started at this time. All plants were grown under short day conditions (8 h light / 16 h dark photoperiod) at photon flux density of 150  $\mu\text{mol m}^{-2} \text{s}^{-1}$  and 22°C and 50% relative humidity in the daytime and 17°C and 60% relative humidity at night. The scale bar in A) represents 2 cm. Five plants were grown per line in separate pots at randomized positions and the thermal pictures were arranged in groups after imaging. B-E) n=5 biological replicates per line, mean  $\pm$  SEM, \*\*P<0.001 compared with

## Results

---

accession Col-0.

progressive drought started at this time. There was 220 g water in the soil (37% soil water content) at the onset of the progressive drought.

After 17 days of growth, the water consumption of each line did not differ much and the soil water content for all was around 32% (Fig. 3-29C). However, the leaf surface temperatures of the accessions showed considerable variations (Fig. 3-29A and B). Compared with Col-0 ( $25.5\text{ }^{\circ}\text{C} \pm 0.1^{\circ}\text{C}$ ), the leaf surface temperature of RLD-0 was higher by  $0.7\text{ }^{\circ}\text{C} \pm 0.2\text{ }^{\circ}\text{C}$  while that of Cvi-0 was  $2.2\text{ }^{\circ}\text{C} \pm 0.4\text{ }^{\circ}\text{C}$  lower. In the same conditions, Ler-0 showed a minor decrease of leaf surface temperature compared with Col-0.

During the progressive drought, both RLD-0 and Cvi-0 showed delayed patterns in water consumption, while that of Ler-0 was similar to that of Col-0 (Fig. 3-29C). During this period, Col-0 showed an increase of leaf area from  $2\text{ cm}^2 \pm 0.1\text{ cm}^2$  to  $183\text{ cm}^2 \pm 4\text{ cm}^2$  (its maximum leaf area) in four weeks (Fig. 3-29D). RLD-0 showed a comparable leaf area at the onset of the experiment, but it generated a  $9\% \pm 2\%$  higher maximum leaf area during the same period, while both Ler-0 and Cvi-0 had similar leaf area at the beginning generated a 40% smaller maximum leaf area (Fig. 3-29D).

At the end of the progressive drought, all the accessions showed the same tendency for above-ground dry biomass as they did for maximum leaf area, except Ler-0 which had a smaller leaf area but comparable biomass to Col-0 (Fig. 3-29E). Regarding that at the end of the progressive drought all accessions used the same amount of water, it is expected that accessions accumulated more biomass would have a higher WUE. Col-0 achieved a WUE of  $2.0\text{ g/L} \pm 0.1\text{ g/L}$  (Fig. 3-29F) while an enhanced WUE by a factor of 1.2 was observed in accession RLD-0 compared with Col-0. The WUE of Cvi-0 was lowered by 1.7-fold (Fig. 3-29F) and Ler-0 showed comparable WUE as Col-0 (Fig. 3-29F).

Taken together, the "cool" leaf temperature accession, Cvi-0, had both reductions of biomass and WUE compared with Col-0 while the "hot" leaf temperature accession RLD-0 achieved  $13\% \pm 4\%$  enhanced WUE at no expense to biomass accumulation (Fig. 3-29 A, B, E and F).

### 3.3.1.5 Gas exchange analysis of Arabidopsis accessions under well-watered and progressive drought conditions

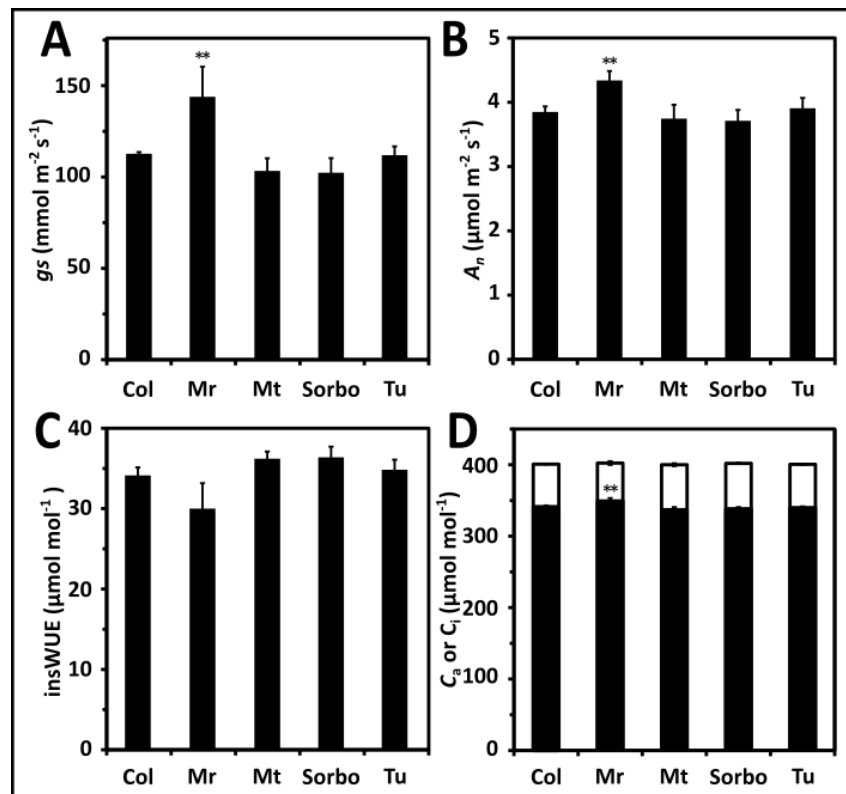


Figure 3-30 Gas exchange analysis of Arabidopsis accession Col-0 (Col), Mr-0 (Mr), Mt-0 (Mt), Sorbo and Tu-0 (Tu). Stomatal conductance ( $g_s$ ) A) and net carbon assimilation rate ( $A_n$ ) B) with whole rosette measurements of these accessions were determined at a photon flux density of  $150 \mu\text{mol m}^{-2} \text{s}^{-1}$ , an external  $\text{CO}_2$  level of  $420 \mu\text{mol mol}^{-1}$  and a vapor pressure deficit of  $13 \pm 2 \text{ Pa kPa}^{-1}$ . InsWUE C) defined as the ratio of  $A_n$  to  $g_s$  and D)  $\text{CO}_2$  concentration at ambient ( $C_a$ , white columns) and intercellular  $\text{CO}_2$  concentration ( $C_i$ , black columns) were determined. 30 d  $\pm$  2 d old plants grown under well-watered conditions ( $\text{SWP} \geq -0.02 \text{ bar}$ ) were used to perform the gas exchange analysis. All plants were grown under short day conditions (8 h light / 16 h dark photoperiod) at photon flux density of  $150 \mu\text{mol m}^{-2} \text{s}^{-1}$ , and  $22^\circ \text{C}$  and 50% relative humidity in the day time and  $17^\circ \text{C}$  and 60% relative humidity at night. A-D)  $n=3$  biological replicates with three technical replicates, mean  $\pm$  SEM, \*\* $P < 0.001$  compared with accession Col.

To study the physiological basis of natural variations in the WUE of various Arabidopsis accessions, a gas exchange analysis was conducted using 30 days  $\pm$  2 days Col-0, Mr-0, Mt-0, Sorbo and Tu-0 at a photon flux density of  $150 \mu\text{mol m}^{-2} \text{s}^{-1}$ , an external  $\text{CO}_2$  level of  $420 \mu\text{mol mol}^{-1}$ , and a vapor pressure deficit of  $13 \text{ Pa kPa}^{-1} \pm 2 \text{ Pa kPa}^{-1}$ . Mt-0, Sorbo, and Tu-0 did not show significant differences in  $A_n$  (net carbon assimilation rate),  $g_s$  (stomatal conductance), insWUE (instantaneous WUE) and  $C_a - C_i$  ( $\text{CO}_2$  gradient between ambient and intercellular space) compared with Col-0.

However, accession Mr-0 had a 13% higher  $A_n$ , which was achieved through the combined effects of 28% higher  $g_s$  and 10% lower  $\text{CO}_2$  gradient  $C_a - C_i$  compared with Col-0, which lowered the insWUE of Mr-0 by 12% (Fig. 3-30A-D).

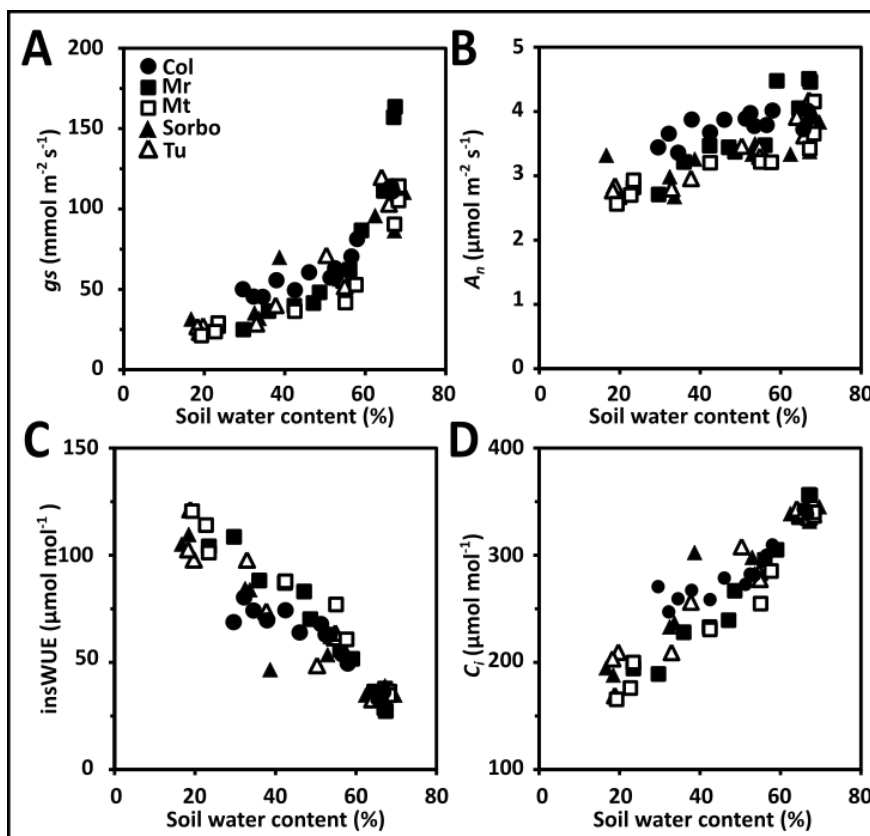


Figure 3-31 Enhanced insWUE in Arabidopsis accessions by reduced soil water content. Stomatal conductance ( $g_s$ ) A) and net carbon assimilation rate ( $A_n$ ) B) of whole rosette measurements of Col-0 (Col, filled circles), Mr-0 (Mr, filled squares), Mt-0 (Mt, open squares), Sorbo (filled triangles) and Tu-0 (Tu, open triangles) were determined at a photon flux density of  $150 \mu\text{mol m}^{-2} \text{s}^{-1}$ , an external  $\text{CO}_2$  level of  $420 \mu\text{mol mol}^{-1}$  and vapor pressure deficit of  $13 \pm 2 \text{ Pa kPa}^{-1}$ . InsWUE C) defined as the ratio of  $A_n$  to  $g_s$  and D)  $\text{CO}_2$  concentration in intercellular space ( $C_i$ ) were determined. Three plants for each line were used to conduct the gas exchange measurements. All plants were grown under short day conditions (8 h light / 16 h dark photoperiod) at a photon flux density of  $150 \mu\text{mol m}^{-2} \text{s}^{-1}$  and  $22^\circ\text{C}$  and 50% relative humidity in the day time and  $17^\circ\text{C}$  and 60% relative humidity at night. A-D)  $n=3$  biological replicates, single measurements for each data point with three technical replicates.

With the depletion of soil water content from 70% to 20%, the  $g_s$  and  $C_i$  of all accessions dropped by 7-fold and 2.3-fold (Fig. 3-31A and D) while  $A_n$  only had 1.3-fold reduction (Fig. 3-31B). The  $A_n$  responded less to soil water content was due to the counterbalance of the reduced  $g_s$  by the 5-fold  $C_a - C_i$  (Fig. 3-31D). As a consequence, the insWUE of these accessions showed more than a two-fold enhancement under 20% soil water content than under 70% (Fig. 3-31C).

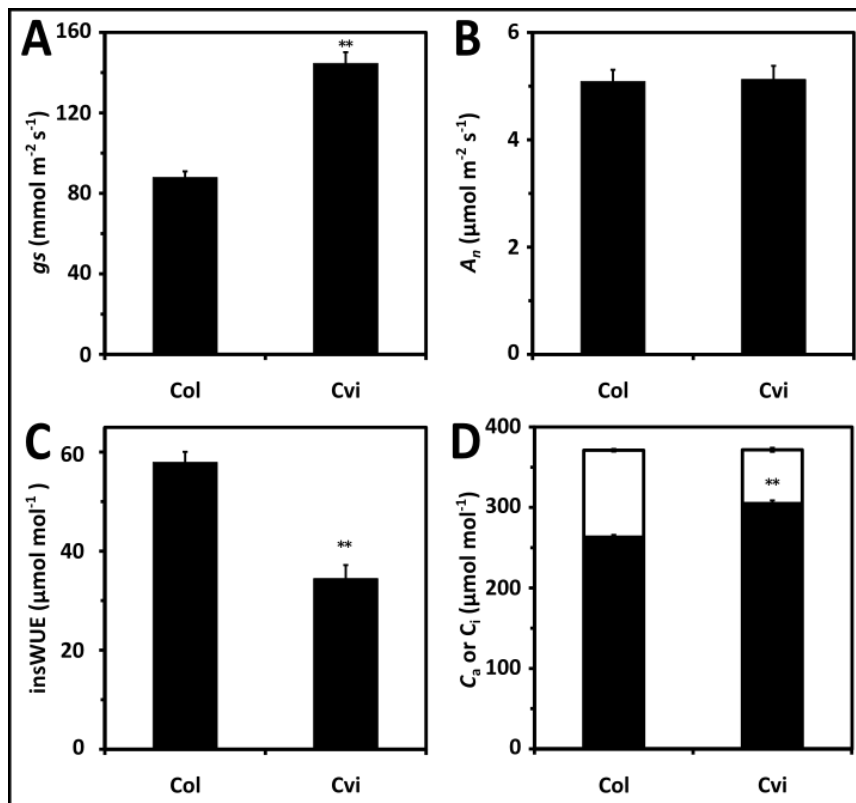


Figure 3-32 Lower insWUE in Arabidopsis accession Cvi-0. Stomatal conductance ( $g_s$ ) A) and net carbon assimilation rate ( $A_n$ ) B) of Col-0 (Col) and Cvi-0 (Cvi) determined at a photon flux density of  $200 \mu\text{mol m}^{-2} \text{s}^{-1}$ , an external  $\text{CO}_2$  level of  $380 \mu\text{mol mol}^{-1}$ , and a vapor pressure deficit of  $15 \text{ Pa kPa}^{-1} \pm 1 \text{ Pa kPa}^{-1}$ . InsWUE C) defined as the ratio of  $A_n$  to  $g_s$ , D) ambient  $\text{CO}_2$  concentration ( $C_a$ , white columns), and intercellular  $\text{CO}_2$  concentration ( $C_i$ , black columns) were determined. Single leaf measurements of 30-day-old Col and Cvi plants grown under well-watered conditions ( $\text{SWP} \geq -0.02 \text{ bar}$ ) were used to perform gas exchange analysis. All plants were grown under short day conditions (8 hours light/16 hours dark photoperiod) at photon flux density of  $150 \mu\text{mol m}^{-2} \text{s}^{-1}$  and  $22^\circ\text{C}$  and 50% relative humidity in the day time,  $17^\circ\text{C}$  and 60% relative humidity at night. A-D)  $n=3$  biological replicates with five technical replicates, mean  $\pm$  SEM, \*\* $P < 0.001$  compared with accession Col.

Independent gas exchange measurements were performed on single leaves of Arabidopsis accessions Col-0 and Cvi-0 grown under well-watered conditions. The  $A_n$  of Cvi-0 did not differ from that of Col-0, while its  $g_s$  was higher by  $56\% \pm 7\%$ , which led to an insWUE lower by a factor of 1.6 (Fig. 3-32A-C). Further analysis revealed  $29\% \pm 2\%$  lower  $C_a - C_i$  in Cvi-0, which was caused by  $29 \mu\text{mol mol}^{-1} \pm 2 \mu\text{mol mol}^{-1}$  higher intercellular  $\text{CO}_2$  than the level in Col-0. (Fig. 3-32D).

### 3.3.1.6 Stomatal aperture and size contribute to leaf temperature differences between Col-0 and Cvi-0

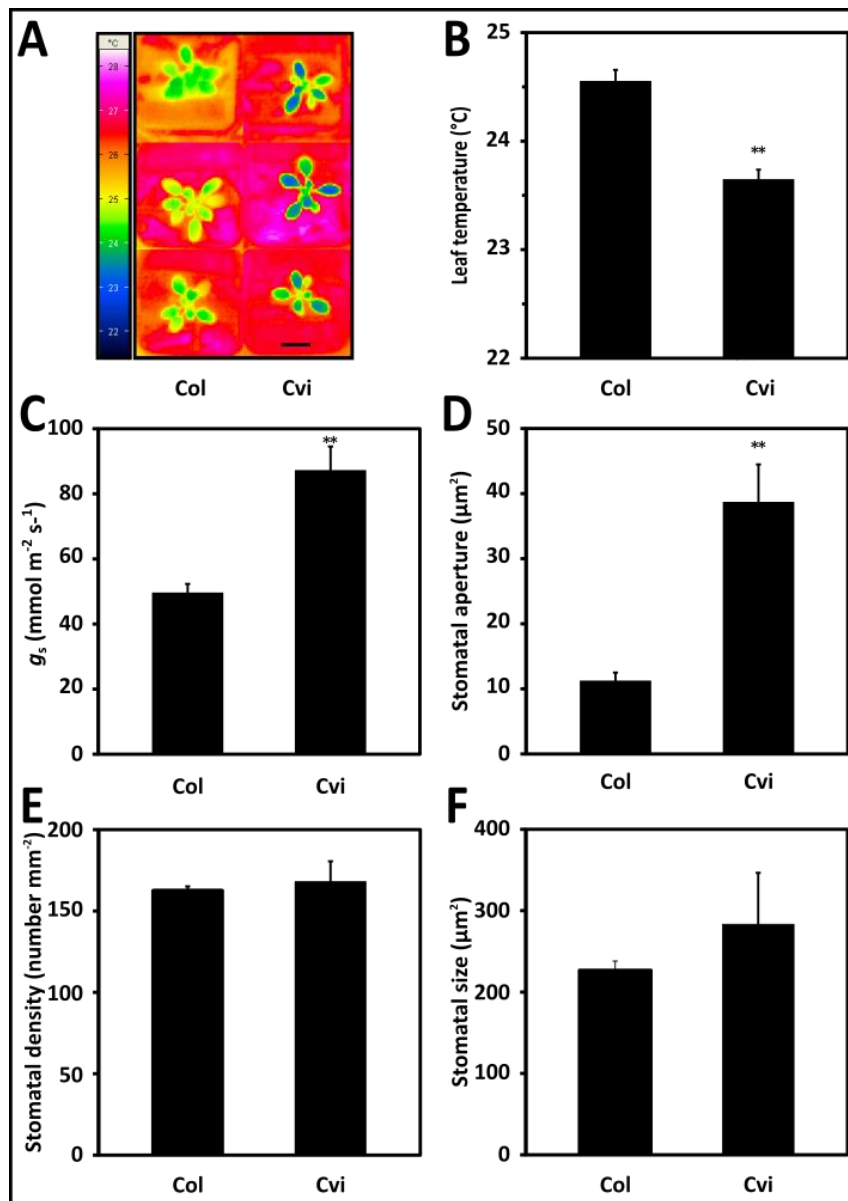


Figure 3-33 Cool leaf temperature and high stomatal conductance in accession Cvi-0 caused by larger stomatal pores and stomatal size. After the determination of the thermogram A), leaf surface temperature B) as shown in A) and stomatal conductance ( $g_s$ ) C) of 26-day-old plants of Col-0 (Col) and Cvi-0 (Cvi), stomatal aperture (defined as oval area of the stomatal pore) D), stomatal density (number per mm<sup>2</sup>) E) and stomatal size (defined as the area of stomatal pores) F) were measured using comparable leaves detached from these plants. The scale bar in A) represents 2 cm. Stomatal conductance B) was determined at a photon flux density of 200 μmol m<sup>-2</sup>s<sup>-1</sup>, an external CO<sub>2</sub> level of 380 μmol mol<sup>-1</sup> and a vapor pressure deficit of 23 Pa kPa<sup>-1</sup> ± 1 Pa kPa<sup>-1</sup>. All plants were grown under well-watered conditions. Plants grown condition as described in Fig. 3-26. A-F) n=3 biological replicates, mean ± SEM, \*\*P<0.001 compared with accession Col.



The reduced WUE of the accession Cvi-0 was proved to be caused by a maintained  $A_n$  and enhanced  $g_s$  which are the consequences of either increased stomatal density, stomatal size or stomatal aperture. To understand this, stomatal parameters were determined by observing separated epidermal peels from 26-day-old Col-0 and Cvi-0 leaves under a microscope, directly after thermal imaging and gas exchange measurements. The leaf surface temperatures and stomatal conductance were confirmed again (Fig. 3-33 A-C). Stomatal apertures (defined as the area of stomatal pores) of Col-0 averaged in  $11.3 \mu\text{m}^2 \pm 1 \mu\text{m}^2$  while those of Cvi-0 were three times larger (Fig. 3-33 D). Cvi-0 did not differ from Col in stomatal density (Fig. 3-33 E) but produced larger stomata by a factor of 1.3 (Fig. 3-33 F). Taken together, the enhanced  $g_s$  of Cvi-0 was caused by larger stomata and bigger stomatal aperture.

### 3.3.2 Quantitative trait locus mapping of cool leaf temperature gene MPK12 and its function in the regulation of WUE

#### 3.3.2.1 Variation in leaf surface temperature during the progressive drought

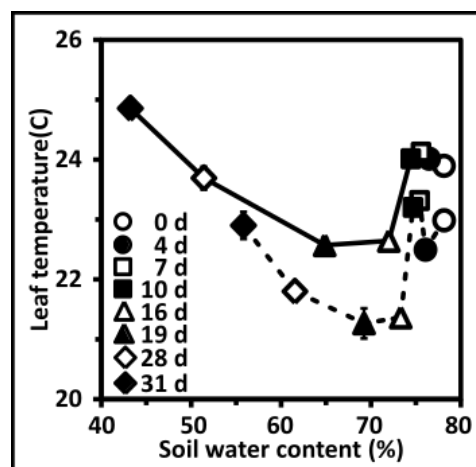


Figure 3-34 Leaf surface temperatures of Col-0 and Cvi-0 in relation to the depletion of soil water content. Seven-day-old seedlings were transferred into soil and were grown under well-watered conditions for another seven days. After covering the pots, 18-day-old plantlets were subjected to the progressive drought. Thermogram was taken to determine leaf temperatures of both Col-0 (Col; solid line) and Cvi-0 (Cvi; dotted line). Symbols indicate days after watering ceased. Experimental design and growth condition as described in Fig. 3-1.  $n=3$  biological replicates for each data point, mean  $\pm$  SEM.

Since a variation in leaf surface temperatures was observed between Arabidopsis accessions Col-0 and Cvi-0, an attempt was made to identify the genes responsible

for the cool-leaf-temperature trait. To achieve this, a high through-put method and a stable phenotype were needed. Thermal imaging was used to detect leaf surface temperatures of Col-0, Cvi-0, and their offspring. In order to eliminate variations in leaf surface temperature caused by environmental factors, each measurement was performed in the controlled ambient conditions in a phyto-chamber.

In addition, leaf temperatures in response to different soil water content were compared for Col-0 and Cvi-0 over five weeks' progressive drought to find the optimum conditions that showed the biggest leaf temperature difference. A reduction in soil water content from 80% to 70% systematically resulted in at least a 1 °C reduction in leaf surface temperature, from 24 °C to 23 °C for Col-0 and from 23 °C to 21 °C for Cvi-0 (Fig. 3-34). Further depletion of soil water below 70% led to reduced differences in leaf surface temperatures (Fig. 3-34). Taken together, leaf surface temperatures of 37-day-old plants grown under well-watered conditions (>70% soil water content) were chosen as a readout for the phenotype for the following QTL mapping.

### **3.3.2.2 Leaf surface temperatures of Col-0, Cvi-0 and reciprocal F1 and F2 generations**

After determination of the optimum conditions for distinguishing leaf surface temperatures, one cross was performed with Col-0 (female parent) and Cvi-0 (male parent). Reciprocal F1 plants from several independent cross events were confirmed as heterozygous and were allowed to self-pollinate to propagate F2 seeds. Ninety-six F2 seeds were sown in the soil as a first mapping population. The leaf surface temperatures of Col-0, Cvi-0, reciprocal F1, and F2 plants were analyzed (Fig. 3-35A-C). Cvi-0 showed "cool" leaf temperatures, averaging 21.8 °C, while Col-0 and the reciprocal F1 hybrid were up to 1.3 °C higher (Fig. 3-35B). Further analysis of distributions of leaf temperatures showed the normal distribution in Col-0, Cvi-0 and

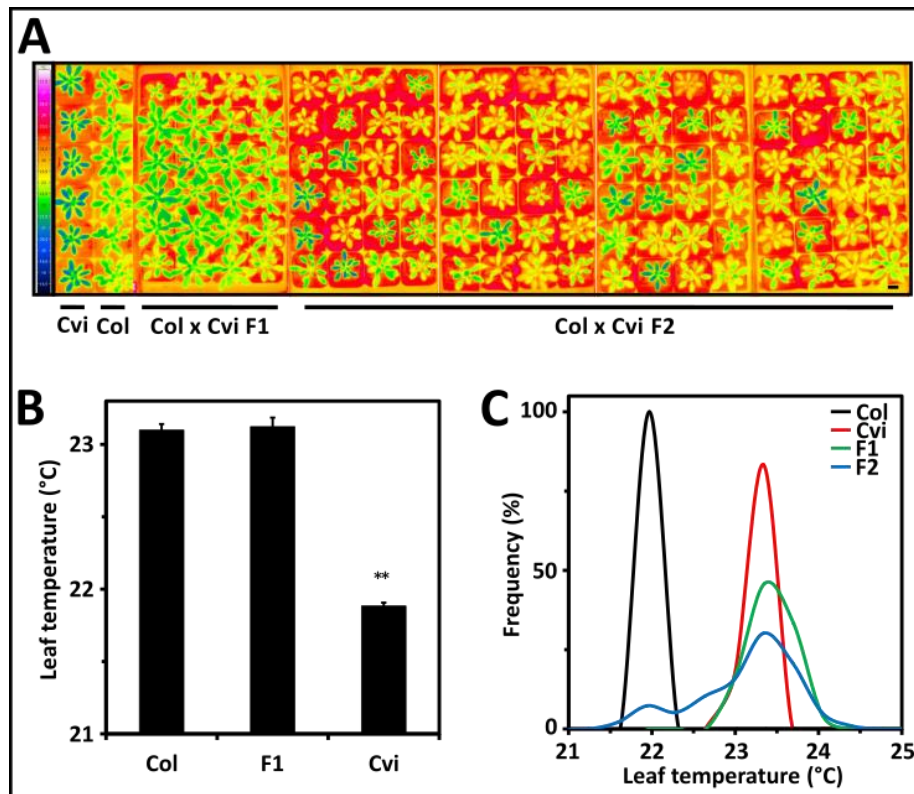


Figure 3-35 Leaf temperatures of Col-0, Cvi-0 and their reciprocal F1 and F2 generations. A) Thermogram of Col-0 (Col), Cvi-0 (Cvi) and reciprocal F1 and F2 generations and B) leaf surface temperature values of parental lines and F1 generation shown in A) and C) distributions of leaf temperature of Col (black line), Cvi (red line) and Col x Cvi F1 (green line) and F2 (blue line). Plants were 37 days old and grown under short day conditions (8 h light /16 h dark photoperiod) at photon flux density of  $150 \mu\text{mol m}^{-2} \text{s}^{-1}$  and  $22^\circ\text{C}$  and 50% relative humidity in daytime and  $17^\circ\text{C}$  and 60% relative humidity at night and under well-watered conditions ( $\text{SWP} \geq -0.02$  bar). The scale bar donates 2cm. B and C)  $n=6$  biological replicates for Col and Cvi and  $n=24$  for F1 generation, mean  $\pm$  SEM. \*\* $P < 0.001$  compared with wild type Col. F2 population contains 96 plants and were used to analyze the leaf temperature distribution in C).

F1 lines, while that of F2 lines followed Mendel's first law, showing 24 plants with "cool" leaf temperatures like Cvi-0 and 72 plants with "hot" leaf temperatures like Col-0 (Fig. 3-35C). To summarize, these results imply that a single QTL locus is responsible for leaf temperature phenotypes, and the Col allele is dominant while Cvi allele is recessive.

### 3.3.2.3 Leaf surface temperatures of Col-0, Cvi-0, and recombinant inbred lines

The leaf temperature was further analyzed by studying RILs. Generation of RILs needs one intercross between parental lines Col-0 and Cvi-0 to create recombinants which

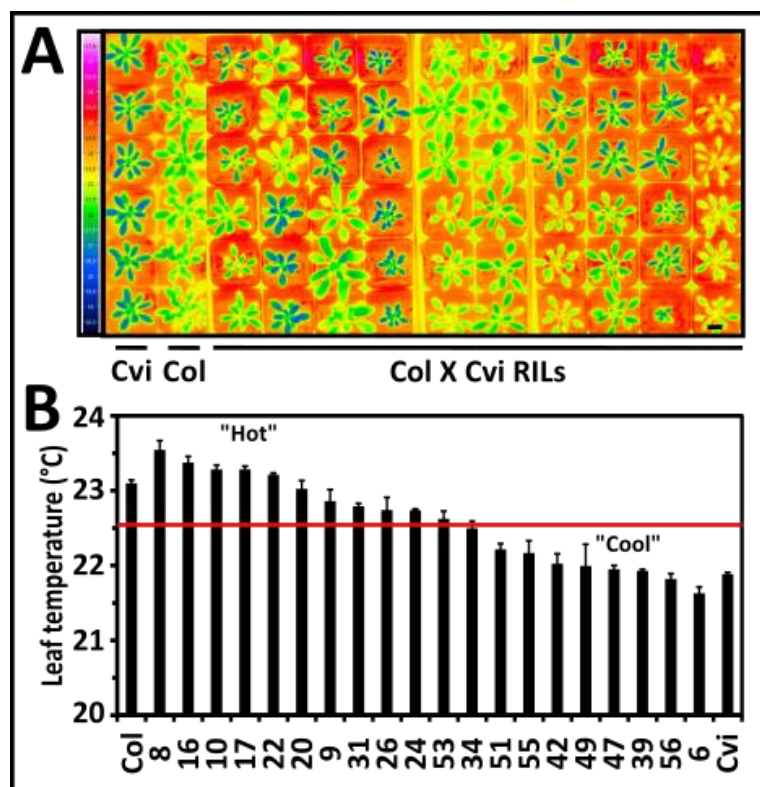


Figure 3-36 Leaf surface temperatures of Col-0, Cvi-0, and their RILs. Thermogram A) displayed with false color and leaf temperature values B) of Col-0, Cvi-0, and RILs (independent lines are indicated by numbers). 37 days old plants grew under the conditions as described in Fig. 3-34. The scale bar in A) equals 2 cm. RILs with the "hot" leaf temperature and "cool" leaf temperature were partitioned by the red solid line. B)  $n=6$  biological replicates for parental lines Col and Cvi and  $n=3$  for RILs, mean  $\pm$  SEM,  $**P<0.001$  compared with wild type.

are then inbred to isogenicity through seven cycles of self-crosses (Crow, 2007). A RIL possesses a permanent set of recombination events. A core set of 20 RILs consisting of defined recombination events (see Fig. 3-37B in the next section) were used in this study to investigate the variations in their leaf temperatures. Thermogram of 37-day-old RILs grown under well-watered conditions was analyzed and the results showed considerable variations in leaf temperature. Nine of twenty RILs below the red line displayed "cool" leaf temperatures while other RILs above the red line had "hot" leaf temperatures (Fig. 3-36A and B). This classification would facilitate to find the loci responsible for the variations in leaf temperatures afterward.

### 3.3.2.4 Mapping the QTL locus responsible for the leaf surface temperature

The phenotype of the organisms is determined by the genotype, the epigenetic

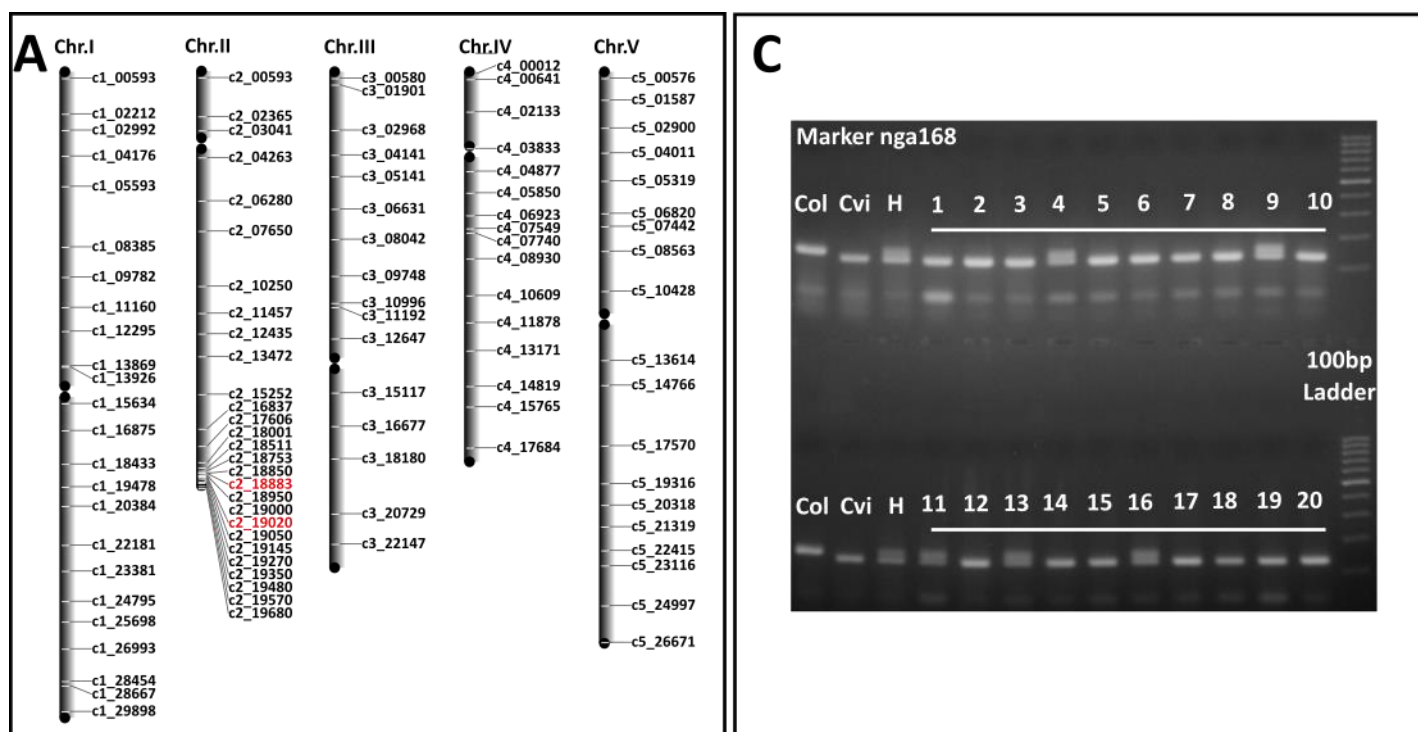
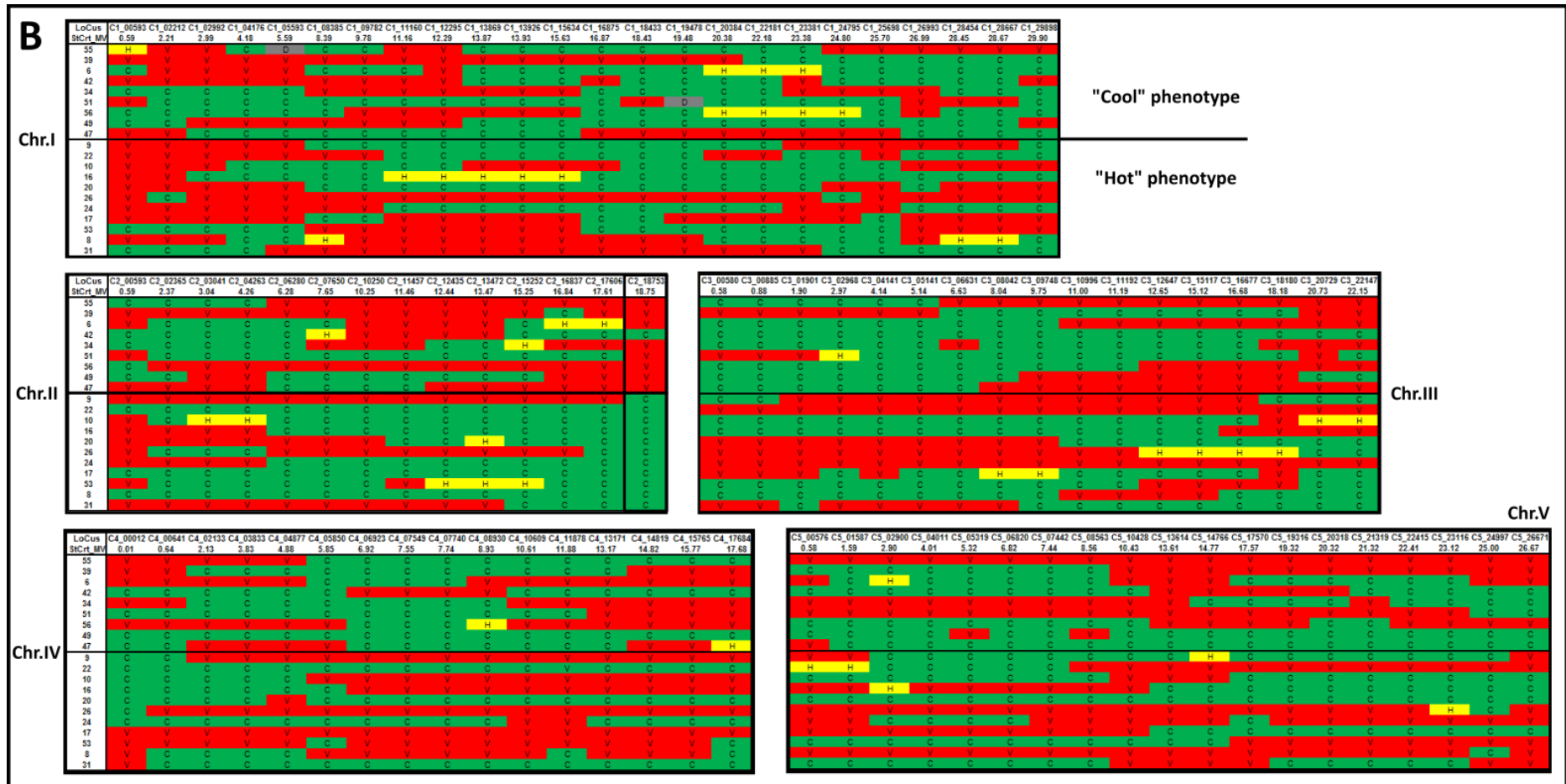


Figure 3-37 Genome and genotype of Col, Cvi and their F2 and RILs populations. Schematic presentation of SNP markers between parental lines distributed on five chromosomes A) were designed by (Simon *et al.*, 2008). 14 additional markers at the end of chromosome 2 were generated for fine mapping. Red highlights two markers flanking the target gene. B) Known genotypes of RILs on five chromosomes (five blocks shown here) were downloaded (<http://publiclines.versailles.inra.fr/page/8>) and were aligned according to their leaf temperature phenotypes (above the black line running through the middle of blocks are "hot" leaf temperature phenotypes while below are "cool" leaf temperature phenotypes). Green, red, and yellow represent Col-like genotype (C), Cvi-like genotype (V) and heterozygous genotype (H) respectively. The black frame at the end of chromosome two indicates the possible locus responsible for leaf temperature traits. C) Genotypes of plantlets showing "cool leaf temperature" phenotype in figure 3-34, using marker nga168 on chromosome 2 close to c2\_18753. Labels with Col, Cvi, and H represent genotypes of Col, Cvi and their F1 generation (H). Numbers 1 to 20 indicates individual F2 lines.

Results



factors, and the environmental factor (Davies *et al.*, 2012; Feil and Fraga, 2011). In this study, the epigenetic factors are ignored, and the environmental factors are also not considered owing to the homogeneity of the growth conditions of plants. In this case, the phenotypes of plants are assumed to be determined by their genotypes. The Cvi-0 x Col-0 RILs have been used to build a genetic map with 90 markers spaced roughly 1.4 Mb apart on five chromosomes of *Arabidopsis* (Fig. 3-37A). Genotypes of 20 RILs (Fig. 3-37B) were generated by (Simon *et al.*, 2008), and the data was downloaded from <http://publiclines.versailles.inra.fr/page/8>. The genotypes were aligned according to the leaf temperature phenotypes of 20 RILs (Fig. 3-36A and B). The alignment results are shown in Fig. 3-37B, in which five blocks represent five chromosomes. Green, red, and yellow cells indicate Col-like genotype (C), Cvi-like genotype (V) and heterozygous genotype (H) respectively. Each block is separated into two parts by a black line. Above the black lines are "hot" leaf temperature phenotypes while below are "cool" leaf temperature phenotypes. The black frame at the end of chromosome two indicates the possible locus responsible for leaf temperature traits, because the genotypes in this region explain the most of the phenotypes of 20 RILs (Fig. 3-37B). "Since the chance of a crossover producing recombination between genes is directly related to the distance between two genes, the lower the frequency of recombination between two markers, the closer they are situated on a chromosome" (Semagn *et al.*, 2006). The closer to the end of chromosome two, there tend to be fewer recombination events (Fig. 3-37B), which indicates that the candidate locus explaining leaf temperature variations should be close to the marker c2\_18753, which shows a single recombination event (Fig. 3-37B).

In addition, another proof was obtained by aligning the genotypes of reciprocal F2 plants that showed "cool" leaf temperatures in Fig. 3-35C. Electrophoresis results of the nga168 marker, which is located at 16800 kb on chromosome two, did not show Col genotype, implying that the "cool" leaf temperature phenotype was linked to marker nga168 (Fig. 3-37C). Taken together, these results restrict the gene responsible for leaf temperature variation between Col-0 and Cvi-0 to the region from marker c2\_18753 to the end of chromosome two.

### 3.3.2.5 Recombination events in F2 mapping population

In order to identify the gene responsible for the leaf temperature trait within the restricted region, 14 additional markers between 18001Kb and 19680Kb (the end of chromosome two) were generated (Fig. 3-37A). Alignments of the phenotypes and the genotypes of 20 RILs showed no recombination event between markers c2\_18753, c2\_19680 and the gene "Cool1" (Fig. 3-38A). To narrow down the region still further, a large F2 mapping population of 1000 plants was generated, and their phenotypes and genotypes were collected. Three data sets were obtained. Set one was "cool" leaf temperature phenotype with Cvi genotype (V) (Fig. 3-38B). Set two was "hot" leaf temperature phenotype with heterozygous genotype (H) (Fig. 3-38B) and set three was "hot" leaf temperature phenotype with Col genotype (C) (Fig. 3-38B). Recombination events can be identified using the data from set one and two, but not set three for the reason that it is hard to distinguish the "hot" leaf temperature phenotype between Col-like and heterozygous-like F2 lines. After analyzing the F2 population, 20 F2 lines had recombination events in the region between 18001 Kb and 19680 Kb (Fig. 3-38B). Twelve recombination events occurred for marker c2\_18001 at the left border and nine events for marker c2\_19680 at the right border (Fig. 3-38B). Recombination events were reduced when the markers were approaching to the gene responsible for the leaf temperature phenotype (Fig. 3-38B). The f2-9-05 line showed a single recombination event (Fig. 3-38B) because it displayed Cvi-like phenotype (Fig. 3-38D) with a heterozygous genotype at the marker c2\_18883 and a Cvi genotype at the marker c2\_18950 (Fig. 3-38C), implying the gene should be after the marker c2\_18883. Moreover, the F2-3-02 line also had one recombination event (Fig. 3-38B) owing to the closest mismatch of heterozygous phenotype (Fig. 3-38C) and Cvi genotype at the marker c2\_19050 (Fig. 3-38D). Finally, the candidate gene was flanked between the markers c2\_18883 (left border) and c2\_19020 (right border) and located within a chromosome DNA fragment of 137 Kb (Fig. 3-38B).



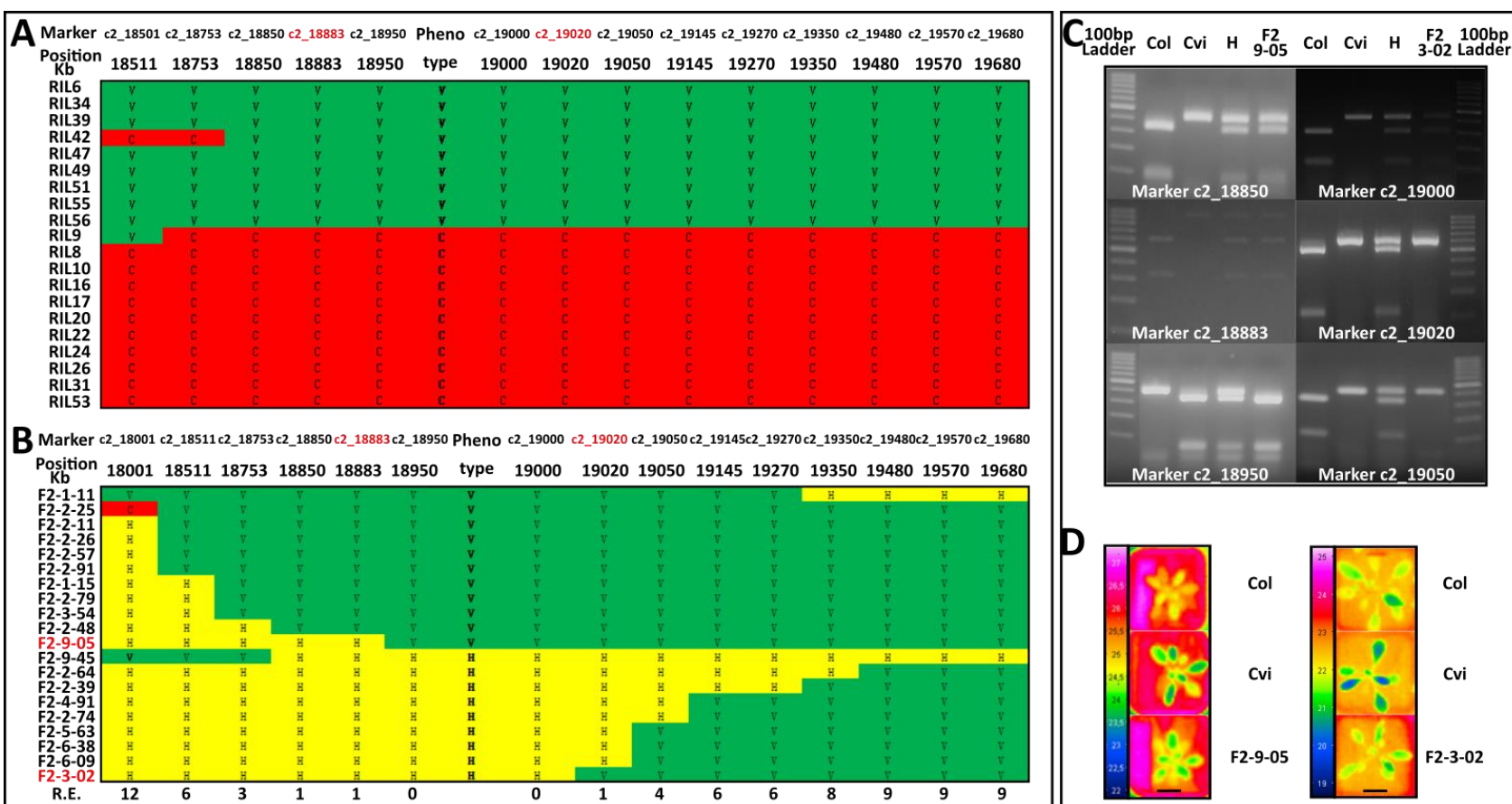


Figure 3-38 Fine mapping of the Cvi "cool" leaf temperature gene to a 137kb region on chromosome 2. A) Recombination events in Col X Cvi F2 mapping population. A) Recombination events in a 1Mb region between marker c2\_18511 and c2\_19680 for RILs and B) recombination events in a 1.6Mb region between marker c2\_18001 and c2\_19680 for the F2 generation. Color codes as described in figure 3-23. C) Genotypes of two Col X Cvi F2 individuals which defined flanking markers and their D) phenotypes. Labels are displayed on the top of electrophoresis pictures. Scale bars in D) donate 2cm. Names of markers are shown at the bottom of each picture.

### 3.3.2.6 Candidate genes

Table 3-3 Candidate gene list between marker c2\_18883 and marker c2\_19020. Gene IDs, names, and descriptions are shown in the table. Gene IDs highlighted in green indicates their priority to be tested.

Gene (18.883-19.020)	Other name	Description
AT2G45900	PNSP	Phosphatidylinositol N-acetylglucosaminyltransferase subunit P-related.
AT2G45910	U-box kinase	U-box domain-containing protein kinase family protein.
AT2G45920	U-box ubiquitin	U-box domain-containing protein.
AT2G45930	-	Unknown protein.
AT2G45940	DUF295	Protein of unknown function.
AT2G45950	SK20	SKP1-like 20 (SK20).
AT2G45960	PIP1B	A member of the plasma membrane intrinsic protein subfamily PIP1.
AT2G45970	CYP86A8	Encodes a member of the CYP86A subfamily of cytochrome p450 genes.
AT2G45980	-	Unknown protein.
AT2G45990	-	Unknown protein.
AT2G46000	-	Unknown protein.
AT2G46020	BRM	Encodes an SWI/SNF chromatin remodeling ATPase.
AT2G46030	UBC6	Ubiquitin conjugating enzyme E2.
AT2G46040	ARID	ARID/BRIGHT DNA-binding domain;ELM2 domain protein.
AT2G46050	PPR-like	Pentatricopeptide repeat (PPR-like) superfamily protein.
AT2G46060	TPR	Transmembrane protein-related.
AT2G46070	MPK12	Encodes a MAP kinase protein.
AT2G46080	BYPASS	Protein BYPASS related.
AT2G46090	Lcbk2	Encodes a putative sphingosine kinase (SphK).
AT2G46100	NTF2	Nuclear transport factor 2 (NTF2) family protein.
AT2G46110	KPHMT1	Encodes a ketopentoate hydroxymethyltransferase.
AT2G46120	tRNA	Pre-tRNA; tRNA-Glu.
AT2G46130	WRKY43	Member of WRKY Transcription Factor.
AT2G46140	LEA1	Late embryogenesis abundant protein.
AT2G46150	LEA2	Late embryogenesis abundant protein.
AT2G46160	RING	RING/U-box superfamily protein.
AT2G46170	RFP	Reticulon family protein.
AT2G46180	GC4	Protein predicted to be a Golgi apparatus structural component.
AT2G46190	MGFP	Mitochondrial glycoprotein family protein.
AT2G46192	-	Other RNA
AT2G46200	-	Unknown protein.
AT2G46210	FAD	Fatty acid/sphingolipid desaturase.
AT2G46220	DUF2358	Uncharacterized conserved protein.
AT2G46225	ABIL1	Encodes a subunit of the WAVE complex.
AT2G46230	PIN	PIN domain-like family protein.

AT2G46240	BAG6	A member of Arabidopsis BAG (Bcl-2-associated athanogene) proteins.
AT2G46250	Myosin	Myosin heavy chain-related.
AT2G46255	MIR159C	Encodes a microRNA that targets several MYB family members.
AT2G46260	-	BTB/POZ/Kelch-associated protein.
AT2G46270	GBF3	encodes a bZIP G-box binding protein.
AT2G46280	TRIP-1	Encodes a homolog of mammalian TGF-beta receptor interacting protein.
AT2G46290	WD40	Transducin/WD40 repeat-like superfamily protein.
AT2G46300	LEA3	Late embryogenesis abundant (LEA) hydroxyproline-rich glycoprotein family.
AT2G46308	-	Unknown protein.
AT2G46310	CRF5	CRF5 encodes one of the six cytokinin response factors.
AT2G46320	-	Mitochondrial substrate carrier family protein.
AT2G46330	-	AGP16:Encodes arabinogalactan protein (AGP16).

The identified region flanked by markers c2\_19883 and c2\_19020 includes 47 genes (Table 3-3). To make the process of identifying the gene responsible for leaf temperature more efficient, a short gene list was generated according to the alignment analysis of amino acid between Col-0 and Cvi-0 and the analysis of guard cell gene expression in Columbia. The nucleotide sequences of the candidate genes were downloaded from <http://signal.salk.edu/atg1001/3.0/gebrowser.php> and were translated into amino acid sequences using an online tool, EMBOSS Transeq ([http://www.ebi.ac.uk/Tools/st/emboss\\_transeq/](http://www.ebi.ac.uk/Tools/st/emboss_transeq/)). Subsequently, alignments of amino acid sequences in Col-0 and Cvi-0 were performed for each candidate gene (data not shown). Genes showing an amino acid difference between Col and Cvi had priority to be tested. In addition, guard cells gene expression data for each candidate gene of Col-0 was downloaded from <http://bar.utoronto.ca/efp/cgi-bin/efpWeb.cgi>. Genes with high expression levels in guard cells were tested firstly. As a result, genes such as AT2G45910, AT2G46070, AT2G46080, AT2G46090, AT2G46140, AT2G46150, AT2G46250, AT2G46280, and AT2G46310 acquired priority to be tested by both Cvi transformants with wild type Col alleles, and by Col knockout mutants.

### 3.3.2.7 MPK12 is the gene responsible for "cool" leaf surface temperature

Cvi transformants with wild type Col alleles were generated by first cloning nine Col-0 genes with their endogenous promoters into pBI121 vector, and then transforming these constructs into wild type Cvi-0 plants through floral dip, and selecting for

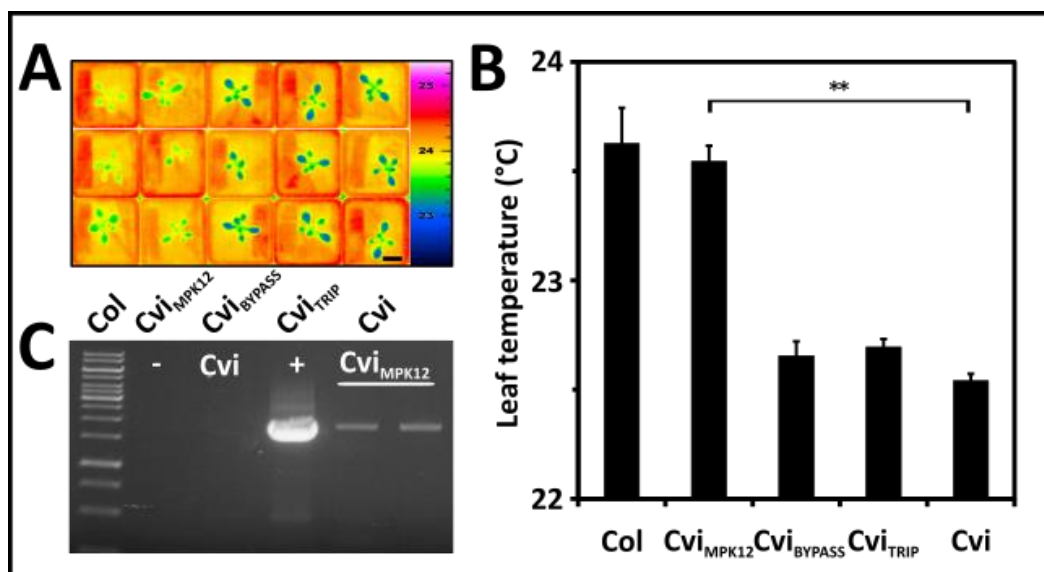


Figure 3-39 Increased leaf surface temperature of Cvi transformants homozygous for Col MPK12 allele. Enhanced leaf surface temperatures in Cvi transformants homozygous for Col MPK12 allele A), and B) thermogram and leaf surface temperatures of Cvi transformants. Plants were 20 days old and grown under short day conditions (8 hours light / 16 hours dark photoperiod) at photon flux density of  $150 \mu\text{mol m}^{-2} \text{s}^{-1}$ , and  $22^\circ\text{C}$  and 50% relative humidity in the daytime and  $17^\circ\text{C}$  and 60% relative humidity at night. The scale bar denotes 2 cm. C) Electrophoresis result indicates two successful transformation events. Water (-) and Cvi served as negative controls, PSK :: MPK12 plasmid DNA (+) served as positive control. A-B)  $n=3$  biological replicates, mean  $\pm$  SEM,  $**P < 0.001$  compared with corresponding wild types.

homozygous lines as carried out for RCAR1 (Ma *et al.*, 2009). Successful transformants were identified by selecting stay-green seedlings grown on 1/2 sugar MS medium containing antibiotics kanamycin. The T1 transformants were then grown in soil for three months to amplify T2 seeds. Subsequently, leaf temperatures of transgenic lines harboring three genes (AT2G46070, AT2G46080, and AT2G46280 respectively) were analyzed (marked in Table 3-3). During this period, the MPK12 gene (AT2G46070), one of the candidate genes, was identified by another group to be responsible for the WUE of plants through an analysis of carbon isotope compositions of an RILs population derived from Ler-0 and Cvi-0. The leaf surface temperatures of our transgenic lines were analyzed and confirmed the results of MPK12 (At2G46070) being Cool1. Among these candidates, the Cvi line homozygous for the Col MPK12 allele (Cvi<sub>MPK12</sub>) showed a Col-like phenotype, with a leaf surface temperature of more than  $1^\circ\text{C}$  higher than Cvi -0 wild type, while transgenic lines homozygous for other Col alleles did not show any leaf temperature differences (Fig. 3-39A and B). Electrophoresis data of the transgenic line Cvi<sub>MPK12</sub> confirmed that

target constructs were transformed into Cvi-0 wild type plants (Fig. 3-39C).

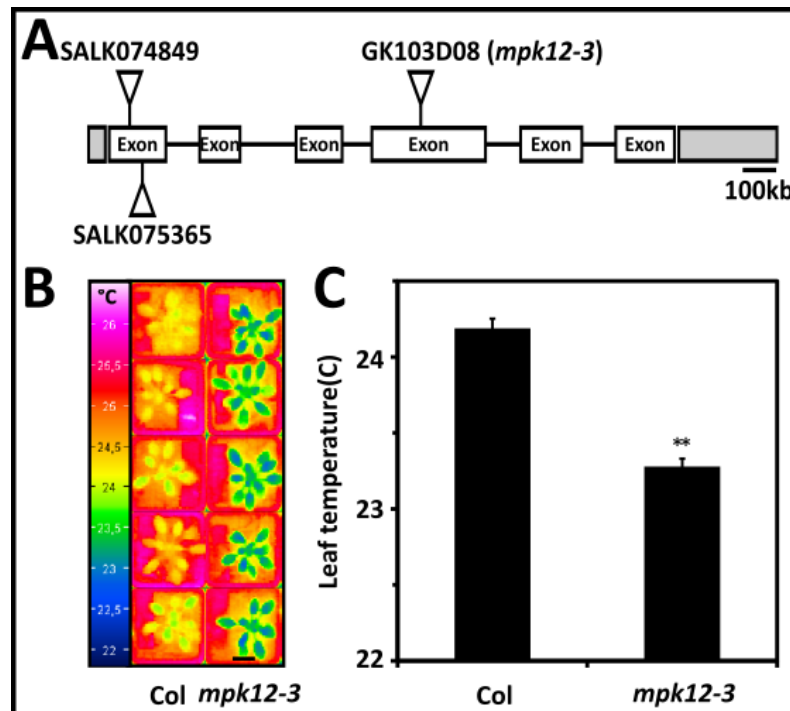


Figure 3-40 Reduced leaf surface temperature of knockout MPK12 mutant *mpk12-3* in Columbia background. A) Available T-DNA insertion lines and their insertion positions. B) Thermogram and C) leaf surface temperatures of *mpk12-3* mutants. Plants were 28 days old and grown under well-watered conditions. Growth conditions as described in Fig. 3-38. The scale bar donates 2 cm. B-C) n=5 biological replicates, mean  $\pm$  SEM, \*\*P<0.001 compared with wild type Col.

In addition, available knockout lines from the five candidate genes (AT2G46070, AT2G46080, AT2G46090, AT2G46140 and AT2G46250) in accession Col-0 background were analyzed and the results of the MPK12 knockout line (*mpk12-3*) is shown. The MPK12 gene consists of six exons and five introns. Three knockout lines are available in the NASC stock center (Fig. 3-40A). The insertion sites of SALK074849 and SALK075365 are located in the first exon and that of GK103D08 in the fourth exon. SALK074849 and SALK075365 have been reported either not to be homozygous or no T-DNA insertion event occurred (Lee, J. S. *et al.*, 2009), whereas the insertion of GK103D08 was proven to be a homozygous *mpk12* knockout. Analysis of thermal imaging showed a Cvi-like phenotype, 0.9 °C lower leaf surface temperature in *mpk12-3* plants compared with wild type Col -0 (Fig. 3-40B and C).

Taken together, these results demonstrate that MPK12 is the gene contributing to the variation in leaf surface temperatures between Col-0 and Cvi-0.

### 3.3.2.8 Amino acid alignments of MPK12

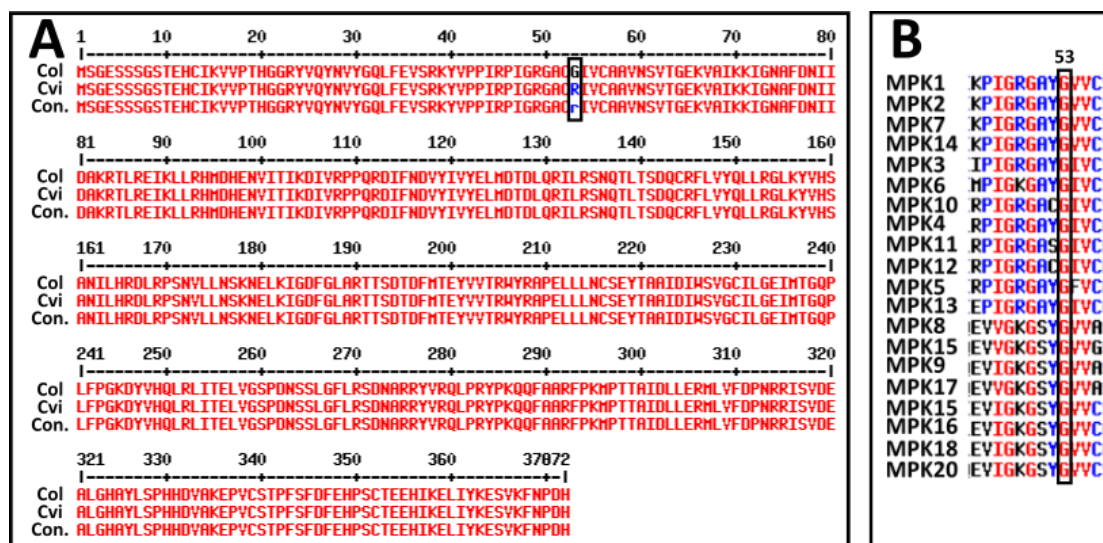


Figure 3-41 Alignment of deduced amino acid sequence of MPK12. A) Alignment of deduced amino acid sequence of MPK12 between Col-0 and Cvi-0. The black frame highlights the substitution from glycine of Col to arginine of Cvi. B) Alignment of deduced amino acid sequence of MPK12 compared to all other MPKs presented in Columbia. The black frame at position 53 highlights the conserved glycine A) and B) Texts on the left side indicate either names of accessions or names of MPKs, and "Con." means consensus sequence. Numbers in the picture are the position of amino acid residues. Red represents a high consensus value (90%) while blue (between 50% and 90%) and black (lower than 50%) indicate lower consensus.

In order to obtain a first hint for the variation in leaf temperature, the alignment of the amino acid sequence of MPK12 in Col-0 and Cvi-0 was analyzed. The result indicates a single substitution from glycine to arginine at residue 53, which falls within the kinase domain of the MPK12 protein (Fig. 3-41A). Further alignments of all MPKs from Arabidopsis Col-0 (Fig. 3-41B) and other available organisms (data not shown) showed that the substitution with arginine is unique for Cvi-0, while all other species showed strong conservation of a glycine residue at site 53.

### 3.3.2.9 Water use efficiency conferred by the MPK12 gene

It has been demonstrated that the gene MPK12 plays a crucial role in controlling the WUE (Des Marais *et al.*, 2014). To confirm this and understand how MPK12 confers on plants water productivity during the progressive drought, both Col knockout mutant *mpk12-3* and transgenic Cvi<sub>MPK12</sub> lines were evaluated. The procedure of progressive drought is the same as described in Fig. 3-1. In the well-watered phase of

progressive drought, the knockout of the MPK12 gene in Col-0 resulted in a reduction in both leaf surface temperature and rosette size compared with wild type Col-0 (Fig.

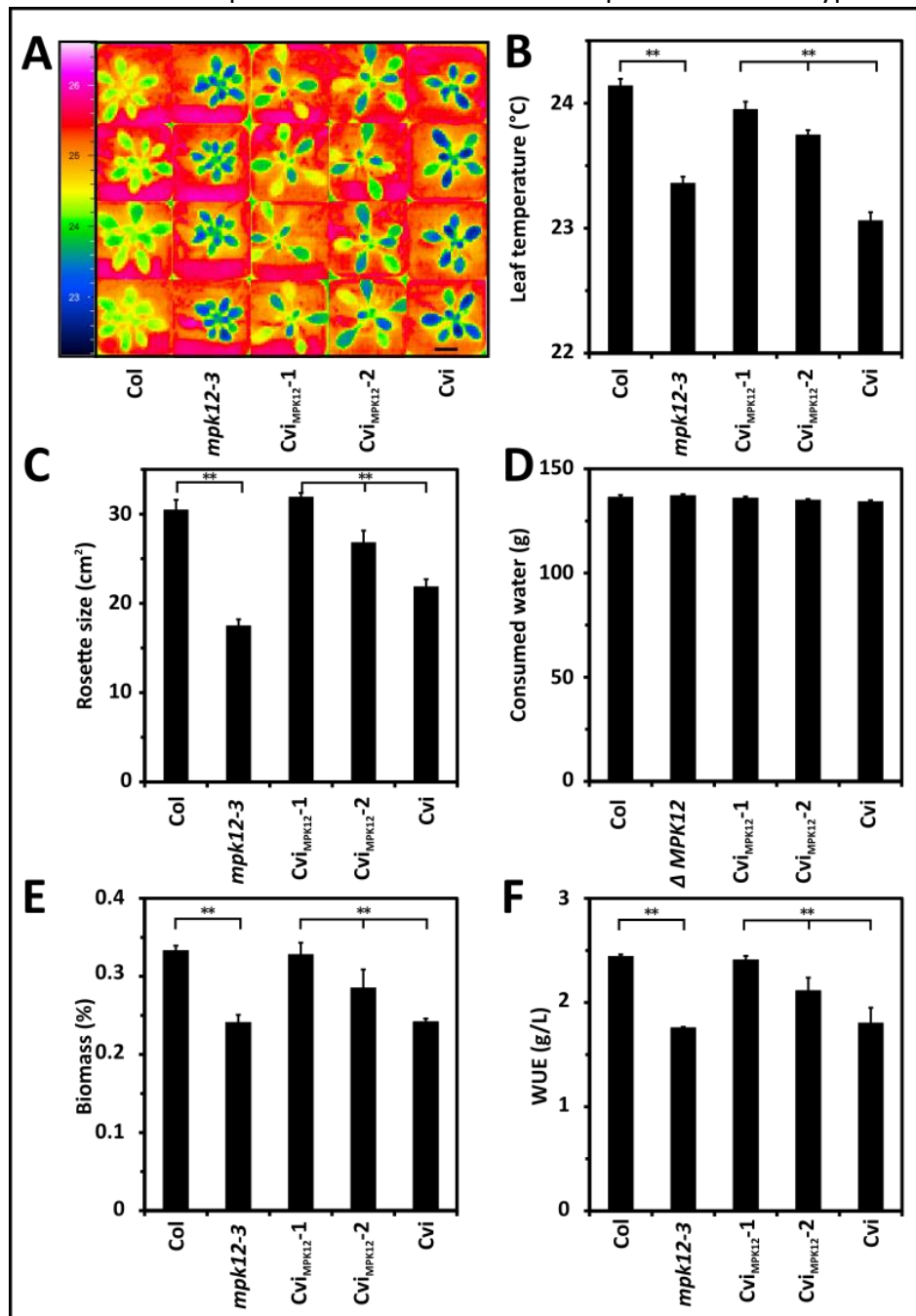


Figure 3-42 Water use efficiency conferred by MPK12 gene. A) Thermogram of wild type Col-0, Cvi-0, Col knockout mutant *mpk12-3* and independent Cvi transformants harboring Col MPK12 allele - *Cvi<sub>MPK12-1</sub>* and *Cvi<sub>MPK12-2</sub>*, grown for 40 days under short day conditions (8 h light / 16 h dark photoperiod) at a photon flux density of  $150 \mu\text{mol m}^{-2} \text{s}^{-1}$ ,  $22^\circ\text{C}$  and 50% relative humidity in daytime and  $17^\circ\text{C}$  and 60% relative humidity at night, and under well-watered conditions (SWP  $\geq -0.02$  bar). Four plants per line were grown in separate pots at randomized positions, and thermal pictures were arranged in groups after imaging. B) Leaf temperatures from data shown in A) and leaf area C) as projected rosette size. The scale bar in A) donates 2 cm. Consumed water D), above-ground dry biomass E) and WUE F) were determined at the end of eight weeks' progressive drought. A-F)  $n=4$  biological

replicates, mean  $\pm$  SEM. \*\* $P < 0.001$  compared with corresponding wild types.

3-42A-C). In contrast, transformed Cvi with the Col MPK12 allele conferred increased leaf surface temperatures with bigger rosette sizes than wild type Cvi-0 (Fig. 3-42A-C). At the end of the progressive drought, the biomass of Col-0 averaged  $0.33 \text{ g} \pm 0.01 \text{ g}$ , and it had consumed  $136 \text{ g} \pm 1 \text{ g}$  water. Knockout mutant *mpk12-3* generated 26% less biomass despite consuming the same amount of water as Col-0, and hence had a lower WUE by a factor of 1.4. Moreover, Cvi-0 accumulated  $0.24 \text{ g} \pm 0.003 \text{ g}$  biomass and consumed  $134 \text{ g} \pm 1 \text{ g}$  water by the end of the progressive drought. Independent Cvi transformants harboring the MPK12 Col allele - Cvi<sub>MPK12-1</sub> and Cvi<sub>MPK12-2</sub> - generated up to 35% more biomass than Cvi-0 wild type plants despite consuming the same amount of water, therefore displaying an enhanced WUE by a factor of 1.3 (Fig. 3-42D-F).

### **3.4 Nighttime stomatal opening and stomatal oscillation of Arabidopsis**

Plants lose water mainly through the stomata, which is caused by the leaf-to-air VPD (Caird *et al.*, 2007). VPD is defined as the difference between the vapor pressure in the air at a given temperature and the saturation vapor pressure in the air at the same temperature (Abteu and Melesse, 2013). The substomatal cavity of the leaf is assumed to be close to saturation vapor pressure (Farquhar and Raschke, 1978), which indicates inevitable water efflux from the substomatal cavity to the atmosphere in cases of stomatal opening according to the Fick's law of diffusion. In the daytime, light-induced stomatal opening (Roelfsema and Hedrich, 2005) leads to substantial water loss in plants. In the dark, stomata close, but incomplete stomatal closure at night was reported in both C3 and C4 plants with considerable variations among species (Caird *et al.*, 2007). Genetic variations in nighttime stomatal opening were also investigated in Arabidopsis and the tested accessions displayed up to 3-fold differences (Christman *et al.*, 2008). Three near isogenic lines derived from either Ler-0 and Cvi-0, or Col-0 and Sf-0 crosses, which showed divergent  $\delta^{13}\text{C}$  or daytime stomatal conductance, exhibited significant differences in nighttime stomatal conductance compared with their parental lines. The analysis of NILs revealed one QTL responsible for the nighttime stomatal opening (Christman *et al.*, 2008), but no gene responsible for it has been identified yet.



The phenomenon of autonomic, cyclic opening, and closing movements of stomata has been described in the past as either cyclic variation in stomatal aperture or stomatal oscillation (Barrs, 1971; Cowan, 1972). This phenomenon is widespread in different plant species and the period of oscillation in most of these species varies from 10 to 50 minutes (Barrs, 1971; Barrs and Klepper, 1968; Caird *et al.*, 2007; Cardon *et al.*, 1994; Farquhar and Cowan, 1974; Teoh and Palmer, 1971). Stomatal oscillation requires a pulse or step changes in a plant's environment. Such changes could be any factor affecting stomatal aperture (Barrs, 1971). The oscillation of stomata can be observed directly using a microscope (Kuiper, 1961; Went, 1944) and indirectly by measuring related plant properties, including stomatal conductance, net carbon assimilation rate, transpiration rate, leaf water status, and stem parameter (Barrs, 1971). Physiological and model studies explain that stomatal oscillation is the result of the positive feedback responses of stomatal apertures to changes in ambient conditions, such as light and temperature, and negative feedback responses to the alternation of plant water potential (Cowan, 1972; Raschke, 1970). Moreover, Raschke still suggested the existence of a third feedback loop in the stomatal oscillation, which involves the response of stomatal aperture to the concentration of CO<sub>2</sub> in intercellular spaces, possibly because of the role of CO<sub>2</sub> in controlling the generation and degradation of osmotica in guard cells (Raschke, 1970). Although successes have been made in explaining this phenomenon, no report illustrates up to now the variation in stomatal oscillation within a single species.

In this chapter, analysis of variations in nighttime stomatal conductance and the period of stomatal oscillation between *Arabidopsis* accessions Col-0 and Cvi-0 are presented through gas exchange measurements. Col-0 showed less open stomata at night and short oscillation periods compared to Cvi-0 that had more open stomata in the dark and long periods of oscillation. With the aim of searching for QTL responsible for these two traits, both the nighttime stomatal conductance and the oscillation periods were analyzed by using F1 plants and RILs derived from Col-0 and Cvi-0. Both traits of Cvi plants harboring Col MPK12 allele were assessed further. The MPK12 gene was shown to explain the variations in nighttime stomatal opening in RILs, but not the variations in stomatal oscillation period. However, novel quantitative trait loci at the end of chromosome two and three were shown to be the

likely cause of the stomatal oscillation trait.

### **3.4.1 Quantitative trait locus analysis of nighttime stomatal opening and stomatal oscillation in Arabidopsis**

#### **3.4.1.1 The phenomena of nighttime stomatal opening and stomatal oscillation**

The nighttime stomatal opening and stomatal oscillation were observed (Fig. 3-43 A and B) through the day-night-day, whole-rosette gas exchange measurements using well-watered, 20 days  $\pm$  8 days old Arabidopsis plants. For each gas exchange measurement, the air with 380  $\mu\text{mol mol}^{-1}$  of  $\text{CO}_2$  and 12  $\text{mmol mol}^{-1}$  of water vapor were continuously supplied. No external light source was mounted over either the ring chamber or the cuvette, and temperature control was switched off. Therefore, the photon flux density and temperature in the ring chamber and the cuvette were dependent on the light source and temperature in the growth chamber. The light regime, light intensity, and leaf temperature of the gas exchange measurements are displayed in Fig. 3-43C and D. According to the illumination regime, three phases of the gas exchange measurement were defined: the dark phase, the phase of transition between dark and daytime, and the daytime phase.

During the dark phase (from 18:00 to 9:00), no illumination occurred, and temperatures in the ring chamber ( $T_{ring}$ ) were around 22 °C (Fig. 3-43C and D).  $\text{CO}_2$  concentration in the ring chamber ( $C_a$ ) was maintained at 380  $\mu\text{mol mol}^{-1}$  (Fig. 3-43E) and the concentration of water vapor ( $W_a$ ) was stabilized at 14  $\text{mmol mol}^{-1}$  (Fig. 3-43E), somehow higher than the supplied value, indicating that the stomata were not fully closed. The  $W_a$  and the nighttime  $T_{ring}$  resulted in leaf-to-air VPDs reaching approximately 15 Pa  $\text{kPa}^{-1}$  at night (Fig. 3-43F). Under these conditions, the nighttime stomatal opening of both the Col-0 and Cvi-0 was reflected by the nighttime transpiration rate ( $E_{night}$ ) and nighttime stomatal conductance ( $g_{s-night}$ ). Col-0 had a  $E_{night}$  ranging from 0.2  $\text{mmol m}^{-2} \text{s}^{-1}$  to 0.6  $\text{mmol m}^{-2} \text{s}^{-1}$ , a  $g_{s-night}$  ranging from 13  $\text{mmol m}^{-2} \text{s}^{-1}$  to 35  $\text{mmol m}^{-2} \text{s}^{-1}$ , while  $E_{night}$  of Cvi-0 varied from 0.4  $\text{mmol m}^{-2} \text{s}^{-1}$  to 0.8  $\text{mmol m}^{-2} \text{s}^{-1}$ , and  $g_{s-night}$  varied from 25  $\text{mmol m}^{-2} \text{s}^{-1}$  to 60  $\text{mmol m}^{-2} \text{s}^{-1}$ . (Fig. 3-43A and B). In addition, Cvi-0 had a predawn (from 2:00 to 9:00) increase in  $E_{night}$  from 0.5  $\text{mmol m}^{-2} \text{s}^{-1}$  to 0.8  $\text{mmol m}^{-2} \text{s}^{-1}$  and  $g_{s-night}$  from 25  $\text{mmol m}^{-2} \text{s}^{-1}$  to 60  $\text{mmol m}^{-2} \text{s}^{-1}$ .

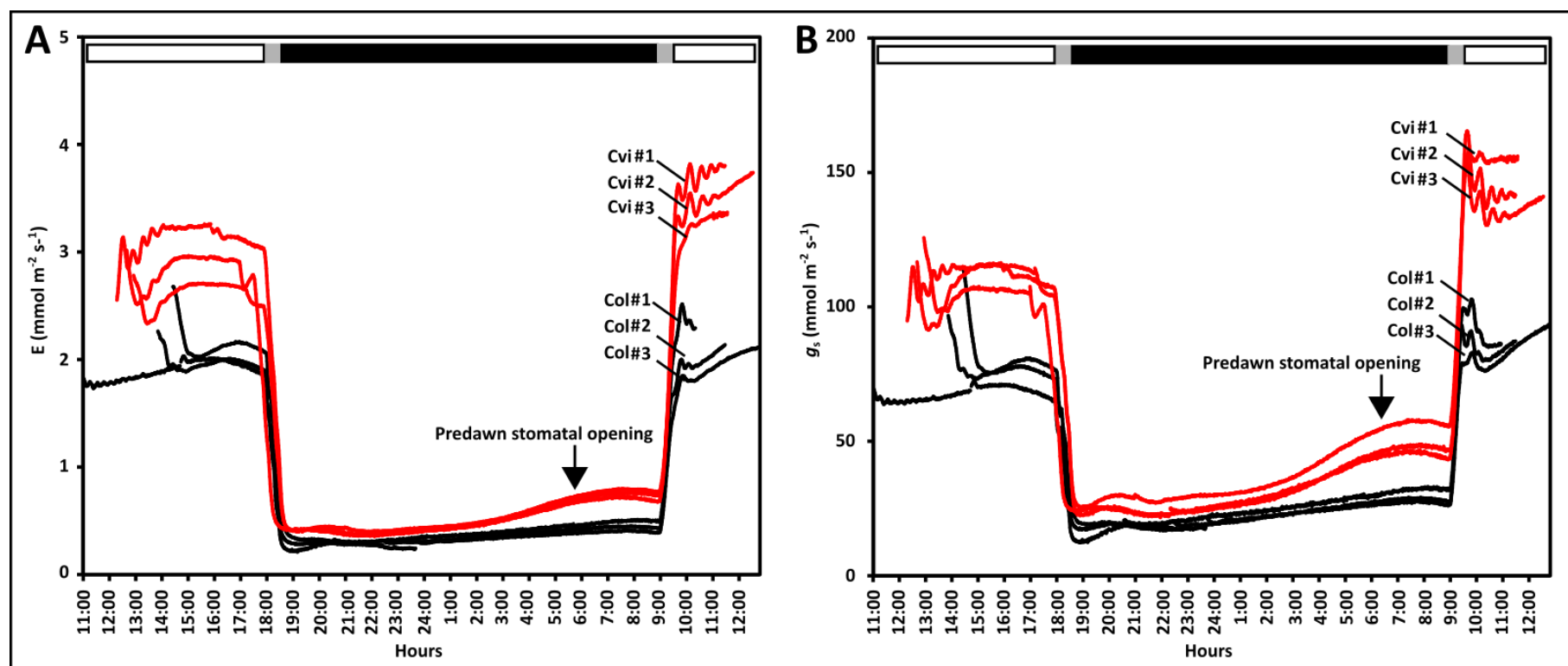
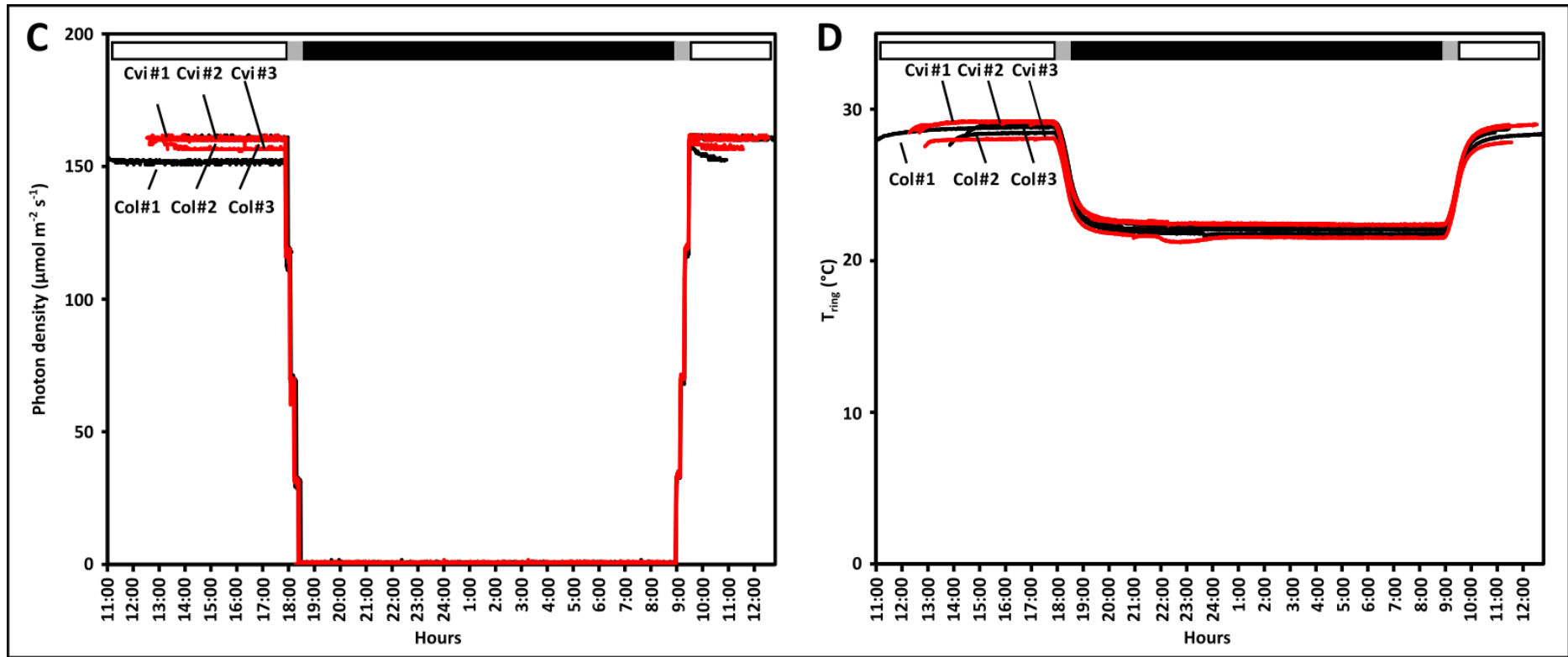
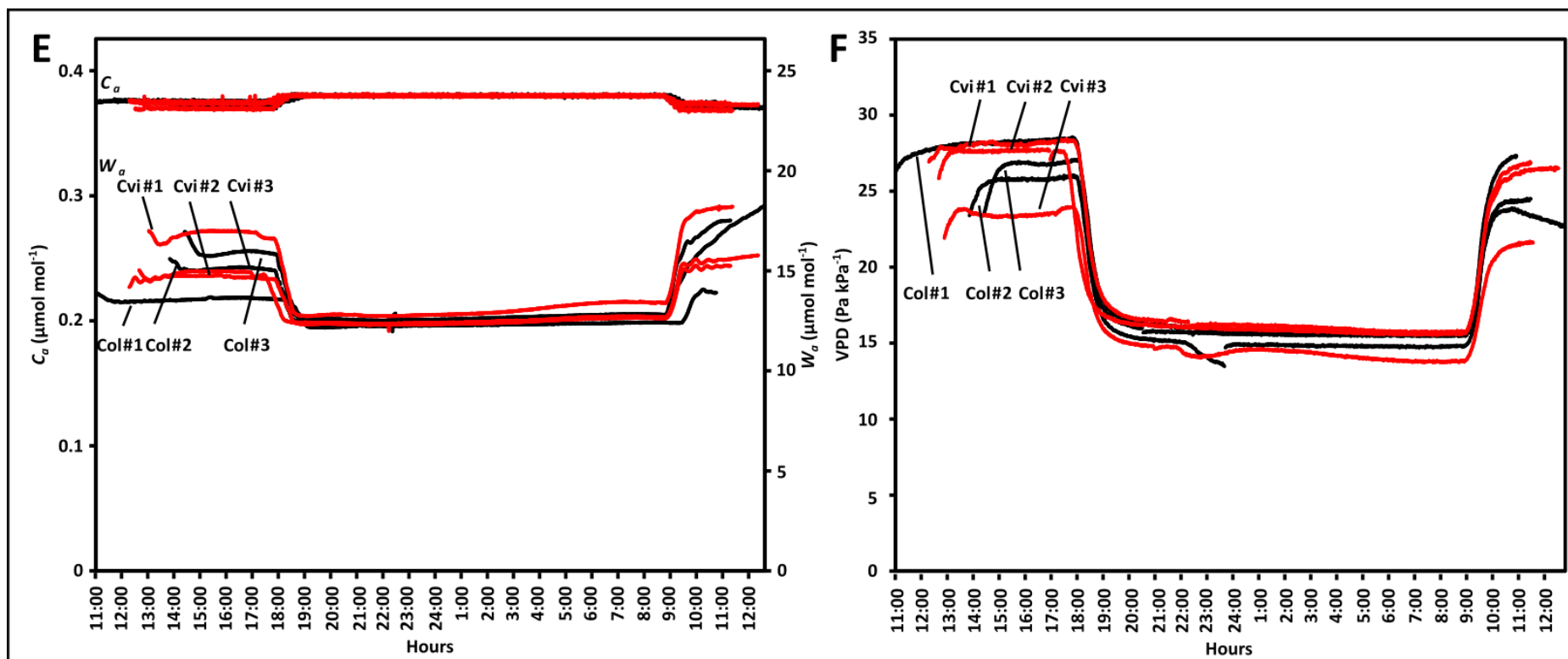


Figure 3-43 Nighttime stomatal opening and stomatal oscillation of Arabidopsis accessions Col-0 and Cvi-0. Nighttime stomatal opening and stomatal oscillation were indicated by A) the transpiration rate ( $E$ ) and B) stomatal conductance ( $g_s$ ) of 20  $\pm$  8 days old Col-0 (black lines) and Cvi-0 (red lines). Determination of  $E$  and  $g_s$  were achieved simultaneously in the gas exchange measurements. Individual plants are labeled with numbers #1, #2, and #3. The light regime and photon flux density C), ring chamber temperature ( $T_{ring}$ ) D),  $CO_2$  ( $C_a$ ) and  $H_2O$  concentration ( $W_a$ ) E), and leaf-to-air VPD F) over time of the day-and-night gas exchange measurements are depicted. Bars on the top of each figure represent the illumination phase (white), the phase of transition from illumination to darkness or darkness to illumination (gray), and the dark phase (black). Black arrows indicate the predawn stomatal opening in Cvi-0 accession. All plants were grown under short day (8h light / 16h dark photoperiod) at a photon flux density of  $150 \mu mol m^{-2} s^{-1}$ , at a temperature of  $22^\circ C$  and 50% relative humidity in the daytime and a temperature of  $17^\circ C$  and 60% relative humidity at night, and under well-watered conditions ( $SWP \geq -0.02$  bar). A-F) Each curve is a single measurement of an individual plant.  $n=3$  biological replicates for Col-0 and Cvi-0.





During the phase of transition from dark to light (9:00 to 9:30), the light intensity increased stepwise from  $0 \mu\text{mol m}^{-2} \text{s}^{-1}$  to  $150 \mu\text{mol m}^{-2} \text{s}^{-1}$  (Fig. 3-43C), and  $T_{ring}$  increased from  $22 \text{ }^{\circ}\text{C}$  to  $27 \text{ }^{\circ}\text{C}$  (Fig. 3-43D). The ambient  $\text{CO}_2$  in the ring chamber decreased slightly (Fig. 3-43E), while  $W_a$  increased steadily from  $12.5 \text{ mmol mol}^{-1}$  to up to  $17 \text{ mmol mol}^{-1}$  (Fig. 3-43E). The increase of  $T_{ring}$  and  $W_a$  caused an increase of leaf-to-air VPDs from  $15 \text{ Pa kPa}^{-1}$  to up to  $27 \text{ Pa kPa}^{-1}$  (Fig. 3-43F). The unsteady state of the environmental conditions at the transition phase triggered the oscillation of the E (Fig. 3-43A) and  $g_s$  (Fig. 3-43B) of Col-0 and Cvi-0.

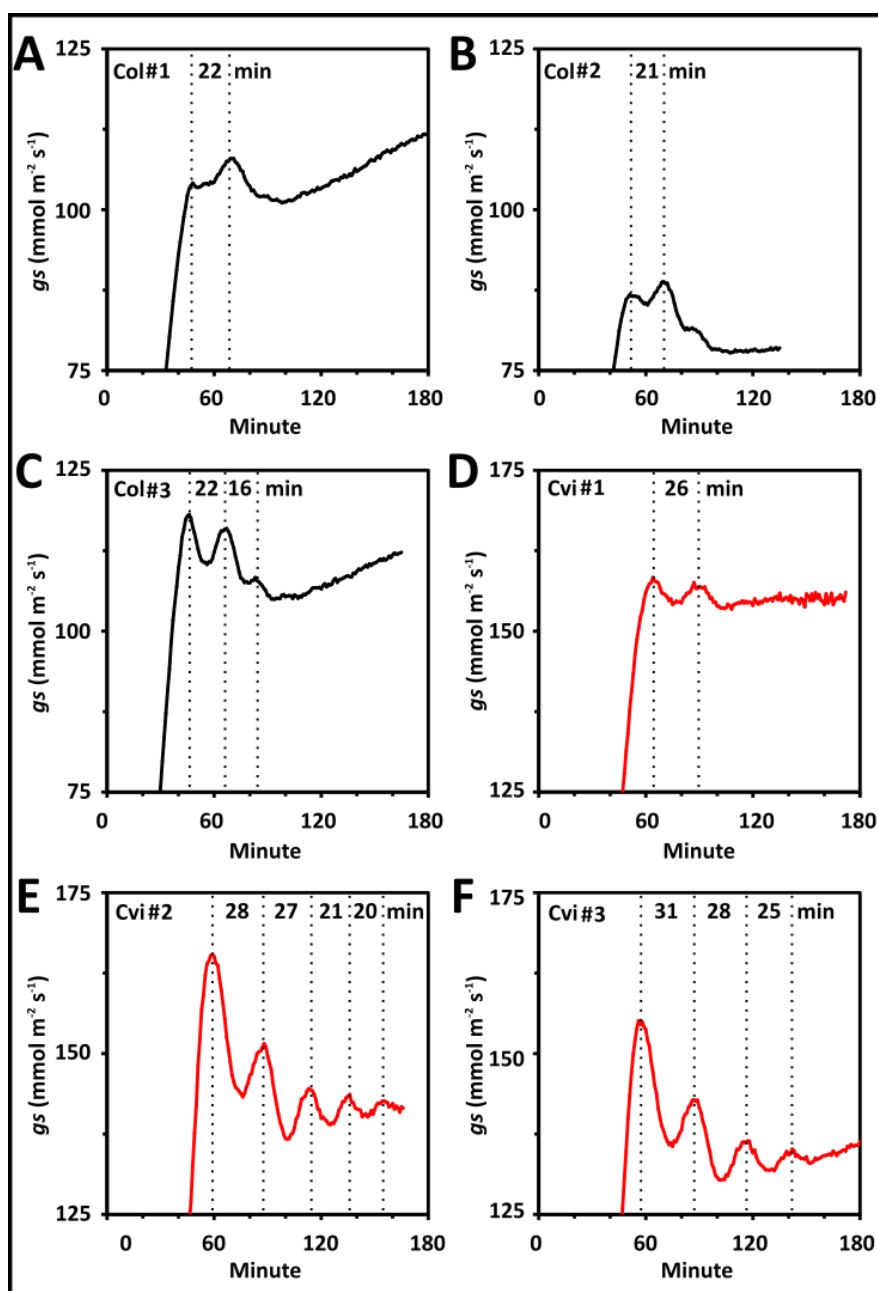


Figure 3-44 Stomatal oscillations of Arabidopsis accessions Col-0 and Cvi-0. The enlargement

of stomatal conductance between 9:00 and 12:00 in Fig. 3-43B presents the details of the stomatal conductance oscillations of Col-0 (black lines) and Cvi-0 (red lines). Individual lines are labeled in the top left corner of each figure. The vertical dotted lines indicate the times of the crests of each oscillation event and the number between the dotted lines indicates the period (length in minutes) of the corresponding oscillation cycle. The gas exchange measurement conditions and growth conditions of plants were as described as in Fig. 3-42. Curves shown in A-F) were single measurements.

During the daytime phase (9:30 to 17:30), light intensity stabilized at  $150 \mu\text{mol m}^{-2} \text{s}^{-1}$  (Fig. 3-43C) and  $T_{ring}$  remained at  $27 \text{ }^\circ\text{C}$  (Fig. 3-43D). Other conditions such as  $C_a$ ,  $W_a$ , and VPD also became stable (Fig. 3-43E and F). The oscillations in  $E$  and  $g_s$  of Col-0 as well as Cvi-0 were damped and finally disappeared. (Fig. 3-43A and B).

The enlargement of stomatal conductance between 9:00 and 12:00 in Fig. 3-43B provides details about the cycles, amplitude, and periods of oscillation. The cycles of oscillation varied considerably (Fig. 3-44A-F). Two of three individual Col-0 plants had one cycle (Fig. 3-44A and B), while the other one had two cycles (Fig. 3-44C). Moreover, one of three independent Cvi plants experienced only one cycle (Fig. 3-44D), while the others had more than three cycles (Fig. 3-44E-F). The half of the difference between the stomatal conductance at the first crest and stomatal conductance at the first trough was used to describe the amplitude of each oscillation. Using this method of calculation, the three Col-0 plants had amplitudes of  $0.2 \text{ mmol m}^{-2} \text{ s}^{-1}$ ,  $0.4 \text{ mmol m}^{-2} \text{ s}^{-1}$ , and  $4 \text{ mmol m}^{-2} \text{ s}^{-1}$  (Fig. 3-44A-C), while the three independent Cvi plants had amplitudes of  $1.5 \text{ mmol m}^{-2} \text{ s}^{-1}$ ,  $15 \text{ mmol m}^{-2} \text{ s}^{-1}$ , and  $10 \text{ mmol m}^{-2} \text{ s}^{-1}$  (Fig. 3-44D-F). These results do not suggest that differences in the cycles and amplitude of the oscillations were caused by genetic differences between Col-0 and Cvi-0. However, the periods of the oscillations were quite stable in the Col and Cvi accessions (Fig. 3-44A-F). Col #1 and Col #2 had periods of 20 and 21 minutes respectively (Fig. 3-44A and B). The oscillations of Col #3 occurred over a period of 22 minutes in the first oscillation cycle and 16 minutes in the second cycle (Fig. 3-44C). Cvi had longer oscillation periods than Col-0 (Fig. 3-44D-F). Cvi #1 had only one cycle with an oscillation period of 26 minutes (Fig. 3-44D); Cvi #2 and Cvi #3 had several oscillation cycles and displayed period lengths of 30, 28, 25, 20 minutes and 30, 28, 25 minutes respectively (Fig. 3-44E-F).

### 3.4.1.2 Mapping the locus responsible for nighttime stomatal opening

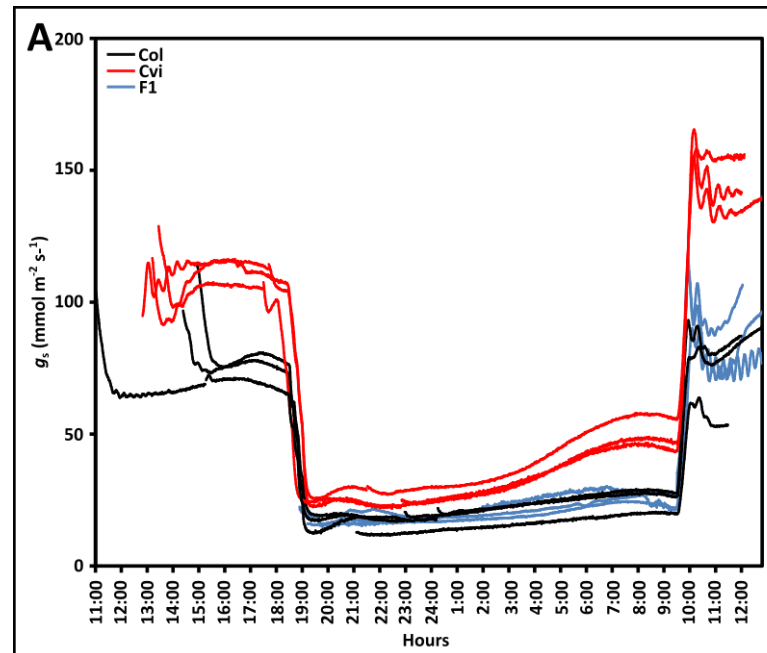
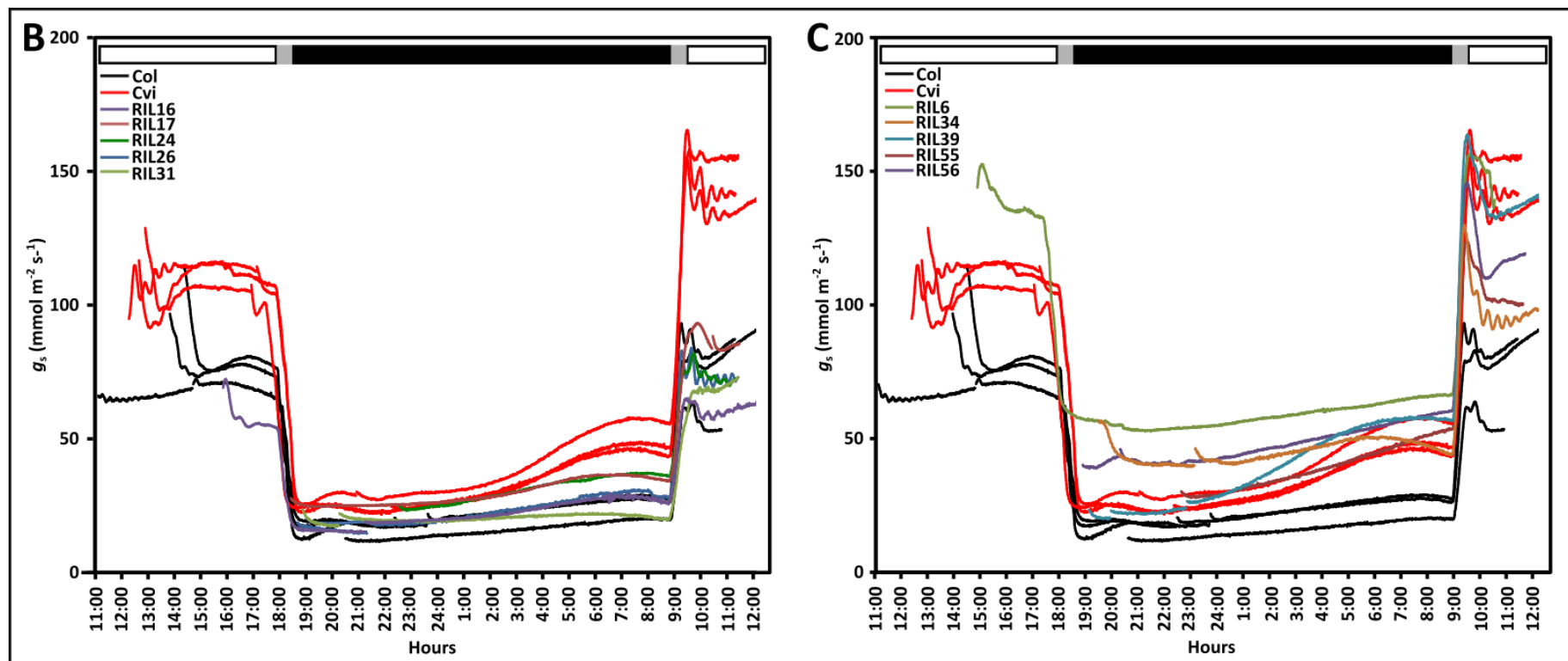


Figure 3-45 Nighttime stomatal openings and stomatal oscillations of F1 hybrids and RILs derived from Arabidopsis accessions Col-0 and Cvi-0. Nighttime stomatal openings and stomatal oscillations were indicated by the stomatal conductance ( $g_s$ ) of 20  $\pm$  8-day-old Col-0 (black lines), Cvi (red lines), F1 (blue lines) A) and RILs in B and C). The stomatal conductance of RIL16, RIL17, RIL24, RIL26, and RIL31 are presented in B) and RIL6, RIL34, RIL39, RIL55, and RIL56 are presented in C). The color codes in B and C) are indicated in the top left corner of each figure. The conditions of gas exchange measurements and growth conditions of plants are as described in figure 3-43. A-C) Each curve is a single measurement of an individual plant.  $n=3$  biological replicates for Col-0, Cvi-0, F1 hybrid, and  $n=1$  for RILs.





## Results

Table 3-4 Nighttime stomatal conductance of Arabidopsis accessions Col-0, Cvi-0 and their F1 hybrids and RILs populations. Nighttime stomatal conductance in the table is the average value of the stomatal conductance in the dark. "-" means no measurement. n=3 for parental lines, F1 hybrid, and n=1 for RILs.

		Nighttime stomatal conductance												
Lines		Col-0	Cvi-0	F1	RIL6	RIL16	RIL17	RIL24	RIL26	RIL31	RIL34	RIL39	RIL55	RIL56
	<b>1</b>	16	33	22	59	21	29	22	28	20	45	39	39	48
<b>Replicates</b>	<b>2</b>	22	32	22	-	-	-	-	-	-	-	-	-	-
	<b>3</b>	23	39	19	-	-	-	-	-	-	-	-	-	-
<b>Mean</b>		20	35	21	59	21	29	22	28	20	45	39	39	48



Figure 3-46 Alignment of genotypes and nighttime stomatal conductance phenotypes of Col, Cvi and their RILs populations. Known genotypes of RILs on five chromosomes (five blocks shown here) were downloaded (<http://publiclines.versailles.inra.fr/page/8>) and aligned according to their stomatal conductance at night compared with parental lines. Higher stomatal conductance at night is presented above the black line in the middle of each block while lower stomatal conductance at night was shown below the black line in each block. The black frame at the end of chromosome two indicates the possible locus responsible for nighttime stomatal opening. Green, red, and yellow represent the Col-like genotype (C), Cvi-like genotype (V) and heterozygous genotype (H) respectively. Gray indicates missing data (D).

To investigate the genetic variation in nighttime stomatal openings, the F1 hybrids derived from Col-0 and Cvi-0 were analyzed. Three independent F1 plants displayed Col-like nighttime stomatal conductance (Fig. 3-45A), and the values averaged 22  $\text{mmol m}^{-2} \text{s}^{-1}$ , 22  $\text{mmol m}^{-2} \text{s}^{-1}$ , 19  $\text{mmol m}^{-2} \text{s}^{-1}$ ; these values are comparable to those of the three individual Col-0 plants (16  $\text{mmol m}^{-2} \text{s}^{-1}$ , 22  $\text{mmol m}^{-2} \text{s}^{-1}$ , 23  $\text{mmol m}^{-2} \text{s}^{-1}$ ) (Table 3-4). These results reveal that nighttime stomatal opening is inheritable, and lower stomatal conductance is a dominant trait. Moreover, the nighttime stomatal conductance of 11 RILs was also analyzed. RIL16, RIL17, RIL24, RIL26, and RIL31 displayed Col-like stomatal conductance in the dark (Fig. 3-45B), and none of their values were as high as the nighttime stomatal conductance of Cvi-0 plants (35  $\text{mmol m}^{-2} \text{s}^{-1}$  on average) (Table 3-4). The other RILs, including RIL6, RIL34, RIL39, RIL55, and RIL56, displayed Cvi-like stomatal conductance at night (Fig. 3-45C), and the values varied from 39  $\text{mmol m}^{-2} \text{s}^{-1}$  to 59  $\text{mmol m}^{-2} \text{s}^{-1}$  (Table 3-4).

The genotypes of the RILs were then aligned according to the nighttime stomatal opening phenotypes of 10 RILs. The alignment results are displayed in Fig. 3-46; the five blocks represent five chromosomes and the green, red, and yellow colors indicate a Col-like genotype (C), Cvi-like genotype (V) and heterozygous genotype (H) respectively. Each block is separated into two parts by a black line. Above the black line are lines having higher stomatal conductance at night, while lines with lower stomatal conductance at night are below the black line. The genotypes at the end of chromosome two and close to the marker c2\_18753 explain most of the phenotypes of the 10 RILs (Fig. 3-46). These results indicate that the candidate locus explaining variations in nighttime stomatal opening should be close to marker c2\_18753.

### **3.4.1.3 Mapping the loci responsible for the oscillation period**

Genetic analysis was also performed with the aim of identifying the locus responsible for the variations in the oscillation periods of Col-0 and Cvi-0. Owing to the uncertainty of the occurrence of oscillation cycles, the oscillation period of the first cycle (from the first crest to the second crest) was used as a readout of the phenotype in the following analysis. The F1 hybrids derived from Col-0 and Cvi-0 were analyzed first. Three independent F1 plants had Col-like oscillation periods, and the values were 21 minutes, 21 minutes, and 17 minutes (Table 3-5). These results indicate that periods of stomatal oscillation are inheritable, and the short period

Table 3-5 Oscillation periods of stomatal conductance of Arabidopsis accessions Col-0 and Cvi-0 and their genetic populations. The period of oscillation presented in the table is the time difference between the first and second crest of an oscillation. "N" indicates that a gas exchange measurement was performed but no oscillation was observed. "-" indicates that no gas exchange measurement was performed. Number 1, 2, 3 are independent measurements of each line.

	Period of first oscillation cycle			Mean
	1	2	3	
Col-0	22	21	22	22
Cvi-0	26	28	31	28
Col X Cvi F1	21	21	17	20
RIL6	N	N	-	/
RIL8	16	N	N	16
RIL9	28	-	-	28
RIL10	21	-	-	21
RIL16	30	-	-	30
RIL17	22	N	-	22
RIL20	21	-	-	21
RIL22	20	-	-	20
RIL24	24	20	-	22
RIL26	23	20	20	21
RIL31	19	17	N	18
RIL34	30	24	-	27
RIL39	24	N	-	24
RIL42	21	27	-	24
RIL47	N	N	N	/
RIL49	27	30	25	27
RIL51	N	-	-	/
RIL53	18	-	-	18
RIL55	25	N	N	25
RIL56	21	24	N	23

phenotype is dominant. Moreover, the oscillation periods of the 11 RILs presented in Fig. 3-45B and C were analyzed, but some of these RILs did not experience oscillation. To collect enough oscillation events, twenty-nine additional gas exchange measurements were performed using the same experimental setup and an enlarged population of RILs. RIL8, RIL10, RIL17, RIL20, RIL22, RIL26, RIL31, and RIL56 had Col-like oscillation periods (Table 3-5). The other RILs, including RIL9, RIL34, RIL16, and RIL49, had Cvi-like oscillation periods (Table 3-5). The remaining RILs, including RIL24, RIL42, RIL55, and RIL56, had either two contradictory values or ambiguous oscillation periods (Table 3-5). These unclear results are needed to be confirmed further. The genotypes of the RILs with assured phenotypes were then aligned according to their oscillation periods, and the results reveal that loci close to marker c2\_18753 at the end of chromosome two and c3\_22147 at the end of chromosome three (Fig. 3-47) may be responsible for the variations in the oscillation periods of Col-0 and Cvi-0.

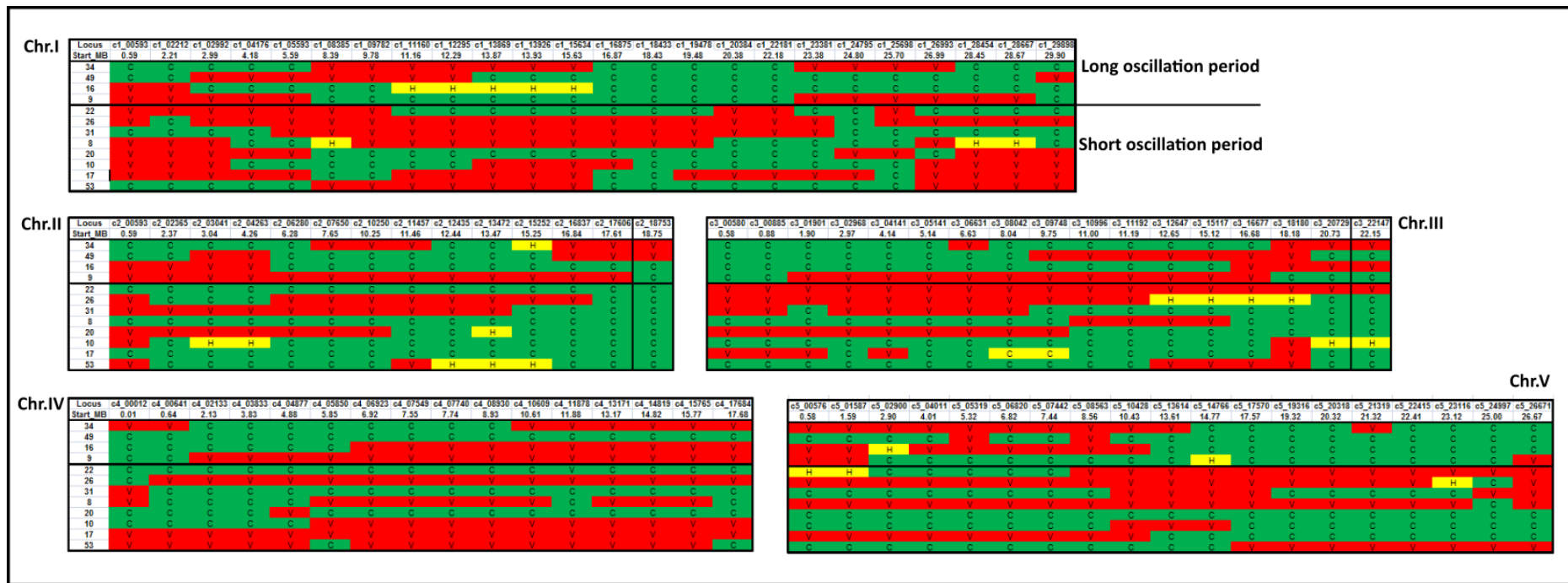


Figure 3-47 Alignment of genotypes and oscillation period phenotypes of Col, Cvi and their RILs populations. The known genotypes of RILs on five chromosomes (five blocks shown here) were downloaded (<http://publiclines.versailles.inra.fr/page/8>) and aligned according to the periods of the first oscillation cycles (from first crest to the second crest) of 12 RILs compared with parental lines. The part above the black line in the middle of each block is the long oscillation period phenotype and the part below the line is the short oscillation period phenotype. The black frames at the end of chromosome two and three indicate the possible locus responsible for the period of stomatal oscillation. Green, red, and yellow represent the Col-like genotype (C), Cvi-like genotype (V), and heterozygous genotype (H) respectively. Gray indicates missing data (D).

## 3.4.2 The MPK12 gene is responsible for nighttime stomatal opening but not for oscillation periods

### 3.4.2.1 Nighttime stomatal opening controlled by the MPK12 gene

The QTL loci responsible for variations in nighttime stomatal opening and oscillation periods include the region close to marker c2\_18753 at the end of chromosome two. This result implied that MPK12 gene may be responsible for these two traits. Therefore, Cvi<sub>MPK12-1</sub> line was used to perform gas exchange measurements (Fig. 3-48). The setup of this experiment was not exactly the same as illustrated in Fig. 3-43C-F. In this experiment, the comparable single leaves of  $37 \pm 4$ -day-old *Arabidopsis* plants grown under well-watered conditions were clamped into the cuvette. During the gas exchange measurements,  $380 \mu\text{mol mol}^{-1}$  CO<sub>2</sub> and  $12 \text{ mmol mol}^{-1}$  water vapor were supplied continuously. After 16 hours of darkness, illumination was available for four hours. According to this light regime, three phases were defined, including a dark phase, a phase of transition from darkness to daytime, and a daytime phase (9:30 to 13:00). During the dark phase, temperatures in the cuvette ( $T_{\text{cuvette}}$ ) of all tested lines was around  $19 \text{ }^{\circ}\text{C}$ , and the CO<sub>2</sub> concentration in the cuvette ( $C_a$ ) was around  $380 \mu\text{mol mol}^{-1}$ . Water vapor concentration ( $W_a$ ) stabilized at  $12 \text{ mmol mol}^{-1}$  and together with the  $T_{\text{ring}}$  resulted in approximately  $12.5 \text{ Pa kPa}^{-1}$  VPDs for all measurements. Under these conditions, nighttime stomatal opening was again observed in both the Col-0 and Cvi-0 accessions (Fig. 3-48A and B). Col-0 had a  $E_{\text{night}}$  ranging from  $0.3 \text{ mmol m}^{-2} \text{ s}^{-1}$  to  $0.5 \text{ mmol m}^{-2} \text{ s}^{-1}$ , a  $g_{s\text{-night}}$  ranging from  $30 \text{ mmol m}^{-2} \text{ s}^{-1}$  to  $35 \text{ mmol m}^{-2} \text{ s}^{-1}$ , while Cvi-0 displayed consistent higher values of both parameters than Col-0 (Fig. 3-43A and B).

During the phase of transition from dark to light (9:00 to 9:30), the light intensity increased stepwise from 0 to  $180 \mu\text{mol m}^{-2} \text{ s}^{-1}$ , and  $T_{\text{cuvette}}$  increased from  $19 \text{ }^{\circ}\text{C}$  to  $24 \text{ }^{\circ}\text{C}$  (Fig. 3-48C and D).  $C_a$  was maintained at  $380 \mu\text{mol mol}^{-1}$  (Fig. 3-48E).  $W_a$  did not have a clear increase for the measurements of Col-0, while  $W_a$  for the measurements of Cvi-0 increased by  $1 \text{ mmol mol}^{-1}$  (Fig. 3-48E). Leaf-to-air VPD in this phase increased up to  $10 \text{ Pa kPa}^{-1}$  for Col-0 and  $8 \text{ Pa kPa}^{-1}$  for Cvi (Fig. 3-48F). The unsteady state of the environmental conditions at the transition phase triggered oscillations in

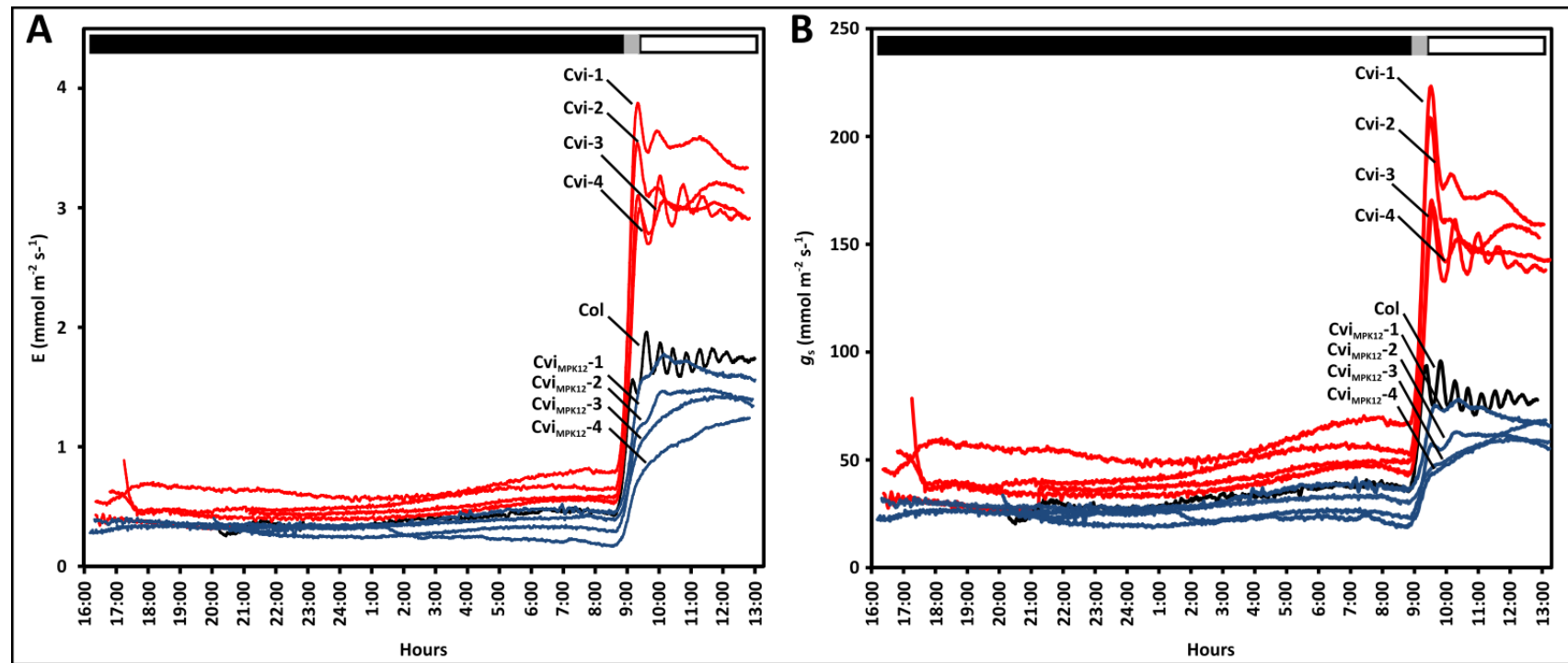
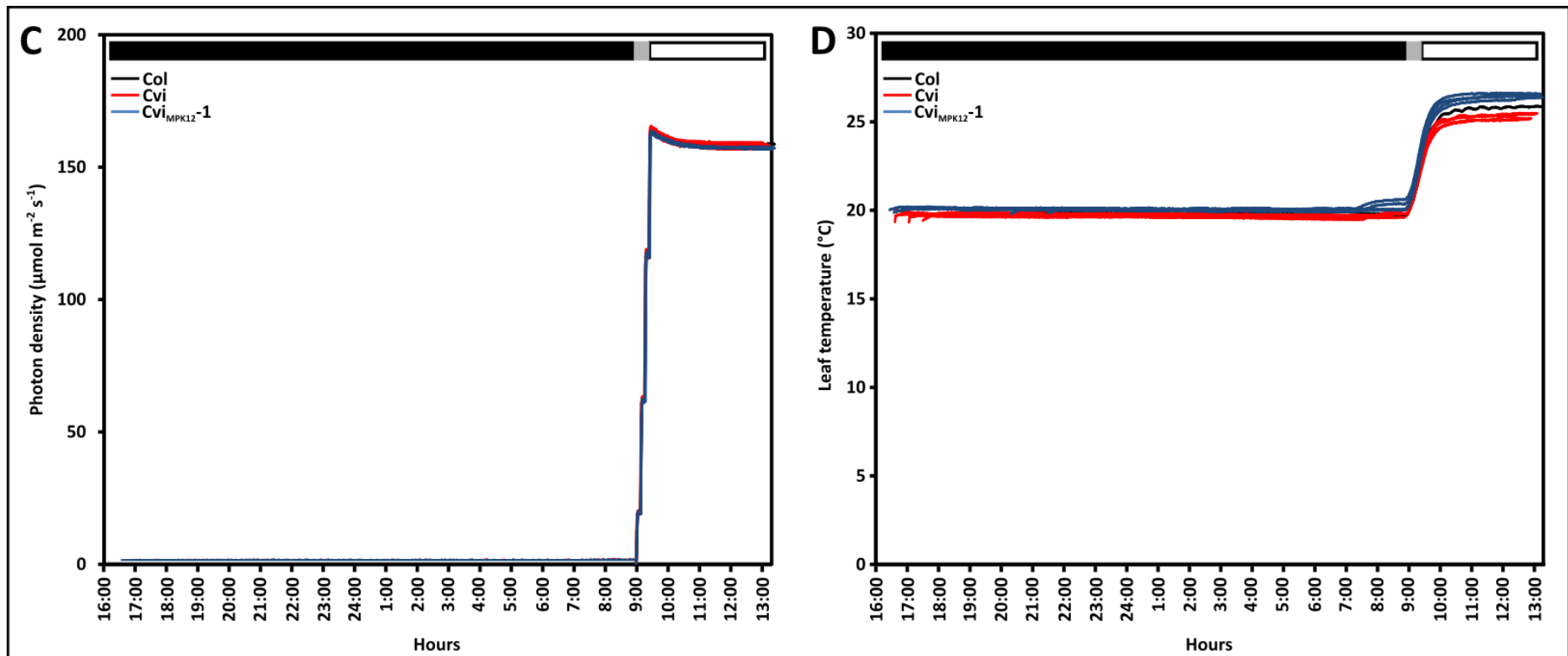
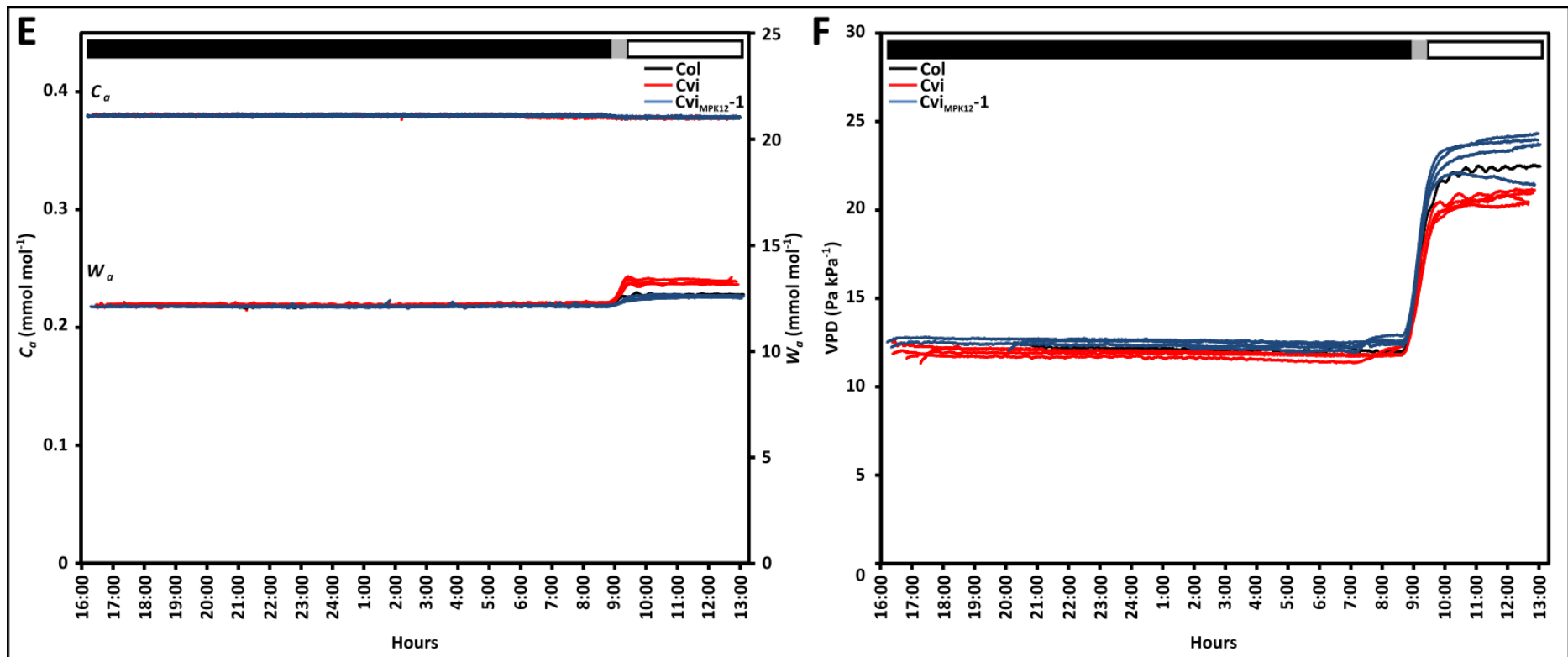


Figure 3-48 Nighttime stomatal opening and stomatal oscillations of Arabidopsis accessions Col-0, Cvi-0 and Cvi plants homozygous for the Col MPK12 allele. Nighttime stomatal opening and stomatal oscillation were indicated by transpiration rate ( $E$ ) A) and stomatal conductance ( $g_s$ ) B) of 37  $\pm$  4-day-old Col-0 (black line), Cvi-0 (red lines) plants and Cvi plants homozygous for the Col MPK12 allele (blue lines). Individual plants are labeled with numbers 1, 2, and 3. The light regime and photon flux density C), leaf temperature D),  $\text{CO}_2$  and  $\text{H}_2\text{O}$  concentration E), and leaf-to-air VPD F) over the time of the day-and-night gas exchange measurements are depicted. The color codes of Fig. 3-48C-F are the same as in A and B, but individual lines are not labeled because of the comparable conditions of these lines. Bars on the top of each figure represent the illumination phase (white), the phase of transition from darkness to illumination (gray), and the dark phase (black). All plants were grown under short day (8 h light / 16 h dark photoperiod) at a photon flux density of  $150 \mu\text{mol m}^{-2} \text{s}^{-1}$ , at a temperature of  $22^\circ\text{C}$  and 50% relative humidity in the daytime and a temperature of  $17^\circ\text{C}$  and 60% relative humidity at night, and under well-watered conditions ( $\text{SWP} \geq -0.02$  bar). A-E) Each curve is a single measurement of an individual plant.  $n=1$  biological replicate for Col-0 and  $n=4$  biological replicates for Cvi-0 and Cvi<sub>MPK12-1</sub>.







the Col-0 and Cvi-0 accessions (Fig. 3-48A and B).

During the daytime phase (17:00 to 9:00), light intensity stabilized at  $180 \mu\text{mol m}^{-2} \text{s}^{-1}$ , and leaf temperatures of all tested lines remained around  $25 \text{ }^{\circ}\text{C}$  (Fig. 3-48C and D). Other conditions, including  $C_a$ ,  $W_a$ , and VPD, also became stable (Fig. 3-48E and F). The oscillations of Col-0 and Cvi-0 triggered in the transition phase damped and finally reached homeostasis (Fig. 3-48A and B).

Table 3-6 Nighttime stomatal conductance of Arabidopsis accessions Col-0, Cvi-0, and Cvi plants homozygous for the Col MPK12 allele. In the table, nighttime stomatal conductance is the average value of stomatal conductance in the dark. "-" indicates no measurement. n=1 biological replicate for Col-0 and n=4 biological replicates for Cvi-0 and Cvi<sub>MPK12-1</sub>.

Nighttime stomatal conductance				
Lines		Col-0	Cvi-0	Cvi <sub>MPK12-1</sub>
	1	32	38	29
Replicates	2	-	55	24
	3	-	38	22
	4	-	45	31
	Mean	32	46	26

Analysis of four Cvi<sub>MPK12-1</sub> plants exhibited Col-like nighttime stomatal conductance (Fig. 3-48A and B; Table 3-6), and the values averaged  $22 \text{ mmol m}^{-2} \text{ s}^{-1}$ ,  $22 \text{ mmol m}^{-2} \text{ s}^{-1}$ , and  $19 \text{ mmol m}^{-2} \text{ s}^{-1}$ ; these values are comparable to the  $32 \text{ mmol m}^{-2} \text{ s}^{-1}$  of Col-0. These results revealed that the Col MPK12 allele could lower the stomatal conductance of Cvi in the dark.

### 3.4.2.2 Oscillation periods are not controlled by the MPK12 gene

Oscillation periods were further analyzed to determine the role of the MPK12 gene in this phenomenon. As in the analysis of the RILs, the oscillation period in the first cycle was used as the phenotype. Consistent with the results of the oscillation periods when using a ring chamber (see Fig. 3-44 and Table 3-5), Col-0 had a period of around 20 minutes (Fig. 3-49A; Table 3-7). Moreover, Cvi-0 had longer periods than Col-0 and the values of the oscillation period of Cvi-0 were 35 minutes, 38 minutes, 38 minutes and 35 minutes (Fig. 3-49B-E; Table 3-7). Analyzed results of Cvi-0 plants

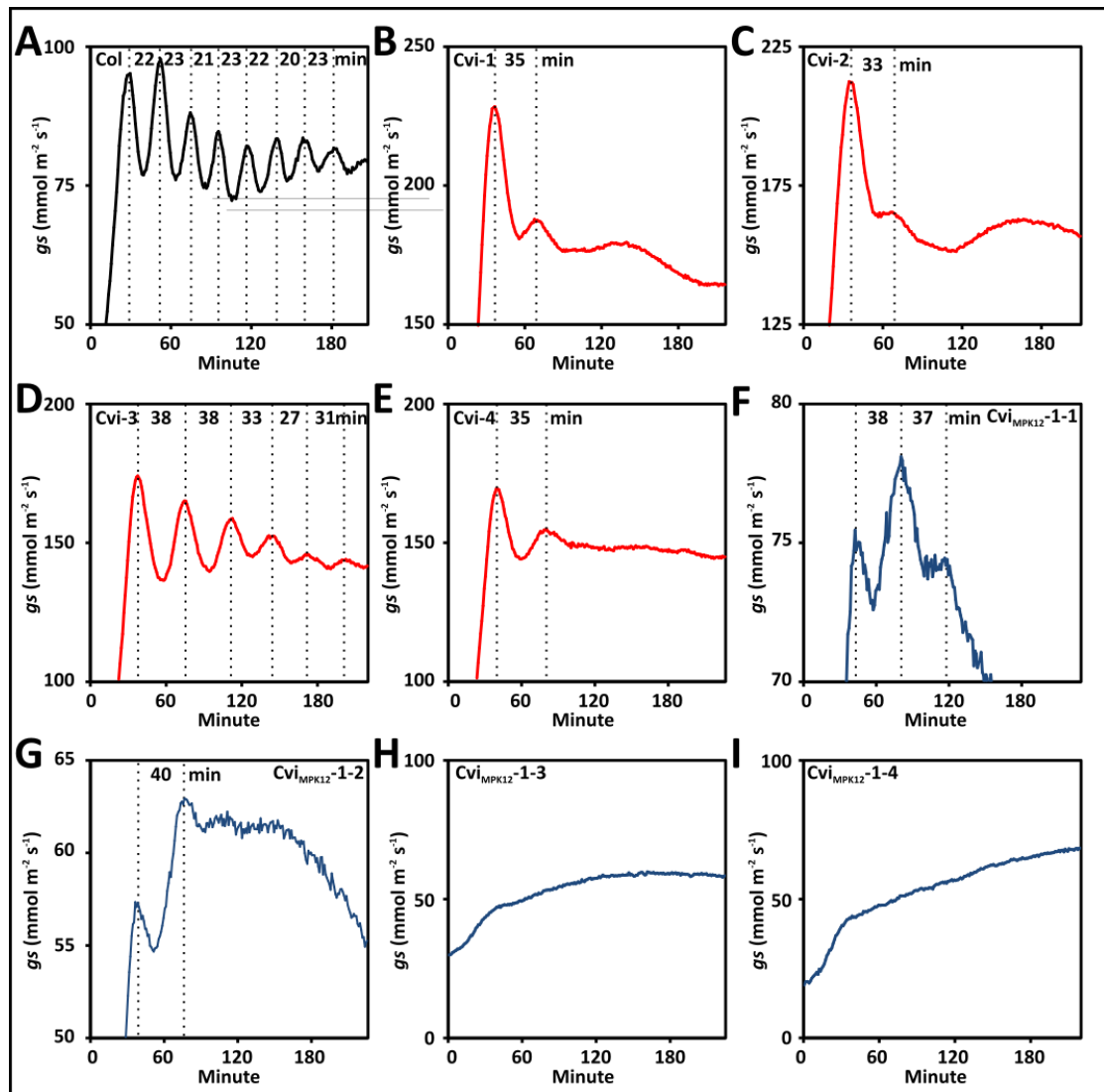


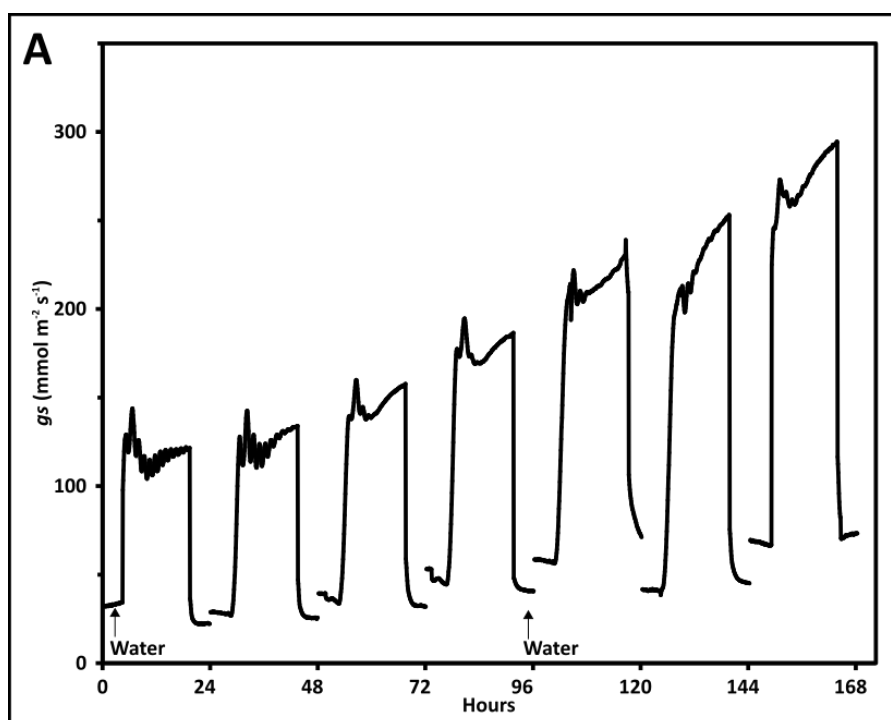
Figure 3-49 Stomatal oscillation of *Arabidopsis* accessions Col-0, Cvi-0 and Cvi plants homozygous for the Col MPK12 allele. The enlargement of stomatal conductance between 9:00 and 13:00 in Fig. 3-48B presents the details of the stomatal conductance oscillations of Col-0 (black lines), Cvi-0 (red lines), and Cvi plants homozygous for the Col MPK12 allele (blue lines). Individual lines are labeled in the top left or right corner of each figure. The vertical, dotted lines indicate the time of the crests of each oscillation event, and the numbers between the dotted lines indicate the periods (length in minutes) of the corresponding oscillation events. The gas exchange measurement conditions and growth conditions of the plants are as described in Fig. 3-48. Curves shown in A-I) are single measurements.

homozygous for Col MPK12 allele displayed that two of four plants had oscillations with one cycle, and the periods were 38 minutes and 40 minutes (Fig. 3-49F and G; Table 3-7), while the other two did not experience oscillation (Fig. 3-49H and I; Table 3-7). These results do not support the assumption that the MPK12 gene may explain the variations in the oscillation periods of Col-0 and Cvi-0.

Table 3-7 Oscillation periods of stomatal conductance of Arabidopsis accessions Col-0, Cvi-0 and Cvi plants homozygous harboring the Col MPK12 allele. Oscillation periods in the table are periods of the first oscillation cycles; these periods are the time difference between the first and second crests of the oscillations. "N" indicates that gas exchange measurements were performed, but no oscillation was observed. "-" indicates that no gas exchange measurements were performed. Individual measurements are presented in the table. The biological replicates are numbered with 1 to 4.

Lines	Period of the first oscillation cycle			
	Col-0	Cvi-0	Cvi <sup>MPK12-1</sup>	
Replicates	1	22	35	38
	2	-	33	40
	3	-	38	N
	4	-	35	N
Mean	22	35	39	

### 3.4.3 Stomatal oscillation does not occur at random



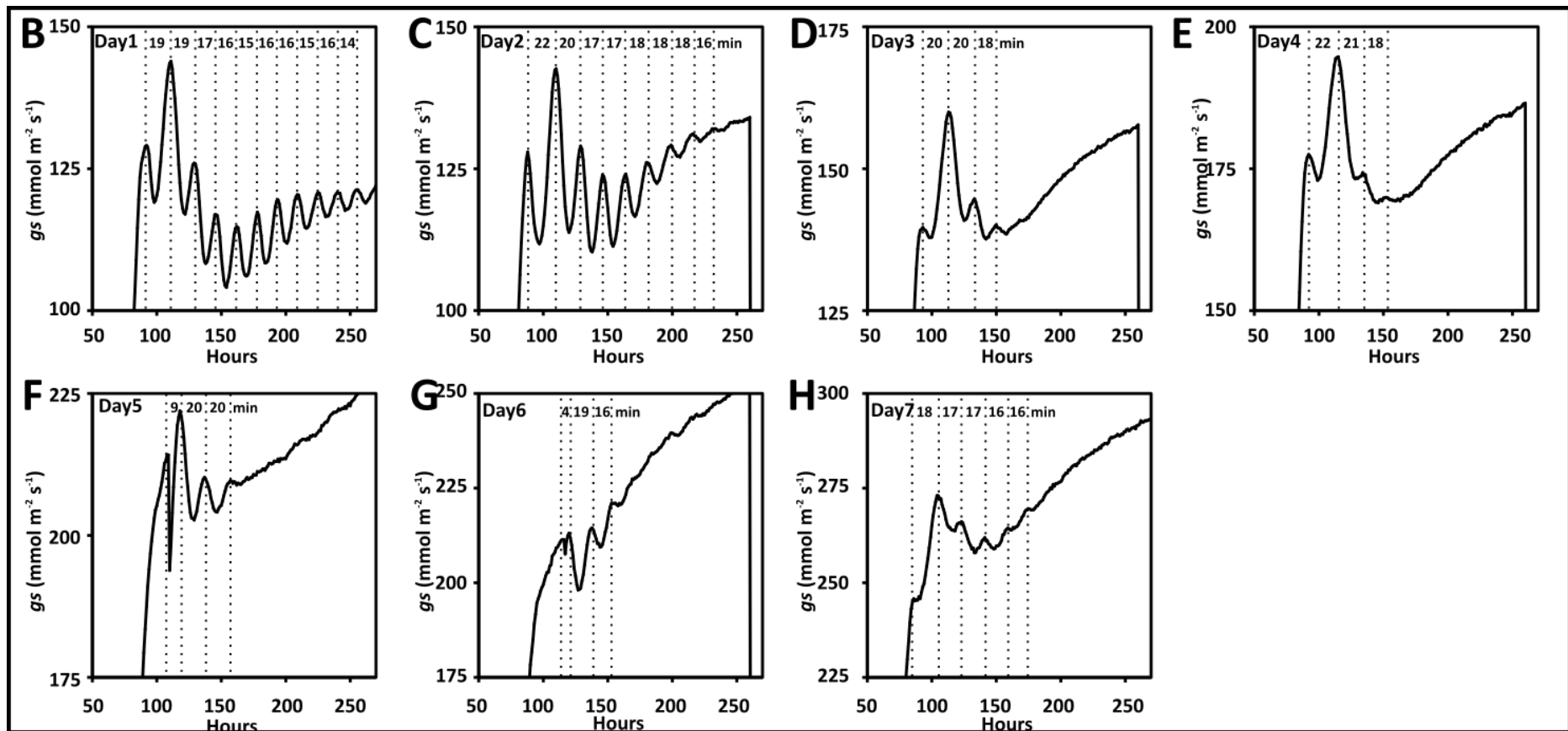


Figure 3-50 Stomatal oscillation does not occur at random and maybe associated with soil water availability. Stomatal conductance A) of the Col-0 plant was recorded in seven days and experienced oscillation during each day. Arrows indicate the time of watering. Magnified pictures of seven oscillation events B-H) show the details of each oscillation event. Days are labeled in the top left corner of each figure. The vertical dotted lines indicate the time of the crests of each oscillation event and the numbers between the dotted lines indicate periods (length in minute) of the corresponding oscillation cycles. Gas exchange measurement conditions and growth conditions of plants are as described in Fig. 3-43. F and G). Oscillations were disturbed at the first oscillation crests of days 5 and 6 because of the replacement of the drier and the CO<sub>2</sub> absorber. A-H) Single measurement of one Col-0 plant.

Former observations of stomatal oscillations (see Fig. 3-44, Table 3-5, Fig. 3-49, and Table 3-7) displayed the uncertainty of the occurrence of stomatal oscillation and also the cycle numbers in oscillation events. To investigate whether oscillations occur occasionally and whether cycles of oscillation occur randomly, a seven-day continuous gas exchange measurements were performed on Col-0. The experimental setup was similar to that illustrated in Fig. 3-43C-F. During the measurements, the plants were not disturbed except the replacement of the drier and the CO<sub>2</sub> absorber. In addition, water was given at night on day one and four (Fig. 3-50A). The oscillations of the Col-0 plants occurred each day (Fig. 3-50A-H), which revealed that stomatal oscillation did not occur randomly. However, the cycles of oscillation showed considerable variations (Fig. 3-50A-H). The oscillations on the first day consisted of ten cycles (Fig. 3-50B), and the number of cycles declined to eight in the second day (Fig. 3-50C). A significant decrease in the number of cycles happened on days three and four, only two cycles occurred (Fig. 3-50D and E). The only difference in environmental factors during this period was the water content of the soil, and when this difference was realized, water was administered at night on day four. Two cycles of stomatal oscillation occurred on days five and six (Fig. 3-50F and G), and the number of cycles increased to five on day seven (Fig. 3-50H). These results suggest that soil water content may be associated with the number of oscillation cycles.

## 4. Discussion

### 4.1 Drought assay system

Drought occurs frequently during the growth season of plants and affects their yield production. Breeding crops with enhanced drought resistance would help stabilize yield. Many studies investigated drought resistance of plants in the past. In recent years, high-throughput phenotyping systems were developed to explore and identify genes involved in the drought stress response of plants. However, few of these researches resulted in the transfer of the knowledge into the field. Some scientists attribute the failure to the complexity of plants' adaption responses to drought according to the facts that the expression level of hundreds of genes are up- or down-regulated during drought, and the gene expression also displayed spatial-temporal variations (Wilkins *et al.*, 2010; Zhou *et al.*, 2007). However, Blum (2011) pointed that although a lot of genes are involved in drought stress, only a small portion of them are related to the drought resistance at the whole plant level, and the spatial-temporal variations in gene expression level may be due to the different tissue water content. Furthermore, he concluded that the failure is caused by the incapability of "recognizing and targeting the correct trait and phenotype under the exact relevant stress conditions", rather than the complexity of the drought resistance (Blum, 2011).

Typically, experimental methods exerting drought on plants includes deficit irrigation and progressive drought. The deficit irrigation simulates the repeated rain-drought scenario which occurs in nature. It is also a commonly used irrigation regimes in the high-throughput plant phenotyping platform in which the controlled drought is exerted by administrating limited amount of water automatically. However, this irrigation regime may give rise to some uncertainties. The repeated watering may lead to a non-uniform soil water distribution in potted experiments with low SWC and big containers. It has been reported that reducing soil water content from 40% to 20% in silt loamy soil results in a reduction of hydraulic conductance from  $1 \text{ cm h}^{-1}$  to  $10^{-5} \text{ cm h}^{-1}$ , while soil water potential was only reduced by a factor of 10, from  $-0.1 \text{ bar}$  to  $-1 \text{ bar}$  (Mualem, 1976; Saxton *et al.*, 1986). Therefore, the water diffusivity would be slowed down during the processes of water infiltration and redistribution in soil. Moreover, water moves not only downward into the deep soil, but also



upward into the atmosphere owing to the evapotranspiration (evaporation from the soil surface and transpiration of plants). The consequence of both reduced water diffusivity and evapotranspiration is that the soil water of potted plants which are subjected to low soil water content may have a vertically non-uniform distribution where the upper part contains more water than the lower part. As a consequence, the roots may predominantly distribute at the top layers of the soil owing to the hydrotropism of roots. In such cases, plants may not be subjected to the designed SWC regime, and of course, which perturbs results. In addition, well-watered control plants in the deficit irrigation scheme may also display unusual behavior, such as poor growth at 80% SWC (Fig. 3-2E), which may be caused by water logging. Water logging occurs when soil water content is higher than field capacity, i.e. the maximum water been held by the soil or other growth mediums. The excess water in the growth mediums results in an oxygen deficiency which can damage the root system and affects the plants' water uptake and growth (Irfan *et al.*, 2010). Although the experiment design for 80% SWC did not exceed the field capacity, a Parafilm was covered on the surface of each pot, and hence may cause oxygen deficiency in the soil.

Another commonly used method for studying the drought is the progressive drought induced by stop watering. This method eliminates the potential problems with iterative watering because water loss in the progressive drought is a spontaneous process. However, the duration of the progressive drought till terminal stress is reported to be quite short in the literature - commonly 10 to 20 days (Erice *et al.*, 2010; Matos *et al.*, 2008; Riccardi *et al.*, 1998). Such a short duration is caused by a fast evapotranspiration of bare soil, typically more than 60% within two weeks (Fig. 3-1A). Although plants respond fast to the drought in the stomatal regulation, such a short duration may not allow plants to fully acclimate to drought stress. However, this disadvantage can be easily avoided in a prolonged progressive drought in which pots are covered to prevent evaporation. This setup allows a slower water loss, and therefore a prolonged period of plant growth. The advantage of the prolonged progressive drought was demonstrated in this study where terminal stress was reached after 8 weeks of drought. Classifying the severity of drought (discussed later) in the prolonged progressive drought displayed a 4 weeks well-watered phase, 2.5 weeks mild-drought phase and 2 weeks severe drought phase (Fig. 3-1B and C), while

the traditional progressive drought scenarios had a 0.5 weeks well-watered phase, 1.5 weeks mild drought phase and 1.5 weeks' severe drought phase (Fig. 3-1A). In addition, analysis of insWUE in lines overexpressing RCAR6 and RCAR10 revealed that their advantages in water use mainly occurred in the well-watered phase of the prolonged progressive drought, which lead to an increased biomass at the end of drought. However, such a biomass gain would not be detected when the experiment is performed in a traditional progressive drought, owing to the much shorter well-watered phase. Taken together, the prolonged progressive drought is a suitable system to study drought resistance, and this drought scenario is close to the slow soil drying observed in the field under drought (Barker *et al.*, 2005).

### **Classification of the severity of drought**

The drought phases can be classified as well-watered phase, mild drought stress and severe drought stress according to the soil water content or soil water potential. Without explaining the basis of this, it may lead to difficulties in comparing results from different studies. Pinheiro and Chaves (2011) studied the photosynthesis in response to drought using the data collected from more than 450 recent papers and found that these results were non-comparable. Blum (2011) explained that the non-comparable results may be partially caused by the variable leaf water deficit which, in turn, is related to the soil water status and the air humidity. Undeniably, there is no consensus up to now on what defines a mild and severe drought stress. The difficulty may origin from drought itself because it is a "creeping phenomenon" (Wilhite and Glantz, 1985), and different species have variable sensitivity to the same drought scenario. Wilhite and Glantz (1985) suggested that the definition and classification of agricultural drought should be based on the symptoms of plants. Furthermore, Levitt (1972) raised that plants had evolved sophisticated strategies to maintain relatively high tissue-water potential or endure low tissue water potential under drought. Among these strategies, reduced stomatal conductance is one of the primary responses of plants to drought (Atwell *et al.*, 1999). Abscisic acid is the main phytohormone mediating the stomatal conductance, and the expression of a key enzyme involved in ABA synthesis - 9-cis-epoxycarotenoid dioxygenase (NCED) - has been reported to increase significantly within 15 to 30 minutes after a leaf detachment or dehydration treatment (Xiong, 2003). Also, a fast response (within 15 to 30 minutes) of ABA-mediated stomatal closure in *Arabidopsis* has been reported

(Tanaka *et al.*, 2005). Furthermore, reduced stomatal conductance would lead to reduced transpiration, and in turn, the transpiration is associated with leaf temperature (Gates, 1968). In this study, 60% SWC (SWP = -0.03 bar) was defined as a boundary to distinguish the well-watered phase and mild drought phase for *Arabidopsis*, according to the fact that the leaf temperature of Col-0 in independent experiments started increasing when the SWC was lower than 60% (SWP = -0.03 bar) (Fig. 3-3A; Fig. 3-33). The increase in leaf temperature was associated with a drop of  $g_s$  in a progressive drought experiment (Fig. 3-3B). In addition, a second indicator for classifying the severity of drought is the leaf wilting, which is the consequence of a turgor loss of leaf owing to a reduced cell water content and is regarded as a severe drought symptom (Bray, 1997). In this study, shrinkage of leaf area supports 15% SWC (SWP = -0.5 bar) as the boundary for distinguishing the mild drought stress and severe drought stress for *Arabidopsis* (Fig. 3-1B and C; Fig. 3-27A and B). Although it had already been suggested over 30 years to classify agricultural drought according to plants' response, little effort was invested in this field so far. The reason may be due to the lack of fast techniques to detect the plants' responses to drought, especially to the mild drought. Using the leaf temperature readout as an approximation for stomatal adjustment and reaching the wilting of leaf along with pF measurements (soil water potential) of the soil may provide simple means to classify the drought phases and provide suitable criteria for different plant species. This would help guide the experimental design, facilitate the evaluation of severity of drought and help explain and compare results and the associated drought resistance mechanisms.

In addition to a proper system for evaluating drought resistance, a relevant trait corresponding to drought resistance is important for studying resistance mechanisms. A deeper root, changes in the anthesis to silking interval and differential osmotic adjustment have been used to breed crops with enhanced drought resistance (Blum, 2011). Carbon isotope discrimination has been frequently used to assess plants' WUE (Des Marais *et al.*, 2014; Juenger *et al.*, 2005). The growth of leaf as projected leaf area has been used to screen for genes involved in the regulation of photosynthesis rate in high throughput phenotyping platforms (Tessmer *et al.*, 2013; Zhang *et al.*, 2012). Among these traits, leaf area is directly linked to the plants' productivity because it is the site for interception of light and diffusion of CO<sub>2</sub>, and it also allows

high throughput, non-destructive, and cost-effective analysis.

In agriculture, the yield or the biomass is a major concern. Monitoring the changes of biomass is always a challenge. Prediction of plants' biomass according to leaf area has been attempted in a high throughput plant phenotyping platform in wheat and barley (Golzarian *et al.*, 2011). However, using leaf area as a substitute for biomass should still be seen with caution because it has been reported recently that leaf area is not a reliable tool to predict plants' biomass (Weraduwege *et al.*, 2015). The author found that neither the specific leaf area nor the projected leaf area is correlated to the shoot biomass in *Arabidopsis* which was grown under well-watered conditions and attributed the non-linear relationship to the partition of carbon to the leaf thickness. The partitioning of photosynthetic carbon to the leaf area and leaf thickness is even more complicated during drought. The leaf area has been reported to be reduced during drought (Grant *et al.*, 2010; Rizza *et al.*, 2004), while the leaf thickness increase under water deficit conditions (Ristic and Cass, 1991; Sam *et al.*, 2000). In this study, plotting the projected leaf area against the above-ground dry biomass displayed a triphasic relationship during the progressive drought (Fig. 3-1D). Positive relationships were found in well-watered phase and mild drought phase, while a negative relationship was observed in severe drought phase. Although a positive linear relationship was observed under mild drought, the ratio of biomass to leaf area was higher than that under well-watered conditions, which can be explained by the overlapping leaves and thicker leaves under drought. Moreover, the leaf wilting makes the relationship between leaf area and biomass more intangible.

Classifying the severity of a drought in a prolonged progressive drought system facilitates an evaluation of *Arabidopsis* germplasms to study the mechanisms involved in the adaption of plants during drought. Under well-watered conditions, examining both leaf growth and leaf surface temperature is a powerful tool to identify natural accessions and transgenic lines that combine enhanced WUE and maintenance of growth (Fig. 3-4; Fig. 3-5A and B; Fig. 3-26A-C; Fig. 3-28A and B; Fig. 3-41A-C). Moreover, measuring gas exchange under well-watered or mild stress conditions allow for the analysis of transient changes of plants' transpiration rate ( $E$ ), carbon assimilation rate ( $A_n$ ), intercellular  $\text{CO}_2$  ( $C_i$ ) and instantaneous water use efficiency (insWUE). These parameters, in turn, facilitate to reveal mechanisms

regarding plants' adaption to the variable severity of drought. Furthermore, reaching the leaf wilting point may also facilitate the study of drought tolerance under severe drought conditions, although this is not emphasized in this study.

## **4.2 Potential to enhance water use efficiency in Arabidopsis**

The studies of WUE in plant species emerged in the middle of the twentieth century when the Green Revolution occurred. A slogan "more crop per drop" was raised in recent years (Kijne *et al.*, 2003). Research on this topic over the last three decades have engendered the wide consensus that the WUE of plants can be enhanced under water-limited conditions. Gravimetrically derived, gas-exchange derived and carbon-isotope-discrimination derived WUE under water-limited conditions have been reported to increase by a factor of 1.5 to 2.5 in different species (Medrano, 2002; Ranney *et al.*, 1991; Rizza *et al.*, 2012; Wall *et al.*, 2001). Studies on *Arabidopsis thaliana* have revealed variations in WUE by a factor of two between well-watered and water-limited conditions in accessions Columbia and Langsberg (Masle *et al.*, 2005). Enhanced WUE in Arabidopsis has also been confirmed by using five different Arabidopsis accessions in this study based on the gas exchange measurements during the period of progressive drought (Fig. 3-30C). However, during the last three decades, few successes have been achieved to translate this insight into crops in field conditions. This may be attributed to a lack of knowledge concerning genes or gene networks regulating WUE. In addition, plants with high WUE are reported to be associated with reduced growth and biomass (Blum, 2005; Hausmann *et al.*, 2005; Martin *et al.*, 1999; Munoz *et al.*, 1998), which also restricts the application of this insight into the field. With the aim of exploring genes regulating WUE, and understanding the association between WUE and growth or yield potential, and searching for plants combined high WUE with maintained growth, four issues are highlighted in this study: (1) Whether Arabidopsis plants with ectopic expression of ABA receptors are capable of achieving high WUE. (2) Identifying natural variation genes regulating WUE in Arabidopsis. (3) Whether enhanced WUE is tightly linked to trade-offs in plants' growth or yield. (4) Demonstrating the mechanisms of enhanced WUE and maintained growth.

### **ABA receptors confers enhanced WUE in Arabidopsis**

Water loss of plants mainly occurs through stomatal pores, the movement of which is

best-known to be regulated by ABA-dependent signaling (Raghavendra *et al.*, 2010). The activation of ABA signaling promotes stomatal closure, preventing water loss in plants. However, stomatal closure may also restrict the diffusion of CO<sub>2</sub> into the site of carboxylation, and therefore, affect photosynthesis and plant growth. This delicate balance may be modulated by an RCAR/PYR1/PYL and an associated protein PP2C (Kang *et al.*, 2010; Kuromori *et al.*, 2010; Ma *et al.*, 2009; Park *et al.*, 2009). Caving ABA into the binding pockets of RCAR proteins inhibits the phosphatase activity of PP2Cs, and then activates SNF-related serine/threonine protein kinases, subsequently activates downstream components by phosphorelay and finally mediates the adaption responses of plants to drought in both short-term and long-term manners (Raghavendra *et al.*, 2010). However, the complexity of sensing mechanisms caused by a combination of fourteen RCARs and six PP2Cs (Raghavendra *et al.*, 2010) makes it difficult to understand which RCARs are more efficient in mediating plants' water efficiency. An ectopic expression of a single ABA receptor would make it possible to avoid this complexity and allow for the investigation of the role of specific RCARs in mediating plants' WUE.

In this study, the transgenic lines with an ectopic expression of a single RCAR which were generated by Stefanie V. Tischer (2016) were investigated during progressive drought. They exhibited considerable variations in leaf surface temperature, growth, water use, biomass formation and WUE. Receptors in subfamily I displayed variable results. One of three RCAR1 overexpressing lines exhibited higher leaf temperature in the well-watered phase of progressive drought (Fig. 3-5A and B), as well as more biomass and higher WUE at the end of the progressive drought (Fig. 3-7E and F). RCAR4, another member of subclade I, had a less significant increase in leaf temperature (Fig. 3-5A and B) and WUE (Fig. 3-7F), but exhibited a stunted growth (Fig. 3-5A; Fig. 3-7A and E). The considerable variation in the growth of lines overexpressing RCARs from subclade I might be attributed to the RCAR-mediated induction of leaf senescence reported in a recent study by Zhao *et al.* (2016). By analyzing survival rate of lines with overexpression of the Arabidopsis ABA receptors under drought conditions, Zhao *et al.* (2016) identified RCAR1 as mediating drought resistance. While this study focused on severe drought scenarios and senescence-related processes which is not compatible with the interest of agriculture, our analysis addressed the contribution of RCAR members to WUE. Most of the RCAR

receptors in subclade II were able to confer Arabidopsis plants with enhanced WUE, especially RCAR6, RCAR8, RCAR9 and RCAR10 (Fig. 3-7F). These results are consistent with previously reported conclusions. Transgenic lines with overexpressing RCAR10 have been revealed to have higher insWUE than wild type Col-0 (Pizzio *et al.*, 2013a). Also, transgenic lines overexpressing RCAR8 have been reported to consume less water (Santiago, Rodrigues *et al.*, 2009), which is consistent with the higher leaf temperature and delayed water consumption in this study (Fig. 3-5A and B; Fig. 3-6B). Subclade III receptors, which are considered to be dimeric and less affine receptors (Yoshida *et al.*, 2014), did not contribute to WUE during progressive drought (Fig. 3-7F). However, a hexuple mutant derived from RCAR11/PYR1, namely PYR1<sup>MANDI</sup> (PYR1(Y58H/K59R/V81I/F108A/S122G/F159L)), possesses nanomolar mandipropamid (an agrochemical and ABA agonist) sensitivity in *in vitro* PP2C inhibition assays, and exhibits higher leaf temperature when applying mandipropamid compared with mock PYR1<sup>MANDI</sup> mutant (Park *et al.*, 2015). These results reveal that overexpressing RCAR1, RCAR6, RCAR8, RCAR9, and RCAR10 would confer enhanced WUE, and in addition, increasing the affinity of ABA or ABA agonist to RCARs through editing the amino acid residues in the binding pocket of RCARs may help enhance plants' WUE.

### WUE correlates with $\delta^{13}\text{C}$ but not with $\delta^{18}\text{O}$

The enhanced WUE of transgenic lines overexpressing different RCARs has been further confirmed by analyzing the isotope abundance of plant materials. Consistent with the gravimetric-derived WUE reported during a progressive drought,  $\Delta^{13}\text{C}_{\text{bulk}}$ -derived WUE also indicated that lines with ectopic expression of RCAR1, RCAR6, RCAR8, RCAR9 and RCAR10 discriminated less  $^{13}\text{C}$  (Fig. 3-8A and C) and achieved higher WUE than Col-0 (Fig. 3-8B and D). When plotting gravimetric-derived WUE against  $\Delta^{13}\text{C}_{\text{bulk}}$ -derived WUE, a strong positive association was found (Fig. 3-10C).

Different plant fractions have considerable variations in carbon isotope compositions ( $\delta^{13}\text{C}$ ) (Park and Epstein, 1961). Among these,  $\delta^{13}\text{C}$  in cellulose reflects the isotopic compositions of the primary products of photosynthesis (Hietz *et al.*, 2005). In addition, a majority of carbon assimilated through photosynthesis during the lifespan of the plants' growth translocates to the seeds and thus, the carbon signature in seeds correlates with that in leaf materials (Farquhar and Richards, 1984a; Hubick

and Farquhar, 1989). Indeed, cellulose and seeds displayed a different signature of  $^{13}\text{C}$  compared with that of the leaf (Fig. 3-8A and C; Fig. 3-21D). Similar to the bulk samples, the overexpression RCAR6-3 line exhibited a less discrimination of  $^{13}\text{C}$  in both cellulose and seed, and therefore achieved higher  $\Delta^{13}\text{C}_{\text{cellulose-derived}}$  and  $\Delta^{13}\text{C}_{\text{seed-derived}}$  WUE than wild type Col-0 (Fig. 3-8A and D; Fig. 3-21D and E).

A carbon isotope analysis at high photon flux density conditions further confirmed the enhanced WUE of RCAR lines. Less  $^{13}\text{C}$  discrimination at a high photon flux density has been reported in tomato (Park and Epstein, 1960; Smith *et al.*, 1976) and in *Acacia farnesiana* (Smith *et al.*, 1976). These results reflect that high photon flux densities promotes the photosynthetic capacity of plants and enhances demand for  $\text{CO}_2$ , therefore imposing a strain on the  $\text{CO}_2$  gradients between the atmosphere and the site of carboxylation in the plants' chloroplast. In accordance with this principle, the less  $^{13}\text{C}$  discrimination was also observed in Arabidopsis lines grown at a saturation light and well-watered conditions, but the RCAR6-3 line still exhibited less discrimination of  $^{13}\text{C}$  and higher  $\Delta^{13}\text{C}_{\text{bulk-derived}}$  WUE than wild type Col-0 (Fig. 3-22E). This result reveals that RCAR6-3 can still maintain a high  $\text{CO}_2$  gradient between ambient air and chloroplasts under high photon flux density conditions.

Similarly, heavy isotope of oxygen -  $^{18}\text{O}$  - is enriched in the leaf water relative to the source water owing to the isotope effect during the process of water movement from the soil to the atmosphere via plants (Farquhar *et al.*, 2007). Moreover, oxygen in plants' cellulose originates mainly from leaf water, and a positive relationship between  $\delta^{18}\text{O}$  in the leaf water and that in cellulose has been reported (Yakir and DeNiro, 1990). Thus,  $\delta^{18}\text{O}$  in the plant's organic matter can be used to access the time-integrated leaf water loss through stomata during its growth period. Barbour *et al.* (2000); Barbour and Farquhar (2000); Cabrera-Bosquet *et al.* (2009); Saurer *et al.* (1997) have reported a negative correlation between  $\delta^{18}\text{O}$  or  $\Delta^{18}\text{O}$  of the organic matter and transpiration rate in wheat. In contrast, Sheshshayee *et al.* (2005) has claimed a positive association between  $\delta^{18}\text{O}$  or  $\Delta^{18}\text{O}$  of the organic matter and accumulative transpiration rate in groundnut and rice. According to the simplified equation for estimation of  $\Delta^{18}\text{O}$  at the evaporation site:

$$\Delta_e \approx (\varepsilon^+ + \varepsilon_k)(1 - h) \quad (19)$$



where  $\Delta_e$  is the  $^{18}\text{O}$  enrichment at the evaporation site in the stomata, the  $\varepsilon_k$  is the kinetic fractionation, the  $\varepsilon^+$  is the liquid-vapor equilibrium fractionation and the  $h$  is the humidity which is related to the VPD, Farquhar *et al.* (2007) have explained that the contrasting results are due to the source of variation of transpiration rate ( $E = g_s \times \text{VPD}$ ). If the source of variation of  $E$  is from  $g_s$ , a negative relationship between  $E$  and  $\delta^{18}\text{O}$  appears, while if the source of variation of  $E$  comes from evaporative demand (VPD-induced), then a positive relationship would be observed. A good example has been reported by Barbour and Farquhar (2000) in which a reduced  $E$  caused by lowering  $g_s$  through applying ABA on the leaves results in an enrichment of  $^{18}\text{O}$  in plants' cellulose, while a reduced  $E$  caused by a decreasing VPD through increasing environmental humidity results in a decrease of  $\delta^{18}\text{O}$  in plants' cellulose. However, the results of this study do support an uncorrelation between the  $\delta^{18}\text{O}$  derived from the cellulose of plants harvested at the end of the progressive drought and the leaf temperature (transpiration rate) under well-watered conditions using different *Arabidopsis* transgenic lines with overexpressing single RCARs (Fig. 3-10 H). It is noteworthy that the RCAR6-3, RCAR8 and RCAR9 lines had a 1 °C higher leaf temperature but possessed either a comparable or a lower  $\delta^{18}\text{O}$  than Col-0 (Fig. 3-9B; Fig. 3-10H). The VPD would not be the argument here, because the humidity for all lines was the same in this experiment. Farquhar *et al.* (2007) have suggested that if the source of variation is from  $g_s$ , two factors should be taken into account. First, the kinetic fractionation -  $\varepsilon_k$  - which is determined mainly by stomatal resistance, and therefore a negative correlation would be expected according to the Equation (19). Second, stomatal closure and reduced  $E$  result in an increase of leaf temperature, so that the concentration of water in the stomatal cavity increases, and  $h$  is decreased. This would also lead to an  $^{18}\text{O}$  enrichment according to the formula Equation (19). Moreover, the increased leaf temperature would affect the  $\varepsilon^+$ , but its effect is thought to be negligible (Farquhar *et al.*, 2007). In addition, the enrichment of  $^{18}\text{O}$  at the evaporation site is more than that in the leaf water owing to the Péclet effect that unenriched water from xylem would oppose the diffusion of enriched water from the evaporative site back to the xylem (Farquhar *et al.*, 2007). The consequence of the Péclet effect is that less  $E$  would result in more enriched  $^{18}\text{O}$  in the leaf water. Taken together, none of these factors in the physical process of water movement could explain the comparable or reduced  $\delta^{18}\text{O}$  in high-temperature RCAR lines -

RCAR6-3, RCAR8, and RCAR9.

There might be the possibility that the less enrichment of  $^{18}\text{O}$  is due to forming of the plant organic matter. The major factor controlling the oxygen composition of the organic matter has been concluded to be the exchange of oxygen atoms between water and carbonyl oxygens in triose phosphates via a geminal-diol intermediate (Farquhar *et al.*, 2007), and several studies support a fractionation of 27 ‰ (Barbour *et al.*, 2000; Cernusak *et al.*, 2003; da Silveira Lobo O'Reilly Sternberg, Leonel and DeNiro, 1983). In addition to the exchange of the carbonyl oxygens, there might be other unknown processes controlling the oxygen isotope composition of plants' organic matter (Schmidt *et al.*, 2001). Overexpressing RCAR6, RCAR8, and RCAR9 might affect these processes, and therefore these transgenic lines may display less oxygen enrichment in cellulose.

### **Enhanced WUE with minor trade-off in growth and biomass**

Enhanced WUE is regarded to be associated with reduced growth and small leaf area (Blum, 2005). Martin *et al.* (1999) has reported that breeding tomato plants with high WUE can be achieved by selecting low  $\Delta^{13}\text{C}$  lines of tomato, but selecting low  $\Delta^{13}\text{C}$  alone may identify a subpopulation of small plants. However, in this study, the leaf surface temperatures and rosette size under well-watered conditions provided the first indication of enhancement of WUE with no or minor trade-offs in growth for lines such as RCAR1-1, RCAR6-3 and RCAR10-3 compared with wild type Col-0 (Fig. 3-5A and B). This result is further confirmed by the lack of association between rosette size (under well-watered conditions) and WUE (at the end of progressive drought) as well as by the association between maximum leaf expansion rate (under well-watered conditions) and WUE (Fig. 3-10E and F). Additionally, analysis of five *Arabidopsis* accessions in progressive drought displayed a weak positive correlation between rosette size or maximum leaf expansion rate (under well-watered conditions) and WUE (at the end of progressive drought) rather than a negative correlation (see Fig. 3-28C and D). Taken together, these results suggest that the growth and WUE are not tightly linked, and selection of high WUE does not necessarily lead to reduced growth.

The association between WUE and yield is also intangible (Blum, 2009). Their

relationship can be negative (Matus *et al.*, 1996), positive (Morgan *et al.*, 1993; Sayre *et al.*, 1995; White *et al.*, 1990) or uncorrelated (Monneveux *et al.*, 2007), depending on the species and the environment. In this study, analysis of final above-ground biomass production and WUE of either RCAR overexpressing lines or Arabidopsis accessions displayed a positive correlation in the progressive drought experiments (Fig. 3-10A; Fig. 3-28B). However, in deficit irrigation, RCAR6-3 and RCAR10-4 lines as well as Col-0 plants displayed enhanced WUE with maintained growth under 40% SWC than that of 60% SWC, while those grown under 20% SWC had enhanced WUE but reduced biomass (Fig. 3-24E and F). These results indicate the elusive relationship between biomass and WUE in Arabidopsis, depending on the drought scenarios.

Tardieu (2011) has suggested that plants may benefit from certain genes in one drought scenario, but not in others. For example, genes which confer on plants high WUE may be an advantage in terminal drought, such as progressive drought stress, but not in mild drought stress. However, the results of RCAR6-3 grown under deficit irrigation do not fully support this insight. RCAR6-3 has been shown to generate more biomass and achieve higher WUE in progressive drought compared with Col-0 grown (Fig. 3-7E and F). Under deficit irrigation with 40% SWC (mild drought stress), RCAR6-3 consumed 50% less water and exhibited 70% higher WUE, but it generated comparable final dry biomass compared with Col-0 under the same conditions (Fig. 3-24E and F). These results indicate that the RCAR6 gene is able to confer on plants enhanced WUE with no or minor trade-offs in growth or yield production, not only in terminal drought stress conditions but also in mild drought stress conditions.

### **The enhanced WUE occurs in the early stage of progressive drought**

Both gravimetric-derived WUE and  $\Delta^{13}\text{C}$ -derived WUE provide an integrated measure of WUE in a progressive drought. However, these results do not give information regarding temporal changes of WUE during a progressive drought, which would facilitate an understanding of when overexpression lines and Col-0 differ most with regard to WUE. Changes in leaf area in response to consumed water indicate that the overexpression lines of RCAR1, RCAR6 and RCAR10 exhibited a higher leaf area compared to Col-0 when consuming the same amount of water (Fig. 3-11A, C, E),

which indicates enhanced leaf-area-derived integrative WUE during the course of progressive drought. The data also imply that the advantage of WUE in RCAR lines appears to occur in the early stages of progressive drought, when e.g. 20 g water is consumed (Fig. 3-11A, C, E). Furthermore, the gas exchange analysis in well-watered conditions revealed that RCAR6-3 and RCAR10-4 lines achieved an almost two-fold enhancement of insWUE when compared to Col-0 (Fig. 3-12A-C), but reducing soil water content attenuated this advantage (Fig. 3-13C). These results suggest a higher WUE at the early growth stage, especially the well-watered phase of progressive drought. This conclusion is consistent with the fact that an improvement of yield in wheat was achieved by selection for high WUE in semi-arid area of Australia, owing to that plants had high WUE and grew under stored moisture conditions could control their water use during the earlier part of the growing season so as to avoid the water deficit in the reproductive stage (Condon *et al.*, 2002; Blum, 2009).

### **The dominant role of shoot part in regulating WUE**

Activation of ABA signaling has been demonstrated to mediate not only the short-term stomatal movement, but also the long-term growth of plants (Raghavendra *et al.*, 2010). These long-term adjustments include osmoregulation at the whole plant level, photosynthetic adjustments, and root-specific responses such as the stimulation of root growth for exploring soil moisture (Sharp and Davies, 1985) or the enhancement of the root hydraulic conductivity (Sharipova *et al.*, 2016). Results of the grafting experiment reveal a dominant role of shoot parts in regulating plants' leaf temperature and WUE, but the contribution of the root cannot be excluded owing to the fact that grafts with RCAR10-4 roots had a tentative increase in  $\Delta^{13}\text{C}$ -derived WUE (Fig. 3-19A and B).

At a constant humidity condition, the elevated leaf temperature in transgenic lines is caused by a lower transpiration rate, which could be the consequence of either reduced stomatal opening (stomatal movement), lower stomatal density or smaller size of stomata (stomatal development). Components in ABA signaling are known to control the opening and closing responses of the stomatal aperture (Merlot *et al.*, 2001; Mustilli *et al.*, 2002; Pizzio *et al.*, 2013a; Vahisalu, Kollist, Wang, Nishimura, Chan, Valerio, Lamminmaki *et al.*, 2008). In terms of stomatal development, overexpression RCAR10 lines have been reported to have less dense stomata when

compared with wild type Col (Pizzio *et al.*, 2013a). However, in this study, three independent experiments did not provide a consensus on the effect of overexpressing RCARs on stomatal density and size because leaves with a higher stomatal density tended to possess a smaller stomatal size, and leaves with lower stomatal density tended to have a larger stomatal size (Fig. 3-25A-D, F and G). These results suggest that overexpressing RCARs may affect the stomatal development, while also regulating the relationship between stomatal density and stomatal size. In addition, the compensation effect of stomatal density and size again supports the role of stomatal movement in mediating plants' leaf temperature, transpiration rate, and WUE.

### Physiological basis of enhanced WUE and maintained growth

WUE is defined as the ratio of  $A_n$  to  $g_s$  (insWUE) transiently, the ratio of biomass to transpiration in a plant (gravimetric-derived WUE) over some weeks or the ratio of yield to input water in a field over a crop cycle (economic WUE) (Morison *et al.*, 2008). Enhanced WUE, according to its definition, can be achieved through either an increase of the nominator, decrease of the denominator or a less decline in the nominator than in the denominator. In this study, enhanced WUE of RCAR6-3 and RCAR10-4 grown at a photon flux density of  $150 \mu\text{mol m}^{-2} \text{s}^{-1}$  and under well-watered conditions (Fig. 3-12A-C) is caused by reduced  $g_s$  and maintained  $A_n$ . Similar results were also observed in Arabidopsis accessions Col-0 and Cvi-0, in which stomatal conductance of Cvi-0 was reduced by 50%, while the  $A_n$  was maintained (Fig. 3-31A-C). The maintained  $A_n$  can be explained by Fick's diffusion law (See Equation 6 in Materials and Methods). This law implies that the reduced stomatal conductance can be fully or partially compensated by the enhanced  $\text{CO}_2$  gradient between the ambient atmosphere and intercellular space. However, the intercellular space is not the destination of the  $\text{CO}_2$ . It would further diffuse from intercellular space into the site of carboxylation, and finally, be assimilated to carbohydrates. Similarly, according to Fick's diffusion law, the  $\text{CO}_2$  flux can be written as:

$$A_n = (C_a - C_c) \cdot [1/(1/g_s + (1/g_m))] \quad (20)$$

where the  $A_n$  depends upon the  $\text{CO}_2$  gradient between the atmosphere and chloroplast as well as the total  $\text{CO}_2$  conductance along its diffusion paths. Estimation

of  $g_m$  in two independent experiments through constant J method and curve fitting method support a comparable value among RCAR6-3, RCAR10-4 and Col-0 (Table 3-1; Table 3-2). This is currently the first study to investigate mesophyll conductance in plants manipulating ABA receptors. Flexas *et al.* (2013) have examined the mesophyll conductance in ABA-insensitive and hypersensitive mutants, and the results have indicated that the mutants do not differ from wild type Col in  $g_m$ . The estimated  $C_c$  according to Fick's diffusion law (see Equation 7 in section 2.2.9.2) exhibited a lower value for RCAR6-3 and RCAR10-4 than Col-0 (Fig. 3-15C; Fig. 3-17C). Taken together, the gas exchange measurement displayed in Fig. 3-15 explains that the relatively lesser reduction in  $A_n$  than in total CO<sub>2</sub> conductance for RCAR6-3 is due to the partial compensation of reduced CO<sub>2</sub> conductance by the increased CO<sub>2</sub> gradient. An independent gas exchange measurement displayed in Fig. 3-17 explains that the comparable  $A_n$  and reduced total conductance for RCAR6-3 and RCAR10-4 are due to the full compensation of reduced CO<sub>2</sub> conductance by the increased CO<sub>2</sub> gradient (Fig. 3-17A-C). The varying degrees of compensation of  $g_s$  by  $C_a - C_c$  in these two experiments might be caused by the age of the leaf. It has been reported that the photosynthetic capacity of a leaf displays often a linear, decline after full expansion (Kitajima *et al.*, 1997a; Koike, 1988). This decline leads to a less demand for CO<sub>2</sub>, and therefore, a reduced CO<sub>2</sub> gradient which may explain the partial compensation to reduced  $g_s$  in old leaves of the RCAR6-3 line. The online measurement reveals that RCAR6-3 had a reduced  $A_n$  and  $g_m$  than Col-0 (Fig. 3-18A and B), which is different from the results using the other two methods. However, RCAR6-3 still displayed enhanced WUE (Fig. 3-18A-D). Taken together, in most cases, the reduced CO<sub>2</sub> conductance could be compensated or partially compensated by an enhanced CO<sub>2</sub> gradient, resulting in comparable  $A_n$  and therefore, an enhancement of WUE.

### **ABA receptors conferred advantage in yield potential depends on the light regime**

Yield potential refers to the yield of a crop cultivar when grown in environments to which it is adapted, when nutrients and water are not limiting and when pests and diseases are effectively controlled (Evans and Fischer, 1999). Enhanced WUE is considered to be associated with trade-offs in yield potential (Blum, 2005). In this study, at a photon flux density of 150  $\mu\text{mol m}^{-2} \text{s}^{-1}$  and well-watered conditions, RCAR6-3 and RCAR10-4 lines, which have been shown to possess 40% higher WUE

than Col-0, displayed no or little decrease in total biomass after four months of growth (Fig. 3-21A and B). However, RCAR6-3 lines grown at the photon flux density of  $900 \mu\text{mol m}^{-2} \text{s}^{-1}$  and well-watered conditions exhibited a 9% increase in WUE with an 18% reduction in biomass compared with Col-0 (Fig. 3-22C and E). The diminished benefit in WUE under the high photon flux density than that under low photon flux density is attributed to a more demand for  $\text{CO}_2$  at high light condition and as such, form a steeper  $\text{CO}_2$  gradient between the atmosphere and chloroplast. As a consequence, the  $C_a - C_c$  of RCAR6-3 may not differ too much from Col-0, but the  $g_s$  may still be lower, therefore resulting in a reduced  $A_n$ . In addition, these results may also partially explain the low rate of success when applying high WUE genes from the lab to the field. Crops grown in the field generally experience full sunlight which equals more than a photon flux density of  $2000 \mu\text{mol m}^{-2} \text{s}^{-1}$ , while the experiments conducted in the greenhouse or growth cabinet are typically controlled at the non-saturated photon flux density range. The high WUE conferred by certain genes under this condition may fail to be more water productive in field conditions.

### Natural variation of WUE in Arabidopsis

Naturally occurring variations in WUE within a single species are the result of interactions between plants and their living environments and are valuable resources for improving plants' WUE (Assmann, 2013). Ten Arabidopsis accessions were evaluated in this study by measuring their leaf temperatures, growth and gas exchange. Among these accessions, Cvi-0 plants displayed lower leaf temperature in both well-watered conditions and mild-stress conditions, but the difference was attenuated when accompanied with the severity of drought (Fig. 3-26; Fig. 3-29; Fig. 3-33; Fig. 3-34). The cooler leaf temperature of Cvi-0 is correlated to its almost two-fold higher stomatal conductance when compared to Col-0. The higher stomatal conductance of Cvi-0 was also reported by (Monda *et al.*, 2011), and this increase has been associated with a more open stomatal aperture. Consistent with Mondain's results, Cvi-0, in this study, also had a more open stomatal aperture (Fig. 3-33D), which may partially be attributed to its larger stomata size (Fig. 3-33F). The natural variations in leaf temperature were also found in Arabidopsis accessions Van-0 and RLD-0. The former displayed a lower leaf temperature under well-watered conditions, while the latter exhibited elevated leaf temperature under mild-stress conditions (Fig. 3-26A-B; Fig. 3-29A-B). According to our knowledge, this is the first investigation

conducted concerning the natural variations of leaf temperature in Arabidopsis. Accessions showing variations in leaf temperature were also more variable in leaf growth and biomass accumulation. The cool leaf temperature accessions - Cvi-0 and Van-0 - had lower and comparable leaf area, respectively, when compared with Col-0 under well-watered conditions (Fig. 3-26A and C). However, both accumulated less biomass at the end of the progressive drought (Fig. 3--26C; Fig. 3-27E). The "hot" accession RLD-0 generated more biomass at the end of progressive drought (Fig. 3-29 E). All accessions depleted all accessible water within the soil and as such, exhibited lower WUE for Cvi-0 and Van-0 (Fig. 3-27 F) and higher WUE for RLD-0 (Fig. 3-29 F). Taken together, three accessions of Arabidopsis indicated more variation in leaf temperature, leaf growth, biomass, and WUE. Water use efficiency of Cvi-0 has been investigated in several studies, and has been shown to discriminate more  $^{13}\text{C}$  and have less WUE than common used accessions (Des Marais *et al.*, 2014; Juenger *et al.*, 2005; Masle *et al.*, 2005; Mckay *et al.*, 2003), while accession Van-0 has not yet been reported on. The Russian accession - rld-2 - has been investigated by Mckay *et al.* (2003), but it is doubtful that they used the same RLD-0 accession as was used in this study because their rld-2 line showed a similar WUE to Cvi-0 owing to a similar  $\delta^{13}\text{C}$  value, while our results displayed a higher WUE of RLD-0 than that of Cvi-0 in a progressive drought experiment (Fig. 3-29F).

In order to adapt to challenging environmental conditions, plants need to coordinate the relationship between growth and survival, which involves complex processes and generates simultaneous variations of different traits (Juenger, 2013). The study regarding the variation of a single trait is relatively straightforward. For example, investigating the variation of WUE through either a gravimetric method (the ratio between dry biomass to consumed water), or a gas exchange measurement (the ratio between net carbon assimilation rate to stomatal conductance), or carbon isotope discrimination help explore the varieties with enhanced WUE within species (Medrano, 2002; Ranney *et al.*, 1991; Rizza *et al.*, 2012; Wall *et al.*, 2001). However, the responses of plants are not quite as simple because the variations of certain traits may associate with the variations of other traits (Juenger, 2013). The advantages of selecting a single trait may be offset by other traits which are negatively related (Mckay *et al.*, 2003). Mckay *et al.* (2003) have found a positive correlation between WUE and flowering time. Turner *et al.* (2001) have pointed out



that yield is generally positively correlated with the length of crop duration and a reduction of crop duration leads to a loss of yield. A negative correlation between WUE and carbon isotope discrimination as well as positive association between carbon isotope discrimination and yield were also found in various crops under different growth conditions (Hall *et al.*, 1994; Matus *et al.*, 1995; Monneveux *et al.*, 2007; Morgan *et al.*, 1993; Ngugi *et al.*, 1993; Saranga *et al.*, 2004). In this study, a strong positive correlation between leaf temperature under well-watered conditions and WUE at the end of progressive drought was found in the *Arabidopsis* accessions (Fig. 3-28A). Cool leaf temperature accessions exhibited low WUE and hot leaf temperature accessions displayed high WUE (Fig. 3-28A). Moreover, WUE is positively correlated with final above-ground dry biomass (Fig. 3-28B), which is due to the fact that all of the plants consumed the same amount of water. Therefore, high WUE accessions generate more biomass and low WUE accessions generate less. This insight has proven to be successful in rain-fed Mediterranean-type agricultural settings where most of the precipitation occurs prior to growing season (Des Marais *et al.*, 2016). When accompanied by less rainfall afterward, varieties with high WUE achieved high yield and varieties with low WUE achieved less yield. A number of studies claim that the advantages of yield decrease as rainfall increases because plants with high WUE generally grow more slowly than plants with low WUE (Des Marais *et al.*, 2016; Juenger, 2013). However, our results do not support this finding. Leaf area, or maximum leaf expansion rate, under well-watered conditions displays a weak positive association with WUE at the end of a progressive drought (Fig. 3-28C and D). In comparison with Cvi-0, other *Arabidopsis* accessions which displayed higher WUE had larger leaf area and faster leaf expansion rate under well-watered conditions (Fig. 3-26C; Fig. 3-27B, C and F; Fig. 3-28C and D). These results suggest that high WUE is not tightly linked reduced growth. Therefore, an indirect selection of both leaf temperature and leaf growth under well-watered conditions (less time-consuming than other methods) may facilitate to find the varieties and identify the genes which combine enhanced WUE with increased growth or yield, and further help uncover the possible mechanisms and translate the insight - "more crop per drop" - into field (Fig. 3-4; Fig. 3-28E and F).

## **Physiological and molecular basis of enhanced WUE in *Arabidopsis* accessions**

The genetic variations of leaf temperature are implications that certain QTLs contribute to these variations. Analysis of RILs and F2 populations derived from Col-0 and Cvi-0 revealed that a single QTL - MPK12 - can explain their genetic variation in leaf temperature (Fig. 3-24A; Fig. 3-25A and B; Fig. 3-26A-C). Earlier results from Des Marais et al. (Des Marais *et al.*, 2014) have indicated that MPK12 is one of five QTLs which is able to explain the variation of  $\delta^{13}\text{C}$  (positively correlated with WUE) between Arabidopsis accession Ler and Cvi, and Ler-MPK12 allele confers on NIL-delta2.1 plants (near isogenic line containing a small introgression from the Cvi genome in a Ler background) higher WUE after 20 days of growth under well-watered conditions. However, their study did not rule out that the correlation between WUE and plants' growth. In this study, a progressive drought analysis revealed that *mpk12* loss of function mutant in Col background had a cooler leaf temperature, smaller leaf area under well-watered conditions, less dry biomass and lower WUE at the end of the drought when compared with Col-0 (Fig. 3-42A-F). Similarly, Cvi<sup>MPK12</sup> plants exhibited hotter leaf temperature, larger leaf area under well-watered conditions, more biomass and higher WUE at the end of the drought when compared with Cvi-0 (Fig. 3-42A-F). These results are consistent with the associations among leaf temperature, leaf growth, biomass and WUE in different Arabidopsis accessions, and document the role of MPK12 in controlling plants' growth and WUE.

The physiological basis of less WUE is that the Cvi MPK12 allele is less responsive to ABA-mediated inhibition of stomatal opening and is more responsive to short-term changes in VPD, and it also confers plants with constitutively larger stomata (Des Marais *et al.*, 2014). Similarly, the 1.3-fold larger stomata size of Cvi-0 was also observed in comparison to Col-0 in this study (Fig. 3-33F). However, this could not fully explain the 1.7-fold higher stomatal conductance of Cvi-0 (Fig. 3-33C). The full compensation needs to take the stomatal aperture into account, although a larger stomatal aperture may be partially attributed to the increased stomatal size (Fig. 3-33D). Since the temperature difference between Col-0 and Cvi-0 is similar to that between Col-0 and *mpk12* mutant, or Cvi-0 and Cvi<sup>MPK12</sup> transgenic lines, I speculate that the larger stomatal size may also not fully explain the variations in stomatal conductance among these lines. Moreover, the lower WUE of lines containing the MPK12 Cvi allele may also be partially attributed to the higher nighttime stomatal

opening, since water loss at night is not accompanied by carbon gain (Fig. 3-48A and B; Table 3-6).

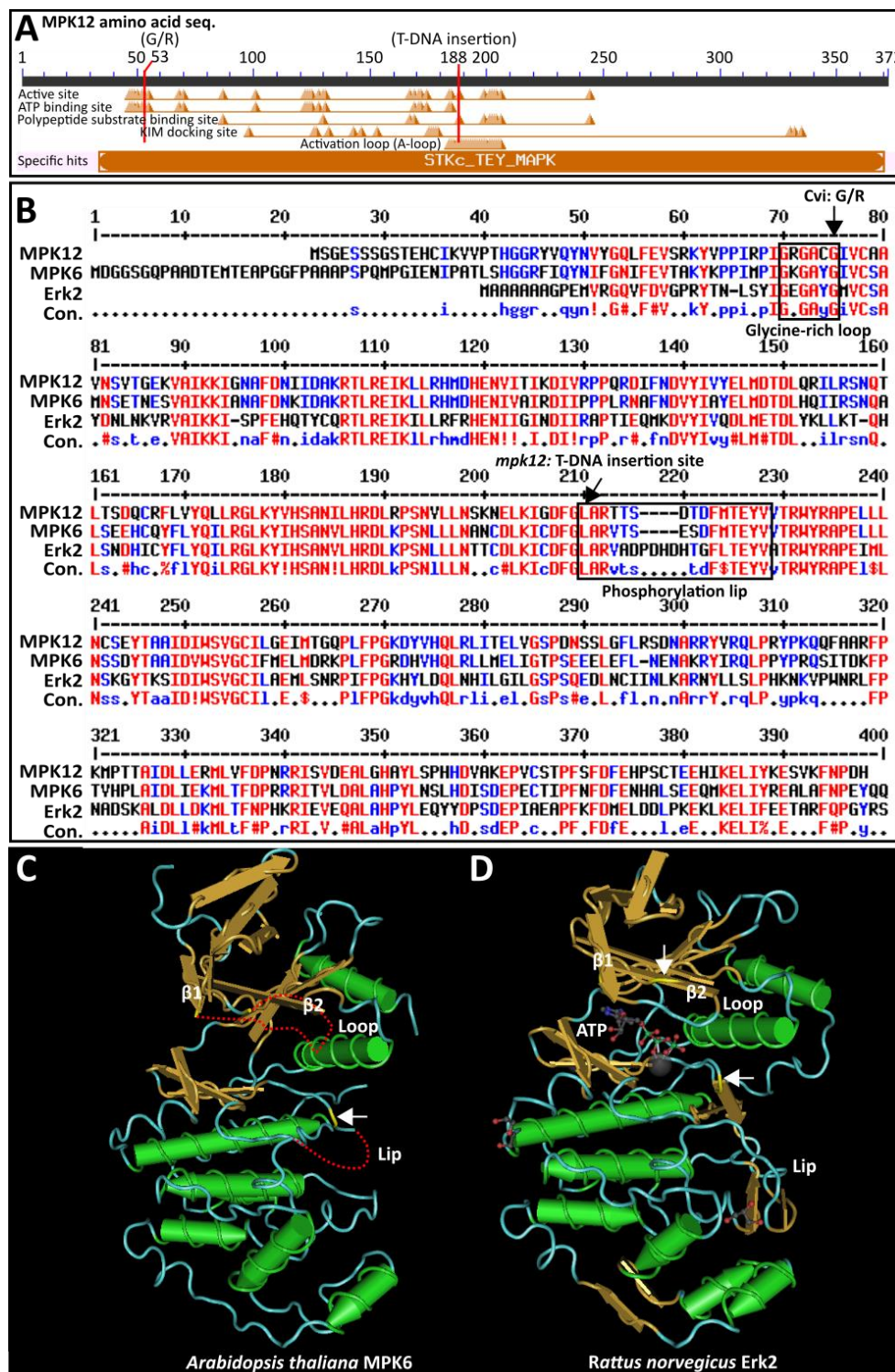


Figure 4-1 Protein structure of MPK12 homologous. A) The predicted conserved domain of MPK12 using the NCBI online tool. The orange peaks indicate hits of amino acid residuals in the functional region of the protein. The red lines indicate the positions of substitution from glycine to arginine in Cvi MPK12 allele and T-DNA insertion site of knockout mutant *mpk12*. B)

Amino acid alignment of Arabidopsis MPK12, MPK6 and Rattus Erk2. The glycine-rich loop and phosphorylation lip are highlighted in the black frames. The positions of substitution from glycine to arginine in Cvi MPK12 allele and T-DNA insertion site of knockout mutant *mpk12* are indicated by arrows. Texts on the left side indicate either name of accessions or names of MPKs, and "Con." means consensus sequence. Numbers in the picture are the position of amino acid residuals. Red represents a high consensus value (90%) while blue (between 50% and 90%) and black (lower than 50%) indicate lower consensus. C) The protein structure of *Arabidopsis thaliana* MPK6 and *Rattus norvegicus* Erk2. The missing parts are indicated by the red dotted lines. The  $\beta$ 1, glycine-rich loop,  $\beta$ 2 structure, phosphorylation lip and ATP molecule are highlighted in both MPK6 and Erk2. The white arrows indicate either the position of substitution from glycine to arginine in Cvi MPK12 allele or the T-DNA insertion site of knockout mutant *mpk12*. The protein structure is downloaded from Cn3D macromolecular structure viewer (<https://www.ncbi.nlm.nih.gov/Structure/CN3D/cn3d.shtml>).

Conserve domain prediction of MPK12 using the NCBI conserved domain online tool displayed an STKc\_TFY\_MAPK conserved domain of MPK12 protein ranging from amino acid residual 35 to residual 372 (Fig. 4-1A). The single substitution from glycine to arginine at residue 53 in accession Cvi-0 falls into the ATP binding site, and T-DNA insertion site of *mpk12* knockout mutant occurs at the activation loop of the MPK12 protein (Fig. 4-1A). Until recently, Wang *et al.* (2016) solved the first plant's MAP kinase structure using MPK6. The predicted secondary structure displayed that the residual 53 lies between  $\beta$ 1 and  $\beta$ 2, and the *mpk12* mutant insertion site lies between  $\beta$ 8 and  $\beta$ 9 which is close to the activation loop (Wang *et al.*, 2016) (Fig. 4-1B). The crystal structure of the Arabidopsis MPK6 protein indicates that the single substitution from glycine to arginine occurs at the glycine-rich loop, which is reported to be a part of ATP binding pocket (Wang *et al.*, 2016) (Fig. 4-1B-D). In MPK6, glycine-rich loop together with  $\beta$ 1 and  $\beta$ 2, form a  $\beta$ -L- $\beta$  structure with which  $\alpha$ C,  $\alpha$ D, L5, L7,  $\beta$  7,  $\beta$  8, DFG motif in L12 and Lys92 in  $\beta$ 3 form an ATP binding pocket (Wang *et al.*, 2016). (Huse and Kuriyan, 2002) have reported that the glycine-rich loop plays an important role in binding and orienting ATP or its derivatives in many protein kinases. Alignments of all MPKs from Arabidopsis Col-0 (Fig. 3-41B) and other available organisms (data not shown) revealed that the substitution with arginine is unique for Cvi-0. In addition, most kinases are activated by phosphorylation of specific residues in the phosphorylation lip. Insertion of the T-DNA in the phosphorylation lip of MPK12 affects its activation. Jammes *et al.* (2009) have demonstrated that MPK12 acts as a positive regulator of ABA signaling in guard cells, and revealed that ABA and H<sub>2</sub>O<sub>2</sub> are able to enhance the kinase activity of MPK12. Therefore, the unique amino acid substitution at the glycine loop in Cvi-0 or T-DNA

insertion at the phosphorylation lip in Col-0 may interrupt the phosphorelay to the substrate, therefore affecting the signal transduction and finally, affecting physiological responses.

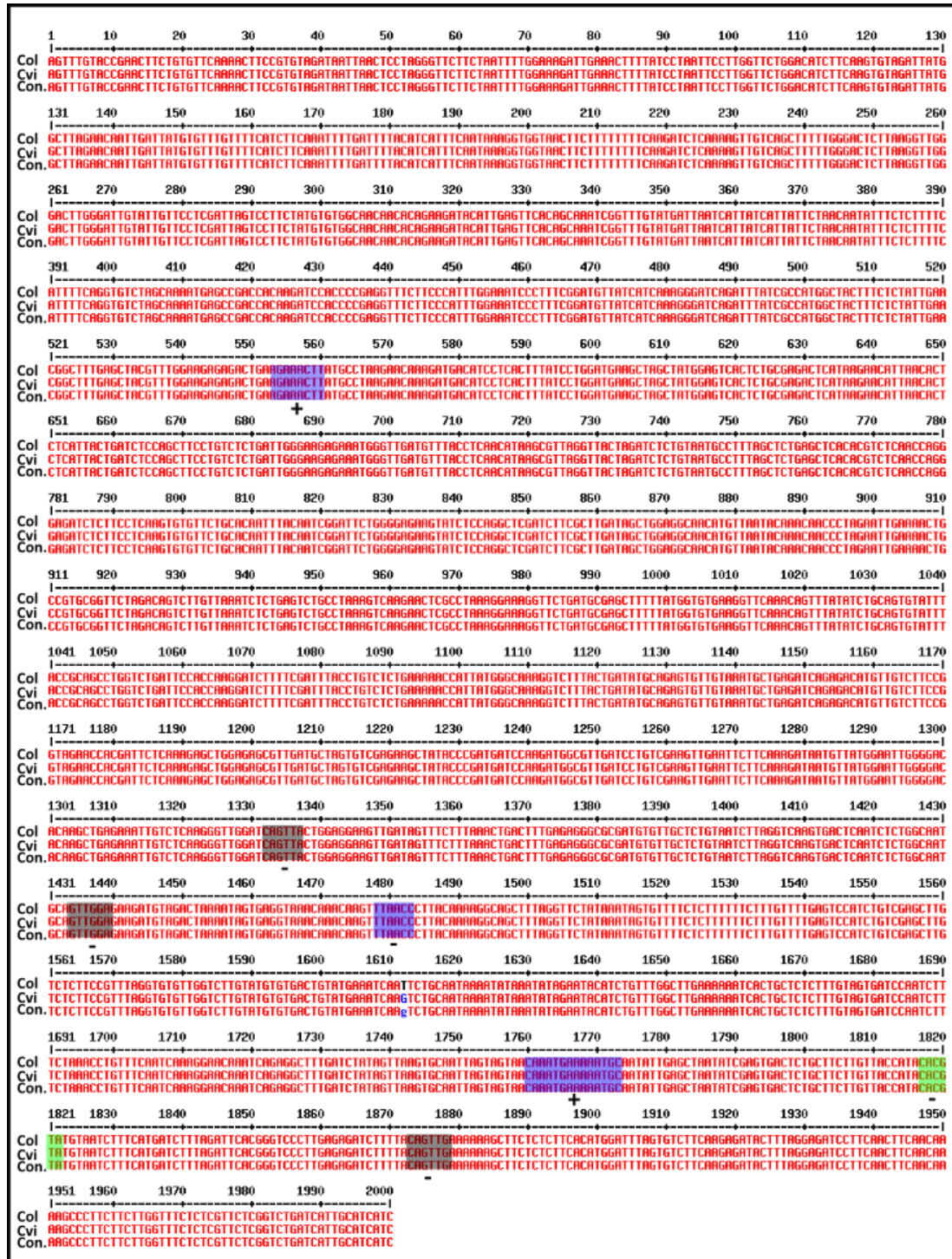


Figure 4-2 Alignment of the promoter sequence in *Col* and *Cvi*. Text on the left displays the name of the corresponding nucleotide sequence and "Con." means consensi sequence. Numbers in the picture indicate the position of nucleotide. The red color represents a high consensus value (90%) while blue represents a middle

value (between 50% and 90%) and black a low consensus value (lower than 50%). Colored boxes are predicted elements in the promoter region. The functional analysis on promoter was done using the Plant Care database.

The MPK12 gene is highly expressed in guard cells (Jammes *et al.*, 2009), which is consistent with its role in regulating plants' stomatal conductance and leaf temperature. The alignment of the artificially defined promoter of MPK12 (2 kb upstream of ATG) between Col and Cvi indicated a T to G mutation at the 1621 bp (Fig. 4-2). A promoter analysis using the PlantCARE online tool (<http://bioinformatics.psb.ugent.be/webtools/plantcare/html/>) indicated three light response elements (blue box), one ABA response element (green box) and three drought inducible elements (gray box) located within the 2 Kb promoter region (Fig. 4-2). The single mutation does not fall into any of these boxes, implying that the leaf temperature variation between Arabidopsis accessions Col-0 and Cvi-0 may not be caused by the difference in their promoter. In addition, the predicted elements in promoter region infer the role of the MPK12 gene in response to light, ABA and drought. Indeed, MPK12 has been reported to be involved in ABA-induced stomatal closure, and the impairment of stomatal closure needs both nonfunctional MPK9 and MPK12 due to a redundancy (Jammes *et al.*, 2009). Des Marais *et al.* (2014) have found that lines homozygous for Cvi MPK12 allele were less responsive to ABA-induced inhibition of stomatal opening and more responsive to short-term changes in VPD. In this study, the MPK12 gene is capable of regulating plants' WUE in progressive drought. The knockout mutant *mpk12* in Col-0 background displayed reduced WUE in progressive drought when compared with Col-0, and the transgenic lines Cvi<sub>MPK12</sub> exhibited enhanced WUE than Cvi-0 (Fig. 3-42F).

### **Nighttime stomatal opening**

Gas exchange between plants and atmosphere mainly occurs through stomatal pores at the lower epidermis of a leaf. During the day, for C3 plants, light induces stomatal opening (Roelfsema and Hedrich, 2005), facilitating CO<sub>2</sub> influx into the site of carboxylation in order to form carbohydrates and support life activities. Meanwhile, the H<sub>2</sub>O efflux into the atmosphere removes the excess energy heating the leaf (Gates, 1968). At night, there is no demand for either CO<sub>2</sub> for photosynthesis or H<sub>2</sub>O for cooling the plants and as such, the stomata are supposed to be closed. However, the incomplete stomatal closure has been reported to be a widespread phenomenon

among different species, with the nighttime stomatal conductance ( $g_{s-night}$ ) values varying from 5% to 30% of their daytime stomatal conductance ( $g_{s-day}$ ) depending upon the species and ambient conditions (Caird *et al.*, 2007). A three-fold difference in nighttime stomatal conductance among *Arabidopsis* accessions has also been reported (Christman *et al.*, 2008). In this study, nighttime stomatal opening was confirmed by measuring gas exchange at night using *Arabidopsis* accessions Col-0 and Cvi-0, and is consistent with the results reported by Christman *et al.* (2008), and Cvi-0 exhibited a 1.8-fold higher  $g_{s-night}$  than Col-0 (Fig. 3-45A and Table 3-4). Further analysis of  $g_{s-night}$  in Col x Cvi F1 hybrid and a Col x Cvi RIL population reveals that low  $g_{s-night}$  of Col-0 is a dominant trait, and a single QTL at the end of chromosome two is able to explain the variation in  $g_{s-night}$  of RILs (Fig. 3-45A; Fig. 3-46A; and Table 3-4). Coincidentally, the MPK12 gene identified as regulating the leaf temperature of plants is situated at this genomic region. It has been reported that *Arabidopsis* accessions with a higher  $g_{s-night}$  also display greater  $g_{night}$ , and selection of high  $g_{s-day}$  may lead to an indirect selection of high  $g_{s-night}$  (Christman *et al.*, 2008). Thus, the Cvi-0 plants transformed with the Col MPK12 allele were used to perform gas exchange during the night, and displayed a lower  $g_{s-night}$  than Cvi-0 plants. These results reveal that the MPK12 gene is able to regulate  $g_{s-night}$  as well as  $g_{s-day}$ .

The implications of nighttime stomatal opening have been concluded by (Caird *et al.*, 2007), who suggest nighttime stomatal opening may: (1) facilitate the root nutrition uptake of plants at night; (2) avoid water loss from the roots to dry areas of the soil along the water potential gradient at night; (3) allows plants to have a higher potential for early morning carbon assimilation, when temperatures and VPD are low. These integrated effects of nighttime water use, nighttime nutrition uptake and remobilization imply the indirect effect of nighttime stomatal opening on plant growth (Caird *et al.*, 2007). However, it is important to note that water loss at night is not accompanied by carbon gain. If there is no clear growth benefit from nighttime stomatal opening, reducing nighttime water loss through stomatal pores may be a way to increase plants' WUE, especially for species with high  $g_{s-night}$ .

## Stomatal oscillation

The phenomenon of autonomic, cyclic, opening and closing movements of the

stomata have been described in the past as either cyclic variation in the stomatal aperture or stomatal oscillation (Barrs, 1971; Cowan, 1972). This phenomenon is widespread in different plant species (Barrs, 1971; Barrs and Klepper, 1968; Caird *et al.*, 2007; Cardon *et al.*, 1994; Farquhar and Cowan, 1974; Teoh and Palmer, 1971). It has been suggested that stomatal oscillation is the result of positive feedback responses of the stomatal apertures to changes in ambient conditions, such as light and temperature, as well as negative feedback responses to alternations of the plant-water potential (Cowan, 1972; Raschke, 1970). In this study, the occurrence of stomatal oscillation was always in the morning when illumination was supplied stepwise and temperature increased in half an hour. Switching on the light in the morning induces stomatal opening and the increased temperature promoted a steep increase in VPD (Fig. 3-43F and Fig. 3-48F), which drives the water to escape from plants through the stomatal pores. However, an over abundance of open stomata (always the first peak in an oscillation event) results in water loss which exceeds the water supply from the roots under well-watered conditions, possibly owing to appreciable resistances to water flow within the plant (Skidmore and Stone, 1964). As a result, the water potential decreases in guard cells followed by a reduced turgor, resulting in partial stomatal closure. The reduced transpiration rate leads to a recovery of water potential and turgor in guard cells, and as a result, the stomata reopen. This opening and closing processes occur repeatedly until the stomatal pores achieve optimum size for balancing the speed of water loss and water uptake. However, there were two cases that no oscillation was observed in the morning (Fig. 3-49H and I). This may not mean that there was no oscillation occurring in response to the changing environments, but the oscillations of stomata were not synchronized.

The period of oscillation found in this study was between 20 min to 30 min, which is in accordance with the reported range of 10 to 50 minutes (Barrs, 1971; Barrs and Klepper, 1968; Caird *et al.*, 2007; Cardon *et al.*, 1994; Farquhar and Cowan, 1974; Teoh and Palmer, 1971). The analysis of variations in the oscillation period (the period of the first cycle) reveals a period of 20 min and 30 min for Col-0 and Cvi-0, respectively. Further analysis of the oscillation period exhibited a 20 min period for the Col x Cvi F1 hybrid, implying a dominant effect of Col alleles. Aligning genotypes of RILs according to the phenotype of the oscillation period revealed two possible QTLs which may explain variations in the oscillation period. One of the loci is at the



end of chromosome two (the region responsible for variations of  $g_{day}$  and  $g_{night}$ ). This result indicates the possibility that there is a genetic association between leaf temperature or  $g_s$  and oscillation period. However, Cvi-0 plants homozygous for the MPK12 gene exhibited an unchanged oscillation period compared with Cvi-0 (Fig. 3-49A-I; Table 3-7), implying that MPK12 is not the gene responsible for variations in the oscillation period. Further research needs to be conducted in order to identify the genes responsible for stomatal oscillation. The implications of stomatal oscillation are rarely reported, but such findings may help stabilize at an optimum stomatal pore size for plants in order to achieve a plant water homeostasis according to the variable environmental cues.

## 5. Appendix

### Repetition progressive drought experiments using wild type Columbia

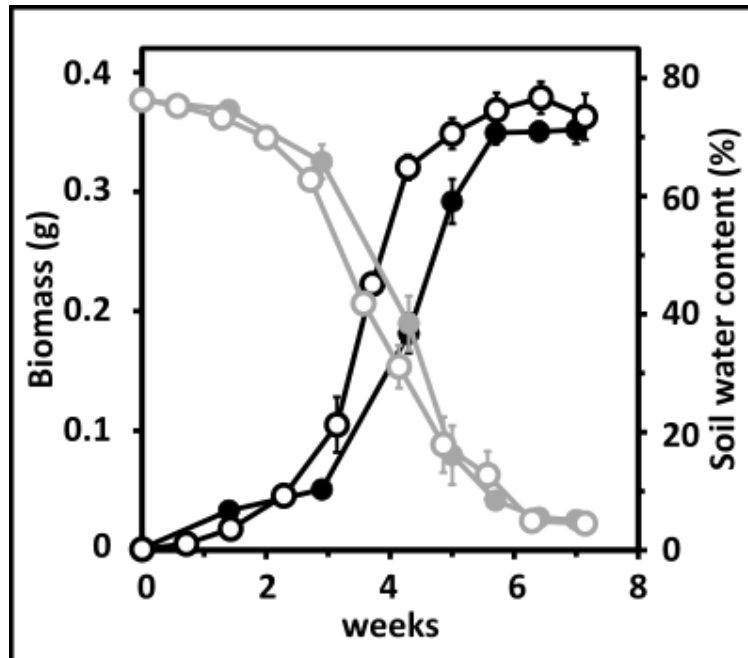


Figure 6-1 Biomass and water consumption in *Arabidopsis thaliana* wild type Columbia during progressive droughts. A) Changes in biomass in gram dry weight (filled black circles for the experiment I and open black circles for the experiment II) together with the soil water content (filled gray circles for the experiment I and open gray circles for experiment II). The approximate soil water content (SWC) was determined by the gravimetric method. All plants in two independent experiments were grown in an 8h light / 16h dark photoperiod at a photon flux density of  $150 \mu\text{mol m}^{-2} \text{s}^{-1}$  and  $22^\circ\text{C}$  and 50% relative humidity in the daytime and  $17^\circ\text{C}$  and 60% relative humidity at night. B)  $n=4$  biological replicates for each data point, mean  $\pm$  SEM.

## Repetition progressive drought experiments using lines overexpressing ABA receptors

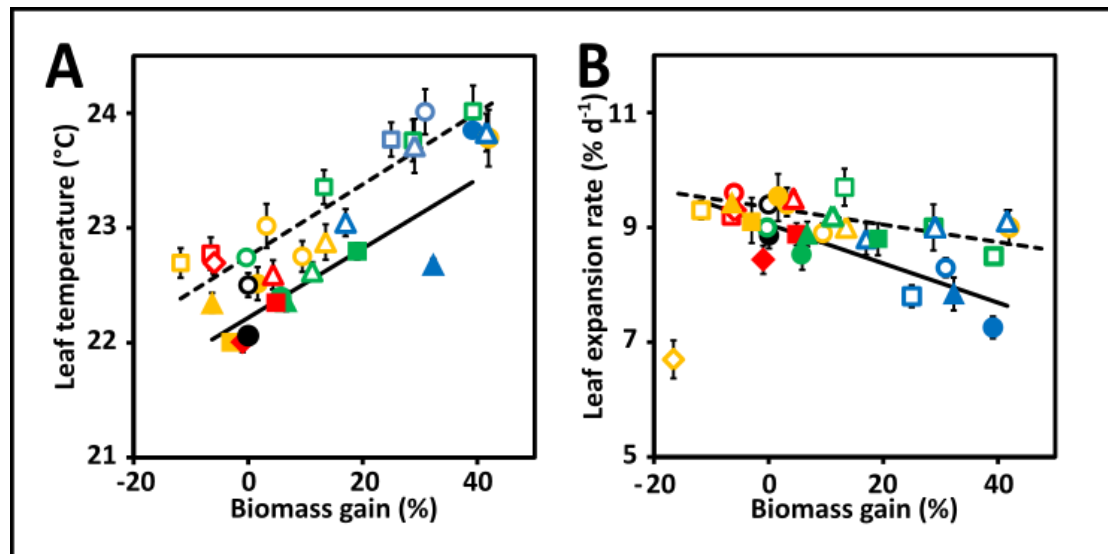


Figure 6-2 Water productivity conferred by ectopic expression of ABA receptors. A) Association of leaf temperature with biomass gain (percentage increase compared with Col). Col (filled circle) accumulated  $0.31 \text{ g} \pm 0.01 \text{ g}$  dry biomass and Col (open circle) accumulated  $0.34 \text{ g} \pm 0.01 \text{ g}$ . Biomass gain was set to 0% for Col. B) Association of leaf expansion rate with biomass gain. Open symbols are the data shown in Fig. 3-10. Filled symbols are the data from an independent experiment. Dotted fitted lines displayed a correlation coefficient of 0.91 ( $P < 0.001$ ) for the association between biomass gain and leaf temperature and of 0.001 ( $P = 0.98$ ) for the association between biomass gain and leaf expansion rate. Solid fitted lines displayed a correlation coefficient of 0.86 ( $P = 0.001$ ) for the association between biomass gain and leaf temperature and of 0.63 ( $P = 0.03$ ) for the association between biomass gain and leaf expansion rate. Growth conditions as described in Fig. 3-5.  $n=4$  biological replicates per data point, mean  $\pm$  SEM.

## Biomass increase of RCAR6-3 and RCAR10-4 in three independent experiments

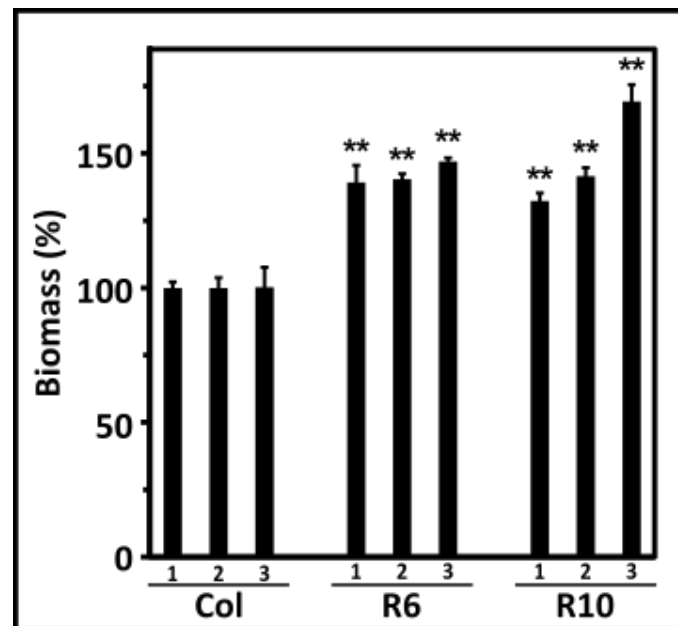


Figure 6-3 Biomass production during progressive droughts. RCAR6-3 (R6) and RCAR10-4 (R10) consistently had a higher biomass yield than Col-0 under progressively drying soil. The mean above-ground biomass of Col-0 was 0.31 g, 0.31 g, and 0.27 g in three independent experiments (numbered 1–3) and the yield of RCAR lines is expressed relative to Col-0. Growth conditions as described in Fig. 3-5.  $n=4$  biological replicates, mean  $\pm$  SEM, \*\* $P < 0.001$  compared with wild type.

## Primers used for identifying genes responsible for a cool leaf temperature trait

Table 5-1 Primers for identifying genes responsible for a "cool" leaf temperature trait.

Primer	Type	Nucleotide sequence (5'-3')	Nucleotide sequence (3'-5')	Annealing temperature	Note
nga168	SSLP	TCGTCTACTGCACTGCCG	GAGGACATGTATAGGAGCCTCG	54	-
c2_18001	CAPS	GTTTCAGCAGTTCCTGATCAATAC	GCTGATCCAGTAACTGTAGCTG	56	BsrDI
c2_18511	CAPS	CAA GAC TCC ATC ACA GCC ATT TG	CTT TGC CTA TTG GAG AGA ATT GAT G	55	XbaII
c2_18753	CAPS	ATA TTT CCA TGC AAC CAA CGC TAC	CAA GGC GTT TAC TTC TCG AAC AA	54	NlaIII
c2_18850	CAPS	GTA CGT GAG ACC TAT GTT CTA TGA	CCT CCA TGA AAT CTC TCC ACC	54	AhaIII
c2_18883	CAPS	GAA TCT TCC ATA GAG GCC ATC GTA G	GTA TAA TTG GAC TGG TTA CAG GCA GC	58	KpnI
c2_18950	CAPS	GAG CGC AAA GGC AGG ATT TTA CG	GAA AGA TGA GTC CCG TTG TAC AGC	57	HindIII
c2_19000	CAPS	GTC GAG AGG GAA CTC CAA CAA AAG	CTG TTT CCT TAA TCT TGA CCT TCT AGC	57	NheI
c2_19020	CAPS	CTC ATC AGC CTG TCT GTA TTA GCA G	CTT TGG CTT CTA CAT CCT GAA CC	57	BglII
c2_19050	CAPS	GAA TCA AAG TGG GCT GGA GCT G	GAG TTG CTT GTC TCC AGG TTT TGG	57	MaeII
c2_19145	CAPS	GTG GTT CAG GGA GCT ACC TAC	CAC CTT GCT TTC GCG TCT GC	56	HhaI
c2_19270	CAPS	CGT AAG TCC CAG AAT ACT AGC AAT ATC C	GAG GGG CTT CTG ACA CCT GTT G	58	EcoRV
c2_19350	CAPS	CAA ACA ATT CTC CAG CTA CTC GAG	GTG CCG TTT GAA GGA ATC AAG AAT G	56	MaeI
c2_19480	CAPS	CCA CTG CAA ATC ACT CGC TCC	GAA GCA ACG AAC GTG GTT AGG	55	HpaII
c2_19570	CAPS	CGG TTA ATC TCG GTA GCA TCC TC	CTC GCA TCA GAT AGT TGG ACT CAA G	57	NlaIII
c2_19680	CAPS	CTA GTC ACT TCT CTG ATG CCA C	GCA TGC ACC ATT CGA GAA TAG AG	55	EcoRV

## Primers used for identifying homozygous T-DNA insertion lines

Table 5-2 Primers for identifying homozygous T-DNA insertion lines.

Primer	Nucleotide sequence (5'-3')	Nucleotide sequence (3'-5')	Annealing temperature
AT2G45910	-	-	-
AT2G46070	CATGATTCGCCGGAGGTATGGCAGGC	GTAGAGAGCCTGCCGGCAAGCGAGGATGATC	57
AT2G46080	CTCGGCAGTCAGGAAGCCTGTTCGCTTGTAGGG	GAGGAGAGCTGGAAGGAAAGCTTGATGGCCTGAAG	57
AT2G46090	CAAGTGGGAGGGCGAGATGGGGAGAATGATAGTC	TCAGGCTGGATGTATGGTCGTATGGGCGACC	56
AT2G46140	GTCGACGGCTCGCGGGCAAGTTAGAGG	CTTGGTGGGCAGCTCGTTGGAGGGATGGTAAGG	57
AT2G46150	-	-	-
AT2G46250	GTTGGTGGGTGGCGTGAAGGCCAGGC	CTCGTGGGTCAGCTCGCACGACTGTCTGG	56
AT2G46280	-	-	-
AT2G46310	-	-	-
GK	ATATTGACCATCATACTCATTGC	-	-
SALK	GCGTGGACCGCTTGCTGCAACT	-	-

Table 5-3 Uniform primers for identifying homozygous T-DNA insertion lines.

Primer	Left border
GK	ATATTGACCATCATACTCATTGC
SALK	GCGTGGACCGCTTGCTGCAACT
SAIL	GCCTTTTCAGAAATGGATAAATAGCCTTGCTTCC

## Primers used for gene cloning

Table 5-4 Primers for cloning genes listed in Table 2-5.

Primer	Nucleotide sequence (5'-3')	Nucleotide sequence (3'-5')	Annealing temperature
AT2G45910	AAAAAGGCGCGCCCGTTCCTGAGGACCATCG	AAAAAGGCGCGCCCCTTTGCTTGGATCGAAGC	55
AT2G46070	AAAAAGGCGCGCCCGATGAAGAGTTTGTACCG	AAAAAGGCGCGCCCTCTCTATACAAAAGGC	55
AT2G46080	AAAAAGGCGCGCCCATCACTAACACAGGGGC	AAAAAGGCGCGCCGTCGGTACAACCTTGATGC	55
AT2G46090	AAAAAGGCGCGCCATCAAGCGAAGATCGAGC	AAAAAGGCGCGCCTGTGACGAAGTAGGATCG	55
AT2G46140	AAAAAGGCGCGCCAGTAGTTGAATGTAGTTGGC	AAAAAGGCGCGCCATTTGACTTTTTCGTCAACG	55
AT2G46150	AAAAAGGCGCGCCCTGATCTACTCTAACACCG	AAAAAGGCGCGCCTGTTTCGAGCCATGTAACG	55
AT2G46250	AAAAAGGCGCGCCCTAGTGAAGTCTCTGAAGC	AAAAAGGCGCGCCGAACCTCAAGTTAAGATTCC	55
AT2G46280	AAAAAGGCGCGCCATAACGGCGAGCGTCTTGGC	AAAAAGGCGCGCCGAAAGAGAACTTTTCCTCC	55
AT2G46310	AAAAAGGCGCGCCTGTTTGTGTAATGGTGGTGG	AAAAAGGCGCGCCACTGTTTTGCGTAGACATGG	55

## Strains used in this study

Table 5-5 Strains used in this study.

Strain list No.	Organism	Strain	Vector/Plasmid	Resistance
6143	Arabidopsis thaliana	C58pGV3101	<i>pBI121 pUbox :: Ubox</i>	Kan and Rif
6086	Arabidopsis thaliana	C58pGV3101	<i>pBI121 pMPK12 :: MPK12</i>	Kan and Rif
6089	Arabidopsis thaliana	C58pGV3101	<i>pBI121 pBYPASS :: BYPASS</i>	Kan and Rif
6087	Arabidopsis thaliana	C58pGV3101	<i>pBI121 pLcbk2 :: Lcbk2</i>	Kan and Rif
6071	Arabidopsis thaliana	C58pGV3101	<i>pBI121 pLEA1 :: LEA1</i>	Kan and Rif
6090	Arabidopsis thaliana	C58pGV3101	<i>pBI121 pLEA2 :: LEA2</i>	Kan and Rif
6088	Arabidopsis thaliana	C58pGV3101	<i>pBI121 pMyosinhc :: Myosinhc</i>	Kan and Rif
6144	Arabidopsis thaliana	C58pGV3101	<i>pBI121 pTRIP :: TRIP</i>	Kan and Rif
6072	Arabidopsis thaliana	C58pGV3101	<i>pBI121 pCRF5 :: CRF5</i>	Kan and Rif



## 6. References

- Abtew, W. and Melesse, A.M.** (2013) *Evaporation and evapotranspiration. Measurements and estimations / Wossenu Abtew, Assefa Melesse*. Dordrecht, London: Springer.
- Agrawal, G.K.** (2001) Screening of the Rice Viviparous Mutants Generated by Endogenous Retrotransposon Tos17 Insertion. Tagging of a Zeaxanthin Epoxidase Gene and a Novel OsTATC Gene. *PLANT PHYSIOLOGY*, 125, 1248–1257.
- Ahlfors, R., Macioszek, V., Rudd, J., Brosché, M., Schlichting, R., Scheel, D. and Kangasjärvi, J.** (2004) Stress hormone - independent activation and nuclear translocation of mitogen - activated protein kinases in *Arabidopsis thaliana* during ozone exposure. *The Plant Journal*, 40, 512–522.
- Apel, I.P.** (1967) On changes occurring rhythmically in the uptake of CO<sub>2</sub> in leaves, 3–9.
- Apel, I.P.** (1966) Rhythmic changes of the stomatal aperture and of CO<sub>2</sub> uptake in barley cotyledons, 279–288.
- Arend, M., Schnitzler, J.-P., Ehltling, B., Hansch, R., Lange, T., Rennenberg, H., Himmelbach, A., Grill, E. and Fromm, J.** (2009) Expression of the *Arabidopsis* mutant ABI1 gene alters abscisic acid sensitivity, stomatal development, and growth morphology in gray poplars. *PLANT PHYSIOLOGY*, 151, 2110–2119.
- Assmann, S.M.** (2013) Natural variation in abiotic stress and climate change responses in *Arabidopsis*: implications for twenty-first-century agriculture. *International Journal of Plant Sciences*, 174, 3–26.
- Atwell, B.J., Kriedemann, P.E., Turnbull, C.G.N., Eamus, D. and Bieleski, R.L.** (1999) *Plants in action. Adaption in nature, performance in cultivation/editors, Brian J. Atwell, Paul E. Kriedemann, Colin G.N. Turnbull ; co-editors, Derek Eamus, Roderick L. Bieleski ; consulting editor, Graham Farquhar*. South Yarra: Macmillan Education Australia.
- Audran, C., Borel, C., Frey, A., Sotta, B., Meyer, C., Simonneau, T. and Marion-Poll, A.** (1998) Expression studies of the zeaxanthin epoxidase gene in *Nicotiana plumbaginifolia*. *PLANT PHYSIOLOGY*, 118, 1021–1028.
- Barber, J.** (2009) Photosynthetic energy conversion: natural and artificial. *Chemical Society reviews*, 38, 185–196.
- Barbour, M.M., Cernusak, L.A., Whitehead, D., Griffin, K.L., Turnbull, M.H., Tissue, D.T. and Farquhar, G.D.** (2005) Nocturnal stomatal conductance and implications for modelling  $\delta^{18}\text{O}$  of leaf-respired CO<sub>2</sub> in temperate tree species. *Functional Plant Biology*, 32, 1107–1121.
- Barbour, M.M. and Farquhar, G.D.** (2000) Relative humidity- and ABA-induced variation in carbon and oxygen isotope ratios of cotton leaves. *Plant Cell Environ*, 23, 473–485.
- Barbour, M.M., Schurr, U., Henry, B.K., Wong, S.C. and Farquhar, G.D.** (2000) Variation in the oxygen isotope ratio of phloem sap sucrose from castor bean. Evidence in support of the Pécelet effect. *PLANT PHYSIOLOGY*, 123, 671–680.

- Barker, T., Campos, H., Cooper, M., Dolan, D., Edmeades, G., Habben, J., Schussler, J., Wright, D. and Zinselmeier, C.** (2005) Improving drought tolerance in maize. *Plant Breed. Rev.*, 25, 173–253.
- Barrs, H.D.** (1971) Cyclic Variations in Stomatal Aperture, Transpiration, and Leaf Water Potential Under Constant Environmental Conditions. *Annu. Rev. Plant. Physiol.*, 22, 223–236.
- Barrs, H.D. and Klepper, B.** (1968) Cyclic Variations in Plant Properties under Constant Environmental Conditions. *Physiol Plant*, 21, 711–730.
- Belin, C., Franco, P.-O. de, Bourbousse, C., Chaignepain, S., Schmitter, J.-M., Vavasseur, A., Giraudat, J., Barbier-Brygoo, H. and Thomine, S.** (2006) Identification of features regulating OST1 kinase activity and OST1 function in guard cells. *PLANT PHYSIOLOGY*, 141, 1316–1327.
- Berger, J.D. and Ludwig, C.** (2014) Contrasting adaptive strategies to terminal drought-stress gradients in Mediterranean legumes: phenology, productivity, and water relations in wild and domesticated *Lupinus luteus* L. *Journal of Experimental Botany*, 65, 6219–6229.
- Bernacchi, C.J., Portis, A.R., Nakano, H., Caemmerer, S. von and Long, S.P.** (2002) Temperature response of mesophyll conductance. Implications for the determination of Rubisco enzyme kinetics and for limitations to photosynthesis in vivo. *PLANT PHYSIOLOGY*, 130, 1992–1998.
- Bertsch, A. and Domes, W.** (1969) CO<sub>2</sub>-Exchange in amphistomatic leaves. I. The influence of the distribution of stomata on both leaf surfaces upon CO<sub>2</sub>-transport. *Planta*, 85, 183–193.
- Billings, W.D., Golley, F., Lange, O.L., Olson, J.S., Rimmert, H., Rundel, P.W., Ehleringer, J.R. and Nagy, K.A., eds.** (1989) *Stable Isotopes in Ecological Research*. New York, NY: Springer New York.
- Blum, A.** (2005) Drought resistance, water-use efficiency, and yield potential—are they compatible, dissonant, or mutually exclusive? *Aust. J. Agric. Res.*, 56, 1159.
- Blum, A.** (2009) Effective use of water (EUW) and not water-use efficiency (WUE) is the target of crop yield improvement under drought stress. *Field Crops Research*, 112, 119–123.
- Blum, A.** (2011) Drought resistance—is it really a complex trait? *Functional Plant Biology*, 38, 753–757.
- Boudsocq, M., Barbier-Brygoo, H. and Laurière, C.** (2004) Identification of nine sucrose nonfermenting 1-related protein kinases 2 activated by hyperosmotic and saline stresses in *Arabidopsis thaliana*. *Journal of Biological Chemistry*, 279, 41758–41766.
- Bourzac, K.** (2013) Water. The flow of technology. *Nature*, 501, S4–S6.
- Bray, E.A.** (1997) Plant responses to water deficit. *Trends in plant science*, 2, 48–54.
- Brooks, A. and Farquhar, G.D.** (1985) Effect of temperature on the CO<sub>2</sub>/O<sub>2</sub> specificity of ribulose-1,5-bisphosphate carboxylase/oxygenase and the rate of respiration in the light. Estimates from gas-exchange measurements on spinach. *Planta*, 165, 397–406.
- Brown, K.W. and Rosenberg, N.J.** (1970) Influence of leaf age, illumination, and

- upper and lower surface differences on stomatal resistance of sugar beet (*Beta vulgaris*) leaves. *Agronomy Journal*, 62, 20–24.
- Brun, W.A.** (1961) Photosynthesis & transpiration from upper & lower surfaces of intact banana leaves. *PLANT PHYSIOLOGY*, 36, 399–405.
- Burnett, E.C., Desikan, R., Moser, R.C. and Neill, S.J.** (2000) ABA activation of an MBP kinase in *Pisum sativum* epidermal peels correlates with stomatal responses to ABA. *Journal of Experimental Botany*, 51, 197–205.
- Cabrera-Bosquet, L., Molero, G., Nogues, S. and Araus, J.L.** (2009) Water and nitrogen conditions affect the relationships of Delta <sup>13</sup>C and Delta <sup>18</sup>O to gas exchange and growth in durum wheat. *Journal of Experimental Botany*, 60, 1633–1644.
- Caemmerer, S. von and Farquhar, G.D.** (1981) Some relationships between the biochemistry of photosynthesis and the gas exchange of leaves. *Planta*, 153, 376–387.
- Caird, M.A., Richards, J.H. and Donovan, L.A.** (2007) Nighttime stomatal conductance and transpiration in C3 and C4 plants. *PLANT PHYSIOLOGY*, 143, 4–10.
- Cardinale, F., Meskiene, I., Ouaked, F. and Hirt, H.** (2002) Convergence and divergence of stress-induced mitogen-activated protein kinase signaling pathways at the level of two distinct mitogen-activated protein kinase kinases. *The Plant cell*, 14, 703–711.
- Cardon, Z.G., Mott, K.A. and Berry, J.A.** (1994) Dynamics of patchy stomatal movements, and their contribution to steady-state and oscillating stomatal conductance calculated using gas-exchange techniques. *Plant Cell Environ*, 17, 995–1007.
- Cassman, K. and Liska, A.J.** (2007) Food and fuel for all. Realistic or foolish? *Biofuels, Bioprod. Bioref.*, 1, 18–23.
- Castiglioni, P., Warner, D., Bensen, R.J., Anstrom, D.C., Harrison, J., Stoecker, M., Abad, M., Kumar, G., Salvador, S., D'Ordine, R., Navarro, S., Back, S., Fernandes, M., Targolli, J., Dasgupta, S., Bonin, C., Luethy, M.H. and Heard, J.E.** (2008) Bacterial RNA Chaperones Confer Abiotic Stress Tolerance in Plants and Improved Grain Yield in Maize under Water-Limited Conditions. *PLANT PHYSIOLOGY*, 147, 446–455.
- Cavender-Bares, J., Sack, L. and Savage, J.** (2007) Atmospheric and soil drought reduce nocturnal conductance in live oaks. *Tree Physiology*, 27, 611–620.
- Cernusak, L.A., Wong, S.C. and Farquhar, G.D.** (2003) Oxygen isotope composition of phloem sap in relation to leaf water in *Ricinus communis*. *Functional Plant Biol.*, 30, 1059.
- Chang, L. and Karin, M.** (2001) Mammalian MAP kinase signalling cascades. *Nature*, 410, 37–40.
- Changnon, S.A.** (2009) Removing the Confusion Over Droughts and Floods. The Interface Between Scientists and Policy Makers. *Water International*, 5, 10–18.
- Chaves, M.M., Maroco, J.P. and Pereira, J.S.** (2003) Understanding plant responses to drought — from genes to the whole plant. *Functional Plant Biol.*, 30, 239.

- Chaves, M.M., Flexas, J. and Pinheiro, C.** (2008) Photosynthesis under drought and salt stress. Regulation mechanisms from whole plant to cell. *Annals of Botany*, 103, 551–560.
- Cheng, W.-H., Endo, A., Zhou, L., Penney, J., Chen, H.-C., Arroyo, A., Leon, P., Nambara, E., Asami, T. and Seo, M.** (2002) A unique short-chain dehydrogenase/reductase in Arabidopsis glucose signaling and abscisic acid biosynthesis and functions. *The Plant cell*, 14, 2723–2743.
- Choi, H.-i., Park, H.-J., Park, J.H., Kim, S., Im, M.-Y., Seo, H.-H., Kim, Y.-W., Hwang, I. and Kim, S.Y.** (2005) Arabidopsis calcium-dependent protein kinase AtCPK32 interacts with ABF4, a transcriptional regulator of abscisic acid-responsive gene expression, and modulates its activity. *PLANT PHYSIOLOGY*, 139, 1750–1761.
- Christman, M.A., Richards, J.H., McKay, J.K., Stahl, E.A., Juenger, T.E. and Donovan, L.A.** (2008) Genetic variation in Arabidopsis thaliana for night-time leaf conductance. *Plant, cell & environment*, 31, 1170–1178.
- Christmann, A., Grill, E. and Huang, J.** (2013) Hydraulic signals in long-distance signaling. *Current opinion in plant biology*, 16, 293–300.
- Christmann, A., Hoffmann, T., Teplova, I., Grill, E. and Muller, A.** (2005) Generation of active pools of abscisic acid revealed by in vivo imaging of water-stressed Arabidopsis. *PLANT PHYSIOLOGY*, 137, 209–219.
- Christmann, A., Moes, D., Himmelbach, A., Yang, Y., Tang, Y. and Grill, E.** (2006) Integration of abscisic acid signalling into plant responses. *Plant biology (Stuttgart, Germany)*, 8, 314–325.
- Colcombet, J. and Hirt, H.** (2008) Arabidopsis MAPKs: a complex signalling network involved in multiple biological processes. *The Biochemical journal*, 413, 217–226.
- Condon, A.G., Richards, R.A., Rebetzke, G.J. and Farquhar, G.D.** (2002) Improving intrinsic water-use efficiency and crop yield. *Crop Science*, 42, 122–131.
- Cowan, I.R.** (1972) Oscillations in stomatal conductance and plant functioning associated with stomatal conductance: Observations and a model. *Planta*, 106, 185–219.
- Cox, E.F.** (1968) Cyclic Changes in Transpiration of Sunflower Leaves in a Steady Environment. *J Exp Bot*, 19, 167–175.
- Crow, J.F.** (2007) Haldane, Bailey, Taylor and recombinant-inbred lines. *Genetics*, 176, 729–732.
- LSL O'Reilly and DeNiro, M.J.D.** (1983) Biogeochemical implications of the isotopic equilibrium fractionation factor between the oxygen atoms of acetone and water. *Geochimica et Cosmochimica Acta*, 47, 2271–2274.
- Daley, M.J. and Phillips, N.G.** (2006) Interspecific variation in nighttime transpiration and stomatal conductance in a mixed New England deciduous forest. *Tree Physiology*, 26, 411–419.
- Danquah, A., Zelicourt, A. de, Boudsocq, M., Neubauer, J., Frei dit Frey, N., Leonhardt, N., Pateyron, S., Gwinner, F., Tamby, J.-P., Ortiz-Masia, D., Marcote, M.J., Hirt, H. and Colcombet, J.** (2015) Identification and characterization of an ABA-activated MAP kinase cascade in Arabidopsis thaliana. *The Plant journal : for cell and molecular biology*, 82, 232–244.

- Davies, N.B., Krebs, J.R. and West, S.A.** (2012) *An introduction to behavioural ecology*. 4th edn. Chichester: Wiley-Blackwell.
- Dawson, T.E., Burgess, S.S.O., Tu, K.P., Oliveira, R.S., Santiago, L.S., Fisher, J.B., Simonin, K.A. and Ambrose, A.R.** (2007) Nighttime transpiration in woody plants from contrasting ecosystems. *Tree Physiology*, 27, 561–575.
- del Pozo, O., Pedley, K.F. and Martin, G.B.** (2004) MAPKKK $\alpha$  is a positive regulator of cell death associated with both plant immunity and disease. *The EMBO journal*, 23, 3072–3082.
- Des Marais, D.L., Auchincloss, L.C., Sukamtoh, E., McKay, J.K., Logan, T., Richards, J.H. and Juenger, T.E.** (2014) Variation in MPK12 affects water use efficiency in Arabidopsis and reveals a pleiotropic link between guard cell size and ABA response. *Proceedings of the National Academy of Sciences of the United States of America*, 111, 2836–2841.
- Des Marais, D.L., Razzaque, S., Hernandez, K.M., Garvin, D.F. and Juenger, T.E.** (2016) Quantitative trait loci associated with natural diversity in water-use efficiency and response to soil drying in *Brachypodium distachyon*. *Plant Science*.
- Dingkuhn, M., Johnson, D.E., Sow, A. and Audebert, A.Y.** (1999) Relationships between upland rice canopy characteristics and weed competitiveness. *Field Crops Research*, 61, 79–95.
- Dodd, A.N., Parkinson, K. and Webb, A.A.R.** (2004) Independent circadian regulation of assimilation and stomatal conductance in the *ztl-1* mutant of Arabidopsis. *New Phytologist*, 162, 63–70.
- Dodd, A.N., Salathia, N., Hall, A., Kévei, E., Tóth, R., Nagy, F., Hibberd, J.M., Millar, A.J. and Webb, A.A.R.** (2005) Plant circadian clocks increase photosynthesis, growth, survival, and competitive advantage. *Science*, 309, 630–633.
- Döhring, T., Koefferlein, M., Thiel, S. and Seidlitz, H.K.** (1996) Spectral shaping of artificial UV-B irradiation for vegetation stress research. *Journal of plant physiology*, 148, 115–119.
- Dongmann, G., Nürnberg, H.W., Förstel, H. and Wagener, K.** (1974) On the enrichment of H<sub>2</sub><sup>18</sup>O in the leaves of transpiring plants. *Radiat Environ Biophys*, 11, 41–52.
- Donovan, L.A., Gris , D.J., West, J.B., Pappert, R.A., Alder, N.N. and Richards, J.H.** (1999) Predawn disequilibrium between plant and soil water potentials in two cold-desert shrubs. *Oecologia*, 120, 209–217.
- Donovan, L.A., Richards, J.H. and Linton, M.J.** (2003) MAGNITUDE AND MECHANISMS OF DISEQUILIBRIUM BETWEEN PREDAWN PLANT AND SOIL WATER POTENTIALS. *Ecology*, 84, 463–470.
- Easlon, H.M., Nemali, K.S., Richards, J.H., Hanson, D.T., Juenger, T.E. and McKay, J.K.** (2014) The physiological basis for genetic variation in water use efficiency and carbon isotope composition in Arabidopsis thaliana. *Photosynthesis research*, 119, 119–129.
- Ehrler, W.L., Nakayama, F.S. and Bavel, C.H.M.** (1965) Cyclic Changes in Water Balance and Transpiration of Cotton Leaves in a Steady Environment. *Physiol Plant*, 18, 766–775.

- Eisenreich, W., Bacher, A., Arigoni, D. and Rohdich, F.** (2004) Biosynthesis of isoprenoids via the non-mevalonate pathway. *Cellular and molecular life sciences : CMLS*, 61, 1401–1426.
- Endo, A., Sawada, Y., Takahashi, H., Okamoto, M., Ikegami, K., Koiwai, H., Seo, M., Toyomasu, T., Mitsunashi, W., Shinozaki, K., Nakazono, M., Kamiya, Y., Koshiba, T. and Nambara, E.** (2008) Drought induction of Arabidopsis 9-cis-epoxycarotenoid dioxygenase occurs in vascular parenchyma cells. *PLANT PHYSIOLOGY*, 147, 1984–1993.
- Erice, G., Louahlia, S., Irigoyen, J.J., Sanchez-Diaz, M. and Avice, J.-C.** (2010) Biomass partitioning, morphology and water status of four alfalfa genotypes submitted to progressive drought and subsequent recovery. *Journal of plant physiology*, 167, 114–120.
- Ethier, G.J. and Livingston, N.J.** (2004) On the need to incorporate sensitivity to CO<sub>2</sub> transfer conductance into the Farquhar-von Caemmerer-Berry leaf photosynthesis model. *Plant Cell Environ*, 27, 137–153.
- Evans, L.T. and Fischer, R.A.** (1999) Yield Potential. *Crop Science*, 39, 1544.
- Evans, JR, Sharkey, T.D., Berry, J.A. and Farquhar, G.D.** (1986) Carbon isotope discrimination measured concurrently with gas exchange to investigate CO<sub>2</sub> diffusion in leaves of higher plants. *Functional Plant Biology*, 13, 281–292.
- FAOSTAT.** (2006) FAO data for agriculture: statistics database. See <http://faostat.fao.org/faostat/collections?versionZext&hasbulkZ0&subsetZagriculture>.
- Faria, T., Silvério, D., Breia, E., Cabral, R., Abadia, A., Abadia, J., Pereira, J.S. and CHAVES, M.M.** (1998) Differences in the response of carbon assimilation to summer stress (water deficits, high light and temperature) in four Mediterranean tree species. *Physiologia Plantarum*, 102, 419–428.
- Farooq, M., Wahid, A., Kobayashi, N., Fujita, D. and Basra, S.M.A.** (2009) Plant drought stress. Effects, mechanisms and management. *Agron. Sustain. Dev.*, 29, 185–212.
- Farquhar, G.D., Cernusak, L.A. and Barnes, B.** (2007) Heavy water fractionation during transpiration. *PLANT PHYSIOLOGY*, 143, 11–18.
- Farquhar, G.D. and Cowan, I.R.** (1974) Oscillations in Stomatal Conductance: The Influence of Environmental Gain. *PLANT PHYSIOLOGY*, 54, 769–772.
- Farquhar, G.D., Ehleringer, J.R. and Hubick, K.T.** (1989) Carbon Isotope Discrimination and Photosynthesis. *Annu. Rev. Plant. Physiol. Plant. Mol. Biol.*, 40, 503–537.
- Farquhar, G.D. and Raschke, K.** (1978) On the Resistance to Transpiration of the Sites of Evaporation within the Leaf. *PLANT PHYSIOLOGY*, 61, 1000–1005.
- Farquhar, G.D. and Richards, R.A.** (1984a) Isotopic Composition of Plant Carbon Correlates With Water-Use Efficiency of Wheat Genotypes. *Functional Plant Biol*, 11, 539–552.
- Farquhar, G.D. and Richards, R.A.** (1984b) Isotopic Composition of Plant Carbon Correlates With Water-Use Efficiency of Wheat Genotypes. *Aust J Plant Physio.*, 11, 539.
- Farquhar, G.V., Caemmerer, S. von and Berry, J.A.** (1980) A biochemical model of

- photosynthetic CO<sub>2</sub> assimilation in leaves of C3 species. *Planta*, 149, 78–90.
- Feil, R. and Fraga, M.F.** (2011) Epigenetics and the environment: emerging patterns and implications. *Nature reviews. Genetics*, 13, 97–109.
- Finkelstein, R.** (2013) Abscisic Acid synthesis and response. *The Arabidopsis book / American Society of Plant Biologists*, 11, e0166.
- Finkelstein, R., Gampala, S.S.L., Lynch, T.J., Thomas, T.L. and Rock, C.D.** (2005) Redundant and distinct functions of the ABA response loci ABA-INSENSITIVE (ABI) 5 and ABRE-BINDING FACTOR (ABF) 3. *Plant molecular biology*, 59, 253–267.
- Flexas, J., Escalona, J.M. and Medrano, H.** (1999) Water stress induces different levels of photosynthesis and electron transport rate regulation in grapevines. *Plant Cell Environ*, 22, 39–48.
- Flexas, J., Ortuno, M.F., Ribas-Carbo, M., Diaz-Espejo, A., Florez-Sarasa, I.D. and Medrano, H.** (2007) Mesophyll conductance to CO<sub>2</sub> in Arabidopsis thaliana. *The New phytologist*, 175, 501–511.
- Flexas, J., Niinemets, U., Galle, A., Barbour, M.M., Centritto, M., Diaz-Espejo, A., Douthe, C., Galmes, J., Ribas-Carbo, M., Rodriguez, P.L., Rossello, F., Soolanayakanahally, R., Tomas, M., Wright, I.J., Farquhar, G.D. and Medrano, H.** (2013) Diffusional conductances to CO<sub>2</sub> as a target for increasing photosynthesis and photosynthetic water-use efficiency. *Photosynthesis research*, 117, 45–59.
- Flexas, J., Ribas-Carbó, M., Diaz-Espejo, A., Galmés, J. and Medrano, H.** (2008) Mesophyll conductance to CO<sub>2</sub>: current knowledge and future prospects. *Plant, cell & environment*, 31, 602–621.
- Franks, S.J., Sim, S. and Weis, A.E.** (2007) Rapid evolution of flowering time by an annual plant in response to a climate fluctuation. *Proceedings of the National Academy of Sciences of the United States of America*, 104, 1278–1282.
- Frye, C.A., Tang, D. and Innes, R.W.** (2001) Negative regulation of defense responses in plants by a conserved MAPKK kinase. *Proceedings of the National Academy of Sciences*, 98, 373–378.
- Fujii, H., Chinnusamy, V., Rodrigues, A., Rubio, S., Antoni, R., Park, S.-Y., Cutler, S.R., Sheen, J., Rodriguez, P.L. and Zhu, J.-K.** (2009) In vitro reconstitution of an abscisic acid signalling pathway. *Nature*, 462, 660–664.
- Fujii, H., Verslues, P.E. and Zhu, J.-K.** (2007) Identification of two protein kinases required for abscisic acid regulation of seed germination, root growth, and gene expression in Arabidopsis. *The Plant cell*, 19, 485–494.
- Fujii, H. and Zhu, J.-K.** (2009) Arabidopsis mutant deficient in 3 abscisic acid-activated protein kinases reveals critical roles in growth, reproduction, and stress. *Proceedings of the National Academy of Sciences of the United States of America*, 106, 8380–8385.
- Fujita, Y., Nakashima, K., Yoshida, T., Katagiri, T., Kidokoro, S., Kanamori, N., Umezawa, T., Fujita, M., Maruyama, K., Ishiyama, K., Kobayashi, M., Nakasone, S., Yamada, K., Ito, T., Shinozaki, K. and Yamaguchi-Shinozaki, K.** (2009) Three SnRK2 protein kinases are the main positive regulators of abscisic acid signaling in response to water stress in Arabidopsis. *Plant & cell physiology*, 50, 2123–2132.
- Furihata, T., Maruyama, K., Fujita, Y., Umezawa, T., Yoshida, R., Shinozaki, K. and**

- Yamaguchi-Shinozaki, K.** (2006) Abscisic acid-dependent multisite phosphorylation regulates the activity of a transcription activator AREB1. *Proceedings of the National Academy of Sciences of the United States of America*, 103, 1988–1993.
- Garg, A.K., Kim, J.-K., Owens, T.G., Ranwala, A.P., Choi, Y.D., Kochian, L.V. and Wu, R.J.** (2002) Trehalose accumulation in rice plants confers high tolerance levels to different abiotic stresses. *Proceedings of the National Academy of Sciences*, 99, 15898–15903.
- Gates, D.M.** (1968) Transpiration and leaf temperature. *Annual Review of Plant Physiology*, 19, 211–238.
- Geerts, S. and Raes, D.** (2009) Deficit irrigation as an on-farm strategy to maximize crop water productivity in dry areas. *Agricultural Water Management*, 96, 1275–1284.
- Geiger, D., Scherzer, S., Mumm, P., Stange, A., Marten, I., Bauer, H., Ache, P., Matschi, S., Liese, A., Al-Rasheid, K.A.S., Romeis, T. and Hedrich, R.** (2009) Activity of guard cell anion channel SLAC1 is controlled by drought-stress signaling kinase-phosphatase pair. *Proceedings of the National Academy of Sciences of the United States of America*, 106, 21425–21430.
- Genty, B., Briantais, J.-M. and Baker, N.R.** (1989) The relationship between the quantum yield of photosynthetic electron transport and quenching of chlorophyll fluorescence. *Biochimica et Biophysica Acta (BBA)-General Subjects*, 990, 87–92.
- Ghashghaie, J., Badeck, F.-W., Lanigan, G., Nogués, S., Tcherkez, G., Deléens, E., Cornic, G. and Griffiths, H.** (2003) Carbon isotope fractionation during dark respiration and photorespiration in C3 plants. *Phytochemistry reviews*, 2, 145–161.
- Glantz, M.H. and Katz, R.W.** (1977) When is a drought a drought? *Nature*, 267, 192–193.
- Gleick, P.H. and Serageldin, I.** (2014) *The world's water. The biennial report on freshwater resources*. Washington, District of Columbia: Island Press.
- Golzarian, M.R., Frick, R.A., Rajendran, K., Berger, B., Roy, S., Tester, M. and Lun, D.S.** (2011) Accurate inference of shoot biomass from high-throughput images of cereal plants. *Plant methods*, 7, 2.
- Gosti, F., Bertauche, N., Vartanian, N. and Giraudat, J.** (1995) Abscisic acid-dependent and -independent regulation of gene expression by progressive drought in *Arabidopsis thaliana*. *Molec. Gen. Genet.*, 246, 10–18.
- Gowda, V.R.P., Henry, A., Yamauchi, A., Shashidhar, H.E. and Serraj, R.** (2011) Root biology and genetic improvement for drought avoidance in rice. *Field Crops Research*, 122, 1–13.
- Grant, O.M., Johnson, A.W., Davies, M.J., James, C.M. and Simpson, D.W.** (2010) Physiological and morphological diversity of cultivated strawberry (*Fragaria×ananassa*) in response to water deficit. *Environmental and Experimental Botany*, 68, 264–272.
- Grassini, P., Eskridge, K.M. and Cassman, K.G.** (2013) Distinguishing between yield advances and yield plateaus in historical crop production trends. *Nature communications*, 4, 2918.



- Grulke, N.E., Alonso, R., Nguyen, T., Cascio, C. and Dobrowolski, W.** (2004) Stomata open at night in pole-sized and mature ponderosa pine. Implications for O<sup>3</sup> exposure metrics. *Tree Physiology*, 24, 1001–1010.
- Gu, J.-F., Qiu, M. and Yang, J.-C.** (2013) Enhanced tolerance to drought in transgenic rice plants overexpressing C 4 photosynthesis enzymes. *The Crop Journal*, 1, 105–114.
- Gudesblat, G.E., Iusem, N.D. and Morris, P.C.** (2007) Guard cell-specific inhibition of Arabidopsis MPK3 expression causes abnormal stomatal responses to abscisic acid and hydrogen peroxide. *The New phytologist*, 173, 713–721.
- Guzel Deger, A., Scherzer, S., Nuhkat, M., Kedzierska, J., Kollist, H., Brosche, M., Unyayar, S., Boudsocq, M., Hedrich, R. and Roelfsema, M.R.G.** (2015) Guard cell SLAC1-type anion channels mediate flagellin-induced stomatal closure. *The New phytologist*, 208, 162–173.
- Hall, A.E., Richards, R.A., Condon, A.G., Wright, G.C. and Farquhar, G.D.** (1994) Carbon isotope discrimination and plant breeding. *Plant breeding reviews*, 12, 81–113.
- Hamlyn G. Jones, ed.** (2004) *Incorporating Advances in Plant Pathology*: Elsevier.
- Harley, P.C., Loreto, F., Di Marco, G. and Sharkey, T.D.** (1992) Theoretical Considerations when Estimating the Mesophyll Conductance to CO<sub>2</sub> Flux by Analysis of the Response of Photosynthesis to CO<sub>2</sub>. *PLANT PHYSIOLOGY*, 98, 1429–1436.
- Harrison, S.J., Mott, E.K., Parsley, K., Aspinall, S., Gray, J.C. and Cottage, A.** (2006) A rapid and robust method of identifying transformed Arabidopsis thaliana seedlings following floral dip transformation. *Plant methods*, 2, 1.
- Hausmann, N.J., Juenger, T.E., Sen, S., Stowe, K.A., Dawson, T.E. and Simms, E.L.** (2005) QUANTITATIVE TRAIT LOCI AFFECTING  $\delta^{13}\text{C}$  AND RESPONSE TO DIFFERENTIAL WATER AVAILABILITY IN ARABIDOPSIS THALLANA. *Evolution*, 59, 81–96.
- Hietz, P., Wanek, W. and Dunisch, O.** (2005) Long-term trends in cellulose delta13 C and water-use efficiency of tropical Cedrela and Swietenia from Brazil. *Tree Physiology*, 25, 745–752.
- Himmelbach, A., Hoffmann, T., Leube, M., Hohener, B. and Grill, E.** (2002) Homeodomain protein ATHB6 is a target of the protein phosphatase ABI1 and regulates hormone responses in Arabidopsis. *The EMBO journal*, 21, 3029–3038.
- Hopmans, P.A.** (1969) Types of stomatal cycling and their water relations in bean leaves. *Zeitschrift fur Pflanzenphysiologie*.
- Huai, J., Wang, M., He, J., Zheng, J., Dong, Z., Lv, H., Zhao, J. and Wang, G.** (2008) Cloning and characterization of the SnRK2 gene family from Zea mays. *Plant cell reports*, 27, 1861–1868.
- Hubbart, J.A., Kavanagh, K.L., Pangle, R., Link, T. and Schotzko, A.** (2007) Cold air drainage and modeled nocturnal leaf water potential in complex forested terrain. *Tree Physiology*, 27, 631–639.
- Hubick, K. and Farquhar, G.** (1989) Carbon isotope discrimination and the ratio of carbon gained to water lost in barley cultivars. *Plant Cell Environ*, 12, 795–804.

- Hunt, L.A., Impens, I.I. and Lemon, E.R. (1968) Estimates of the Diffusion Resistance of Some Large Sunflower Leaves in the Field. *PLANT PHYSIOLOGY*, 43, 522–526.
- Huse, M. and Kuriyan, J. (2002) The Conformational Plasticity of Protein Kinases. *Cell*, 109, 275–282.
- Hwa, C.-M. and Yang, X.-C. (2008) The AtMKK3 pathway mediates ABA and salt signaling in Arabidopsis. *Acta Physiologiae Plantarum*, 30, 277–286.
- Ichimura, K., Shinozaki, K., Tena, G., Sheen, J., Henry, Y., Champion, A., Kreis, M., Zhang, S., Hirt, H., Wilson, C., Heberle-Bors, E., Ellis, B.E., Morris, P.C., Innes, R.W., Ecker, J.R., Scheel, D., Klessig, D.F., Machida, Y., Mundy, J., Ohashi, Y. and Walker, J.C. (2002) Mitogen-activated protein kinase cascades in plants. A new nomenclature. *Trends in plant science*, 7, 301–308.
- Imes, D., Mumm, P., Böhm, J., Al - Rasheid, K.A.S., Marten, I., Geiger, D. and Hedrich, R. (2013) Open stomata 1 (OST1) kinase controls R-type anion channel QUAC1 in Arabidopsis guard cells. *The Plant Journal*, 74, 372–382.
- Ingram, J. and Bartels, D. (1996) THE MOLECULAR BASIS OF DEHYDRATION TOLERANCE IN PLANTS. *Annual review of plant physiology and plant molecular biology*, 47, 377–403.
- Irfan, M., Hayat, S., Hayat, Q., Afroz, S. and Ahmad, A. (2010) Physiological and biochemical changes in plants under waterlogging. *Protoplasma*, 241, 3–17.
- Iuchi, S., Kobayashi, M., Taji, T., Naramoto, M., Seki, M., Kato, T., Tabata, S., Kakubari, Y., Yamaguchi-Shinozaki, K. and Shinozaki, K. (2001a) Regulation of drought tolerance by gene manipulation of 9-cis-epoxycarotenoid dioxygenase, a key enzyme in abscisic acid biosynthesis in Arabidopsis. *The Plant journal : for cell and molecular biology*, 27, 325–333.
- Iuchi, S., Kobayashi, M., Taji, T., Naramoto, M., Seki, M., Kato, T., Tabata, S., Kakubari, Y., Yamaguchi-Shinozaki, K. and Shinozaki, K. (2001b) Regulation of drought tolerance by gene manipulation of 9-cis-epoxycarotenoid dioxygenase, a key enzyme in abscisic acid biosynthesis in Arabidopsis. *The Plant Journal*, 27, 325–333.
- Iuchi, S., Kobayashi, M., Yamaguchi-Shinozaki, K. and Shinozaki, K. (2000) A stress-inducible gene for 9-cis-epoxycarotenoid dioxygenase involved in abscisic acid biosynthesis under water stress in drought-tolerant cowpea. *PLANT PHYSIOLOGY*, 123, 553–562.
- Ivey, C.T. and Carr, D.E. (2012) Tests for the joint evolution of mating system and drought escape in *Mimulus*. *Annals of Botany*, 109, 583–598.
- James, J.J., Alder, N.N., Muhling, K.H., Lauchli, A.E., Shackel, K.A., Donovan, L.A. and Richards, J.H. (2006) High apoplastic solute concentrations in leaves alter water relations of the halophytic shrub, *Sarcobatus vermiculatus*. *Journal of Experimental Botany*, 57, 139–147.
- Jammes, F., Song, C., Shin, D., Munemasa, S., Takeda, K., Gu, D., Cho, D., Lee, S., Giordo, R. and Sritubtim, S. (2009) MAP kinases MPK9 and MPK12 are preferentially expressed in guard cells and positively regulate ROS-mediated ABA signaling. *Proceedings of the National Academy of Sciences*, 106, 20520–20525.
- Jammes, F., Song, C., Shin, D., Munemasa, S., Takeda, K., Gu, D., Cho, D., Lee, S.,

- Giordo, R., Sritubtim, S., Leonhardt, N., Ellis, B.E., Murata, Y. and Kwak, J.M.** (2009) MAP kinases MPK9 and MPK12 are preferentially expressed in guard cells and positively regulate ROS-mediated ABA signaling. *Proceedings of the National Academy of Sciences of the United States of America*, 106, 20520–20525.
- Jasechko, S., Sharp, Z.D., Gibson, J.J., Birks, S.J., Yi, Y. and Fawcett, P.J.** (2013) Terrestrial water fluxes dominated by transpiration. *Nature*, 496, 347–350.
- Jensen, M.K., Hagedorn, P.H., Torres-Zabala, M. de, Grant, M.R., Rung, J.H., Collinge, D.B. and Lyngkjaer, M.F.** (2008) Transcriptional regulation by an NAC (NAM-ATAF1,2-CUC2) transcription factor attenuates ABA signalling for efficient basal defence towards *Blumeria graminis* f. sp. *hordei* in *Arabidopsis*. *The Plant journal : for cell and molecular biology*, 56, 867–880.
- Jensen, M.K., Lindemose, S., Masi, F. de, Reimer, J.J., Nielsen, M., Perera, V., Workman, C.T., Turck, F., Grant, M.R., Mundy, J., Petersen, M. and Skriver, K.** (2013) ATAF1 transcription factor directly regulates abscisic acid biosynthetic gene NCED3 in *Arabidopsis thaliana*. *FEBS open bio*, 3, 321–327.
- Juenger, T.E.** (2013) Natural variation and genetic constraints on drought tolerance. *Current opinion in plant biology*, 16, 274–281.
- Juenger, T.E., McKay, J.K., Hausmann, N., Keurentjes, J.J.B., Sen, S., Stowe, K.A., Dawson, T.E., Simms, E.L. and Richards, J.H.** (2005) Identification and characterization of QTL underlying whole-plant physiology in *Arabidopsis thaliana*. Delta13C, stomatal conductance and transpiration efficiency. *Plant Cell Environ*, 28, 697–708.
- Kanemasu, E.T. and Tanner, C.B.** (1969) Stomatal Diffusion Resistance of Snap Beans. II. Effect of Light. *PLANT PHYSIOLOGY*, 44, 1542–1546.
- Kang, J., Hwang, J.-U., Lee, M., Kim, Y.-Y., Assmann, S.M., Martinoia, E. and Lee, Y.** (2010) PDR-type ABC transporter mediates cellular uptake of the phytohormone abscisic acid. *Proceedings of the National Academy of Sciences of the United States of America*, 107, 2355–2360.
- Kavar, T., Maras, M., Kidrič, M., Šuštar-Vozlič, J. and Meglič, V.** (2008) Identification of genes involved in the response of leaves of *Phaseolus vulgaris* to drought stress. *Mol Breeding*, 21, 159–172.
- Khanna-Chopra, R., Srivalli, B. and Ahlawat, Y.S.** (1999) Drought induces many forms of cysteine proteases not observed during natural senescence. *Biochemical and biophysical research communications*, 255, 324–327.
- Khokhlatchev, A.V., Canagarajah, B., Wilsbacher, J., Robinson, M., Atkinson, M., Goldsmith, E. and Cobb, M.H.** (1998) Phosphorylation of the MAP Kinase ERK2 Promotes Its Homodimerization and Nuclear Translocation. *Cell*, 93, 605–615.
- Kijne, J.W., Barker, R. and Molden, D.J.** (2003) *Water productivity in agriculture. Limits and opportunities for improvement*. Oxon, Cambridge, MA: CABI Pub. in association with the International Water Management Institute.
- Kitajima, K., Mulkey, S. and Wright, S.** (1997a) Decline of photosynthetic capacity with leaf age in relation to leaf longevities for five tropical canopy tree species. *American Journal of Botany*, 84, 702.
- Kitajima, K., Mulkey, S. and Wright, S.** (1997b) Decline of photosynthetic capacity

- with leaf age in relation to leaf longevities for five tropical canopy tree species. *American Journal of Botany*, 84, 702.
- Kobayashi, Y., Murata, M., Minami, H., Yamamoto, S., Kagaya, Y., Hobo, T., Yamamoto, A. and Hattori, T.** (2005) Abscisic acid - activated SNRK2 protein kinases function in the gene - regulation pathway of ABA signal transduction by phosphorylating ABA response element - binding factors. *The Plant Journal*, 44, 939–949.
- Kobayashi, Y., Yamamoto, S., Minami, H., Kagaya, Y. and Hattori, T.** (2004) Differential activation of the rice sucrose nonfermenting1–related protein kinase2 family by hyperosmotic stress and abscisic acid. *The Plant cell*, 16, 1163–1177.
- Koike, T.** (1988) Leaf Structure and Photosynthetic Performance as Related to the Forest Succession of Deciduous Broad - Leaved Trees1. *Plant Species Biology*, 3, 77–87.
- Koiwai, H., Nakaminami, K., Seo, M., Mitsunashi, W., Toyomasu, T. and Koshiba, T.** (2004) Tissue-specific localization of an abscisic acid biosynthetic enzyme, AAO3, in Arabidopsis. *PLANT PHYSIOLOGY*, 134, 1697–1707.
- Koncz, C. and Schell, J.** (1986) The promoter of TL-DNA gene 5 controls the tissue-specific expression of chimaeric genes carried by a novel type of Agrobacterium binary vector. *Molec Gen Genet*, 204, 383–396.
- Kooyers, N.J.** (2015) The evolution of drought escape and avoidance in natural herbaceous populations. *Plant Science*, 234, 155–162.
- Kriedemann, P.E.** (1968) Some photosynthetic characteristics of citrus leaves. *Australian Journal of Biological Sciences*, 21, 895–906.
- Kuhn, J.M., Boisson-Dernier, A., Dizon, M.B., Maktabi, M.H. and Schroeder, J.I.** (2006) The protein phosphatase AtPP2CA negatively regulates abscisic acid signal transduction in Arabidopsis, and effects of abh1 on AtPP2CA mRNA. *PLANT PHYSIOLOGY*, 140, 127–139.
- Kuiper, P.J.C.** (1961) The effects of environmental factors on the transpiration of leaves, with special reference to stomatal light response. *Meded. Landbouwhogeschool, Wageningen*, 61, 1–49.
- Kulik, A., Wawer, I., Krzywińska, E., Bucholc, M. and Dobrowolska, G.** (2011) SnRK2 protein kinases—key regulators of plant response to abiotic stresses. *Omics: a journal of integrative biology*, 15, 859–872.
- Kumar, J., ed.** (2001) *Gnetics of flowering time in chichpea and its bearing on productivity in the semi-arid environment*: Elsevier.
- Kuromori, T., Miyaji, T., Yabuuchi, H., Shimizu, H., Sugimoto, E., Kamiya, A., Moriyama, Y. and Shinozaki, K.** (2010) ABC transporter AtABCG25 is involved in abscisic acid transport and responses. *Proceedings of the National Academy of Sciences of the United States of America*, 107, 2361–2366.
- Kuzuyama, T.** (2014) Mevalonate and Nonmevalonate Pathways for the Biosynthesis of Isoprene Units. *Bioscience, Biotechnology, and Biochemistry*, 66, 1619–1627.
- Kwak, J.M., Murata, Y., Baizabal-Aguirre, V.M., Merrill, J., Wang, M., Kemper, A., Hawke, S.D., Tallman, G. and Schroeder, J.I.** (2001) Dominant negative guard cell K<sup>+</sup> channel mutants reduce inward-rectifying K<sup>+</sup> currents and light-induced

- stomatal opening in Arabidopsis. *PLANT PHYSIOLOGY*, 127, 473–485.
- Lasceve, G., Leymarie, J. and Vavasseur, A.** (1997) Alterations in light - induced stomatal opening in a starch - deficient mutant of Arabidopsis thaliana L. deficient in chloroplast phosphoglucomutase activity. *Plant, cell & environment*, 20, 350–358.
- Lebaudy, A., Pascaud, F., Véry, A.-A., Alcon, C., Dreyer, I., Thibaud, J.-B. and Lacombe, B.** (2010) Preferential KAT1-KAT2 heteromerization determines inward K<sup>+</sup> current properties in Arabidopsis guard cells. *Journal of Biological Chemistry*, 285, 6265–6274.
- Lee, J.S., Wang, S., Sritubtim, S., Chen, J.-G. and Ellis, B.E.** (2009) Arabidopsis mitogen-activated protein kinase MPK12 interacts with the MAPK phosphatase IBR5 and regulates auxin signaling. *The Plant journal : for cell and molecular biology*, 57, 975–985.
- Lee, S.C., Lan, W., Buchanan, B.B. and Luan, S.** (2009) A protein kinase-phosphatase pair interacts with an ion channel to regulate ABA signaling in plant guard cells. *Proceedings of the National Academy of Sciences of the United States of America*, 106, 21419–21424.
- Levitt, J.** (1972) *Responses of plants to environmental stresses*: Academic press New York.
- Levy, P.E., Meir, P., Allen, S.J. and Jarvis, P.G.** (1999) *The effect of aqueous transport of CO<sub>2</sub> in xylem sap on gas exchange in woody plants*.
- Li, J., Wang, X.-Q., Watson, M.B. and Assmann, S.M.** (2000) Regulation of abscisic acid-induced stomatal closure and anion channels by guard cell AAPK kinase. *Science*, 287, 300–303.
- Lian, H.-L.** (2004) The Role of Aquaporin RWC3 in Drought Avoidance in Rice. *Plant and Cell Physiology*, 45, 481–489.
- Lichtenthaler, H.K.** (1999) THE 1-DEOXY-D-XYLULOSE-5-PHOSPHATE PATHWAY OF ISOPRENOID BIOSYNTHESIS IN PLANTS. *Annual review of plant physiology and plant molecular biology*, 50, 47–65.
- Lindemose, S., O'Shea, C., Jensen, M.K. and Skriver, K.** (2013) Structure, function and networks of transcription factors involved in abiotic stress responses. *International journal of molecular sciences*, 14, 5842–5878.
- López-Castañeda, C. and Richards, R.A.** (1994) Variation in temperate cereals in rainfed environments III. Water use and water-use efficiency. *Field Crops Research*, 39, 85–98.
- Lovell, J.T., Juenger, T.E., Michaels, S.D., Lasky, J.R., Platt, A., Richards, J.H., Yu, X., Easlon, H.M., SEN, S. and McKay, J.K.** (2013) Pleiotropy of FRIGIDA enhances the potential for multivariate adaptation. *Proceedings. Biological sciences / The Royal Society*, 280, 20131043.
- Ludlow, M.M. and Muchow, R.C.** (1990) A Critical Evaluation of Traits for Improving Crop Yields in Water-Limited Environments. In *A critical evaluation of traits for improving crop yields in water-limited environments* (Ludlow MM, Muchow RC, ed): Elsevier, pp. 107–153.
- Ma, Y., Szostkiewicz, I., Korte, A., Moes, D., Yang, Y., Christmann, A. and Grill, E.**

- (2009) Regulators of PP2C phosphatase activity function as abscisic acid sensors. *Science (New York, N.Y.)*, 324, 1064–1068.
- Malone, M.** (1993) Hydraulic Signals. *Philos Trans R Soc Lond B Biol Sci*, 341, 33.
- Manzaneda, A.J., Rey, P.J., Anderson, J.T., Raskin, E., Weiss-Lehman, C. and Mitchell-Olds, T.** (2015) Natural variation, differentiation, and genetic trade-offs of ecophysiological traits in response to water limitation in *Brachypodium distachyon* and its descendent allotetraploid *B. hybridum* (Poaceae). *Evolution; international journal of organic evolution*, 69, 2689–2704.
- Mao, X., Zhang, H., Tian, S., Chang, X. and Jing, R.** (2010) TaSnRK2. 4, an SNF1-type serine/threonine protein kinase of wheat (*Triticum aestivum* L.), confers enhanced multistress tolerance in *Arabidopsis*. *Journal of Experimental Botany*, 61, 683–696.
- Marin, E., Nussaume, L., Quesada, A., Gonneau, M., Sotta, B., Hugueney, P., Frey, A. and Marion-Poll, A.** (1996) Molecular identification of zeaxanthin epoxidase of *Nicotiana plumbaginifolia*, a gene involved in abscisic acid biosynthesis and corresponding to the ABA locus of *Arabidopsis thaliana*. *The EMBO journal*, 15, 2331–2342.
- Marks, C.O. and Lechowicz, M.J.** (2007) The ecological and functional correlates of nocturnal transpiration. *Tree Physiology*, 27, 577–584.
- Maroco, J.P., Pereira, J.S. and Manuela Chaves, M.** (2000) Growth, photosynthesis and water-use efficiency of two C4 Sahelian grasses subjected to water deficits. *Journal of Arid Environments*, 45, 119–137.
- Martin, B., Tauer, C.G. and Lin, R.K.** (1999) Carbon isotope discrimination as a tool to improve water-use efficiency in tomato. *Crop Science*, 39, 1775–1783.
- Masle, J., Gilmore, S.R. and Farquhar, G.D.** (2005) The ERECTA gene regulates plant transpiration efficiency in *Arabidopsis*. *Nature*, 436, 866–870.
- Matos, A.R., Gigon, A., Laffray, D., Petres, S., Zuily-Fodil, Y. and Pham-Thi, A.-T.** (2008) Effects of progressive drought stress on the expression of patatin-like lipid acyl hydrolase genes in *Arabidopsis* leaves. *Physiologia Plantarum*, 134, 110–120.
- Matus, A., Slinkard, A.E. and van Kessel, C.** (1995) Carbon isotope discrimination and indirect selection for seed yield in lentil. *Crop Science*, 35, 679–684.
- Matus, A., Slinkard, A.E. and van Kessel, C.** (1996) Carbon isotope discrimination and indirect selection for transpiration efficiency at flowering in lentil (*Lens culinaris* Medikus), spring bread wheat (*Triticum aestivum* L.) durum wheat (*T. turgidum* L.), and canola (*Brassica napus* L.). *Euphytica*, 87, 141–151.
- Mckay, J.K., Richards, J.H. and Mitchell-Olds, T.** (2003) Genetics of drought adaptation in *Arabidopsis thaliana*. I. Pleiotropy contributes to genetic correlations among ecological traits. *Mol Ecol*, 12, 1137–1151.
- McKay, J.K., Richards, J.H., Nemali, K.S., SEN, S., Mitchell-Olds, T., Boles, S., Stahl, E.A., Wayne, T. and Juenger, T.E.** (2008) Genetics of drought adaptation in *Arabidopsis thaliana* II. QTL analysis of a new mapping population, KAS-1 x TSU-1. *Evolution; international journal of organic evolution*, 62, 3014–3026.
- Medrano, H.** (2002) Regulation of Photosynthesis of C3 Plants in Response to Progressive Drought. Stomatal Conductance as a Reference Parameter. *Annals of Botany*, 89, 895–905.

- Meinzer, F.C., Sharifi, M.R., Nilsen, E.T. and Rundel, P.W.** (1988) Effects of manipulation of water and nitrogen regime on the water relations of the desert shrub *Larrea tridentata*. *Oecologia*, 77, 480–486.
- Melcher, K., Ng, L.-M., Zhou, X.E., Soon, F.-F., Xu, Y., Suino-Powell, K.M., Park, S.-Y., Weiner, J.J., Fujii, H. and Chinnusamy, V.** (2009) A gate–latch–lock mechanism for hormone signalling by abscisic acid receptors. *Nature*, 462, 602–608.
- Merlot, S., Gosti, F., Guerrier, D., Vavasseur, A. and Giraudat, J.** (2001) The ABI1 and ABI2 protein phosphatases 2C act in a negative feedback regulatory loop of the abscisic acid signalling pathway. *The Plant Journal*, 25, 295–303.
- Meyer, S., Mumm, P., Imes, D., Endler, A., Weder, B., Al - Rasheid, K.A.S., Geiger, D., Marten, I., Martinoia, E. and Hedrich, R.** (2010) AtALMT12 represents an R - type anion channel required for stomatal movement in Arabidopsis guard cells. *The Plant Journal*, 63, 1054–1062.
- Mikołajczyk, M., Awotunde, O.S., Muszyńska, G., Klessig, D.F. and Dobrowolska, G.** (2000) Osmotic stress induces rapid activation of a salicylic acid–induced protein kinase and a homolog of protein kinase ASK1 in tobacco cells. *The Plant cell*, 12, 165–178.
- Mitra, J.** (2001) Genetics and genetic improvement of drought resistance in crop plants. *Curr. Sci*, 80, 758–763.
- Mittler, R., Merquiol, E., Hallak - Herr, E., Rachmilevitch, S., Kaplan, A. and Cohen, M.** (2001) Living under a ‘dormant’ canopy: a molecular acclimation mechanism of the desert plant *Retama raetam*. *The Plant Journal*, 25, 407–416.
- Miyazono, K.-i., Miyakawa, T., Sawano, Y., Kubota, K., Kang, H.-J., Asano, A., Miyauchi, Y., Takahashi, M., Zhi, Y. and Fujita, Y.** (2009) Structural basis of abscisic acid signalling. *Nature*, 462, 609–614.
- Monda, K., Negi, J., Iio, A., Kusumi, K., Kojima, M., Hashimoto, M., Sakakibara, H. and Iba, K.** (2011) Environmental regulation of stomatal response in the Arabidopsis Cvi-0 ecotype. *Planta*, 234, 555–563.
- Monneveux, P., Sheshshayee, M.S., Akhter, J. and Ribaut, J.-M.** (2007) Using carbon isotope discrimination to select maize (*Zea mays* L.) inbred lines and hybrids for drought tolerance. *Plant Science*, 173, 390–396.
- Morgan, J.A., LeCain, D.R., McCaig, T.N. and Quick, J.S.** (1993) Gas exchange, carbon isotope discrimination, and productivity in winter wheat. *Crop Science*, 33, 178–186.
- Morgan, J.M.** (1984) Osmoregulation and Water Stress in Higher Plants. *Annu. Rev. Plant. Physiol.*, 35, 299–319.
- Morison, J.I.L., Baker, N.R., Mullineaux, P.M. and Davies, W.J.** (2008) Improving water use in crop production. *Philosophical transactions of the Royal Society of London. Series B, Biological sciences*, 363, 639–658.
- Mualem, Y.** (1976) A new model for predicting the hydraulic conductivity of unsaturated porous media. *Water resources research*, 12, 513–522.
- Munoz, P., Voltas, J., Araus, J.L., Igartua, E. and Romagosa, I.** (1998) Changes over time in the adaptation of barley releases in north-eastern Spain. *Plant Breeding*, 117, 531–535.

- Murray, M.G. and Thompson, W.F.** (1980) Rapid isolation of high molecular weight plant DNA. *Nucleic acids research*, 8, 4321–4326.
- Musselman, R.C. and Minnick, T.J.** (2000) Nocturnal stomatal conductance and ambient air quality standards for ozone. *Atmospheric Environment*, 34, 719–733.
- Mustilli, A.-C.** (2002) Arabidopsis OST1 Protein Kinase Mediates the Regulation of Stomatal Aperture by Abscisic Acid and Acts Upstream of Reactive Oxygen Species Production. *THE PLANT CELL ONLINE*, 14, 3089–3099.
- Mustilli, A.-C., Merlot, S., Vavasseur, A., Fenzi, F. and Giraudat, J.** (2002) Arabidopsis OST1 protein kinase mediates the regulation of stomatal aperture by abscisic acid and acts upstream of reactive oxygen species production. *The Plant cell*, 14, 3089–3099.
- Nakashima, K., Fujita, Y., Kanamori, N., Katagiri, T., Umezawa, T., Kidokoro, S., Maruyama, K., Yoshida, T., Ishiyama, K. and Kobayashi, M.** (2009) Three Arabidopsis SnRK2 protein kinases, SRK2D/SnRK2.2, SRK2E/SnRK2.6/OST1 and SRK2I/SnRK2.3, involved in ABA signaling are essential for the control of seed development and dormancy. *Plant and Cell Physiology*, 50, 1345–1363.
- Nambara, E. and Marion-Poll, A.** (2005) Abscisic acid biosynthesis and catabolism. *Annual review of plant biology*, 56, 165–185.
- Negi, J., Matsuda, O., Nagasawa, T., Oba, Y., Takahashi, H., Kawai-Yamada, M., Uchimiya, H., Hashimoto, M. and Iba, K.** (2008) CO<sub>2</sub> regulator SLAC1 and its homologues are essential for anion homeostasis in plant cells. *Nature*, 452, 483–486.
- Nelson, D.E., Repetti, P.P., Adams, T.R., Creelman, R.A., Wu, J., Warner, D.C., Anstrom, D.C., Bensen, R.J., Castiglioni, P.P., Donnarummo, M.G., Hinchey, B.S., Kumimoto, R.W., Maszle, D.R., Canales, R.D., Krolkowski, K.A., Dotson, S.B., Gutterson, N., Ratcliffe, O.J. and Heard, J.E.** (2007) Plant nuclear factor Y (NF-Y) B subunits confer drought tolerance and lead to improved corn yields on water-limited acres. *Proceedings of the National Academy of Sciences of the United States of America*, 104, 16450–16455.
- Ngugi, E.C., Galwey, N.W. and Austin, R.B.** (1993) Genotype × environment interaction in carbon isotope discrimination and seed yield in cowpea (*Vigna unguiculata* L. Walp.). *Euphytica*, 73, 213–224.
- Nishimura, N., Hitomi, K., Arvai, A.S., Rambo, R.P., Hitomi, C., Cutler, S.R., Schroeder, J.I. and Getzoff, E.D.** (2009) Structural mechanism of abscisic acid binding and signaling by dimeric PYR1. *Science*, 326, 1373–1379.
- Nishimura, N., Yoshida, T., Kitahata, N., Asami, T., Shinozaki, K. and Hirayama, T.** (2007) ABA-Hypersensitive Germination1 encodes a protein phosphatase 2C, an essential component of abscisic acid signaling in Arabidopsis seed. *The Plant journal : for cell and molecular biology*, 50, 935–949.
- North, H.M., Almeida, A. de, Boutin, J.-P., Frey, A., To, A., Botran, L., Sotta, B. and Marion-Poll, A.** (2007) The Arabidopsis ABA-deficient mutant *aba4* demonstrates that the major route for stress-induced ABA accumulation is via neoxanthin isomers. *The Plant journal : for cell and molecular biology*, 50, 810–824.
- Nunes, M.A., Bierhuizen, J.F. and Ploegman, C.** (1968) STUDIES ON PRODUCTIVITY



- OF COFFEE. I. EFFECT OF LIGHT, TEMPERATURE AND CO<sub>2</sub> CONCENTRATION ON PHOTOSYNTHESIS OF COFFEA ARABICA. *Acta Botanica Neerlandica*, 17, 93–102.
- Okamoto, M., Tanaka, Y., Abrams, S.R., Kamiya, Y., Seki, M. and Nambara, E.** (2009) High humidity induces abscisic acid 8'-hydroxylase in stomata and vasculature to regulate local and systemic abscisic acid responses in Arabidopsis. *PLANT PHYSIOLOGY*, 149, 825–834.
- Oki, T. and Kanae, S.** (2006) Global hydrological cycles and world water resources. *Science (New York, N.Y.)*, 313, 1068–1072.
- Ortiz-Masia, D., Perez-Amador, M.A., Carbonell, J. and Marcote, M.J.** (2007) Diverse stress signals activate the C1 subgroup MAP kinases of Arabidopsis. *FEBS letters*, 581, 1834–1840.
- Park, J.-J., Jin, P., Yoon, J., Yang, J.-I., Jeong, H.J., Ranathunge, K., Schreiber, L., Franke, R., Lee, I.-J. and An, G.** (2010) Mutation in Wilted Dwarf and Lethal 1 (WDL1) causes abnormal cuticle formation and rapid water loss in rice. *Plant molecular biology*, 74, 91–103.
- Park, R. and Epstein, S.** (1960) Carbon isotope fractionation during photosynthesis. *Geochimica et Cosmochimica Acta*, 21, 110–126.
- Park, R. and Epstein, S.** (1961) Metabolic fractionation of C(13) & C(12) in plants. *PLANT PHYSIOLOGY*, 36, 133–138.
- Park, S.-Y., Fung, P., Nishimura, N., Jensen, D.R., Fujii, H., Zhao, Y., Lumba, S., Santiago, J., Rodrigues, A., Chow, T.-F.F., Alfred, S.E., Bonetta, D., Finkelstein, R., Provart, N.J., Desveaux, D., Rodriguez, P.L., McCourt, P., Zhu, J.-K., Schroeder, J.I., Volkman, B.F. and Cutler, S.R.** (2009) Abscisic acid inhibits type 2C protein phosphatases via the PYR/PYL family of START proteins. *Science (New York, N.Y.)*, 324, 1068–1071.
- Park, S.-Y., Peterson, F.C., Mosquna, A., Yao, J., Volkman, B.F. and Cutler, S.R.** (2015) Agrochemical control of plant water use using engineered abscisic acid receptors. *Nature*, 520, 545–548.
- Parkhurst, D.F. and Gates, D.M.** (1966) Transpiration resistance and energy budget of *Populus sargentii* leaves. *Nature*, 210, 172–174.
- Pei, Z.** (1998) Role of Farnesyltransferase in ABA Regulation of Guard Cell Anion Channels and Plant Water Loss. *Science*, 282, 287–290.
- Pilot, G., Lacombe, B., Gaymard, F., Chérel, I., Boucherez, J., Thibaud, J.-B. and Sentenac, H.** (2001) Guard Cell Inward K<sup>+</sup> Channel Activity in Arabidopsis Involves Expression of the Twin Channel Subunits KAT1 and KAT2. *Journal of Biological Chemistry*, 276, 3215–3221.
- Pimentel, D., Berger, B., Filiberto, D., Newton, M., Wolfe, B., Karabinakis, E., Clark, S., Poon, E., Abbett, E. and Nandagopal, S.** (2004) Water resources: agricultural and environmental issues. *BioScience*, 54, 909–918.
- Pinheiro, C. and Chaves, M.M.** (2011) Photosynthesis and drought: can we make metabolic connections from available data? *Journal of Experimental Botany*, 62, 869–882.
- Pizzio, G.A., Rodriguez, L., Antoni, R., Gonzalez-Guzman, M., Yunta, C., Merilo, E., Kollist, H., Albert, A. and Rodriguez, P.L.** (2013a) The PYL4 A194T mutant

- uncovers a key role of PYR1-LIKE4/PROTEIN PHOSPHATASE 2CA interaction for abscisic acid signaling and plant drought resistance. *PLANT PHYSIOLOGY*, 163, 441–455.
- Pizzio, G.A., Rodriguez, L., Antoni, R., Gonzalez-Guzman, M., Yunta, C., Merilo, E., Kollist, H., Albert, A. and Rodriguez, P.L.** (2013b) The PYL4 A194T mutant uncovers a key role of PYR1-LIKE4/PROTEIN PHOSPHATASE 2CA interaction for abscisic acid signaling and plant drought resistance. *PLANT PHYSIOLOGY*, 163, 441–455.
- Pons, T.L., Flexas, J., Caemmerer, S. von, Evans, J.R., Genty, B., Ribas-Carbo, M. and Brugnoli, E.** (2009) Estimating mesophyll conductance to CO<sub>2</sub>: methodology, potential errors, and recommendations. *Journal of Experimental Botany*, erp081.
- Poorter, H. and Nagel, O.** (2000) The role of biomass allocation in the growth response of plants to different levels of light, CO<sub>2</sub>, nutrients and water. A quantitative review. *Aust J Plant Physio.*, 27, 1191.
- Qin, X. and Zeevaart, J.A.D.** (1999) The 9-cis-epoxycarotenoid cleavage reaction is the key regulatory step of abscisic acid biosynthesis in water-stressed bean. *Proceedings of the National Academy of Sciences*, 96, 15354–15361.
- Raghavendra, A.S., Gonugunta, V.K., Christmann, A. and Grill, E.** (2010) ABA perception and signalling. *Trends in plant science*, 15, 395–401.
- Ranney, T.G., Bir, R.E. and Skroch, W.A.** (1991) Comparative drought resistance among six species of birch (*Betula*). Influence of mild water stress on water relations and leaf gas exchange. *Tree Physiology*, 8, 351–360.
- Raschke, K.** (1970) Stomatal Responses to Pressure Changes and Interruptions in the Water Supply of Detached Leaves of *Zea mays* L. *PLANT PHYSIOLOGY*, 45, 415–423.
- Rawson, H.M. and Clarke, J.M.** (1988) Nocturnal Transpiration in Wheat. *Aust J Plant Physio.*, 15, 397.
- Ray, D.K., Ramankutty, N., Mueller, N.D., West, P.C. and Foley, J.A.** (2012) Recent patterns of crop yield growth and stagnation. *Nature communications*, 3, 1293.
- Rebetzke, G.J., Condon, A.G., Farquhar, G.D., Appels, R. and Richards, R.A.** (2008) Quantitative trait loci for carbon isotope discrimination are repeatable across environments and wheat mapping populations. *TAG. Theoretical and applied genetics. Theoretische und angewandte Genetik*, 118, 123–137.
- Rebetzke, G.J., Condon, A.G., Richards, R.A. and Farquhar, G.D.** (2002) Selection for Reduced Carbon Isotope Discrimination Increases Aerial Biomass and Grain Yield of Rainfed Bread Wheat. *Crop Science*, 42, 739.
- Riboni, M., Galbiati, M., Tonelli, C. and Conti, L.** (2013) GIGANTEA enables drought escape response via abscisic acid-dependent activation of the florigens and SUPPRESSOR OF OVEREXPRESSION OF CONSTANS. *PLANT PHYSIOLOGY*, 162, 1706–1719.
- Riccardi, F., Gazeau, P., Vienne, D. de and Zivy, M.** (1998) Protein changes in response to progressive water deficit in maize quantitative variation and polypeptide identification. *PLANT PHYSIOLOGY*, 117, 1253–1263.
- Richards, J.H. and Caldwell, M.M.** (1987) Hydraulic lift: substantial nocturnal water

- transport between soil layers by *Artemisia tridentata* roots. *Oecologia*, 73, 486–489.
- Riederer, M. and Schreiber, L.** (2001) Protecting against water loss: analysis of the barrier properties of plant cuticles. *Journal of Experimental Botany*, 52, 2023–2032.
- Ristic, Z. and Cass, D.D.** (1991) Leaf Anatomy of *Zea mays* L. in Response to Water Shortage and High Temperature. A Comparison of Drought-Resistant and Drought-Sensitive Lines. *Botanical Gazette*, 152, 173–185.
- Rizza, F., Badeck, F.W., Cattivelli, L., Lidestri, O., Di Fonzo, N. and Stanca, A.M.** (2004) Use of a Water Stress Index to Identify Barley Genotypes Adapted to Rainfed and Irrigated Conditions. *Crop Science*, 44, 2127.
- Rizza, F., Ghashghaie, J., Meyer, S., Matteu, L., Mastrangelo, A.M. and Badeck, F.-W.** (2012) Constitutive differences in water use efficiency between two durum wheat cultivars. *Field Crops Research*, 125, 49–60.
- Robert, N., Merlot, S., N'guyen, V., Boisson-Dernier, A. and Schroeder, J.I.** (2006) A hypermorphic mutation in the protein phosphatase 2C HAB1 strongly affects ABA signaling in *Arabidopsis*. *FEBS letters*, 580, 4691–4696.
- Rodrigues, M.L., Pacheco, C. and Chaves, M.M.** (1995) Soil-plant water relations, root distribution and biomass partitioning in *Lupinus albus* L. under drought conditions. *J Exp Bot*, 46, 947–956.
- Roelfsema, M.R.G. and Hedrich, R.** (2005) In the light of stomatal opening: new insights into 'the Watergate'. *The New phytologist*, 167, 665–691.
- Roelfsema, M.R.G., Levchenko, V. and Hedrich, R.** (2004) ABA depolarizes guard cells in intact plants, through a transient activation of R<sup>-</sup> and S<sup>-</sup> type anion channels. *The Plant Journal*, 37, 578–588.
- Rubio, S., Rodrigues, A., Saez, A., Dizon, M.B., Galle, A., Kim, T.-H., Santiago, J., Flexas, J., Schroeder, J.I. and Rodriguez, P.L.** (2009) Triple loss of function of protein phosphatases type 2C leads to partial constitutive response to endogenous abscisic acid. *PLANT PHYSIOLOGY*, 150, 1345–1355.
- Saez, A., Robert, N., Maktabi, M.H., Schroeder, J.I., Serrano, R. and Rodriguez, P.L.** (2006) Enhancement of abscisic acid sensitivity and reduction of water consumption in *Arabidopsis* by combined inactivation of the protein phosphatases type 2C ABI1 and HAB1. *PLANT PHYSIOLOGY*, 141, 1389–1399.
- Sam, O., Jerez, E., Dell'Amico, J. and Ruiz-Sanchez, M.C.** (2000) Water stress induced changes in anatomy of tomato leaf epidermes. *Biologia Plantarum*, 43, 275–277.
- Sambrook, J. and Russell, D.W.** (2001) Molecular cloning: a laboratory manual 3rd edition. *Coldspring-Harbour Laboratory Press, UK*.
- Santiago, J., Dupeux, F., Round, A., Antoni, R., Park, S.-Y., Jamin, M., Cutler, S.R., Rodriguez, P.L. and Márquez, J.A.** (2009) The abscisic acid receptor PYR1 in complex with abscisic acid. *Nature*, 462, 665–668.
- Santiago, J., Rodrigues, A., Saez, A., Rubio, S., Antoni, R., Dupeux, F., Park, S., Márquez, J.A., Cutler, S.R. and Rodriguez, P.L.** (2009) Modulation of drought resistance by the abscisic acid receptor PYL5 through inhibition of clade A PP2Cs. *The Plant Journal*, 60, 575–588.

- Saranga, Y., Jiang, C., Wright, R.J., Yakir, D. and Paterson, A.H.** (2004) Genetic dissection of cotton physiological responses to arid conditions and their inter-relationships with productivity. *Plant, cell & environment*, 27, 263–277.
- Sato, A., Sato, Y., Fukao, Y., Fujiwara, M., Umezawa, T., Shinozaki, K., Hibi, T., Taniguchi, M., Miyake, H., Goto, D.B. and Uozumi, N.** (2009) Threonine at position 306 of the KAT1 potassium channel is essential for channel activity and is a target site for ABA-activated SnRK2/OST1/SnRK2.6 protein kinase. *The Biochemical journal*, 424, 439–448.
- Saurer, M., Aellen, K. and Siegwolf, R.** (1997) Correlating  $\delta^{13}\text{C}$  and  $\delta^{18}\text{O}$  in cellulose of trees. *Plant, cell & environment*, 20, 1543–1550.
- Saxton, K.E., Rawls, W., Romberger, J.S. and Papendick, R.I.** (1986) Estimating generalized soil-water characteristics from texture. *Soil Science Society of America Journal*, 50, 1031–1036.
- Sayre, K.D., Acevedo, E. and Austin, R.B.** (1995) Carbon isotope discrimination and grain yield for three bread wheat germplasm groups grown at different levels of water stress. *Field Crops Research*, 41, 45–54.
- Schmidt, H.-L., Werner, R.A. and Roßmann, A.** (2001)  $^{18}\text{O}$  pattern and biosynthesis of natural plant products. *Phytochemistry*, 58, 9–32.
- Schnyder, H., Schäufele, R., Lötscher, M. and Gebbing, T.** (2003) Disentangling  $\text{CO}_2$  fluxes: Direct measurements of mesocosm-scale natural abundance  $^{13}\text{CO}_2/^{12}\text{CO}_2$  gas exchange,  $^{13}\text{C}$  discrimination, and labelling of  $\text{CO}_2$  exchange flux components in controlled environments. *Plant, cell & environment*, 26, 1863–1874.
- Schwabe, W.W.** (1952) Effects of photoperiodic treatment on stomatal movement.
- Schwartz, S.H., Qin, X. and Zeevaart, J.A.** (2001) Characterization of a novel carotenoid cleavage dioxygenase from plants. *The Journal of biological chemistry*, 276, 25208–25211.
- Schwartz, S.H., Qin, X. and Zeevaart, J.A.D.** (2003) Elucidation of the indirect pathway of abscisic acid biosynthesis by mutants, genes, and enzymes. *PLANT PHYSIOLOGY*, 131, 1591–1601.
- Schweighofer, A., Hirt, H. and Meskiene, I.** (2004) Plant PP2C phosphatases: emerging functions in stress signaling. *Trends in plant science*, 9, 236–243.
- Semagn, K., Bjørnstad, Å. and Ndjioudjop, M.N.** (2006) Principles, requirements and prospects of genetic mapping in plants. *African Journal of Biotechnology*, 5, 2569–2587.
- Sharipova, G., Veselov, D., Kudoyarova, G., Fricke, W., Dodd, I.C., Katsuhara, M., Furuichi, T., Ivanov, I. and Veselov, S.** (2016) Exogenous application of abscisic acid (ABA) increases root and cell hydraulic conductivity and abundance of some aquaporin isoforms in the ABA-deficient barley mutant Az34. *Annals of Botany*.
- Sharkey, T.D., Bernacchi, C.J., Farquhar, G.D. and Singsaas, E.L.** (2007) Fitting photosynthetic carbon dioxide response curves for C(3) leaves. *Plant, cell & environment*, 30, 1035–1040.
- Sharma, P.D.** (2009) *Ecology and environment*. Meerut: Rastogi Publications.
- Sharp, R.E. and Davies, W.J.** (1985) Root growth and water uptake by maize plants in drying soil. *Journal of Experimental Botany*, 36, 1441–1456.

- Sherrard, M.E. and Maherali, H.** (2006) THE ADAPTIVE SIGNIFICANCE OF DROUGHT ESCAPE IN AVENA BARBATA, AN ANNUAL GRASS. *Evol*, 60, 2478.
- Sheshshayee, M.S., Bindumadhava, H., Ramesh, R., Prasad, T.G., Lakshminarayana, M.R. and Udayakumar, M.** (2005) Oxygen isotope enrichment ( $\delta^{18}\text{O}$ ) as a measure of time-averaged transpiration rate. *Journal of Experimental Botany*, 56, 3033–3039.
- Siddique, T., Okeke, B.C., Arshad, M. and Frankenberger, W.T., JR** (2003) Enrichment and isolation of endosulfan-degrading microorganisms. *Journal of environmental quality*, 32, 47–54.
- Silva, L., Pedroso, G., Doane, T.A., Mukome, F. and Horwath, W.R.** (2015) Beyond the cellulose. Oxygen isotope composition of plant lipids as a proxy for terrestrial water balance. *Geochem. Persp. Let.*, 33–42.
- Simon, M., Loudet, O., Durand, S., Berard, A., Brunel, D., Sennesal, F.-X., Durand-Tardif, M., Pelletier, G. and Camilleri, C.** (2008) Quantitative trait loci mapping in five new large recombinant inbred line populations of *Arabidopsis thaliana* genotyped with consensus single-nucleotide polymorphism markers. *Genetics*, 178, 2253–2264.
- Skidmore, E.L. and Stone, J.F.** (1964) Physiological role in regulating transpiration rate of the cotton plant. *Agronomy Journal*, 56, 405–410.
- Skiryicz, A., Vandenbroucke, K., Clauw, P., Maleux, K., Meyer, B. de, Dhondt, S., Pucci, A., Gonzalez, N., Hoeberichts, F., Tognetti, V.B., Galbiati, M., Tonelli, C., van Breusegem, F., Vuylsteke, M. and Inzé, D.** (2011) Survival and growth of *Arabidopsis* plants given limited water are not equal. *Nat Biotechnol*, 29, 212–214.
- Smith, B.N., Oliver, J. and Millan, C.M.** (1976) Influence of carbon source, oxygen concentration, light intensity, and temperature on  $^{13}\text{C}/^{12}\text{C}$  ratios in plant tissues. *Botanical Gazette*, 99–104.
- Smith-Espinoza, C.J., Richter, A., Salamini, F. and Bartels, D.** (2003) Dissecting the response to dehydration and salt (NaCl) in the resurrection plant *Craterostigma plantagineum*. *Plant Cell Environ*, 26, 1307–1315.
- Tischer, S.V. (2016)** "Charakterisierung der Abscisinsäure-Rezeptorkomplexe in *Arabidopsis thaliana*". (Characterization of abscisic acid receptor complexes in *Arabidopsis thaliana*). *Dissertation from Technical University of Munich.*, 65-69 and 117-154
- Steudle, E.** (2000) Water uptake by roots. Effects of water deficit. *Journal of Experimental Botany*, 51, 1531–1542.
- Sunkar, R., Bartels, D. and Kirch, H.-H.** (2003) Overexpression of a stress-inducible aldehyde dehydrogenase gene from *Arabidopsis thaliana* in transgenic plants improves stress tolerance. *The Plant journal : for cell and molecular biology*, 35, 452–464.
- Szostkiewicz, I., Richter, K., Kepka, M., Demmel, S., Ma, Y., Korte, A., Assaad, F.F., Christmann, A. and Grill, E.** (2010) Closely related receptor complexes differ in their ABA selectivity and sensitivity. *The Plant Journal*, 61, 25–35.
- Takahashi, T., Yamamoto, K., Senda, Y. and Tsuzuku, M.** (2005) Predicting individual stem volumes of sugi (*Cryptomeria japonica* D. Don) plantations in mountainous

- areas using small-footprint airborne LiDAR. *J For Res*, 10, 305–312.
- Tan, B., Joseph, L.M., Deng, W., Liu, L., Li, Q., Cline, K. and McCarty, D.R.** (2003) Molecular characterization of the Arabidopsis 9 - cis epoxy-carotenoid dioxygenase gene family. *The Plant Journal*, 35, 44–56.
- Tanaka, Y., Sano, T., Tamaoki, M., Nakajima, N., Kondo, N. and Hasezawa, S.** (2005) Ethylene inhibits abscisic acid-induced stomatal closure in Arabidopsis. *PLANT PHYSIOLOGY*, 138, 2337–2343.
- Tardieu, F.** (1996) Drought perception by plants Do cells of droughted plants experience water stress? *Plant Growth Regul*, 20, 93–104.
- Tardieu, F.** (2011) Any trait or trait-related allele can confer drought tolerance. Just design the right drought scenario. *Journal of Experimental Botany*, 63, 25–31.
- Tardieu, F. and Simonneau, T.** (1998) Variability among species of stomatal control under fluctuating soil water status and evaporative demand. Modelling isohydric and anisohydric behaviours. *Journal of Experimental Botany*, 49, 419–432.
- Teige, M., Scheikl, E., Eulgem, T., Doczi, R., Ichimura, K., Shinozaki, K., Dangl, J.L. and Hirt, H.** (2004) The MKK2 pathway mediates cold and salt stress signaling in Arabidopsis. *Molecular cell*, 15, 141–152.
- Teoh, C.T. and Palmer, J.H.** (1971) Nonsynchronized Oscillations in Stomatal Resistance among Sclerophylls of Eucalyptus umbra. *PLANT PHYSIOLOGY*, 47, 409–411.
- Tessmer, O.L., Jiao, Y., Cruz, J.A., Kramer, D.M. and Chen, J.** (2013) Functional approach to high-throughput plant growth analysis. *BMC systems biology*, 7, 1.
- Thiel, S., Döhring, T., Köfferlein, M., Kosak, A., Martin, P. and Seidlitz, H.K.** (1996) A Phytotron for Plant Stress Research. How Far Can Artificial Lighting Compare to Natural Sunlight? *Journal of plant physiology*, 148, 456–463.
- Thompson, A.J., Jackson, A.C., Parker, R.A., Morpeth, D.R., Burbidge, A. and Taylor, I.B.** (2000) Abscisic acid biosynthesis in tomato: regulation of zeaxanthin epoxidase and 9-cis-epoxy-carotenoid dioxygenase mRNAs by light/dark cycles, water stress and abscisic acid. *Plant molecular biology*, 42, 833–845.
- Torrecillas, A., Galego, R., Pérez-Pastor, A. and Ruiz-Sánchez, M.C.** (1999) Gas exchange and water relations of young apricot plants under drought conditions. *The Journal of Agricultural Science*, 132, 445–452.
- Turnbull, C.G.N., Booker, J.P. and Leyser, H.M.O.** (2002) Micrografting techniques for testing long-distance signalling in Arabidopsis. *The Plant journal : for cell and molecular biology*, 32, 255–262.
- Turner, N.** *Drought resistance and adaptation to water deficits in crop plants.*
- Turner, N., ed.** (1986) *Advances in Agronomy Volume 39*: Elsevier.
- Turner, N.C., Wright, G.C. and Siddique, K.** (2001) Adaptation of grain legumes (pulses) to water-limited environments (Turner, N., ed): Elsevier, pp. 193–231.
- Umezawa, T., Nakashima, K., Miyakawa, T., Kuromori, T., Tanokura, M., Shinozaki, K. and Yamaguchi-Shinozaki, K.** (2010) Molecular basis of the core regulatory network in ABA responses: sensing, signaling and transport. *Plant & cell physiology*, 51, 1821–1839.
- Umezawa, T., Sugiyama, N., Mizoguchi, M., Hayashi, S., Myouga, F.,**

- Yamaguchi-Shinozaki, K., Ishihama, Y., Hirayama, T. and Shinozaki, K.** (2009) Type 2C protein phosphatases directly regulate abscisic acid-activated protein kinases in Arabidopsis. *Proceedings of the National Academy of Sciences of the United States of America*, 106, 17588–17593.
- Umezawa, T., Sugiyama, N., Takahashi, F., Anderson, J.C., Ishihama, Y., Peck, S.C. and Shinozaki, K.** (2013) Genetics and phosphoproteomics reveal a protein phosphorylation network in the abscisic acid signaling pathway in Arabidopsis thaliana. *Sci. Signal.*, 6, rs8-rs8.
- Vahisalu, T., Kollist, H., Wang, Y.-F., Nishimura, N., Chan, W.-Y., Valerio, G., Lamminmaki, A., Brosche, M., Moldau, H., Desikan, R., Schroeder, J.I. and Kangasjarvi, J.** (2008) SLAC1 is required for plant guard cell S-type anion channel function in stomatal signalling. *Nature*, 452, 487–491.
- Vahisalu, T., Kollist, H., Wang, Y.-F., Nishimura, N., Chan, W.-Y., Valerio, G., Lamminmäki, A., Brosché, M., Moldau, H. and Desikan, R.** (2008) SLAC1 is required for plant guard cell S-type anion channel function in stomatal signalling. *Nature*, 452, 487–491.
- Valdés, A.E., Övernäs, E., Johansson, H., Rada-Iglesias, A. and Engström, P.** (2012) The homeodomain-leucine zipper (HD-Zip) class I transcription factors ATHB7 and ATHB12 modulate abscisic acid signalling by regulating protein phosphatase 2C and abscisic acid receptor gene activities. *Plant molecular biology*, 80, 405–418.
- van den Honert, T. H.** (1948) Water transport in plants as a catenary process. *Discuss. Faraday Soc.*, 3, 146.
- Wall, G.W., Brooks, T.J., Adam, N.R., Cousins, A.B., Kimball, B.A., Pinter, P.J., LaMorte, R.L., Triggs, J., Ottman, M.J., Leavitt, S.W., Matthias, A.D., Williams, D.G. and Webber, A.N.** (2001) Elevated atmospheric CO<sub>2</sub> improved Sorghum plant water status by ameliorating the adverse effects of drought. *New Phytol*, 152, 231–248.
- Wang, B., Qin, X., Wu, J., Deng, H., Li, Y., Yang, H., Chen, Z., Liu, G. and Ren, D.** (2016) Analysis of crystal structure of Arabidopsis MPK6 and generation of its mutants with higher activity. *Scientific reports*, 6, 25646.
- Wang, H., Ngwenyama, N., Liu, Y., Walker, J.C. and Zhang, S.** (2007) Stomatal development and patterning are regulated by environmentally responsive mitogen-activated protein kinases in Arabidopsis. *The Plant cell*, 19, 63–73.
- Wang, Z.-Y., Xiong, L., Li, W., Zhu, J.-K. and Zhu, J.** (2011) The plant cuticle is required for osmotic stress regulation of abscisic acid biosynthesis and osmotic stress tolerance in Arabidopsis. *The Plant cell*, 23, 1971–1984.
- Warren, C.R. and Dreyer, E.** (2006) Temperature response of photosynthesis and internal conductance to CO<sub>2</sub>: results from two independent approaches. *Journal of Experimental Botany*, 57, 3057–3067.
- Wasilewska, A., Vlad, F., Sirichandra, C., Redko, Y., Jammes, F., Valon, C., Frei dit Frey, N. and Leung, J.** (2008) An update on abscisic acid signaling in plants and more. *Molecular plant*, 1, 198–217.
- Weigel, D.** (2012) Natural variation in Arabidopsis: from molecular genetics to ecological genomics. *PLANT PHYSIOLOGY*, 158, 2–22.

- Went, F.W.** (1944) Plant Growth Under Controlled Conditions. II. Thermoperiodicity in Growth and Fruiting of the Tomato. *American Journal of Botany*, 31, 135–150.
- Weraduwage, S.M., Chen, J., Anozie, F.C., Morales, A., Weise, S.E. and Sharkey, T.D.** (2015) The relationship between leaf area growth and biomass accumulation in *Arabidopsis thaliana*. *Frontiers in plant science*, 6, 167.
- Werner, C., Schnyder, H., Cuntz, M., Keitel, C., Zeeman, M.J., Dawson, T.E., Badeck, F.-W., Brugnoli, E., Ghashghaie, J., Grams, T.E.E., Kayler, Z.E., Lakatos, M., Lee, X., Máguas, C., Ogée, J., Rascher, K.G., Siegwolf, R.T.W., Unger, S., Welker, J., Wingate, L. and Gessler, A.** (2012) Progress and challenges in using stable isotopes to trace plant carbon and water relations across scales. *Biogeosciences*, 9, 3083–3111.
- White, J.W., Castillo, J.A. and Ehleringer, J.** (1990) Associations between productivity, root growth and carbon isotope discrimination in *Phaseolus vulgaris* under water deficit. *Functional Plant Biology*, 17, 189–198.
- Wilhite, D.A. and Glantz, M.H.** (1985) Understanding. The Drought Phenomenon: The Role of Definitions. *Water International*, 10, 111–120.
- Wilkins, O., Brautigam, K. and Campbell, M.M.** (2010) Time of day shapes *Arabidopsis* drought transcriptomes. *The Plant journal : for cell and molecular biology*, 63, 715–727.
- Xiao, F., Goodwin, S.M., Xiao, Y., Sun, Z., Baker, D., Tang, X., Jenks, M.A. and Zhou, J.-M.** (2004) *Arabidopsis* CYP86A2 represses *Pseudomonas syringae* type III genes and is required for cuticle development. *The EMBO journal*, 23, 2903–2913.
- Xin, Z., Franks, C., Payton, P. and Burke, J.J.** (2008) A simple method to determine transpiration efficiency in sorghum. *Field Crops Research*, 107, 180–183.
- Xing, Y., Jia, W. and Zhang, J.** (2007) AtMEK1 mediates stress-induced gene expression of CAT1 catalase by triggering H<sub>2</sub>O<sub>2</sub> production in *Arabidopsis*. *Journal of Experimental Botany*, 58, 2969–2981.
- Xing, Y., Jia, W. and Zhang, J.** (2008) AtMKK1 mediates ABA-induced CAT1 expression and H<sub>2</sub>O<sub>2</sub> production via AtMPK6-coupled signaling in *Arabidopsis*. *The Plant journal : for cell and molecular biology*, 54, 440–451.
- Xiong, L.** (2003) Regulation of Abscisic Acid Biosynthesis. *PLANT PHYSIOLOGY*, 133, 29–36.
- Xu, J.L., Lafitte, H.R., Gao, Y.M., Fu, B.Y., Torres, R. and Li, Z.K.** (2005) QTLs for drought escape and tolerance identified in a set of random introgression lines of rice. *TAG. Theoretical and applied genetics. Theoretische und angewandte Genetik*, 111, 1642–1650.
- Xu, X., Martin, B., Comstock, J.P., Vision, T.J., Tauer, C.G., Zhao, B., Pausch, R.C. and Knapp, S.** (2008) Fine mapping a QTL for carbon isotope composition in tomato. *TAG. Theoretical and applied genetics. Theoretische und angewandte Genetik*, 117, 221–233.
- Xu, Y., This, D., Pausch, R.C., Vonhof, W.M., Coburn, J.R., Comstock, J.P. and McCouch, S.R.** (2009) Leaf-level water use efficiency determined by carbon isotope discrimination in rice seedlings: genetic variation associated with population structure and QTL mapping. *TAG. Theoretical and applied genetics*.



- Theoretische und angewandte Genetik*, 118, 1065–1081.
- Xu, Z.-Y., Lee, K.H., Dong, T., Jeong, J.C., Jin, J.B., Kanno, Y., Kim, D.H., Kim, S.Y., Seo, M., Bressan, R.A., Yun, D.-J. and Hwang, I.** (2012) A vacuolar beta-glucosidase homolog that possesses glucose-conjugated abscisic acid hydrolyzing activity plays an important role in osmotic stress responses in Arabidopsis. *The Plant cell*, 24, 2184–2199.
- Yakir, D. and Sternberg, L. da S. L.** (2000) The use of stable isotopes to study ecosystem gas exchange. *Oecologia*, 123, 297–311.
- Yang, J., Zhang, J., Wang, Z., Zhu, Q. and Wang, W.** (2001) Remobilization of carbon reserves in response to water deficit during grain filling of rice. *Field Crops Research*, 71, 47–55.
- Yin, P., Fan, H., Hao, Q., Yuan, X., Di Wu, Pang, Y., Yan, C., Li, W., Wang, J. and Yan, N.** (2009) Structural insights into the mechanism of abscisic acid signaling by PYL proteins. *Nature structural & molecular biology*, 16, 1230–1236.
- Yoo, C.Y., Pence, H.E., Jin, J.B., Miura, K., Gosney, M.J., Hasegawa, P.M. and Mickelbart, M.V.** (2010) The Arabidopsis GTL1 transcription factor regulates water use efficiency and drought tolerance by modulating stomatal density via transrepression of SDD1. *The Plant cell*, 22, 4128–4141.
- Yoshida, R.** (2002) ABA-Activated SnRK2 Protein Kinase is Required for Dehydration Stress Signaling in Arabidopsis. *Plant and Cell Physiology*, 43, 1473–1483.
- Yoshida, R., Umezawa, T., Mizoguchi, T., Takahashi, S., Takahashi, F. and Shinozaki, K.** (2006) The regulatory domain of SRK2E/OST1/SnRK2.6 interacts with ABI1 and integrates abscisic acid (ABA) and osmotic stress signals controlling stomatal closure in Arabidopsis. *The Journal of biological chemistry*, 281, 5310–5318.
- Yoshida, T., Fujita, Y., Sayama, H., Kidokoro, S., Maruyama, K., Mizoi, J., Shinozaki, K. and Yamaguchi-Shinozaki, K.** (2010) AREB1, AREB2, and ABF3 are master transcription factors that cooperatively regulate ABRE-dependent ABA signaling involved in drought stress tolerance and require ABA for full activation. *The Plant journal : for cell and molecular biology*, 61, 672–685.
- Yoshida, T., Mogami, J. and Yamaguchi-Shinozaki, K.** (2014) ABA-dependent and ABA-independent signaling in response to osmotic stress in plants. *Current opinion in plant biology*, 21, 133–139.
- Zhang, X., Hause, R.J. and Borevitz, J.O.** (2012) Natural genetic variation for growth and development revealed by high-throughput phenotyping in Arabidopsis thaliana. *G3: Genes Genomes/Genetics*, 2, 29–34.
- Zhao, Y., Chan, Z., Gao, J., Xing, L., Cao, M., Yu, C., Hu, Y., You, J., Shi, H., Zhu, Y., Gong, Y., Mu, Z., Wang, H., Deng, X., Wang, P., Bressan, R.A. and Zhu, J.-K.** (2016) ABA receptor PYL9 promotes drought resistance and leaf senescence. *Proceedings of the National Academy of Sciences of the United States of America*, 113, 1949–1954.
- Zhou, J., Wang, X., Jiao, Y., Qin, Y., Liu, X., He, K., Chen, C., Ma, L., Wang, J., Xiong, L., Zhang, Q., Fan, L. and Deng, X.W.** (2007) Global genome expression analysis of rice in response to drought and high-salinity stresses in shoot, flag leaf, and panicle. *Plant molecular biology*, 63, 591–608.

- Zhu, X.-G., Long, S.P. and Ort, D.R.** (2008) What is the maximum efficiency with which photosynthesis can convert solar energy into biomass? *Current opinion in biotechnology*, 19, 153–159.

---



# Acknowledgements

My Ph.D. study was performed in the laboratory of Prof. Dr. Erwin Grill in the Institute of Botany, Technical University of Munich. I would like to express my special appreciation and thanks to my supervisor Prof. Dr. Erwin Grill for providing me the opportunity to work in his laboratory and carry on this very interesting research project, and for his stimulating advice and constructive criticism during the years of my Ph.D. research, and for working overtime till 12 o'clock on preparing and submitting the publication, and for the critical reading for this manuscript, and translation of the summary into German.

I would also like to thank Prof. Dr. Kay Schneitz and Prof. Dr. Ramon A. Torres Ruiz for participation in my committee.

Special thanks would also give to Dr. Alexander Christmann who gave a lot of help and valuable suggestions on some of my experiments, within which the most impressive one is working the whole day for generating the grafts. I would also like to thank Dr. Farhah Assaad for her critical reading constructive comments for the manuscript of the PNAS.

I have been blessed with a friendly and nice group. They give me a lot of help and support during my Ph.D. years. I would specially thank Stefanie Tischer for generating the valuable germplasms - overexpressing RCAR lines, and Jinghui Liu for her help in conducting the progressive drought experiments, and Christian Kornbauer, Christoph Heidersberger and Eltschig Claudia for their teaching and doing gene cloning, and our gardeners - Michael Schmidt, Held Lisa and Caroline Klaus - for the daily management of plants, and Josef Reischenbeck for making some facilities for our experiments. Special thank would also give to Annelie Welker, Stefanie Tischer and Michael Papacek who did the proofreading for some parts of my thesis and gave a lot of useful suggestions. I would also like to thank Moritz Ruschhaupt for his timely help in answering statistic questions from the journal, and Kowalski Natalie for her help in submitting the dissertation, and Dr. Jin Huang and Ting Cao for their help during the first two years of my Ph.D. research.

I would like to thank Beate Seelinger, Schubert, Ulrike and Bernehrer, Lisa-Marie for their help in daily life and bureaucracy.

I am also very grateful to Prof. Dr. Hans Schnyder and Dr. Rudi Schäufele from Lehrstuhl für Grünlandlehre for providing experimental space and facilities for the determination of mesophyll conductance, and Prof. Dr. Wilhelm Windish and Michael Gertitschke from Lehrstuhls für Tierernährung for the measurement of energy. I would also like to thank Dr. Albert Andreas from EUS in Helmholtz Center Munich for providing the space in the sun simulator chamber for the high photon flux density experiments.

A special thanks to my mother, Lincong Fan, my father, Ercai Yang, my mother-in-law, Minghua Zhang, and father-in-law, Weizheng Liu, for their understanding and support during the period of my Ph.D. study. At the end, I would like express appreciation to my wife Jinghui Liu who gave me a lot of help and support in both work and family.

This work is supported by Deutsche Forschungsgemeinschaft Grants (GR938 and SFB924) and Bayerisches Staatsministerium für Bildung und Kultus, Wissenschaft und Kunst (ForPlanta). The first four years' cost of living in Germany was funded by the State Scholarship fund from the China Scholarship Council of the P.R. China, and the rest of time was funded by Prof. Dr. Erwin Grill's laboratory.



---

---

# Lebenslauf

## Persönliche Daten

---

<b>Name</b>	Zhenyu Yang
<b>Geboren am</b>	13 April 1983, in Xinzhou, V.R.China
<b>Nationalität</b>	Chinesisch
<b>Familienstand</b>	Verheiratete

---

## Ausbildung

---

<b>1998 - 2002</b>	Abitur, die erste Mittelschule von Xinzhou, Shanxi Provinz, V.R. China
<b>2002 - 2006</b>	Studium der Biotechnologie an der Shanxi Agricultural Universität, Shanxi Provinz, V.R. China
<b>2007 - 2010</b>	Studium die Gartenbauwissenschaften an der Northwest Agriculture and forest Universität, Shaanxi Provinz, V.R. China
<b>2010 - 2016</b>	Doktorarbeit am Lehrstuhl für Botanik der Technischen Universität München

---

## Publikationen

---

### **The proceedings of the National Academy of science (PNAS) 2016**

Yang, Zhenyu; Liu, Jinghui; Tischer, Stefanie V.; Christmann, Alexander; Windisch, Wilhelm; Schnyder, Hans; Grill, Erwin (2016) Leveraging abscisic acid receptors for efficient water use in Arabidopsis. Proceedings of the National Academy of Sciences of the United States of America 113, 6791 - 6736.

---